Temperature impact on the consolidation and creep behaviour of compacted clayey soils

Nidal Jarad

UNIVERSITÉ DE LORRAINE

École doctorale EMMA – Énergie Mécanique et Matériaux
Laboratoire d'Énergétique et de Mécanique Théorique et Appliquée

THÈSE

Présentée en vue de l'obtention du grade de

Docteur de l'Université de Lorraine
Science des matériaux
Spécialité : Mécanique des matériaux

Par

Nidal JARAD

Temperature impact on the consolidation and creep behaviour of compacted clayey soils

Impact de la température sur le comportement de consolidation et de fluage des sols argileux compacts

Soutenance prévue le 14 décembre 2016 devant la commission d'examen :

Monsieur Saïd TAÏBI	Professeur - Université du Havre	Rapporteur
Monsieur Yu Jun CUI	Professeur à l'École des Ponts ParisTech	Rapporteur
Monsieur Akbar JAVADI	Professeur - Université d'Exeter (GB)	Examinateur
Madame Farimah MASROURI	Professeur – Université de Lorraine	Directeur de thèse
Monsieur Olivier CUISINIER	Maître de Conférences - Université de Lorraine	Co-directeur de thèse

To my parents

ACKNOWLEDGEMENTS

I would like to thank in deep my supervisor Professor Farimah Masrouri for her continuous support, motivation and invaluable academic guidance throughout this research. I would like to thank deeply my co-supervisor Dr. Olivier Cuisinier for his support, encouragement, and meticulous guidance throughout my period of candidature. Without the support of my supervisors, this thesis would not become a reality. My thanks goes also to Dr. Sandrine Rosin-Paumier for providing me some experimental data. My thanks are also for the secertaries of the laboratory.

I would like also to thank the technical staff in the laboratory of soil mechanics (LEMTA) for their help and support to carry out the experimental work of my research. I also owe gratitude to all my friends and colleagues at the laboratory of my work (LEMTA).

I would like to gratefully acknowledge the financial support for this research through PhD fellowships which provided by Erasmus Mundus Program- EPIC that co-ordinated by Cardiff Metropolitan University and Funded by the EU Commission). My thanks are for Mrs Delphine Laurant for her guidance and support to arrive to France and coordination during my PhD study.

I would like to express my gratitude to Professor Yu Jun Cui at Ecole des Ponts Paris Tech, and Professor Said Taibi at université de Havre for their agreement to be external reviewers of this dissertation. In addition, I would like to thank Professor Akbar Javadi at the University of Exeter for his agreement to be the president of the jury members of this dissertation.

Finally, I would like to express my greatest gratitude to my parents who have been encouraged and supported me. I would like also to extend my gratitude to Wadoud, Zemenu, Luc, Hossein, Ahmed, Saeid, Wahib and all the others I met in the laboratory during my thesis.

Résumé de THÈSE

1. Introduction

Dans un certain nombre de problématiques comme le stockage des déchets radioactives, les sondes géothermiques, le stockage thermique dans des aquifères et l'enfouissement des câbles de haute tension (Reeves et al., 2006), il est indispensable de prendre en compte l'impact de la température sur le comportement hydromécanique des argiles. Pour cette raison, de nombreux travaux ont été effectués pour apprécier les effets de changement de température (Kholghifard et al., 2014).

Ainsi, la température peut avoir un effet important sur les paramètres de consolidation des sols argileux. Towhata et al. (1993), Boudali et al. (1994) et Marques et al. (2004) ont effectué des essais oedométriques thermorégulés sur plusieurs argiles. Leurs résultats montrent une diminution de l'indice des vides sous l'effet de l'augmentation de la température. Tandis que Kholghifard et al. (2014) n'ont pas constatés l'effet de la température sur la variation de l'indice des vides. Burghignoli et al. (2000) expliquent que la variation de l'indice des vides est due essentiellement au réarrangement des grains du sol, la variation de la température, l'histoire de chargement, l'histoire de la température et le temps de chauffage.

Plusieurs chercheurs concluent que le chauffage de sol diminue la contrainte de préconsolidation (Sultan et al., 2002; Moritz, 1995). Contrairement à Mon et al., (2013) qui ont observés une augmentation de la contrainte de préconsolidation avec l'augmentation de la température. La variation des propriétés initiales des éprouvettes telles que l'indice des vides initial et la structure de l'argile peuvent être des raisons de divergences des résultats. La variation des propriétés des éprouvettes est due principalement aux méthodes de préparations, le temps de chauffage et de refroidissement, la contrainte de préconsolidation appliquée et les différentes techniques expérimentales utilisées (Crawford, 1967).

Dans ce contexte, cette étude a examiné l'impact de la température sur le comportement de consolidation et du fluage d'argiles compactées saturées. L'impact de la nature du sol et de son histoire mécanique a été considéré. L'effet de la vitesse de déformation a été étudié pour des températures variant entre 5 et 70 °C et différentes vitesses de déformation utilisant une cellule oedométrique thermorégulée.

2. Matériaux et méthodes

2 .1. Matériaux

Deux argiles saturées et compactées ont été étudiées. L'argile A contient essentiellement de l'illite (77%) mais contient également des proportions de calcite et de kaolinite de 12% et 10% ainsi que des traces de quartz et de feldspath. L'illite est une argile non gonflante (Srodon et al., 1986). L'argile B est un matériau composé de kaolinite, illite et de smectite. Les limites d'Atterberg (AFNOR, 1993) et les courbes de Proctor (AFNOR, 1999) pour les deux argiles ont été déterminées comme indiqué dans le tableau 1. Près de 85% des particules d'argile A ont un diamètre inférieur à 2 μm (classe des argiles), et les 15% restants ont un diamètre inférieur à 20 μm (classe des limons). Près de 72% des particules d'argile B ont un diamètre inférieur à 20 μm (classe des limons), et les 25,5% restants ont un diamètre inférieur à 0,08 mm. L'argile A et L'argile B sont classées comme A3, et A2 respectivement selon la classification du GTR (2000).

Tableau 1. Characteristics d'Argile A et de l'argile B.

Type de sol	Argile A	Argile B
Limite de liquidité (%)	65	43,5
Limite de plasticité (%)	34	19,7
Indice de plasticité (%)	31	23,8
Teneur optimale en humidité (%)	31,3	16,5
La densité sèche maximale (Mg/m^3)	1,43	1,74
Gravité spécifique	2,65	2,65

2 .2. Préparation de l'échantillon

Les poudres de deux matériaux ont été mélangées avec de l'eau distillée à la température ambiante afin que la teneur en eau corresponde à la valeur optimale (à densité sèche maximale), puis maintenu pendant 24 heures pour obtenir l'homogénéité. Les éprouvettes ont été compactés sous charge statique dans un moule rigide en une seule couche pour former des éprouvettes de 71,4 mm de diamètre et de 20 mm de hauteur dont leurs poids représentent la

densité sèche maximale. Une fois l'échantillon est compacté, il est transféré du moule de compactage à la cellule œdométrique.

2.3 Dispositif expérimental

Une vue générale de l'ensemble du dispositif expérimental est donnée sur la figure (1). L'ensemble du système comprend le bâti de charge, cellule œdométrique, dispositif de température et un injecteur d'eau. L'échantillon est introduit dans le dispositif entre deux pierres poreuses. La cellule œdométrique à embase modifiée comprend un système de drainage pour la sortie d'air, la saturation. La pression d'eau interstitielle est mesurée au moyen d'un capteur de pression. Un chargement externe est appliqué à la pièce de pression à l'aide d'une presse.

Le dispositif de régulation thermique alimente le corps de la cellule œdométrique en liquide thermique via des tubes recouverts d'isolants.

Le contrôleur pression-volume est utilisé, comme un injecteur d'eau, afin de saturer l'éprouvette en appliquant une pression interstitielle à la base de l'échantillon.

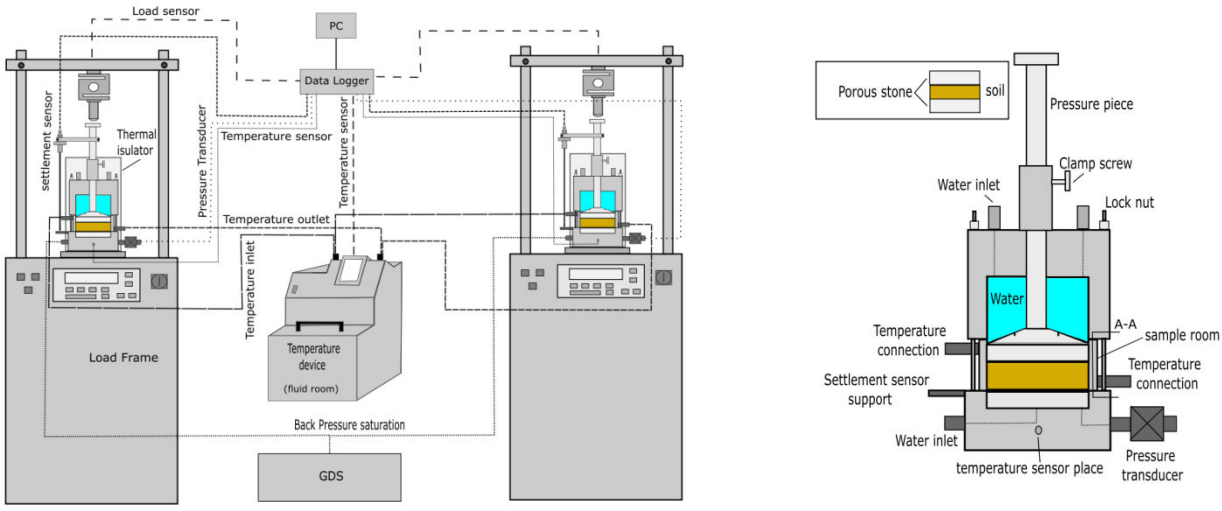

(a) (b)

Figure 1. (a) Schéma de principe de l'appareil (b) cellule oedometric détail

2. 4. Les procédures expérimentales

Après son compactage directement dans la cellule oedométrique, l'éprouvette a été chargée verticalement sous contrainte verticale constante de 10 kPa. Une pression d'eau de l'ordre de 10 kPa a été appliquée pour saturer l'échantillon par l'intermédiaire de la base.

Une fois la saturation achevée, l'éprouvette a été amenée à la température désirée en 48 heures, puis l'essai, CRS, consolidation à vitesse de déformation constante, a été accompli. Dans un essai CRS, l'échantillon est chargé à une vitesse constante de déformation verticale. Le drainage est autorisé uniquement à la surface supérieure de l'échantillon. Pendant l'essai, l'excès de la pression interstitielle, générée par le biais de l'éprouvette, varie du maximum à la base jusqu'à zéro à la surface supérieure. La force de réaction, la déformation axiale, et la pression interstitielle à la base ont été mesurées durant les essais à certains intervalles de temps. L'échantillon a été chargé à partir de 10 kPa jusqu'à 5120 kPa à des vitesse de déformation de 0,002%/min; 0,01%/min; et 0,02 %/min. Pour observer l'influence de la chaleur, l'argile ''A'' a été testée sous des températures de 20; 47,6; 69,2°C à chaque taux de déformation, tandis que l'Argile ''B'' a été testée sous les températures les plus basses et les plus élevées (5,53 et 69,2° C) à chaque taux de déformation.

2.5. Interprétation des résultats

Une distribution parabolique de la pression interstitielle est considérée à travers l'échantillon au cours de l'essai CRS. La contrainte effective peut être évaluée comme suit (Wissa et al. 1971):

$$\sigma' = \sigma - \frac{2}{3}u \qquad (1)$$

Où σ = contrainte totale, et u = la pression interstitielle à la base de l'éprouvette.

Les paramètres mesurés lors des essais isothermiques de consolidation du CRS effectués à diverses températures ont été employés pour déterminer la conductivité hydraulique des sols argileux étudiés à des températures et des taux de déformation comme méthode indirecte de mesure selon l'équation suivante (ASTM, 2008):

$$k_t = \frac{\dot{\varepsilon}_t H_t H_O \gamma_w}{2u} . \frac{1}{10000} \qquad (2)$$

Où : H_t est l'exemple de hauteur à un moment spécifique, t; H_o : est la hauteur initiale de l'échantillon et $\dot{\varepsilon}_t$ est le taux de déformation à un moment spécifique, t, et peut être calculée comme suit:

$$\dot{\varepsilon}_t = \frac{H_{t+1} - H_{t-1}}{H_O} . \frac{1}{t_{t+1} - t_{t-1}} \qquad (3)$$

L'effet de la température sur la conductivité hydraulique des argiles peuvent être mieux compris en termes de la perméabilité intrinsèque, K, comme suit :

$$k_t = \frac{K\gamma_w(T)}{\mu(T)} \qquad (4)$$

Où μ (T) est la viscosité de l'eau interstitielle à l'essai de température.

Les valeurs de coefficient de consolidation des argiles étudiées ont été calculés à un moment donné, t, au cours de l'essai CRS comme l'équation suivante (ASTM, 2008):

$$c_v = \frac{k}{m_v \gamma_w} \qquad (5)$$

Dans lequel, la perméabilité, k, et le coefficient de compressibilité de volume, m_v, développé à un moment donné, t. γ_w est la densité de l'eau à une température donnée.

Au cours de l'essai CRS, le coefficient de compressibilité volume a été déterminé à un moment donné, t, selon l'équation suivante (ASTM, 2008) :

$$m_v = \frac{\varepsilon_{t+1} - \varepsilon_{t-1}}{\sigma_{t+1} - \sigma_{t-1}} . \frac{1}{100} \qquad (6)$$

Qui représente la déformation volumétrique de l'éprouvette d'argile en raison de l'accroissement de la contrainte effective pendant un temps donné, t.

3. Résultats

La figure 2(a) présente la variation de la déformation avec la contrainte effective verticale sous différentes températures pour les essais CRS à 0,01%/min du taux de déformation pour les deux matériaux. La déformation-log σ' courbe pour l'argile A a changé légèrement avec les températures testées, alors qu'il était moins affectée par la température de l'argile B (plus dense que l'Argile A).

Les valeurs de l'indice de compression, qui représente la pente de la ligne de compression, convergent à différentes températures. Les valeurs sont comprises entre 0,188 et 0,213 pour l'argile A à des températures entre 20 et 70 °C, tandis que pour l'argile B, à des températures de 5 et 70 °C, elles varient entre 0,182 et 0,205. En outre, les lignes de compression sont presque parallèles à différents taux de déformation de 0,002; 0,01; 0,02%/min à une certaine température. Les valeurs d' indice de gonflement, obtenu à partir des pentes des lignes de gonflement, à différentes températures varient entre 0,0035 et 0,01 pour l'argile A, et entre 0,011 et 0,019 pour l'argile B. En conséquence, l'indice de compression pour les deux argiles pourrait être considérés comme indépendant de la température et de la vitesse de déformation. En outre, l'ampleur des changements dans les valeurs pour tous les essais sur la même argile indique que l'indice de gonflement n'est pas fortement dépendant de la température et de la vitesse de déformation. La figure 2 (c) présente la variation de l'indice de compression et de gonflement avec la température et la vitesse de déformation pour 9 essais sur l'Argile A et 6 Essais sur l'argile B.

3.1. Influence de la température sur la pression interstitielle

Figure 2 (b) montre la variation de l'excédent de pression interstitielle avec différentes températures. Pour l'argile A, par exemple, à 0,01%/min du taux de déformation, l'excédent maximum de pression interstitielle générée à 69,2°C est de 2,5 fois plus petit qu'à la température ambiante. Pour l'argile B, au même taux de déformation, l'excédent maximum de pression interstitielle générée à 5°C est 2,7 fois plus grand que la pression interstitielle générée à 69,2 °C. L'excédent de pression interstitielle généré, mesurée à la base de l'échantillon, montre une forte dépendance de la température pour les deux argiles. En général, à une déformation donnée, plus la température est basse, plus forte est la pression interstitielle générée à la base du spécimen et que, pour des températures élevées, l'excédent de pression interstitielle générée est petit. En effet, l'apparition de haute perméabilité à hautes températures

à l'addition de l'écoulement d'un seul côté limite l'accumulation de la pression interstitielle dans le spécimen pendant l'essai CRS.

3.2. Influence de la température sur la pression de préconsolidation

La pression de préconsolidation déterminée pour l'argile A pour tous les tests à différentes températures (20; 47,6; 69,2°C) se rapporte qu'il a diminué avec l'augmentation de température comme une représentation linéaire. En comparant les pressions de préconsolidation déterminée pour l'argile B à des températures de 5,53°C et 69,2°C, il a diminué légèrement à haute température, et en conséquence, il pourrait être considéré comme indépendant de la température. La figure 2 (d) montre la variation de la pression de préconsolidation en fonction de la température qui a été déterminé à partir de 9 essais sur l'argile A CRS et 6 Essais sur l'argile B.

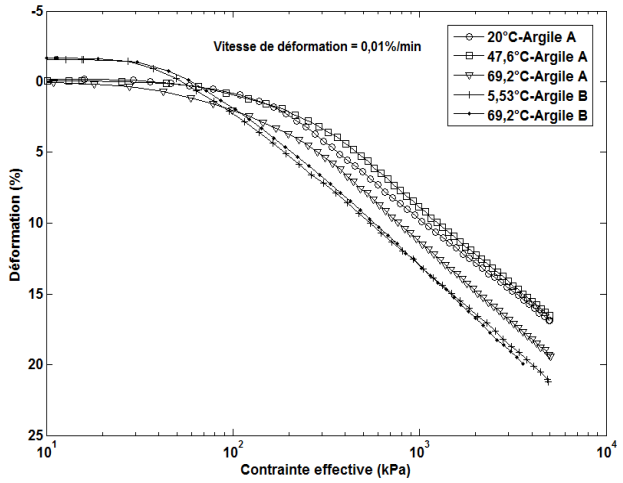

(a)

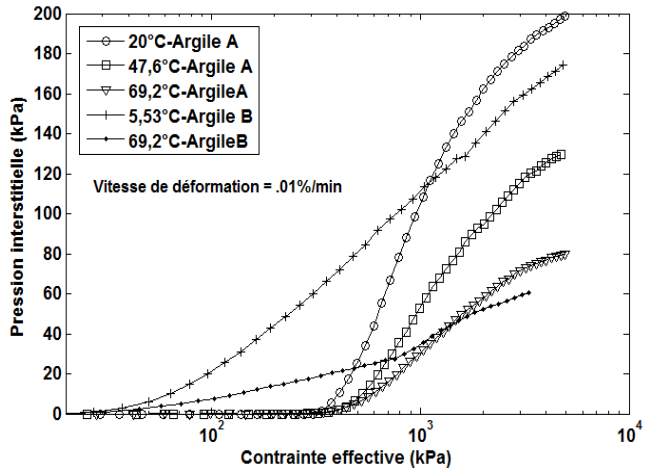

(b)

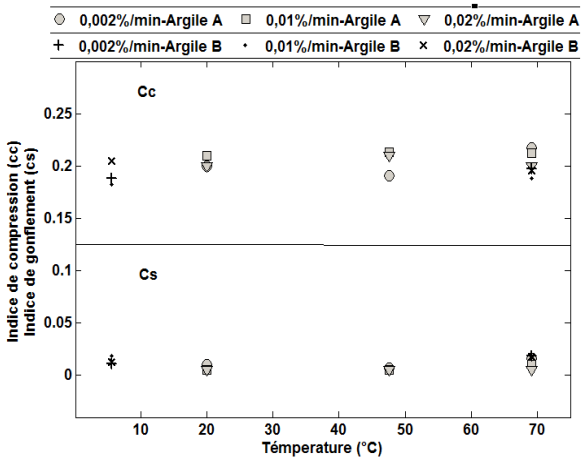

(c)

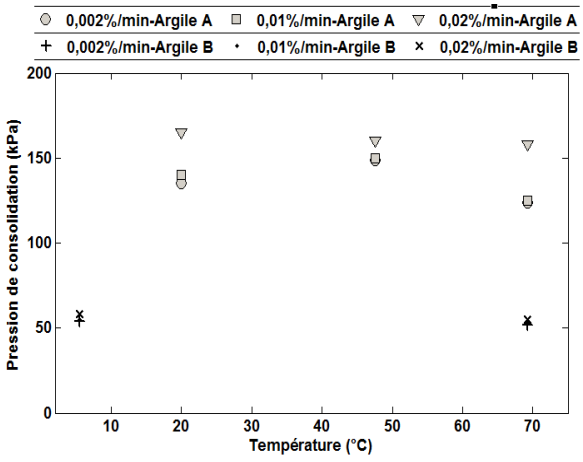

(d)

Figure 2.L'influence de la température sur (a) l'déformation (b) l'pressure interstitlelle (c) l'indice de gonflement de la compression et (d) pression de préconsolidation.

3.3. Influence de la température sur la perméabilité

La figure 3 (a) montre la variation de la conductivité hydraulique et la perméabilité intrinsèque avec la température pour les deux argiles à l'indice de vide spécifique. À la vitesse de déformation spécifique, la conductivité hydraulique de l'argile a augmenté avec l'augmentation de la température pour les températures testées de 20; 47,6; 69,2°C. Pour l'argile B à une vitesse de déformation de 0,01%/min par exemple, la conductivité hydraulique à la température de 69,2 °C augmente jusqu'à environ 3 fois que celle à 5,53 °C. Selon les résultats obtenus des matériaux étudiés, la conductivité hydraulique est fortement dépendante de la température, alors que la variation de la perméabilité intrinsèque avec la température est négligeable. Il n'y a pas de changement important dans l'unité de poids de l'eau avec la température si on le compare avec la viscosité. La valeur de la viscosité de l'eau pure libre change négativement avec la température.

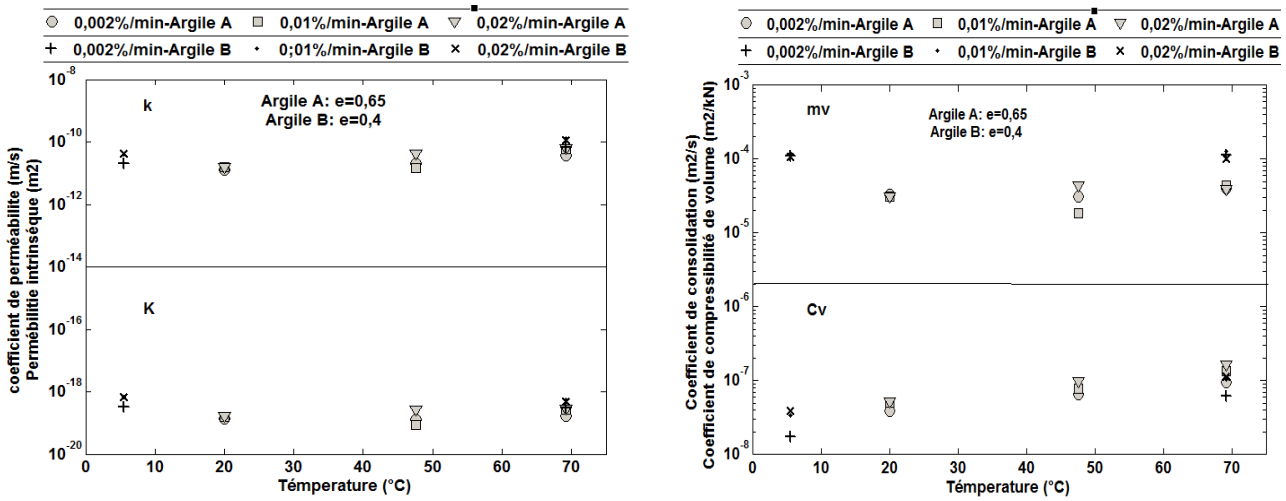

(a) (b)

Figure 3.L'influence de la température sur (a) l'coefficient of perméabilité perméabilité et intrinsèque. (b) l'coefficient de consolidation et l'coefficient de compressibilité de volume.

3.4. Influence de la température sur le coefficient de consolidation

Résultats de la figure 3 (b) montrent l'influence de la température sur le coefficient de consolidation (c_v) à différents taux de déformation à l'indice de vide spécifique. Pour illustrer les résultats au taux de déformation de 0,01%/min pour les argiles étudiées par exemple. Pour l'argile A, à la plus haute température; 69,2 °C; la C_V est $1{,}36\times10^{-7}$ m^2/s, alors que c'est $5{,}05\times10^{-8}$ m^2/s pour la température ambiante, 20°C. Encore une fois, pour l'argile B, le C_v est de $1{,}04\times10^{-7}$ m^2/s à la température de 69,2 °C, alors que c'est $3{,}36\times10^{-8}$ m^2/s à la température 5,53 °C. En fonction de ces résultats, à un certain taux de déformation, la valeur du coefficient de consolidation est plus grande à l'augmentation de température. À une certaine température, la valeur du coefficient de consolidation est plus grande à l'augmentation de taux de déformation. La diminution de la viscosité du squelette du sol et l'eau interstitielle à des températures élevées rend le taux de consolidation supérieur aux basses températures.

3.5. Influence de la température sur le coefficient de compressibilité de volume

Figure 3 (b) montre la variation du coefficient de compressibilité de volume (mv) avec la température à différents taux de déformation pour les argiles étudiées à l'indice de vide spécifique. Par exemple, 0,01%/min du taux de déformation d'Argile A, la valeur de mv au plus et bas les températures les plus élevées (20 et 69,2°C) sont 3,15×10-5 et 4,44×10-5

m2/kN, respectivement. De même, pour l'argile B, les valeur de mv à des températures de 5,53 et 69,2°C sont 1,21×10-4 et 1,26×10-4 m2/kN, respectivement. En fait, les résultats indiquent que le coefficient de compressibilité volume valeurs à tout compte tenu du taux de déformation est environ pas changé avec la température.

3.6. Influence de la température sur l'indice de fluage

Figure 4 montre la variation du l'indice de fluage (cα) avec la température pour les argiles étudiées. L'indice de fluage déterminée pour l'argile A à différentes températures (20; 47,6; 69,2°C) se rapporte qu'il a diminué avec l'augmentation de température. En comparant les indices de fluage déterminé pour l'argile B à des températures de 5,53°C et 69,2°C, il a diminué légèrement à haute température. La raison pourrait être liée à la diminution de la viscosité du squelette du sol et l'eau interstitielle à des températures élevées.

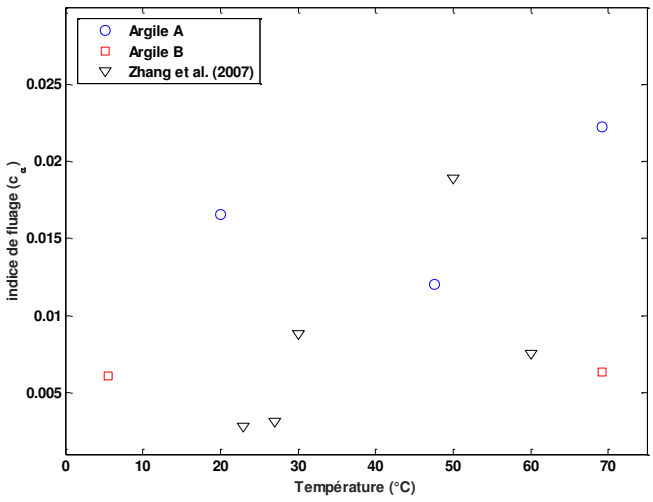

Figure 4.L'influence de la température sur l'indice de fluage.

3.7. Influence de l'argile nature et l'histoire du stress sur le comportement thermo-hydro-mécanique

Les résultats montrent que le comportement contrainte-déformation de l'argile A était pas fortement dépendante de la température, alors qu'il a été moins affectée par la température pour l'argile B. La conductivité hydraulique (k) et le coefficient de consolidation (cv) était supérieure à la température plus élevée, tandis que la pression des pores est inférieure à la température plus élevée.

Les argiles légèrement surconsolidées ont montré un comportement de contraction lors du chauffage, alors que les plus lourdement échantillons consolidés ont montré un comportement de dilatation lors du chauffage.

4. Conclusions

Les résultats de l'étude expérimentale, effectuée sur deux argiles compactées et saturées utilisant une cellule œdométrique de type thermo-régulé pour étudier l'influence de la température sur les caractéristiques de consolidation de l'argile, peuvent être résumé comme suit :

- La variation de l'indice de compression (c_c) et de gonflement (c_S) avec la température et la vitesse de déformation pourrait être considéré comme négligeable.
- La pression de préconsolidation (p_c) diminue en fonction de la température pour l'Argile A, alors qu'elle diminue légèrement pour l'argile B.
- La conductivité hydraulique (k) augmente avec la température, tandis que la perméabilité intrinsèque (K) est indépendante de la température.
- La pression interstitielle (u) diminue avec l'augmentation de la température au cours l'essai CRS.
- Le comportement contrainte-déformation de l'argile A a changé légèrement avec la température, tandis qu'il est moins influencé par la température de l'argile B. Ce résultat entraîne que plus l'argile compactée est dense, moins est affectée par la température.
- Le coefficient de consolidation (c_v) augmente avec la température, alors que la variation du coefficient de compressibilité de volume (m_v) avec la température est considérée comme négligeable.
- L'indice de fluage (c_α) augmente avec la température pour les deux matériaux.
- L'impact étudié des facteurs principaux de l'étude, qui comprend la température, l'argile nature, et de l'histoire du stress sur le comportement des sols argileux compactés a indiqué que ces facteurs pourraient contrôler le comportement thermo-hydro-mécanique des argiles compactées.

Table of contents

List of figures

List of tables

General introduction

Consolidation of clay soils is one of the main challenges in geotechnical and civil engineering. It can be divided into primary and secondary consolidation. The primary compression is governed by the dissipation of pore pressure and the secondary compression is time dependent behaviour. Long term behaviour has a significant effect on the serviceability and stability of structures built on soft soils.

Ground temperature fluctuations are significant in several contexts, including radioactive wastes, hot buried pipes, contaminated landfill sites, aquifer thermal energy storage systems, and buried electricity cables (Reeves et al., 2006; Haehnlein et al., 2010; Mon et al., 2013; Raude et al., 2015). Therefore, the impact of temperature on the short- and long-term consolidation behaviour of soils is a major issue in geotechnical engineering. A better understanding of this phenomenon will help reduce the undesired effects of temperature changes and allow a better selection of design method (Sultan et al., 2002; Cekerevac and Laloui, 2004; Watabe et al., 2012; Kholghifard et al., 2014).

Short- and long-term consolidation properties of clayey soils may be altered after temperature variation. Based on a laboratory study, Abuel-Naga et al. (2005) found that the consolidation rate (c_v) increased as the temperature increased. This was related to the variation of the permeability with temperature. The permeability increases as the temperature increase, which has been shown in many experimental studies including the direct method (Delage et al., 2000; Villar and Lloret, 2004) and indirect method (Towhata et al., 1993; Abuel-Naga et al., 2005). The reduced viscosity of pore water at high temperatures causes an increase in the hydraulic conductivity. However, the intrinsic permeability is independent of temperature (Delage et al., 2009). The mechanical behaviour of clay soils including preconsolidation pressure,

compression index, and swelling index were investigated for different temperatures. Most of the researchers found that heating reduces the preconsolidation pressure (Moritz, 1995; Sultan et al., 2002; Abuel-Naga et al., 2005; François et al., 2007; Tang et al., 2007). Indeed, the softening of the clay at high temperature is caused by the reduction in viscosity of the pore water and soil skeleton. Generally, the increased number of mineral-to-mineral contacts at high temperature causes more plastic strain and a reduction in the elastic domain (Shariatmadari and Saeidijam, 2012). Hence, the preconsolidation pressure decreases at high temperatures. Conversely, positive temperature dependency was observed in a few studies (e.g., Mon et al., 2013). The hardening behaviour of the clay with heating is caused by the enhanced inter-particle forces between the clay particles, which increases the shear stiffness. The results of the isothermal oedometric tests at different temperatures showed that the variations of the compression index (c_c) and swelling index (c_s) with temperature were negligible (Finn, 1951, Campanella and Mitchell, 1968). In contrast, a few researchers observed that c_c (Tsutsumi and Tanaka, 2012) and c_s (Abuel-Naga et al., 2007) change with temperature.

There are still limited studies on the influence of temperature on creep (i.e., long term consolidation behaviour) of soils. Gupta (1964) carried out creep tests at different temperatures and stated that the creep index increases as the temperature increases. A similar result was found by Green (1969), but he noted that the influence of temperature on the creep was dependent on the effective stress level; temperature affected the creep more at lower effective stress levels. By raising the test temperature from 20.0°C up to 90.0°C during the secondary consolidation phase, Towhata et al. (1993) observed a volume contraction of the sample during this phase. This result indicated to the temperature impact on the creep behaviour of clay soil. Burghignoli et al. (1992) noted that thermal loading accelerates the mechanical creep phenomena. The amount or rate of creep increases as the temperature increases because of the reduction in the apparent viscosity of the contacts between particles at higher temperatures (Gupta, 2013).

The long-term consolidation behaviour of clayey soils is strain rate dependent (Leroueil et al., 1985) and is caused by viscous properties of the clay skeleton (Tsutsumi and Tanaka, 2012). Consequently, creep can be assessed in terms of the effect of the strain rate. The influence of temperature on the strain rate-preconsolidation pressure relationship was investigated by very few researchers (e.g., Boudali et al., 1994; Marques et al., 2004). Boudali et al. (1994) performed different constant rate of strain (CRS) consolidation tests at different temperatures

to investigate the viscous behaviour of natural clay. They found that the strain rate-preconsolidation pressure relationship is independent of temperature. A similar behaviour of natural clays was also observed by Marques et al. (2004). Boudali et al. (1994) and Marques et al. (2004) found approximately parallel slopes of the logarithmic strain rate-preconsolidation pressure relationship at different temperatures. However, these studies focused mainly on natural and structured clays.

Compacted clayey soils are used in engineering for example as engineered barriers for the disposal of long-life radioactive wastes at shallow depths; therefore, they are usually subjected to cyclic changes of temperature. Assessment of creep in terms of the strain rate effect at ambient and different temperatures for compacted clay soils was not considered by researchers.

Objective of the thesis

In this context, the main objective of this thesis was to investigate the influence of temperature on the short-and long-term consolidation behaviour of compacted clayey soils. Two different clays were used to study the influence of characteristics and mineralogy on the temperature dependent mechanical and hydraulic behaviours. In addition, the impact of stress history on the temperature dependent mechanical and hydraulic behaviours was studied. Parameters obtained by short-term consolidation are the compression index, swelling index, preconsolidation pressure, excess pore pressure, permeability, coefficient of volume compressibility, and coefficient of consolidation. The parameter obtained by long-term consolidation is the creep index. To characterize the behaviour in terms of the strain rate effect, constant rate of strain consolidation tests (CRS) with different strain rates were performed within the temperature range from 5° C to 70° C using temperature controlled oedometric cells. In comparison with the incremental loading in common oedometer tests, the CRS tests are rapid and provide a large amount of data within a short time. These data are useful for the evaluation of the long-term hydro-mechanical and creep behaviours of clayey soils.

Thesis plan

This study is divided into five chapters. A brief review of each chapter is given as follows:

Chapter1-Literature review

In this chapter, a review for the thermal properties of soil, variation of hydraulic conductivity with temperature in direct method, temperature effect on the short- and long-term

consolidation behaviour of clay soils is presented. Then, the experimental methods used for these studies are exposed. In addition, a review for the modeling of elasto-viscoplastic and thermo-elasto-viscoplastic behaviour of clay is presented. The scientific background needed for understanding the upcoming chapters is provided in this chapter.

Chapter2-Materials characteristics and experimental method

The main characteristics of the studied materials, the design of the experimental devices, and the theory of the performed tests are presented in this chapter. The experimental procedures and program of tests performed in this research are also presented.

Chapter3-Thermo-hydro-mechanical behaviour of illitic clay

In this chapter, the temperature and strain rate effects on the mechanical and hydraulic behaviour of saturated compacted illitic clay are introduced. In detail, the variations of the short- and long-term consolidation characteristics of this material with temperature are studied. The compression index, swelling index, preconsolidation pressure, excess pore pressure, permeability, coefficient of volume compressibility, and coefficient of consolidation are the studied parameters of the short-term consolidation while the creep index is the studied parameter of the long-term behaviour.

Chapter4-Impact of clay nature on the thermo-hydro-mechanical behaviour

The influence of clay characteristics and mineralogy on the temperature dependent mechanical and hydraulic behaviours is presented in this chapter. The results of thermo-hydro-mechanical behaviours of illitic clay and clay composed of kaolinite and illite are compared and presented to explain the clay nature effect. In particular, the comparisons between temperature dependent short- and long-term consolidation parameters for the studied clays are performed and displayed.

Chapter5-Impact of stress history on the thermo-hydro-mechanical behaviour

The effect of over-consolidation ratio (OCR) on the thermo-hydro-mechanical behaviour of compacted clayey soils is given in this chapter. The samples were loaded for different stress histories for both studied materials, and it is divided into lightly and heavily over-consolidated samples. The consolidation characteristics of short-term behaviour of lightly and heavily over-consolidated studied clays are compared and displayed.

Chapter 1 Literature review

1.1 Introduction

The effect of temperature on the hydro-mechanical behaviour of clayey soils is a major issue in geotechnical engineering. Understanding this phenomenon is required for more efficient and economic engineering designs.

An overview of the previous studies concerning the thermo-hydro-mechanical behaviour of clayey soils is discussed in this chapter. The first section focuses on the main thermal properties of soil, its values, and the factors that influence these thermal properties. The second section shows the influence of temperature on the permeability using the direct method tests. The third section presents the variation of short term consolidation characteristics with temperature which includes swelling pressure, compression index, swelling index, preconsolidation pressure, coefficient of consolidation, coefficient of volume compressibility, permeability using indirect method, and variation of normally consolidated and over-consolidated behaviours of clay with temperature. The fourth section highlights the creep behaviour of clayey soils, its theories, mechanisms, and concepts, and the main factors that influence this behaviour. The last section shows the modeling of thermo-hydro-mechanical behaviour of clayey soils which includes the modeling of elasto-viscoplastic and thermo-elasto-viscoplastic behaviour of clayey soils.

1.2 Thermal properties of soil

Soil thermal properties including thermal conductivity, heat capacity and thermal diffusivity are required in many areas of engineering, agronomy, meteorology, and soil science, and in recent years considerable efforts have been put into developing techniques to determine these

properties. Heat flow by conduction in soil may be determined from knowledge of the thermal conductivity and temperature gradient (Abu-Hamdeh, 2003; Lipiec et al., 2007).

1.2.1 Definitions

The thermal conductivity (λ)

The thermal conductivity is the amount of heat passing in unit time through a unit cross sectional area of the soil under a unit temperature gradient applied in the direction of this heat flow (as cited in Farouki, 1981) (Figure 1.1).

$$\lambda = q / [A\,(T_2 - T_1)/l] \quad \textbf{(1.1)}$$

Where q: heat flow (W), A: sectional area (m^2), T: temperature (°K), l: length. The unit dimension is W/ (m·K).

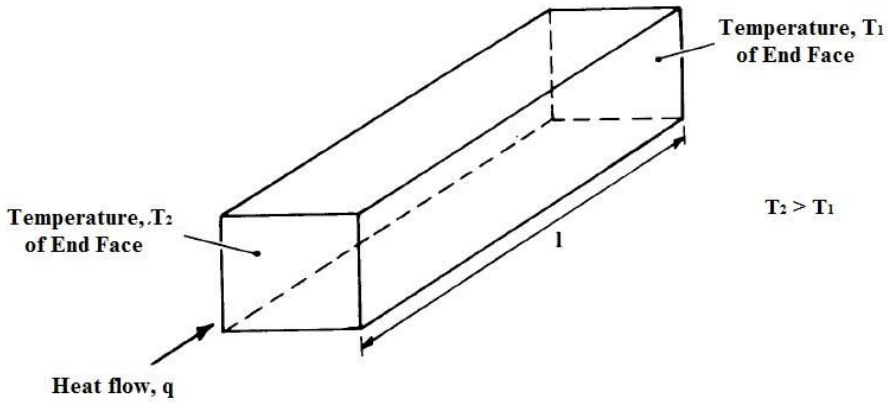

Figure 1.1 Heat flow through soil element (from Farouki, 1981).

Heat capacity (C)

The heat capacity is the energy required to raise the temperature of a unit volume of soil by 1°C (as cited in Farouki, 1981; Peters-Lidard et al., 1998)**.**

$$C = \rho c \quad \textbf{(1.2)}$$

where ρ is the density (g/cm^3) and c is the mass specific heat (cal/g °C).

Thermal diffusivity (α)

The thermal diffusivity is the ratio of thermal conductivity to heat capacity (as cited in Farouki, 1981; Krzeminska et al., 2012).

$$\alpha = \lambda / C \quad \textbf{(1.3)}$$

where the dimensional unit is (mm^2/s).

Some typical values of the thermal properties for soil constituents are indicated in Table 1.1.

Table 1.1 Thermal properties of soil constituents (Campbell & Norman, 1998).

	λ W/ (m·K)	C MJ/(m^3K)	α mm^2/s
Soil minerals	2.5	2.3	1.09
Granite	3	2.2	1.36
Quartz	8.8	2.1	4.19
Organic matter	0.25	2.5	0.10
Water	0.6	4.18	0.14
Ice	2.2	1.9	1.16
Air	0.025	0.001	20.83

1.2.2 Main factors influencing thermal properties

The thermal properties of soil depend on several parameters such as mineralogical composition, grain size of soil, moisture content, dry density, and saturation (Oladunjoye & Sanuade, 2012). These factors can be classified into two groups. The first group is inherent to the soil itself such as mineralogical composition, and the other group of factors can be managed or controlled, at least to a certain extent, by human management, such as water content and dry density.

A) Soil mineralogy

Texture and mineralogical composition of the soil are considered as the factors or properties that are inherent to the soil itself (Pramanik & Aggarwal, 2013; Alnefaie & Abu-Hamdeh, 2013). One of the factors that affect the soil thermal conductivity is its mineral composition (Becker et al., 1992; Misra et al., 1995; Fricke et al., 1997). Based on data collected from sands and gravels, Van Rooyon's correlation (1957) gives the soil thermal conductivity as a function of the mineral type, and granulometry (Becker et al., 1992).

Soil thermal conductivity varies with the mineral composition of the soil. For example, soils which have high quartz content generally have a greater thermal conductivity than soils which have high contents of plagiodase feldspar and pyroxene (Becker et al., 1992).

Tang et al. (2008b) wrote that the mineralogical composition among other factors influences the thermal conductivity of compacted bentonites. They found that the MX80 bentonite had lower thermal conductivity than that studied by Madsen (1998), since it contained a lower fraction of quartz. Tang et al. (2010) analyzed two MX80 bentonite samples in terms of mineralogical effects (effects of the proportion of quartz and montmorillonite) on the thermal conductivity. They concluded that the mineralogical effect was significant on the thermal

conductivity, and that the thermal conductivity of quartz is much higher than other minerals (Tang et al., 2008b).

B) Moisture content

The presence of a small amount of water content in soil improves the thermal contacts because of water bridges (Farouki, 1981), and therefore enhances the thermal conductivity.

The influence of increasing moisture content depends on the type of soil. The increase of water content in sand may spread water films around the larger sand particles than silt and clay, thus increasing the contact area between sand particles, which cause the thermal conductivity to increase. Figure 1.2 shows the relationship between moisture content and thermal conductivity (Farouki, 1981).

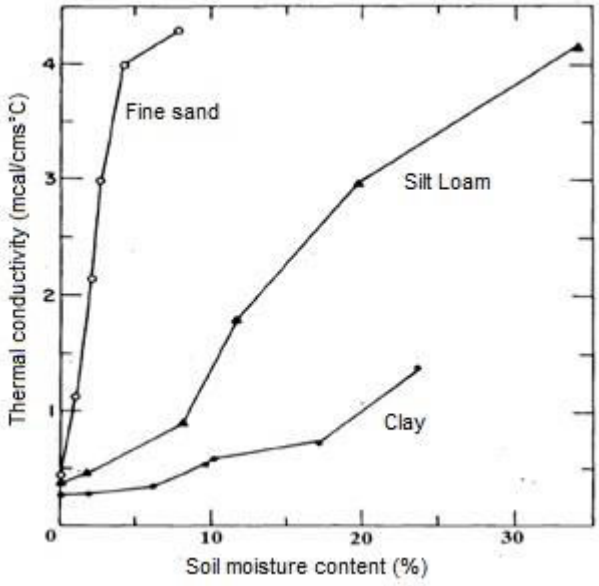

Figure 1.2 Thermal conductivity vs. moisture content (from Farouki, 1981).

In unsaturated soils, the heat capacity is greatly affected by water content because of the high heat capacity of water compared to air and solids (Hanson et al., 2000). If the volume fractions x of the solid, water, and air components present in a unit soil volume are known, the heat capacity will be as following equation:

$$C = x_s C_s + x_w C_w + x_a C_a \quad \textbf{(1.4)}$$

where C_s , C_w and C_a are heat capacities per unit volume of the solid, water and air.

The volumetric heat capacity of soil is a linear function of its air–water composition (Krzeminska et al., 2012). The volumetric heat capacity increases with increasing moisture content (Farouki, 1981). Figure 1.3 indicates the relationship between volumetric heat capacity

and moisture content for a sandy soil at different bulk densities (Alnefaie & Abu-Hamdeh, 2013).

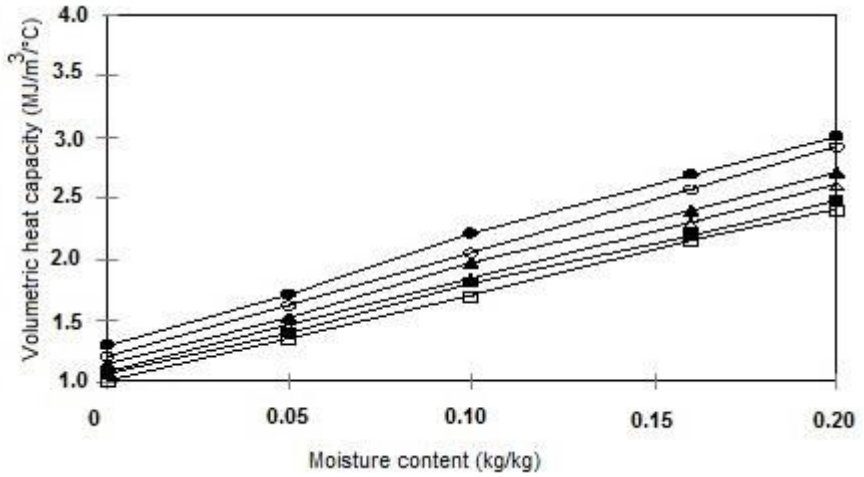

Figure 1.3 Moisture content vs. volumetric heat capacity (from Alnefaie & Abu-Hamdeh, 2013), ■: measured, □: predicted.

Bulk densities: ■, 1200kg/m^3, ▲, 1300kg/m^3, ● :1400kg/m^3

Thermal diffusivity is greatly affected by water content because of the high heat capacity of water compared with air and solids (Hanson et al., 2000). According to Abu Hamdeh (2003), the thermal diffusivity varies with moisture content and soil texture. Sandy soils exhibit a thermal diffusivity peak at a certain moisture content range, but clay soils do not exhibit a sharp thermal diffusivity peak. In fact, the increase of water content in sand increases the contact area between sand particles than clay soils particles because of larger water films around the sand particles. Accordingly, the sand thermal diffusivity increases more than clay since it has higher thermal conductivity which is related positively by water content. Figure 1.4 shows thermal diffusivity as a function of moisture content (Abu Hamdeh, 2003).

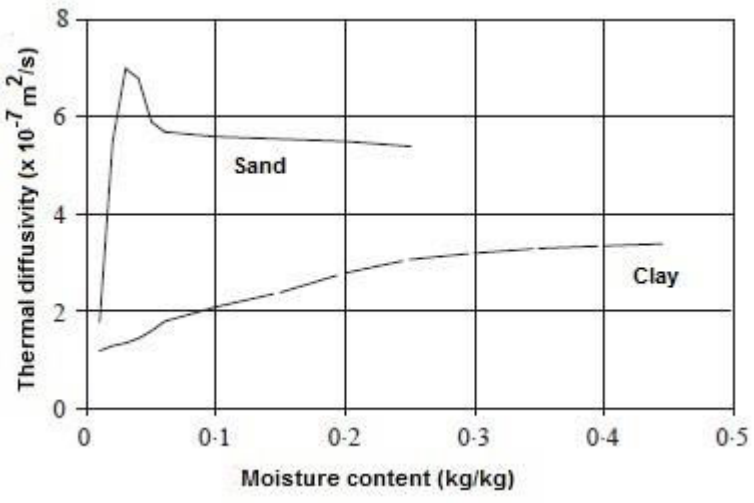

Figure 1.4 Thermal diffusivity as a function of moisture content for clay (from Abu Hamdeh, 2003).

C) Dry density

Another factor that significantly influences the thermal properties of soil is the soil density (Lipiec et al., 2007).

An increase in the dry density of a soil will lead to an increase in its thermal conductivity (Fricke et al., 1997). The increase in thermal conductivity of soil with the dry density increase is primary due to three factors including more solid matter per unit soil volume, less pore air or pore water per unit soil volume, and better heat transfer across the contacts (e.g. Farouki, 1981). Figure 1.5 shows the relationship between thermal conductivity of sandy soil and dry density at constant water content (Farouki, 1981).

Soil density among other factors influences the soil heat capacity (Abu Hamdeh, 2003). Volumetric heat capacity increases with soil density increase (Alnefaie & Abu Hamdeh, 2013). So that, with solids volume fraction increase, the heat capacity of soil increases (Farouki, 1981).

$$C = \rho c \qquad \textbf{(1.5)}$$

ρ: density, and c: mass specific heat. The dimensional unit is $MJ/(m^3/K)$.

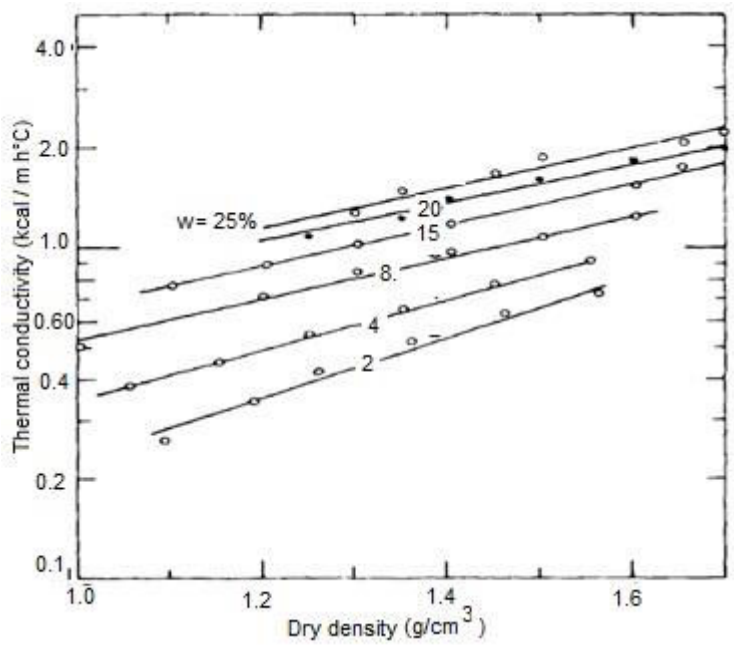

Figure 1.5 Thermal conductivity of sandy soil vs. dry density at constant water content (from Farouki, 1981).

The heat capacity increases with dry density increase due to an increase in the volume of solids fractions, and hence, the thermal diffusivity variation with dry density increase is low (Farouki, 1981). According to the Oladunjoye and Sanuade (2012), there is a weak positive relationship between dry density and thermal diffusivity as shown in Figure 1.6, due to the better conduction of heat resulting from improved contact between the soil grains.

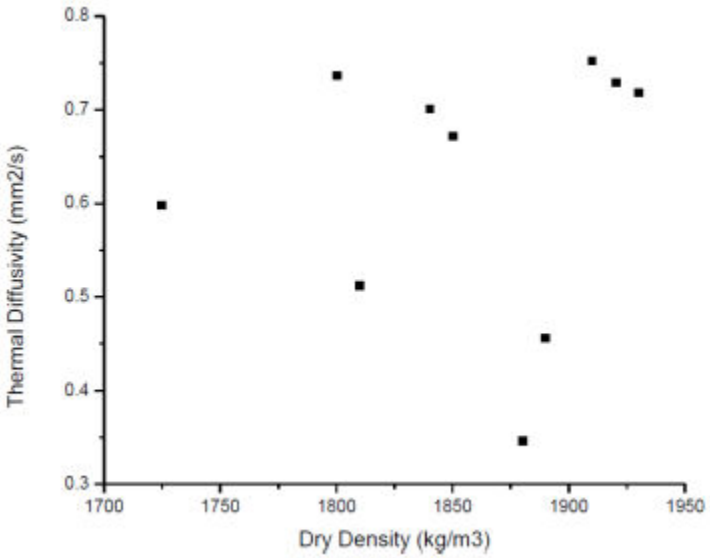

Figure 1.6 Thermal conductivity vs. Dry density (from Oladunjoye and Sanuade, 2012).

1.2.3 Conclusion

This section provided a review to the main thermal properties of soil which includes the thermal conductivity, the heat capacity, and the thermal diffusivity. The main factors which influence the thermal properties of soil are the soil mineralogy, the moisture content and the dry density.

1.3 Effect of temperature on the permeability

The following section includes the experimental investigation of the permeability variation with temperature and an interpretation for these variations.

1.3.1 Experimental investigation

Many researchers investigated experimentally the effect of heat on the coefficient of the hydraulic conductivity. Table 1.2 shows the different researchers' results of the temperature effects on the permeability.

Cho et al. (1999, 2000) measured the hydraulic conductivity of a saturated compacted ca-bentonite through direct method within the temperature range of 20 to 80^0 C. They concluded that as temperature increases, the hydraulic conductivity increases, and the hydraulic conductivity at the temperature of 80^0 C increases up to about three times than those at 20^0 C. They mentioned that the increase of hydraulic conductivity with increasing temperature is affected greatly by the change in the viscosity of water, and the intrinsic permeability is nearly constant (Figure 1.7). Bouazza et al. (2008) and Cho et al. (2011) also found a positive relationship between hydraulic conductivity and temperature.

Tests of constant head hydraulic conductivity have been done on Boom clay at different temperatures between 20° and 90°C and under various isotropic stresses by Delage et al. (2000, 2009) showing that for clayey soils, the changes of hydraulic conductivity were only related to changes in the viscosity of free water with temperature. Therefore, the changes in intrinsic permeability with temperature were not affected by temperature. Figure 1.8 shows the hydraulic conductivity in terms of intrinsic permeability. Ye et al. (2013) also indicated that the hydraulic conductivity of the saturated compacted GMZ01 bentonite increases with temperature rise.

Table 1.2 Temperature effect on the permeability.

No.	Author	Soil	Soil characteristics	Method	Temperature	k variation with T
1	Subba et al. (1953)	A remoulded alluvial soil	Passing through 1 mm sieve.	Constant head	35 to 1000° C	35 to 60° C and above 650° C: Decrease 60 to 650 C: Increase
2	Morin & Silva (1984)	Illite Smectite Siliceous ooze Calcareous ooze	LL: 95%; PL: 43% LL: 270%; PL: 91% LL: 254%; PL: 134% LL: 132%; PL: 73%	Rigid ring cell	Between 22 and 220° C	Increase
3	Cho et al. (1999)	Ca-bentonite	Montmorillonite (70%), feldspar (29%), quartz (1%)	Special apparatus	Between 20 and 80° C	Increase
4	Delage et al. (2000)	Boom clay	- PI=50%, Porosity=40%, Stiff clay	Triaxial	Between 20 and 100° C	Increase
5	Cho et al. (2000)	Ca-bentonite	Montmorillonite (70%), feldspar (29%), quartz (1%)	Special apparatus	Between 20 and 150° C	Increase
6	Romero et al. (2001)	Unsaturated Boom clay	20%-30% kaolinite, 20%-30% illite and 10%-20% smectite, LL=56%,PL=29%	Oedometer	22, 40, 60, and 80° C	Increase
7	Villar & Lloret (2004)	FEBEX bentonite	LL = 98-106 % Montmorillonite (90%)	Oedometer	Between 20 and 80° C	Increase
8	Bouazza et al. (2008)	Geosynthetic clay	Sodium/powder bentonite	Modified Rowe cell	Between 20 and 60° C	Increase

9	Delage et al. (2009)	Boom clay	PI=50%, porosity=40%, stiff clay	Triaxial	Between 20 and 90° C	Increase
10	Villar & Lloret (2010)	FEBEX bentonite	LL = 98-106 % Montmorillonite (90%)	Oedometer	Between 20 and 90° C	Increase
11	Cho W. et al (2011)	Kyungju Ca-bentonite	Montmorillonite (70%), feldspar (29%), quartz (1%)	Cylindrical cell	20 to 150º C	Increase
12	Tsutsumi & Tanaka (2012)	Kasaoka OsakaMa12 Louiseville	LL=62%, PL=36% LL=109%, PL=43% LL=71%, PL=22%	Modified triaxial	Between 10 and 50° C	Increase

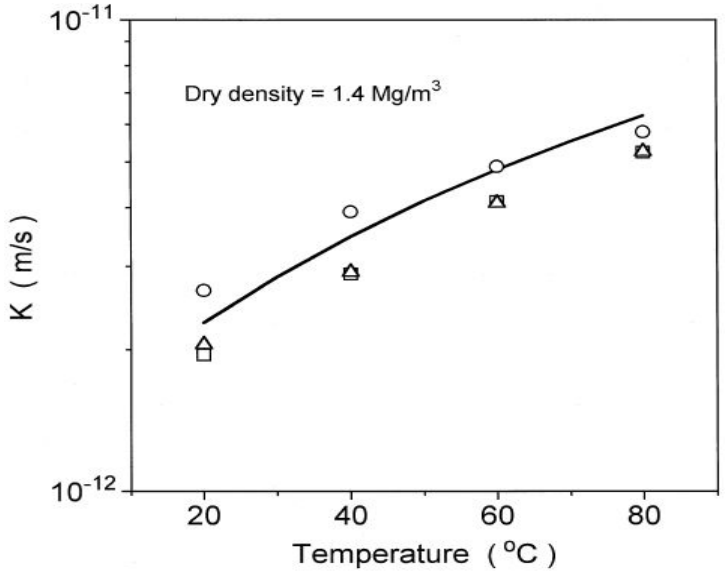

Figure 1.7 Permeability Vs. temperature with dry density of 1.4 Mg/m^3 (from Cho et al., 1999).

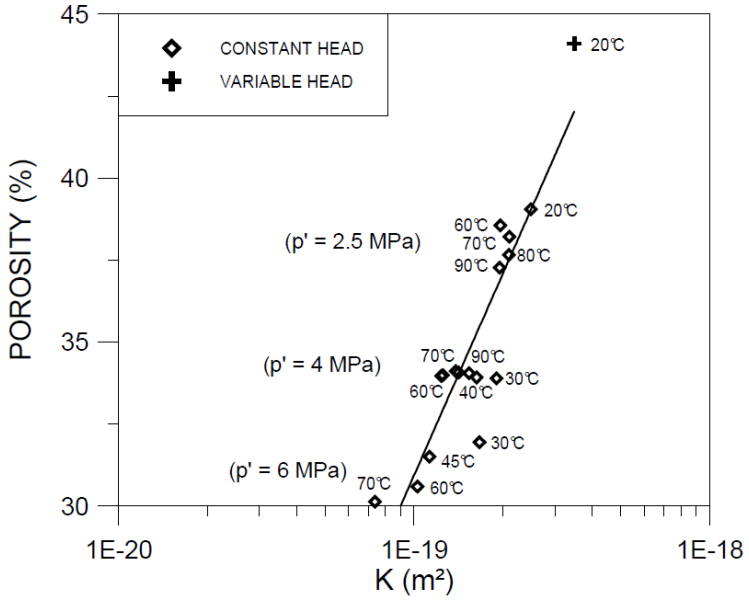

Figure 1.8 Permeability values in terms of intrinsic permeability (from Delage et al., 2000).

1.3.2 Interpretation

Factors that represent or influence the magnitude of the hydraulic conductivity of porous material include, 1) The physical properties of the fluid (soil liquid phase) which includes the viscosity and the unit weight of the fluid, 2) The properties of the solid matrix which describe the size of flow channel between soil particles, 3) The physico-chemical interactions between the soil particles and the permeant (surrounding) fluid which are a function of mineral characteristics of the solid particles as well as the chemical composition of the pore fluid. These interactions also affect the size of the flow channel (Bouazza et al., 2008; Abuel-Naga et al., 2005).

A) Viscosity

At constant void ratio, the increase in hydraulic conductivity is largely affected by the thermal evolution of the liquid properties. An equation was proposed to determine this effect by calculating the intrinsic permeability as a function of the hydraulic conductivity test results at different elevated temperatures,

$$K = \frac{k\mu(T)}{\gamma_w(T)} \qquad (1.6)$$

where, K, k, μ (T) and γ_w(T) are the intrinsic permeability, hydraulic conductivity, pore water viscosity and unit weight at the tested temperature, respectively.

According to test results, there is no important change in the unit weight of water with temperature if we compare it with viscosity. The value of free pure water viscosity changes with temperature (T) as the following equation,

$$\mu(T) = -0.00046575 \ln(T) + 0.00239138 \quad (1.7)$$

The variation of viscosity of water with temperature is the main reason for the change of hydraulic conductivity with temperature. The following equation estimates the ratio between the hydraulic conductivity at tested temperature k(T) and at ambient temperature $k(T_o)$ at certain soil porosity,

$$\frac{k(T)}{k(T_o)} = \frac{\mu(T_o)\gamma_w(T)}{\mu(T)\gamma_w(T_o)} \quad (1.8)$$

where μ(T) and μ(To) are the pore water viscosity at test and room temperature, respectively, and $\gamma_w(T)$ and $\gamma_w(T_o)$ are the pore water unit weight at test and room temperature, respectively.

B) Clay fabric

Changes in the void size due to the effect of temperature on the clay may contribute to the change in hydraulic conductivity with temperature. The potential redistribution of intra and inter particle pores with temperature changes may have an effect on hydraulic properties of soils (Bouazza et al., 2008). However, Morin and Silva (1984) and Delage et al. (2000) found that the effect of temperature on the soil matrix is insignificant for a wide range of temperature. The influence of the volume change of the soil matrix due to temperature is too small to be responsible for the change of the hydraulic conductivity at elevated temperatures (Abuel-Naga et al., 2005).

In fine grained soils, the progressive decrease in tightness of the clay-water link with increased clay water distance leads to a distinction between bound water and free water, and to analyze the effect of temperature on the water flow in clayey soils, the separation of viscosity effects from those related to clay-water interaction seems difficult (Delage et al., 2000).

C) Physico-chemical effect

The magnitude of physico-chemical interactions determines the size of the diffuse double layer which can have an important effect on the size of the flow channel, and thus hydraulic conductivity. The diffuse double layer thickness can be estimated as follows (as cited in Bouazza et al., 2008):

$$\vartheta = \sqrt{\frac{\varepsilon_O KRT}{2F^2 CV}} \quad \textbf{(1.9)}$$

where ε_O= 8.86 * 10^{-12} F/m (permittivity of vacuum), K is relative dielectric permittivity of the pore fluid, R= 8.314 J.mol-1.k (gas constant), T is temperature, F=9.68*10^4 C/mol (faraday constant), c is pore fluid concentration, and v is valence of the prevailing counter ion.

When the temperature increases, the value of the dielectric constant decreases, and there is little variation in the size of the diffuse double layer with temperature. At an elevated temperature, the adsorbed water may be converted into bulk pore water; a higher amount of bulk pore water may be generated due to this conversion leading to an increase of permeability due to an increase in flow channel volume (Cho et al., 1999, Delage et al., 2000). Towhata et al. (1993) concluded the same interpretation.

Shariatmadari and Saeidijam (2012) concluded similar interpretation about the soil permeability increases with high temperature, the volume of adsorbed water held to the soil particles inversely influences the permeability. The decrease in plastic limits with increased temperature is consistent with this analysis (Delage et al., 2000), as commented by Morin and Silva (1986). Derjaguin et al. (1986) indicated that the water adsorbed at the surface of clay particles changes its nature at around 70^{o} C to that of free water, and the increase of the amount and the cross section of free water in pores allow the water transfer through the clay to be easier. However, Morin and Silva (1984) and Delage et al. (2000) found that the effect of temperature on the thickness of the diffuse double layer is insignificant. According to the degree of binding of water to the soil matrix, the water varies from free or unbounded to strongly bound or adsorbed water. In detail, the free water is at distance from the soil particle surface and can flow under normal hydraulic gradient, but the adsorbed water is near the soil particle surface, called diffuse double layer.

1.3.3 Conclusion

This section indicated that the majority of researchers found that the permeability of clay soils increases with temperature increase while the intrinsic permeability is independent of temperature. The main reason for this positive relationship of permeability with temperature is the decreased viscosity with temperature increase. It is observed that the soil porosity and fabric variation with temperature is negligible. Howerer, the physico-chemical interactions could contribute to the permeability change with temperature.

1.4 Effect of temperature on the short term consolidation behaviour of clay soils

The current section discusses the influence of temperature on the soil volume and the short term consolidation characteristics including preconsolidation pressure, compression index (C_c), swelling index (C_s), coefficient of volume compressibility (m_v), coefficient of consolidation (C_v), and permeability (k) measurement using indirect method.

1.4.1 Volume change due to temperature

Many researchers studied the effect of temperature on the volume change of soil upon heating/ cooling cycles at different stress history (Abuel-Naga et al., 2005). The samples of tests varied from normally consolidated state to over-consolidated state under drained and undrained methods.

A) Normally consolidated clay

Thermo-mechanical tests with temperature variation up to 90^0 C were carried out by Towhata et al. (1993) to analyze the effect of high temperature on the volume change of MC clay and bentonite. They found that the normally consolidated clays had a volume contraction at elevated temperature for both MC clay and bentonite (Figure 1.9), and the volume contraction of bentonite is greater than that of MC clay under the same pressure. They suggested that the contraction caused by heating may be due to the clay particles deterioration, and the volume change may increase with the plasticity of clay.

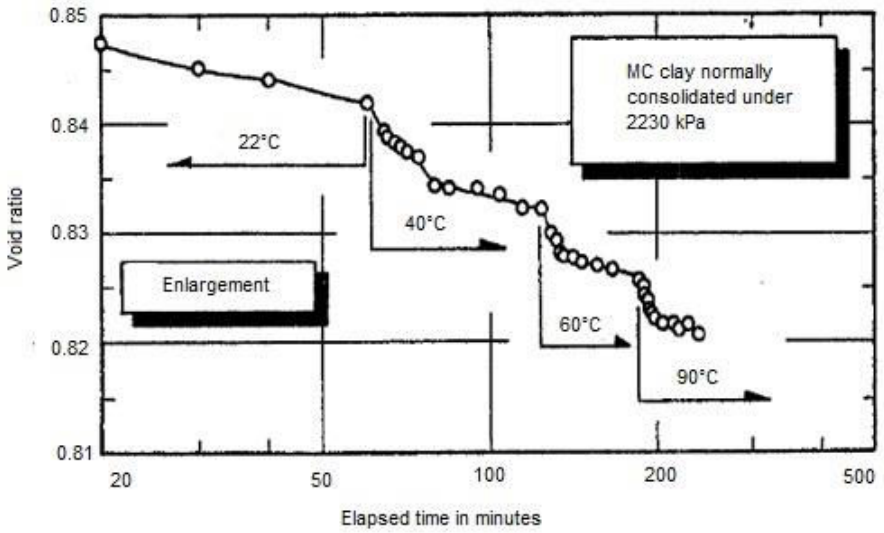

Figure 1.9 Thermally induced volume change of normally consolidated MC clay under 2230 kPa stress.

According to Cekerevac and Laloui (2004), normally consolidated samples of Kaolin clay showed contraction upon heating. They performed drained tests under various thermo-mechanical loading paths with temperature range of 22 to 90^0 C using modified triaxial equipment. Plastic contraction at high temperature (50-60,60-70,70-80, and 80-95^0 C) was observed by Delage et al. (2004) when they conducted triaxial tests on normally consolidated host clay from Belgium (Boom clay). They indicated that expulsion of water caused this thermal contraction, and this behaviour is similar to the standard consolidation. They reported that plastic volumetric strains as a result of contraction had a hardening influence on the soil,

and this plastic contraction is independent of the applied mean effective stress. The same results were already obtained by Sultan et al. (2002).

Abuel-Naga et al. (2005) performed drained modified oedometer tests with different temperatures up to 90^0 C, and different stress conditions to study the thermo-mechanical behaviour of soft Bangkok clay. They found that the normally consolidated samples have nonlinear irreversible contraction, while these samples behaved as over-consolidation state after subjecting to the drained heating/cooling cycle (25-90-25^0 C), and this behaviour depends on the cyclic temperature. They pointed out that the thermally induced volume change is not affected by stress level. The same conclusion is reported by Abuel-Naga et al. (2007a). Using the modified oedometer for drained heating tests, and triaxial for undrained heating tests at different temperatures and different stresses, Abuel-Naga et al. (2007b) found the same results. They mentioned that the induced pore water pressure of normally consolidated samples by temperature is reversible (Figure 1.10). The reversed pore pressure contributes to the irreversible volume deformation of the sample.

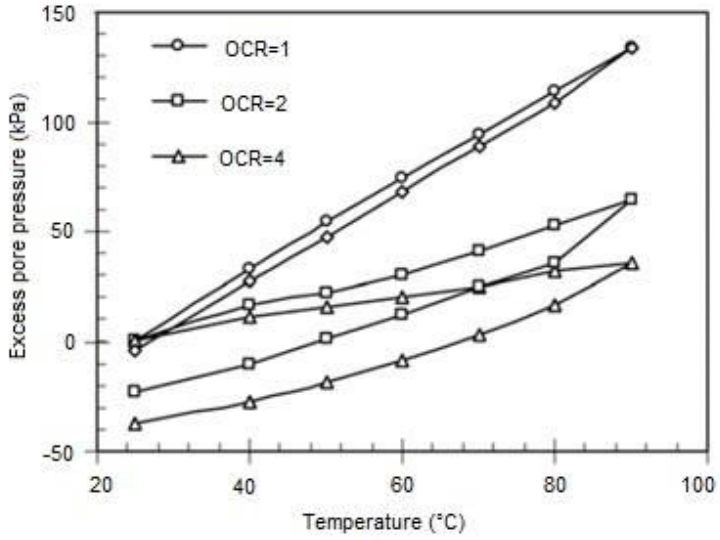

Figure 1.10 Variation of induced pore water pressure at different OCR with temperature.

A reduction in the volume was observed by Shariatmadari and Saeidijam (2011) when they elevated the temperature of compacted bentonite-sand mixture (1:1) sample (PI= 255%) from 25 to 90°C in an oedometer cell. Also, they indicated that the required time for stabilization is less in high temperature because of permeability increase (Figure 1.11). They suggested that this behaviour is related to the effect of temperature on diffuse double layer state (DDL in Eq. 1.9).

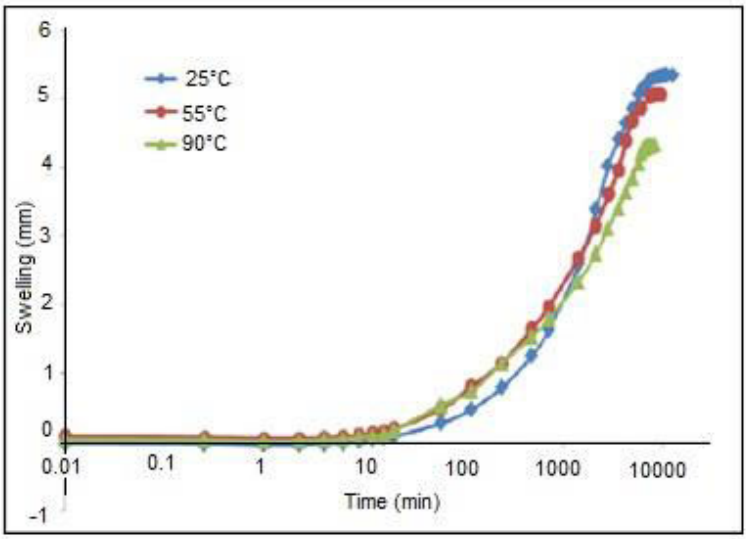

Figure 1.11 The swelling (volume change) of sample at different temperatures in oedometer under 15 kPa (from Shariatmadari and Saeidijam, 2011).

B) Over-consolidated clay

Towhata et al. (1993) also studied the effect of temperature on the over-consolidated samples by firstly unloading the stress level from 2230 kPa to a certain level of pressure between 40 and 1280 kPa, given OCR values from 1.7 to 56. They found expansion behaviour for the lightly over-consolidated samples (OCR=1.7) until 90^0 C, but the contraction behaviour began at 90^0 C. The contraction is attributed to the thermal deterioration of clay skeleton upon heating, while expansion is attributed to the thermal expansion of the pore water that caused swelling of the soil skeleton, and this swelling is related to a decrease in effective stress. For highly over-consolidated samples, they observed volume expansion after heating, and this magnitude increased with OCR increase. Cekerevac and Laloui (2004) loaded and unloaded Kaolin clay specimens to different over-consolidation ratio values (1, 1.2, 1.5, 2, 3, 6, and 12) for drained heating test. They found that the lightly over-consolidated samples (OCR=1.5, and 2) had a thermal contraction behaviour but it is less than the normally consolidated samples, while the highly over-consolidated samples (OCR=12) had a thermal expansion (Figure 1.12). They reported that as the OCR increases, the expansion behaviour increases, or the stress history (OCR) influences the thermal volumetric strain (Figure 1.13). In addition, OCR values at which thermal volumetric strain occurs depend on the soil type.

Abuel-Naga et al. (2005) observed that the over-consolidation ratio (OCR) values influence the thermally induced volumetric strain at various levels of temperature. This means that the volumetric strain converted from contraction behaviour to expansion behaviour after certain OCR values, since the soil changed from the normally consolidated state to the over-consolidated state at a specific temperature value.

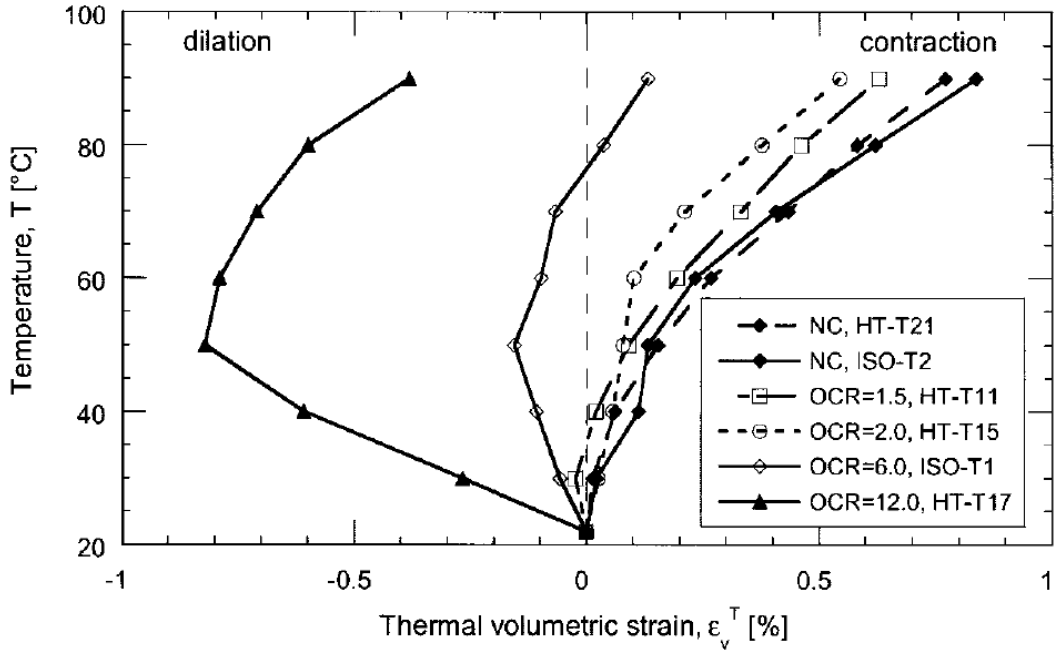

Figure 1.12 Thermal volumetric strain of kaoline Vs. temperature (from Cekerevac and Laloui, 2004).

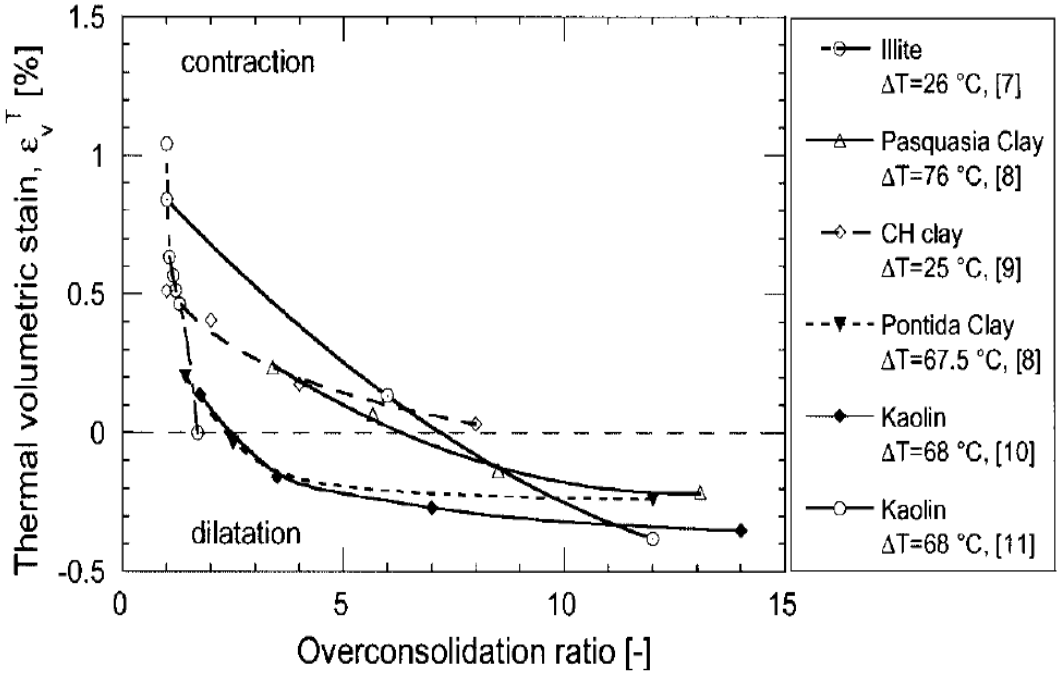

Figure 1.13 Over-consolidation ratio Vs. thermal volumetric strain (from Cekerevac and Laloui, 2004).

C) Interpretation

The physico-chemical changes, soil plasticity and percentage of fines are the main factors that cause the thermo-mechanical behaviour of saturated fine-grained soils, under temperature less than the pore liquid boiling point. The intensity of the thermally induced changes can be determined by the above mentioned factors together. The intensity of the physico-chemical

interactions upon heating can be affected by the soil placticity index, and this index may influence quantitatively the thermally induced volumetric strain (Abuel-Naga et al., 2005).

The intensity of thermally induced volume change of saturated clays depends on the clay mineralogy and the pore fluid chemistry that influence the thermal behaviour of interparticle physico-chemical forces. When the temperature increases by an increment ΔT, the thermal expansion of a volume of pore water ΔV_w , and a volume of soil skeleton ΔV_s equal respectively (As cited in Delage et al., 2000):

$$\Delta V_w = \alpha_w V_w \Delta T \quad \textbf{(1.10)}$$

$$\Delta V_s = \alpha_s V_s \Delta T \quad \textbf{(1.11)}$$

where α_w, and α_s are the thermal expansion coefficient of free water and the thermal expansion coefficient of the solid skeleton respectively.

During a drained heating test, the volumetric strain ε_v is obtained by the following equation (as cited in Delage et al., 2000),

$$\varepsilon_v = \left[\frac{\Delta V_{dr} - (\alpha_w V_w + \alpha_s V_s)\Delta T}{V}\right] \quad \textbf{(1.12)}$$

where, ΔV_{dr} is the total volume of drained water.

In low porosity plastic clays, the adsorbed water is at a distance from the clay platelet, and the vertical pressure on the adsorbed water decreases when the distance increases. The volumetric strain of this type of clay can be observed by the following equation (as cited in Delage et al., 2000),

$$\varepsilon_v = \left[\frac{\Delta V_{dr} - (V\Delta V_a S_S \rho_d + \alpha_s V_s)\Delta T}{V}\right] \quad \textbf{(1.13)}$$

where ΔV_a is the volume of expanded adsorbed water per unit surface of clay mineral and per °C, S_s is the specific surface of the clay and ρ_d the dry unit weight of the soil.

During temperature increase, the interparticle viscous shear resistance of the adsorbed water decreases since the interparticle spacing between particles increases. This movement can be considered as a decrease in viscosity of the adsorbed water layer. The temperature decreases the clay resistance to fabric change and consequently the preconsolidation pressure (Abuel-Naga et al., 2007b).

Inside the elastic limit zone, the mechanical consolidation behaviour generates only reversible volume change because the applied effective stress is less than the clay particles resistance to fabric change which is affected by clay mineralogy, pore water chemistry, and environmental conditions such as temperature (Abuel-Naga et al., 2007b).

d) Conclusion

It is observed that the temperature effect on the volume of clayey soils depends on the mechanical consolidation state of clay. Normally consolidated samples have irreversible contraction under heating, while over-consolidated samples have expansion behaviour under heating.

1.4.2 Conclusion

The influence of temperature on the free swelling parameters and the short-term consolidation characteristics of clayey soils were discussed in this section. It is observed that the preconsolidation pressure decreases with temperature increase. The compression and swelling indices and the coefficient of volume compressibility variations with temperature could be considered negligible. The coefficient of consolidation and permeability increase with temperature increase. In addition, the normally consolidated clay soils contract upon heating, while the over-consolidated samples expand upon heating.

1.4.3 Effect of temperature on the preconsolidation pressure

The preconsolidation pressure is considered as the pseudo-elastic limit which separates ‘‘elastic’’ pre-yield from ‘‘plastic’’ post-yield behaviour in isotropic or oedometric conditions (controls the size of the yield limit) under different temperatures (Laloui and Cekerevac, 2003, 2004, Shariatmadari and Saeidijam, 2012).

Many experimental works had been done by different researchers to study the effect of temperature on the preconsolidation pressure of clays, and the majority of them found that preconsolidation pressure decreases with increase of temperature (Sultan et al., 2002; Marques et al., 2004; Cui et al., 2009; Masin et al., 2011; Hong et al., 2013). Table 1.3 shows the different researchers’ results of the temperature effects on the preconsolidation pressure.

Moritz (1995) conducted CRS (constant rate of strain) oedometer tests with a temperature range between 20 and 70^{o} C on Swedish clay which was extracted from 6m (homogeneous, liquid limit between 81-87 %) and 9m (sulphide stains, liquid limit between 77-85 %) of depth, and he indicated a decrease of preconsolidation pressure with temperature rise (Figure 1.14).

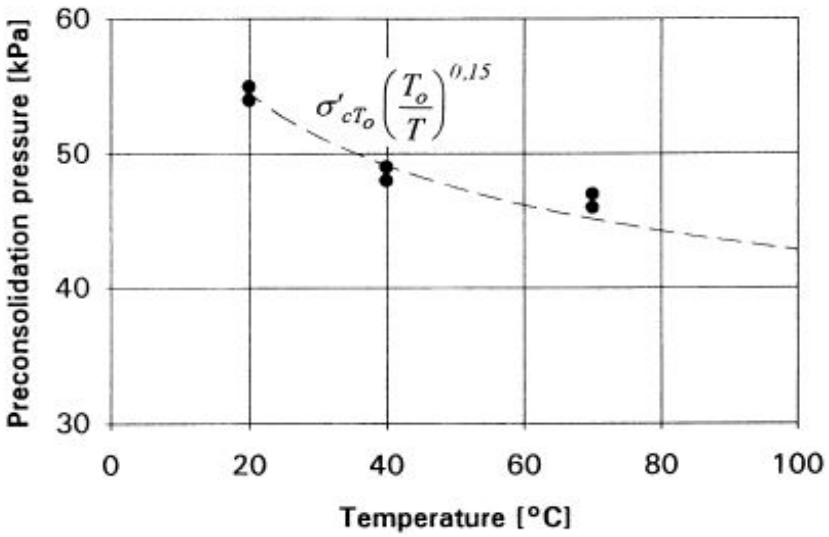

Figure 1.14 Effect of temperature on preconsolidation pressure for tests from 6m (From Moritz, 1995).

From isotropic cell tests carried out on four saturated boom clay samples, Sultan et al. (2002) mentioned an exponential variation of the preconsolidation pressure with temperature. When temperature decreases, preconsolidation pressure increases (Figure 1.15).

Laloui and Cekerevac (2003, 2004) performed an experimental study on saturated remoulded Kaolin (CM clay) to analyze the thermal effect on preconsolidation pressure using a thermomechanical triaxial cell with three different temperatures (22-60-90^{o} C). They found that when temperature increases, preconsolidation pressure decreases by an average of 4 kPa/10°C.

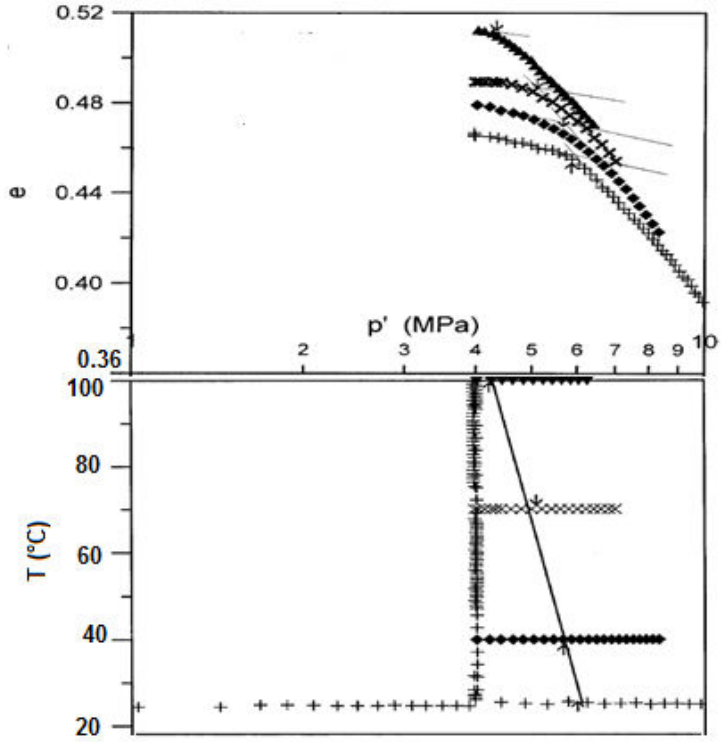

Figure 1.15 Preconsolidation Vs. temperature (From Sultan et al., 2002).

On the other hand, Abuel-Naga et al. (2007b) indicated that the preconsolidation pressure was independent of temperature after modified oedometer tests on saturated soft Bangkok clay with temperature up to 90^{o} c. Abuel-Naga et al. (2005) performed modified oedometer tests on saturated soft Bangkok clay with temperature up to 90^{o} C, and they pointed out negative non-linear relationship of preconsolidation pressure with temperature.

The thermo-mechanical preconsolidation stress depends on both mechanical volumetric plastic strain and thermal volumetric irreversible strain. The nature of the thermal volume change behaviour (See section 1.4.1) influences the value of the preconsolidation pressure (Cekerevac & Laloui, 2004). However, the reduction of the elastic limit with increase in temperature related to the induced thermal effect on preconsolidation pressure (Cekerevac & Laloui, 2004). The following equations represent linear and nonlinear relationship between preconsolidation pressure and temperature respectively (Abuel-Naga et al., 2005):

$$\frac{\sigma'_c(T)}{\sigma'_c(T_o)} = \left[\frac{T_O}{T}\right]^{\alpha} \quad \textbf{(1.14)}$$

$$\frac{\sigma'_c(T)}{\sigma'_c(T_o)} = 1 - \gamma\left[\log\frac{T}{T_o}\right] \quad \textbf{(1.15)}$$

where $\sigma'_c(T_o)$ and $\sigma'_c(T)$ are the preconsolidation pressures at 20° C and tested temperature, respectively, α and γ are the model parameters which depend on the soil type.

The soil parameters in this model depend on the thermally induced volumetric change which was discussed in section 1.4.1.

Table 1.3 Temperature effects on the preconsolidation pressure.

No.	Author	Soil	Soil characteristics	Method	T	P_c Variation with T
1	Moritz (1995)	Swedish clay	From 6m: LL=81-87 %, homogeneous From 9m:LL=77-85 % sulphide stains	Triaxial and CRS tests	20 to 70^{0} C	Decrease
2	Sultan et al. (2002)	Saturated boom clay	Stiff clay PI = 50%	Isotropic cell	20 to 100^{0} C	Decrease (exponential change)
3	Laloui & Cekerevac (2003, 2004)	Remoulded Kaolin (CM clay)	LL = 45% PI = 24% %<2 mm = 45	Triaxial cell	22-60-90^{o} C	Decrease
4	Abuel-Naga et al. (2005)	Natural soft Bangkok	LL=103%, PI=60%, Clay=69%,silt=	Modified oedometer	25 to 90^{0} C	Decrease (non linear) Increase after subjecting to heating cooling cycle

		clay	28%, sand=3%			
5	Tang et al. (2007)	MX80 clay	Unsaturated compacted LL = 520% PI = 474%	Triaxial cell	20 & 60^0 C	Decrease from 1.9 MPa to 0.8 MPa
6	François et al. (2007)	Remoulded unsaturated sandy silt	Clay fraction = 8% Silty fraction = 72% PI = 8.7%	Isotropic cell oedometric cell	22 to 800 C	Decrease
7	Abuel-Naga et al. (2007b)	Saturated natural soft Bangkok clay	LL=103%, PI=60%, clay=69%,silt=28%, sand=3%	Modified oedometer	25 to 90^0 C	Independent

It can be concluded that the preconsolidation pressure decreases with the increase of temperature based on the experimental results.

1.4.4 Effect of temperature on the compressibility parameters

The effect of temperature on the compressibility parameters including compression index (C_c), swelling index (C_s), coefficient of volume compressibility (m_v), and coefficient of consolidation (c_v) have been studied by several researchers. Understanding the effects of temperature changes on the strength and compressibility of soils is important. Some researchers reported that the compressibility changes with temperature (Tanaka et al., 1997). Table 1.4 shows the obtained results of the temperature effects on the consolidation characteristics and others,

Table 1.4 Temperature effects on the consolidation characteristics.

No.	Author	Soil	Soil characteristics	Method	Temperature	variation with T
1	Campanella & Mitchell (1968)	Illite	Remolded Saturated	Drained isotropic cell	24.7, 37.8, 51.4^0 C	C_c is independent
2	Lingnau et al. (1996)	1:1 Mixture bentonite-sand	Compacted Saturated LL=230-250% PI=200%	High pressure and temperature cell/drained	26, 65, and 100^0 C	C_s & C_c are independent
3	Tanaka et al. (1997)	Illitic clays	Reconstituted Saturated LL=30% PI=9%	Drained isotropic cell	28, 65, 100^0 C	Non parallel normally consolidated lines
4	Delage et al. (2000, 2004)	Boom clay	PI=50%, Porosity=40%, Stiff clay, saturated	Drained triaxial	Between 20 and 100° C	C_v & m_v not affected significantly
5	Sultan et al. (2002)	Boom clay	PI=50%, Porosity=40%, Stiff clay, saturated	Drained isotropic cell	23, 40, 70, and 100^0 C	Compression curves converged towards the same limit.
6	Cekerevac &	Kaolin clay	Remoulded	Drained	22, 90° C	C_c is independent

	Laloui (2004) Laloui &Cekerevac (2003)		Saturated LL=40% , PL=24%	triaxial apparatus		
7	Marques et al. (2004)	Sensitive clay from Quebec	Saturated PI= 41 to 49%	Drained oedometer test	between 10 and 50° C	The slope of the compression curve in the over-consolidated domain is not strongly affected
8	Abuel-Naga et al. (2005)	Bangkok clay	Natural, soft, -LL=103%, PI=60%, Clay=69%,silt=28%, sand=3%	Drained modified oedometer	25 to 90° C to 25° C	C_v increases positively
9	François et al. (2007)	Sandy silt	Remoulded Unsaturated Clay fraction = 8% Silty fraction = 72% PI = 8.7%	Isotropic cell Oedometric cell	Between 22 to 80° C.	Compressibility indices are quasi-independent of temperature.
10	Abuel-Naga et al. (2007a)	Bangkok clay	Saturated, natural soft Over-consolidated LL=103%, PI=60%, Clay=69%,silt=28%, sand=3%	Modified oedometer	25 to 90° C	Cc is independent Cs in the lightly over-consolidated samples is increased positively
11	Tang et al. (2008a)	MX80 bentonite	Compacted, unsaturated LL=520% PL=46%	Triaxial apparatus	25 to 80° C	The effect on the compressibility parameters was not significant
12	Cui et al. (2009)	Boom clay	Saturated LL = 59-76% PL=22-26% PI = 37-50%	Drained triaxial tests	25 °C and 70-80 °C	Volumetric strain rate coefficient increased with elevated temperature
13	Shariatmadari & Saeidijam (2011,2012)	Bentonite-sand mixture (1:1)	Compacted, saturated LL = 290% PI = 255%	Drained oedometer	25 to 90°C	a_v and C_c increased at elevated temperature
14	Tsutsumi & Tanaka (2012)	Kasaoka OsakaMa12 Louiseville	LL=62%, PL=36% LL=109%, PL=43% LL=71%, PL=22% Reconstituted, saturated	Drained CRS tests	10 and 50° C	C_s was independent of temperature C_c at 50° C was smaller than that at 100° C.

By using triaxial apparatus, Campanella & Mitchell (1968) found that C_c is independent from temperature after drained isotropic consolidation experiments at different temperatures (24.7, 37.8, 51.4^0 C) on three saturated remolded illite samples. The samples were heated then were loaded (Figure 1.16). Different results were obtained by Tanaka et al. (1997) which showed non parallel normally consolidated lines for the reconstituted illitic clays.

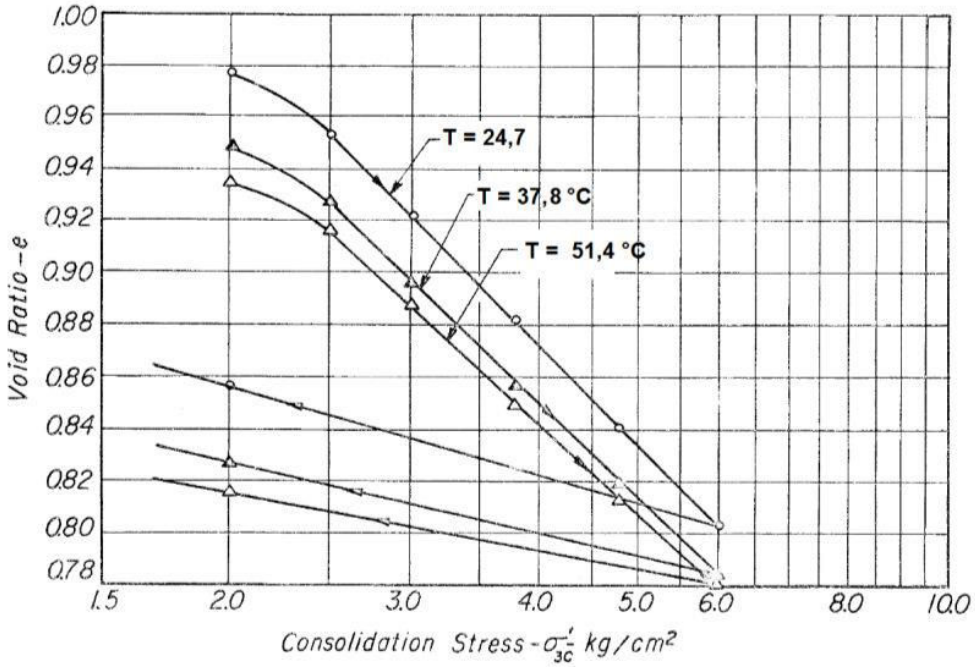

Figure 1.16 consolidation stress Vs. Temperature (from Campanella & Mitchell, 1968).

Delage et al. (2000, 2004) conducted an isotropic compression cell tests with high temperatures on a slightly over-consolidated sample of Boom clay and concluded that the change of c_v and m_v with temperature higher than 60^0 C is not important. Figure 1.17 shows the variation of coefficient of consolidation with temperature (Delage et al., 2000).

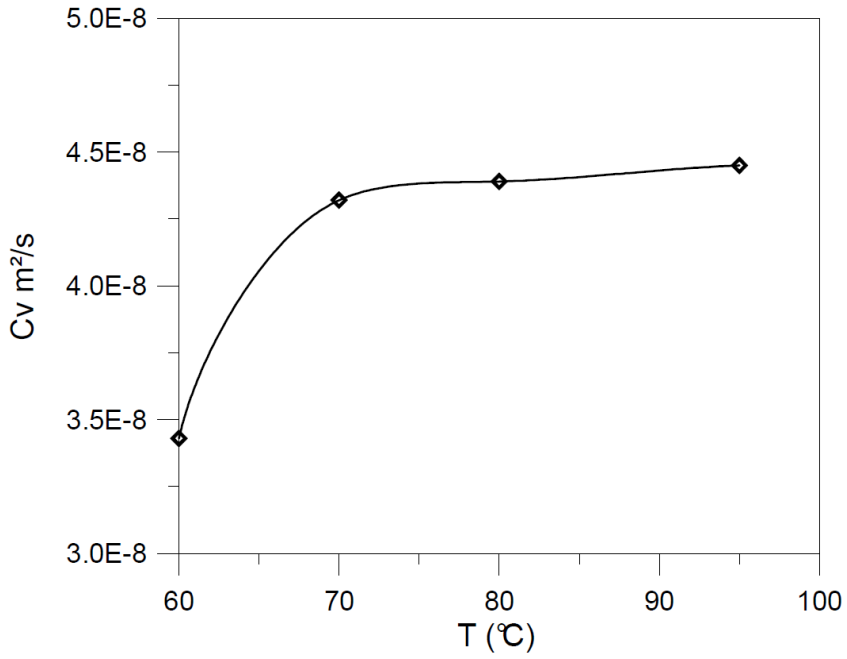

Figure 1.17 Coefficient of consolidation variation with temperature (from Delage et al., 2000).

A comparison between the normal consolidation lines (NCL) of remoulded Kaolin clay at ambient (22^0 C) and high 90^0 C temperatures have been done by Cekerevac & Laloui (2004)

using triaxial apparatus under isotropic pressure. They found that the lines for the two tested temperatures are parallel, and therefore the slopes (C_c) of these lines are also independent of temperature (C_c=0.24 at 22^0 C and C_c=0.23 at 90^0 C). This result is consistent with Laloui & Cekerevac (2003).

After an oedometric experimental study that has been done by Marques et al. (2004) to study the effect of temperature between 10° C and 50^0 C on sensitive clay from Quebec, the results showed that the slope of the compression curve in the over-consolidated domain is affected by the temperature through the test temperature. Ochiai et al. (2005) found that the C_c and C_s of saturated soft Bangkok clay are independent of temperature.

Results of the iso-thermal oedometric experimental program at different temperatures obtained by Abuel-Naga et al. (2005) indicated that the consolidation rate (C_v) of normally consolidated soft Bangkok clay increases with temperature increase. Abuel-Naga et al. (2007a) carried out isothermal consolidation tests on over-consolidated soft Bangkok clay samples at different values of temperature through oedometer apparatus. They observed approximately similar slope (C_c) of compression lines, but the slope of the elastic line (C_s) in the lightly over-consolidated samples increased with temperature as shown in Figure 1.18. These results are consistent with Abuel-Naga et al. (2013).

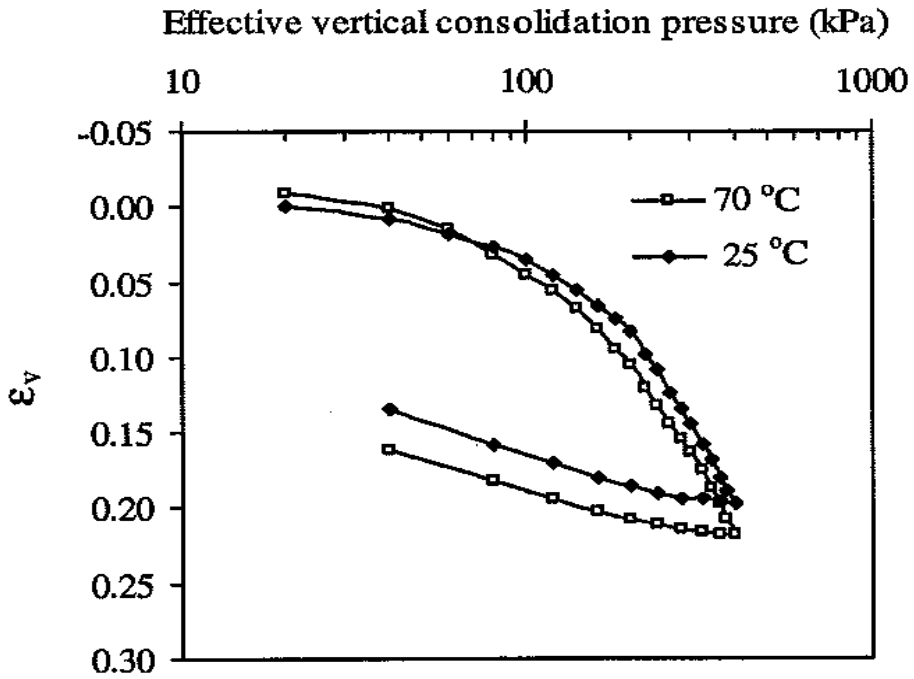

Figure 1.18 Effective vertical stress Vs. vertical strain under different constant temperature (from Abuel-Naga et al., 2005).

On the other hand, Shariatmadari & Saeidijam (2011) examined the effect of elevated temperature on the compressibility of bentonite-sand mixtures (1:1) in oedometer apparatus. They observed that the slopes of consolidation curves (a_v) increased at elevated temperatures (Figure 1.19). When temperature increases, the compression index (C_c) and its quantity increases, since the void ratio at elevated temperature is less.

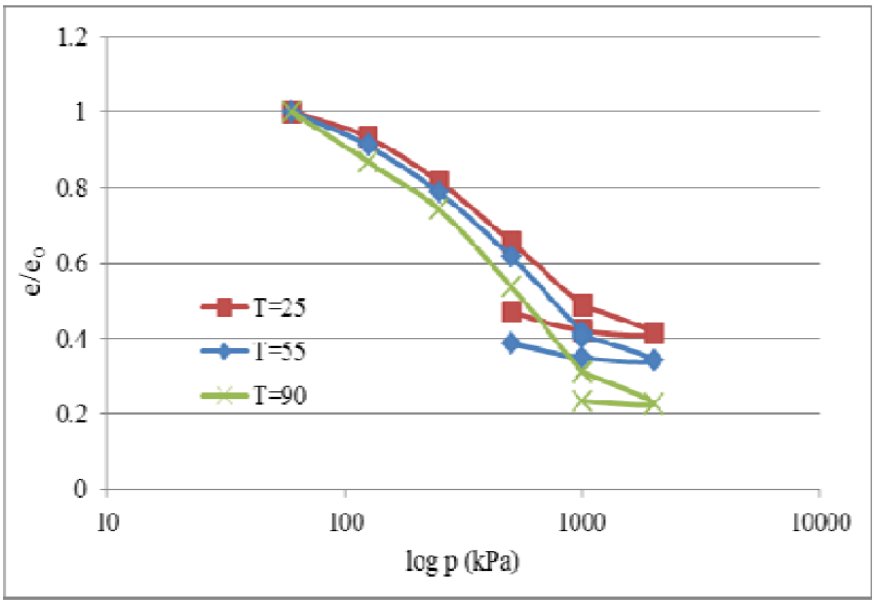

Figure 1.19 Void ratio Vs. compressive stress at different temperatures (from Shariatmadari & Saeidijam, 2011).

According to constant rate of strain tests which were performed by Tsutsumi & Tanaka (2012) on three reconstituted clay samples (Kasaoka, OsakaMa12, and Louiseville) at temperatures of 10^0 C and 50^0 C, the C_c of normally consolidated state at 50^0 C (slope of e-log p curve) was smaller than that at 10^0 C, while they considered that C_s was independent of temperature. Figure 1.20 shows that values of C_c and C_s are identical at different temperatures (Tang et al., 2007).

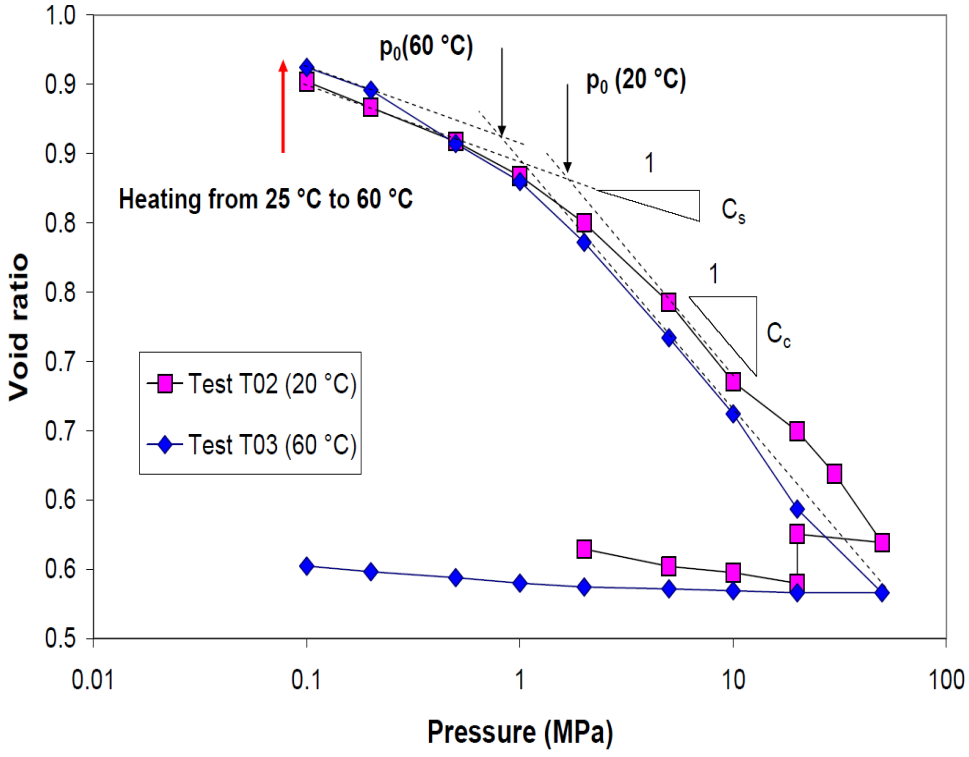

Figure 1.20 Void ratio Vs. pressure at different temperature (from Tang et al., 2007).

The effect of temperature on the compressibility parameters has been studied using isothermal oedometer and isotropic triaxial tests performed at different temperatures. Based on the obtained results, the variation of compression and swelling indices with temperature seems to be negligible. The hydraulic conductivity increases with temperature increase, while the intrinsic permeability could be considered independent of temperature. In fact, the reduced viscosity with temperature increase leads to an increase in the hydraulic conductivity, while the clay fabric is not affected by temperature variation which leads to non changed intrinsic permeability at different temperatures. In addition, the coefficient of consolidation increases with temperature increase since it is a function of the hydraulic conductivity, while the coefficient of volume compressibility variation with temperature is negligible.

1.4.5 Effect of temperature on the permeability (Indirect method)

The indirect method employs the measured parameters obtained from isothermal consolidation tests performed at various temperature levels.

Towhata et al (1993) derived permeability values at different temperatures between 20 and 90°C from the curves of isothermal consolidation tests on bentonite (PI= 421%) and MC clays (PI= 29%) in a rigid ring oedometer as the following equation,

$$k = m_v \gamma_w c_v \qquad (1.16)$$

where γ_w is the unit weight of water, mv is the coefficient of volume compressibility, c_v is the coefficient of consolidation.

They observed that permeability increased with temperature increase due to reduction in viscosity of water. This result is consistent with Abuel-Naga et al. (2005) who used the same method on the soft Bangkok clay (PI= 60%) (Figure 1.21).

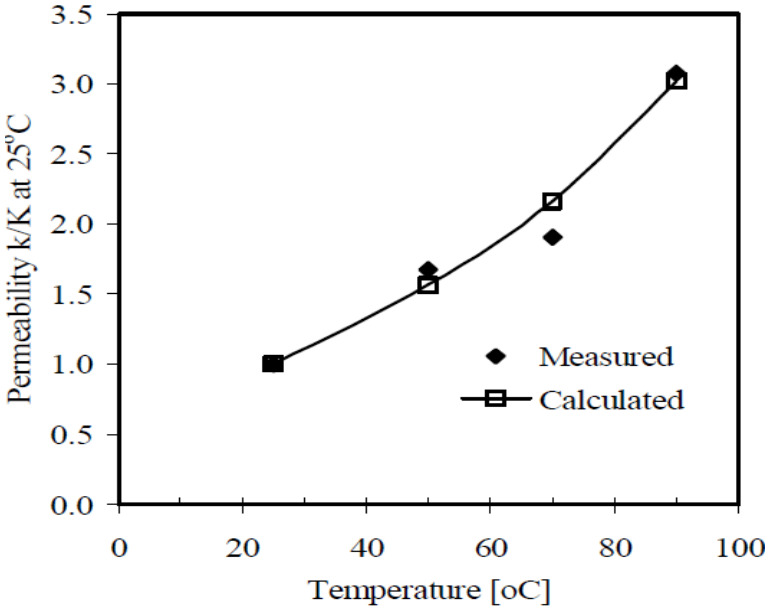

Figure 1.21 Permeability variation with temperature (from Abuel-Naga et al., 2005).

Most of the experimental results based on the indirect method of measuring permeability at different temperatures indicated that the permeability increases with temperature increase. The main reason for permeability increase with temperature is the reduction in the water viscosity at higher temperature.

1.5 Creep in clayey soils

1.5.1 Introduction

The classical theory of one-dimensional consolidation that has been introduced by Terzaghi (1925) considers a unique relationship between effective stress and strain and it is independent of time. After Terzaghi's works, Buisman (1936) noted a continuous deformation of clay during consolidation tests for long time after the dissipation of pore pressure, and this deformation can be represented linearly in semi-logarithmic scale with time (Suhonen, 2010; Jain and Nanda, 2010). The consolidation process is divided into primary and secondary consolidation as shown in Figure 1.22. The primary consolidation is defined as the decrease in the volume with effective stress increase due to pore pressure dissipation. The secondary consolidation or creep is defined as the decrease in volume under constant effective stress due

to continued re-adjustment of clay particles (Das, 2008). The two parameters can be defined as following:

- Primary consolidation : $\Delta e = -c_c \log\sigma'$
- Secondary consolidation: $\Delta e = - c_\alpha \log t$

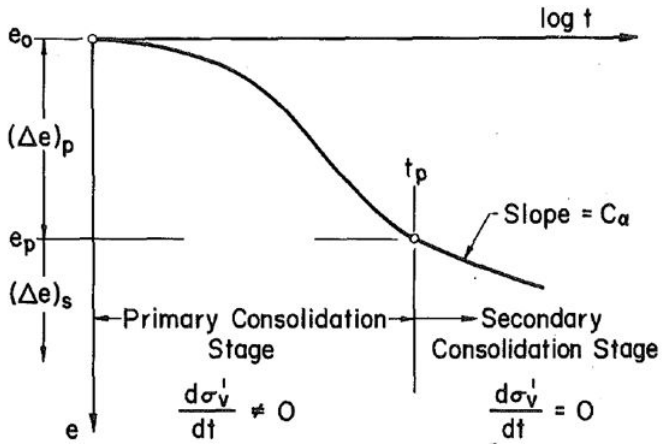

Figure 1.22 Void ratio-logarithm of time relationship showing primary and secondary consolidation behaviour (Gray, 1936).

According to Mesri (1973), the plastic clays and organic soils have greater secondary compression, and he classified the secondary compression in general based on creep index as shown in Table 1.5 (Jain and Atul, 2010). In reality, the clay behaviour is strongly dependent on time (Verruijt, 2012), and the main question would be if creep starts during primary consolidation or after the dissipation of pore pressure.

Table 1.5 Classification of secondary consolidation of clay (Mesri, 1973).

C_α	*Secondary compressibility*
< 0.002	very low
0.002–0.004	low
0.004–0.008	medium
0.008–0.016	high
0.016–0.032	very high

According to the experimental works, the settlement-log time curves are classified into three types called type I, II, and III as shown in Figure 1.23 (Green, 1969 ; Jain and atul, 2010). Type 1 of the curves shows a well defied primary and secondary consolidation curve where the secondary compression represents a straight line after the primary consolidation. These types of curves are a result of subjecting the soil to large pressure increment ratio. Curve III shows acceleration in the rate of secondary consolidation, and it is a result of applying small

load increment ratios to the soil. Curve II is caused by intermediate load increment ratio, and it shows a transition curve that has a behaviour between types I and III (Green, 1969 ; Jain and atul, 2010).

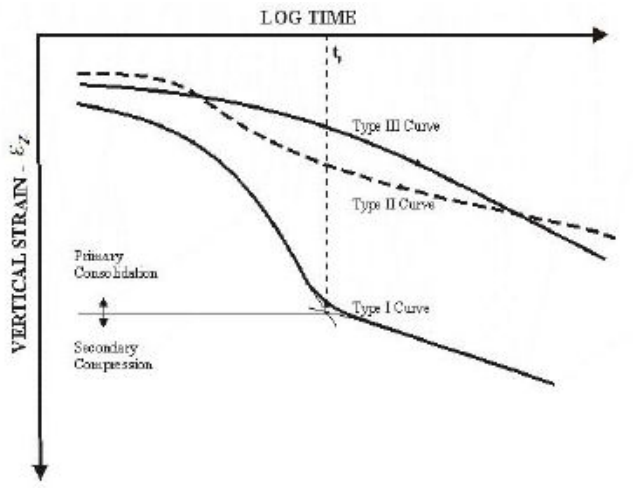

Figure 1.23 Settlement variation with log time resulting from oedometer tests on a saturated clay (from Ladd & Preston 1965).

As it was mentioned before, the main area of debate has been whether creep is significant during primary consolidation. Ladd et al. (1977) presented two different hypotheses, called A and B. It is used as a basic to discuss the creep phenomenon during short time in the laboratory tests and long term in the field. Hypothesis A suggests that creep occurs only after the end of primary consolidation which means after the pore pressure dissipation and hence, the settlement-time curve does not depend on the duration of consolidation. Hypothesis B suggests that creep occurs at least partly during primary consolidation because of a structural viscosity and hence, the settlement-time curve of thick samples coincides with the thin samples settlement-time curve in the secondary consolidation stage since it depends on the duration of consolidation. As shown in Figure 1.24(a), hypothesis A shows a unique end of primary (EOP) strain that is different from hypothesis B. In hypothesis A, the end of primary (EOP) strain of thin and thick samples are equal and this indicates that the end of primary (EOP) strain is independent of primary consolidation duration. On the contrary, hypothesis B indicates that end of primary (EOP) strain is primary consolidation duration dependent, so the end of primary (EOP) strain of thick sample is larger than the EOP strain of thin sample.

Many experimental works studied the creep effects during consolidation process, and there is no agreement between researchers. Mesri et al. (1995) and Aboshi (1973) supported hypothesis A according to their experimental data. Conversely, Taylor (1942), Brinch Hansen

(1969), Barden (1969), and Degago (2011) supported hypothesis B which is based on Suklje's isotaches (1957).

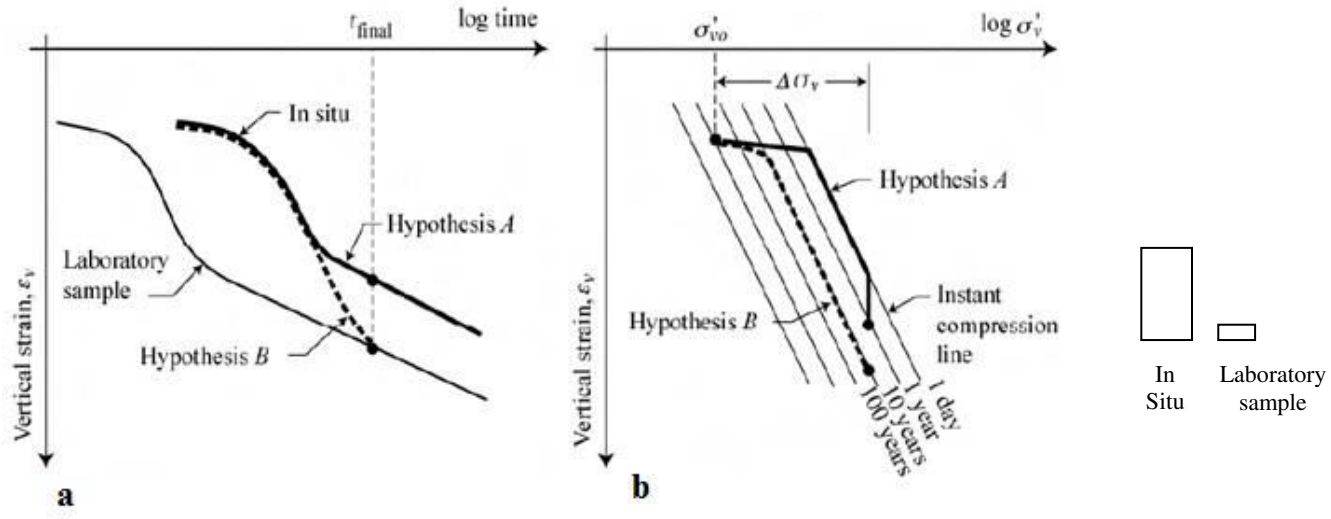

Figure 1.24 Hypotheses A and B for consolidation of clay layers at different thicknesses (after Ladd et al., 1977).

Leroueil (1996) reinterpreted the compression curves of consolidation tests which were performed on Saint-Hilaire clay by Mesri et al. (1995) as shown in Figure 1.25. The figure shows two components of drawings.

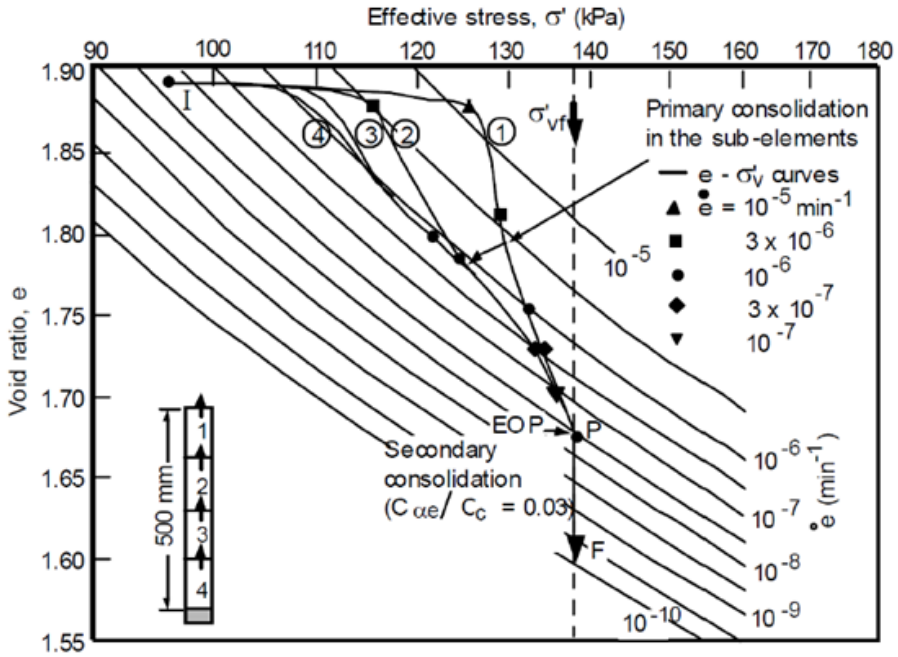

Figure 1.25 Special one-dimensional consolidation test carried out by Mesri et al. (1995) on Saint Hilaire clay and reinterpreted by Leroueil (1996) (from Leroueil, 2006).

Firstly, the primary consolidation is represented by the line starting from the initial condition (I) to the EOP consolidation (point P). During primary consolidation, the compression curve

behaviour depends on the location of the sub-specimens in the sample. The strain rate is the highest value near the drainage boundary (sub-specimen 1) during the early stages of consolidation because of rapid dissipation of excess pore pressure. Thus, the vertical effective stress near the drainage boundary reached the isotaches with highest strain rate. For sub-specimens 3 and 4 (far from the drainage boundary), the strain rates are much smaller during the same period and the effective stress reached the isotaches with lower strain rates. The compression curves of the sub specimens converge when the soil close to the EOP consolidation (point P). Secondly, the stage of secondary consolidation starts after the EOP consolidation, and the sample settlement increases from P to F. A similar behaviour was observed by Imai and Tang (1992) who investigated the consolidation behaviour of clay with 7 sub-specimens connected in series.

Leroueil et al. (1985) investigated the rheological behaviour of clay using constant rate of strain (CRS) consolidation tests in order to observe the time or strain rate effect. The results of these tests are presented in Figure 1.26.

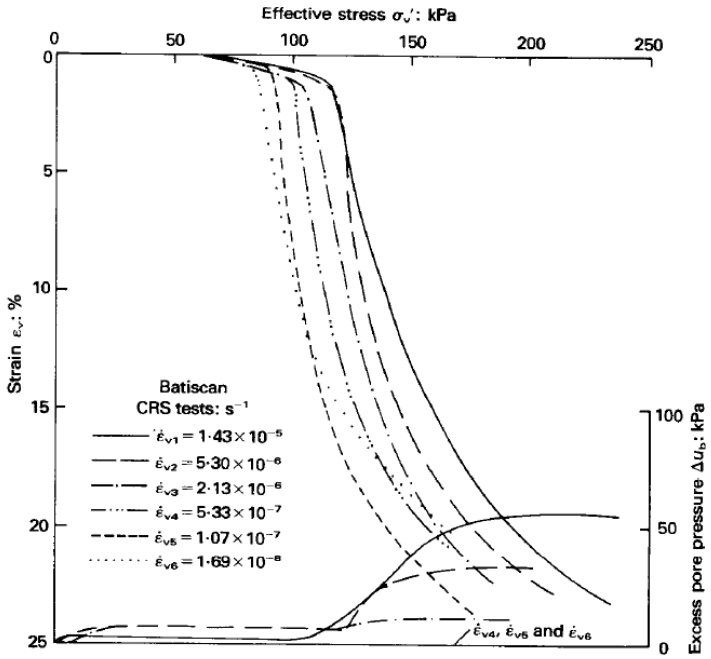

Figure 1.26 CRS tests on the Batiscan clay (from Leroueil et al., 1985).

It is concluded that 1) at a given effective stress, the higher the strain rate, the lower the strain or, under a given strain, the lower the strain rate, the lower the effective stress, 2) the lower the strain rate, the lower the excess pore pressure at the base of the sample, and it is extremely small for strain rates lower than 5.33 x 10^{-7}/s, 3) The compression curve of lower strain rate (1.7 x 10^{-7}/s) intersects the other curves due to cementation.

Many researchers (e.g. Sällfors, 1975; Adachi et al. 1982) observed the same behaviour of clay using constant rate of strain (CRS) tests. The results indicated that the rheological behaviour of clay can be described by a combination of effective stress, strain, and strain rate (σ', ε, $\dot{\varepsilon}$). A unique stress-strain-strain rate relationship which controls the clay behaviour under one dimensional compression can be described by two curves that include the variation of preconsolidation pressure with strain rate, and the normalized stress strain relationship (Leroueil et al, 1985),

$$\sigma'_p = f(\dot{\varepsilon}) \quad \textbf{(1.17)}$$

$$\sigma' / \sigma'_p(\dot{\varepsilon}) = g(\dot{\varepsilon}) \quad \textbf{(1.18)}$$

This unique relationship was observed by Leroueil et al. (1985) after performing a series of different types of oedometer tests (constant rate of strain tests, long term creep tests, controlled gradient tests, multiple stage loading tests) on natural clays.

The experimental results were interpreted by researchers to explain the effect of the clay layer thickness on the compressive strain caused by consolidation. There is no consensus when creep actually starts after or during primary consolidation.

1.5.2 Mechanisms of creep deformation

There are different mechanisms presented by the researchers to explain the creep deformation behaviour. Table 1.6 shows the main mechanisms of creep deformation which were introduced by the existing literature review. Generally, the clay mineralogy plays an important role in the creep deformation. In the macroscopic level, the creep deformation is caused by the rearrangement or adjustment of the clay structure under an effective stress (Das, 2008). In the microscopic level, the creep deformation is caused by the drainage of pore fluid in micropores or due to the structural viscosity of pore fluids (Le et al., 2012, Green, 1969).

Table 1.6 Main mechanisms of creep (from Le et al., 2012).

Author	Mechanism	Main factors
Taylor & Merchant (1940), Terzaghi (1941), Gibson & Lo (1961), Mesri (1973, 2003), Mesri & Godlewski (1977), Crooks et al. (1984).	Breakdown of interparticle bonds	Relative movement of particles, soil structure rearrangement.
Murayama & Shibata (1961), Christensen & Wu (1964), Mitchell (1964), Kwok & Bolton (2010).	Breaking of molecule bonds	Activate energy, temperature and deviatoric stress.

Grim (1962), Gupta (1964), Kuhn & Mitchell (1993).	Sliding particles	Activate energy, contact forces.
De Jong & Verruijt (1965), Berry & Poskitt (1972), Zeevaart (1986), Navarro & Alonso (2001), Mitchell & Soga (2005), Wang & Xu (2006).	Water flows with two drainage structure (Macro– micro structures)	Two levels of soil structures, water flows in two pore structures and deformation of pores.
Terzaghi (1941), Barden (1969), Bjerrum (1967), Garlanger (1972), Christie & Tonks (1985), Graham & Yin (2001).	Structural viscosity	Different viscosity of absorbed water system, clay mineral–water interaction.

1.5.3 Main factors influencing creep

The creep behaviour of clayey soils is influenced by several factors as reported by many researchers. The main factors that were determined by the researchers are sample thickness, load increment ratio, soil vibration, quantity of organic matter, sample disturbance, and the most important factors are pore fluid viscosity, effective stress, and temperature.

A) Pore fluid Viscosity

Schmertmann (1976) performed triaxial tests on dried, compacted kaolinite powder which were saturated with five different pore fluids under constant isotropic consolidation pressure of 350 kPa. Table 1.7 shows viscosity (μ), primary (t_{100}) and secondary (Δt_{sec}) consolidation times, and the creep index (c_α) corresponding to each pore fluid (Schmertmann, 2012). He observed that the creep index increased with the viscosity increase, whereas the creep index due to dry nitrogen gas equals zero. Figure 1.27 shows a linear fit between creep index and the viscosity of the used fluids.

Table 1.7 Consolidation of clay using different pore fluids with different viscosity (μ) (from Schmertmann, 1976).

Fluid	η(cp)	t_{100}(min)	Δt_{sec}(min)	C_α (x10^{-3})
Dry Nitrogen gas	0.02	≈ 0	NA	≈ 0
Methyl Alcohol	0.59	40	900	3.6
Benzene	0.65	7	580	4.8
Distilled Water	1.00	150	1230	6.2
25%/glycerin 75%/water	2.10	230	1080	12.2

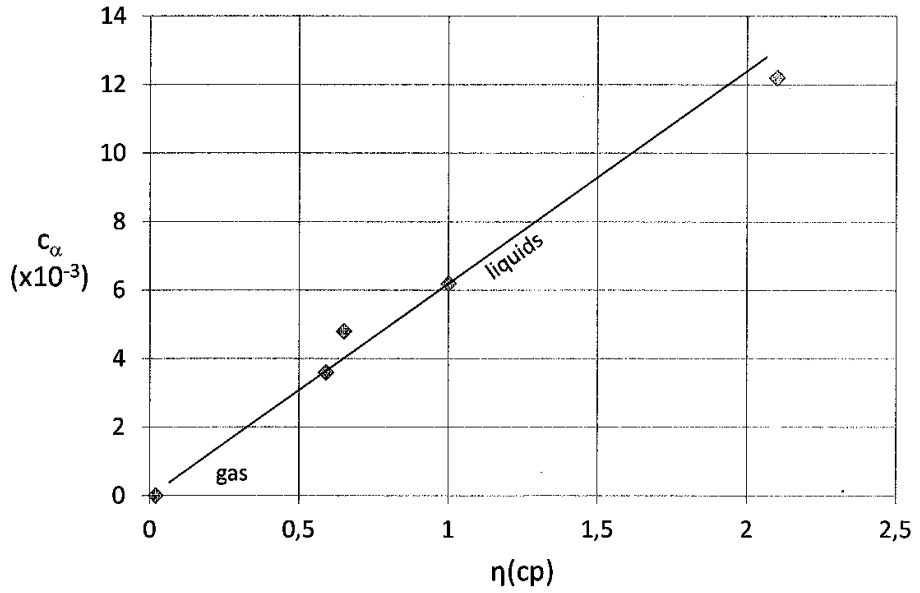

Figure 1.27 Creep index (cα) Variation with viscosity (μ) of powdered, compacted, saturated kaolinite using different pore fluids (from Schmertmann, 1976).

B) Effective stress

There are different opinions about the effect of load level on creep. MacFarlane (1959) observed that the creep index of flocculated kaolinite increased from 3.9 x10^{-3} to 5x10^{-3} when the effective stress of oedometric tests was increased from 300 to 800 kPa. A similar behaviour was observed by Marchall (1960). He performed five triaxial tests on deflocculated extruded BBC clay (PI=11%) and found that the creep index increased from 5.0 to 7.5x10^{-3} when the effective stress increased from 300 to 800 kPa as shown in Figure 1.28 by a linear relationship. However, Newland and Allely (1960) noted that the creep index was approximately independent of effective stress except near the preconsolidation pressure where it increased slightly. Jonas (1964) reported that the creep index is constant after passing the preconsolidation pressure level for silty clay. In contrast, Olson (1965) observed that the creep index of sensitive soil increased up to the preconsolidation pressure then decreased. However, Goldberg (1965) indicated that the creep index of a silty clay increased linearly with effective stress after passing the preconsolidation pressure (Green, 1969).

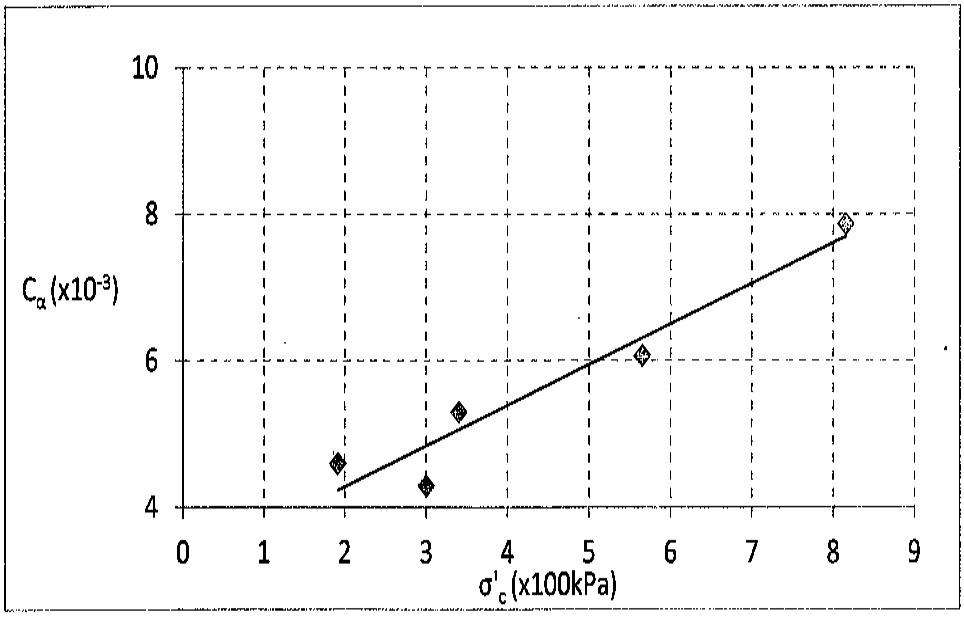

Figure 1.28 Creep index variation with effective stress of deflocculated, extruded BBC clay (from Schmertmann, 2012).

C) Temperature

Although temperature variations could highly affect the creep behaviour, there are still a very few studies on this subject. The rate of one dimensional creep may increase with temperature increase (Edil et al., 1994). Table 1.8 shows the different researcher's results of the temperature effects on the creep index.

Table 1.8 Temperature effect on the creep index.

No.	Author	Soil	Soil characteristics	Method	T	Creep variation with T
1	Gupta (1964)	Undisturbed soil (Haney clay)	LL = 50% PI = 25%	Unconsolidated Undrained triaxial Consolidated undrained triaxial	From 20 to 45^0 C	Strain increased with temperature increase under constant total stress at any time.
2	Green (1969)	Organic & non organic clay (Bryce Clay)	LL = 45.1% -non organic PI = 20.1%-non organic	Oedometric creep	5 to 50^0 C	c_α was more positively affected by temperature under lower effective stress.
3	Eriksson (1992)	Sulphide soils	Sulphide content	Oedometric creep	5 to 60^o C	Creep deformation increase with temperature increase.
4	Towhata et al. (1993)	MC clay	Similar to kaolin mineralogy	Consolidation apparatus	Up to 90^0 C	The amount of secondary contraction is more than the case under room temperature.
5	Moritz (1995)	Undisturbed soil (Sweden)	Water content:84% (6m) Water content:81% (9m)	Consolidated drained triaxial	40 & 70°C	The high temperatures may cause the starting of creep at lower effective stress.
6	Burghignoli et al. (2000)	Reconstituted clay (Todi clay)	LL = 52% PI = 30%	Drained triaxial	25 to 80^o C	The rate of thermal secondary consolidation increases at high temperature.

7	Zhang et al. (2007)	Opalinus Clay Callovo-Oxfordian argillite	Opalinus Clay, γ_d= 2.31 Oxfordian, γ_d = 2.25	Triaxial creep	Up to 60°C	-The creep rate accelerated with temperature increase up to 50°C. -The creep rate slowed at temperature over 50°C.
8	Cui et al. (2009)	Boom clay	LL = 70% PI = 45%	Triaxial test	20 & 40^0 C	The volumetric strain rate increased with temperature increase.

Gupta (1964) investigated the creep behaviour of undisturbed clay using two types of triaxial tests including unconsolidated undrained and consolidated undrained tests within a temperature range between 20 and 45°C. He observed in both types of triaxial tests that the strain was increased with temperature increase under constant total stress for any given time interval. He concluded that the soil will have more energy at high temperature, and this energy will increase the number of the molecules of soil which gained energy. More activation of molecules will lead to more weakening of the bonds and this induces a higher compressibility. During consolidated undrained tests, he also observed that the pore pressure increased with temperature increase. The reduction of net repulsive and attractive forces between particles makes the pore pressure greater at high temperature in this case of tests.

According to Moritz (1995), the high temperatures may cause the starting of creep earlier. He conducted a series of consolidated drained triaxial tests under the in situ stress at temperatures of 40 and 70°C on specimens taken from different depths (6 and 9 m). The results indicated that the vertical deformation and volume change of the specimens increased at high temperature. The vertical deformation increased by 2% at 70°C larger than the deformation at 20.0°C while it closed to the deformation at 40.0°C. Green (1969) found that the creep index was more affected by temperature under lower effective stress or stress level. In general, his results indicated that the magnitude of creep index increased at high temperature.

Zhang et al. (2007) carried out a series of creep tests on two kinds of indurated clays, Callovo-Oxfordian argillite and Opalinus Clay, using triaxial apparatus. The samples were tested under constant isotropic stress between 0.7 and 14 MPa at temperatures up to 60°C. The results indicated that the creep rate was maximum for a temperature of 50°C. They explained that the creep acceleration at high temperature is due to combined two mechanisms, firstly, the reduction of the pore water viscosity with temperature increase that causes a reduction in the shear resistances between particles, and secondly, the release of pore water because of the thermally induced viscosity reduction which results in shrinkage. However, the shear resistances between particles increased at temperatures over 50°C due to more release of adsorbed water films, and this lead to the slowing of the creep rate. Generally, their results

showed that the deformation of clays depends strongly on the adsorbed water films (Figure 1.29).

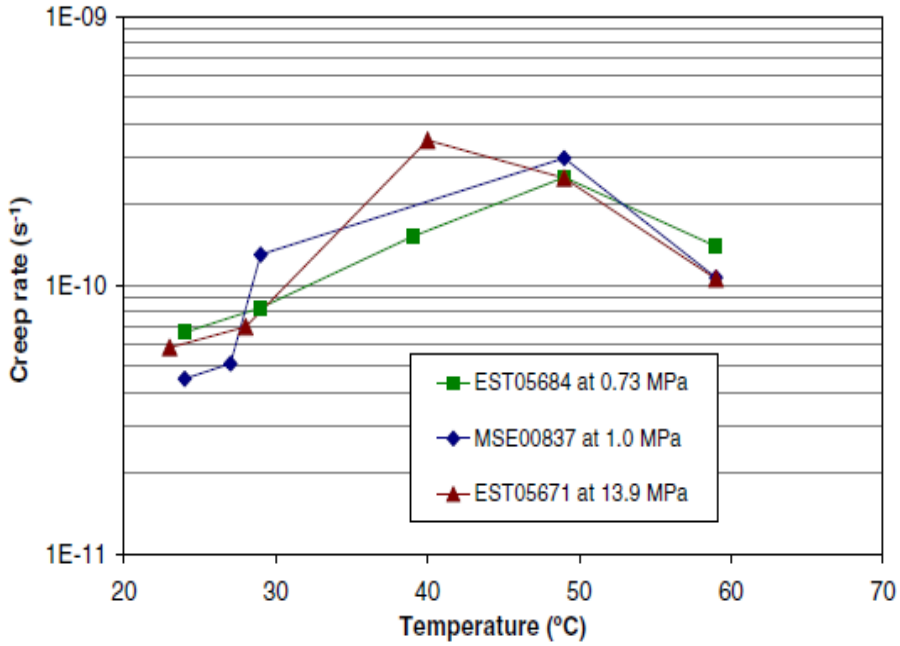

Figure 1.29 Temperature impact on the creep rate of clayey soils (from Zhang et al., 2007).

Towhata (1993) heated a sample of MC clay (similar to kaolin mineralogy) up to 90°c during the secondary consolidation stage to monitor the influence of temperature on the sample volume. He noted a volume contraction immediately after heating, and the amount of contraction was more than the deformation under room temperature. He explained that under heating either the rate of consolidation was accelerated, or the stiffness of the clay skeleton was deteriorated. Figure 1.30 shows the influence of temperature on the sample volume during secondary consolidation period under constant stress of 160 kPa.

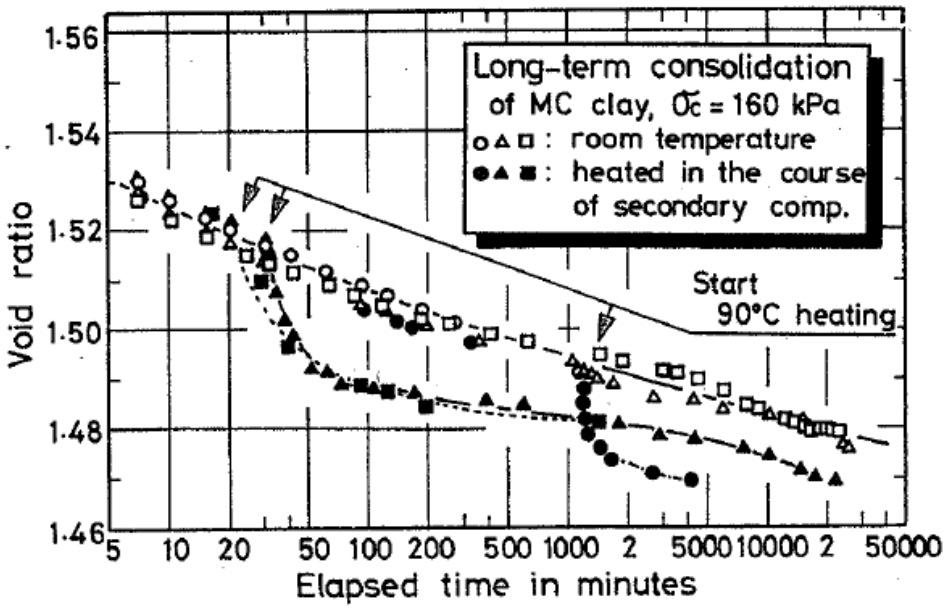

Figure 1.30 Influence of temperature on the sample volume during secondary consolidation (from Towhata, 1993).

Burghignoli et al. (2000) studied the thermal behaviour of reconstituted and natural clays during drained conditions through applying a thermal cycle under constant average effectives stress using triaxial device. Figure 1.31 shows the thermal cycle influence on the volume and the void ratio of the normally consolidated clay with time. The void ratio was reduced during the heating stage (path a-b) more than when it was at constant temperature, then it continued in reduction under constant high temperature (path b-c) but at a lower rate. The reduction in the void ratio might be related to the rearrangement of the soil particles because of heating, but the thermal expansion of the soil grains is very small. When the sample was cooled down (path c-d) to the initial temperature then kept constant at that temperature (path d-e), no change in void ratio was observed. This refers to non significant rearrangement of the particles during these stages. In this case, the void ratio reduction during heating is irreversible. In parallel, the same results were obtained for the volume variation through the thermal cycle except the cooling phase which represented a reduction. They suggested a relationship between the drained thermal behaviour and the time dependent behaviour of the solid skeleton or creep. As shown in Figure 1.32, the linear relationship between the void ratio variation due to the thermal loading (e_{TC}) and those due to creep (e_{CR}) increased with the amplitude of the thermal cycle. In fact, the rearrangement of particles due to heating is an amplification of those caused by the creep deformation of the solid skeleton at constant temperature. Generally, the rate of secondary consolidation may increase at high temperature. This result is consistent with Campanella and Mitchel (1968) and Burghignoli et al. (1992).

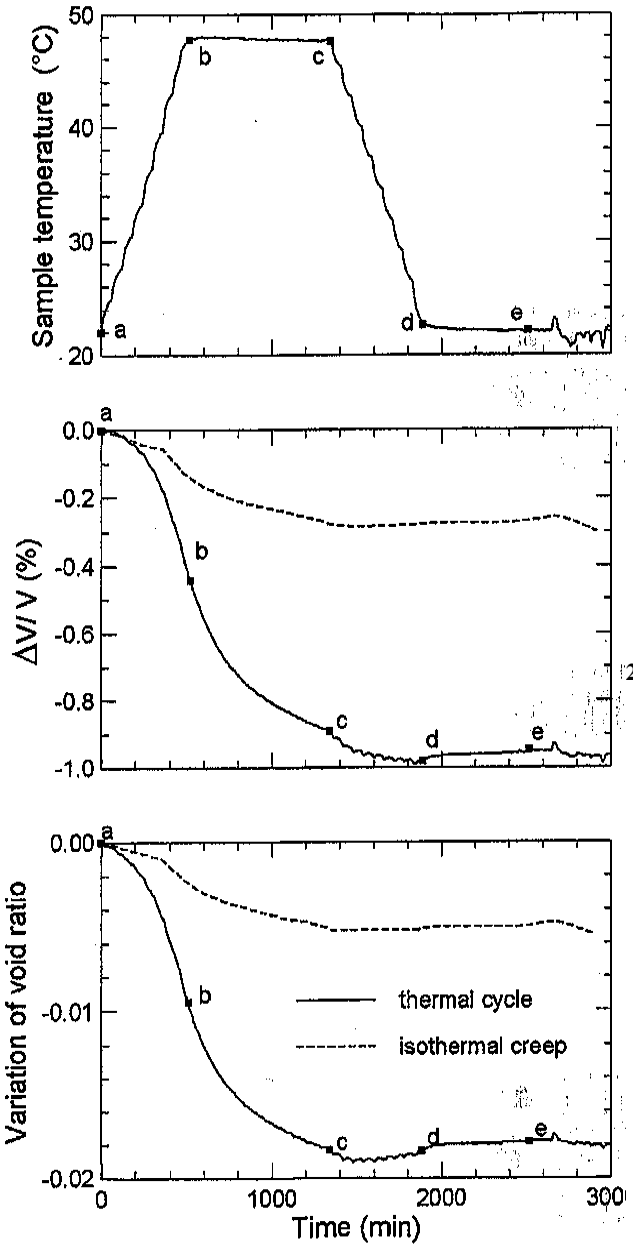

Figure 1.31 Thermal cycle impact on the volume and void ratio of normally consolidated clay with time (from Burghignoli et al., 2000).

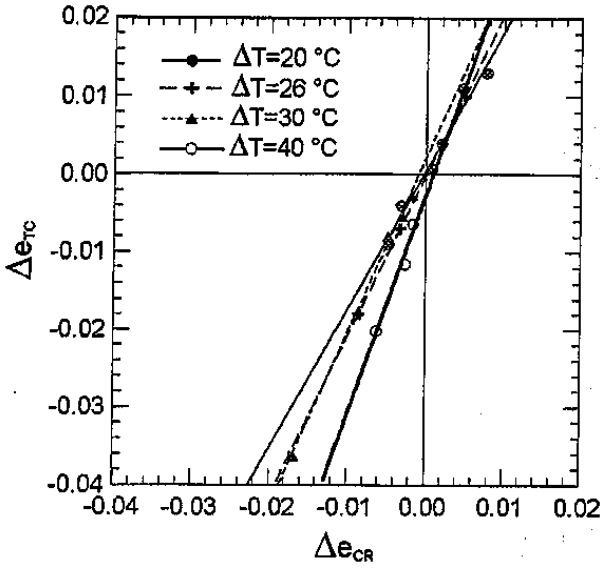

Figure 1.32 e_{TC} Vs. e_{CR} at different thermal cycles for reconstituted clay (from Burghignoli et al., 2000).e_{tc}:void ratio due to thermal loading, e_{cr}:void ratio due to creep.

1.5.4 Creep index (C_α) and compression index (C_c) relationship

Mesri and Godlewski (1977) developed a method for determining the creep index, c_α , as a function of compression index, c_c. This method is based on the result that the magnitude and the behaviour of secondary compression index, c_α, with time ($c_\alpha=\Delta e/\Delta \log t$) is directly related to the magnitude and the behaviour of compression index, C_c, with consolidation stress ($c_c=\Delta e/\Delta \log \sigma'$). The relationship between the creep index and compression index is linear with a constant slope of c_α/c_c. Value of c_α/c_c has a narrow range for each type of soil (see Table 1.9). Figure 1.33 shows an example for the relationship between c_c and c_α for sensitive clay from Canada based on an experimental work. Accordingly, the secondary compression behaviour of any soil can be defined completely by the value of c_α/c_c together with the end of primary (EOP) e-logσ' curve (Mesri and Castro, 1987).

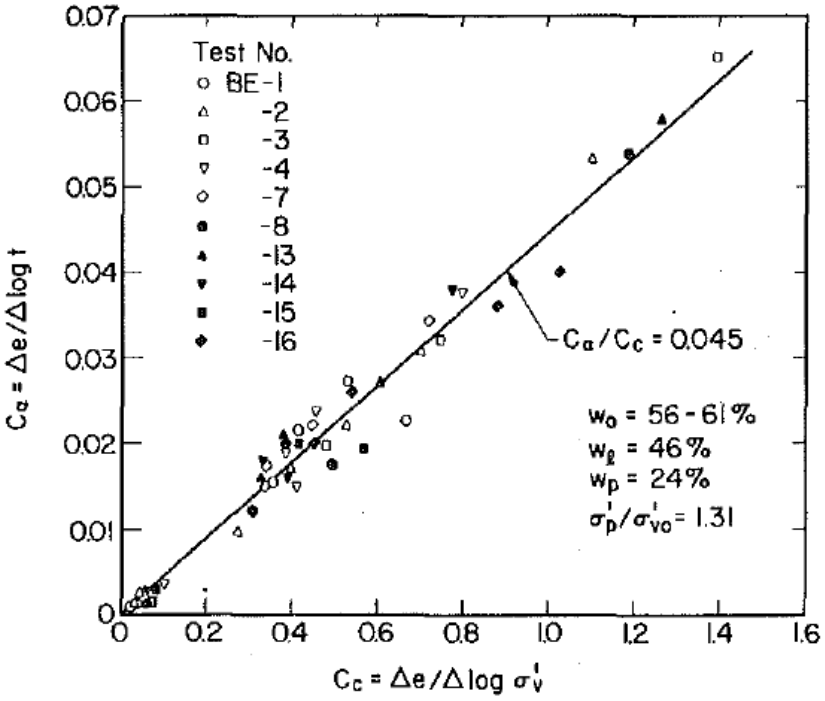

Figure 1.33 c_α-c_c relationship for Berthierville Clay (from Mesri and Castro, 1987).

According to Leroueil et al. (1985), the preconsolidation pressure–strain rate relationship represents the capability of clay skeleton to creep. Figure 1.34 shows the preconsolidation pressure-strain rate relationship for Batiscan clay. Based on the gained experience with soft clays, preconsolidation pressure–strain rate relashinship can be described as a linear function in the logarithmic scale (Yashima et al., 1998):

$$\text{Log } \dot{\varepsilon} = a + \alpha \text{ Log } P_c \qquad \textbf{(1.19)}$$

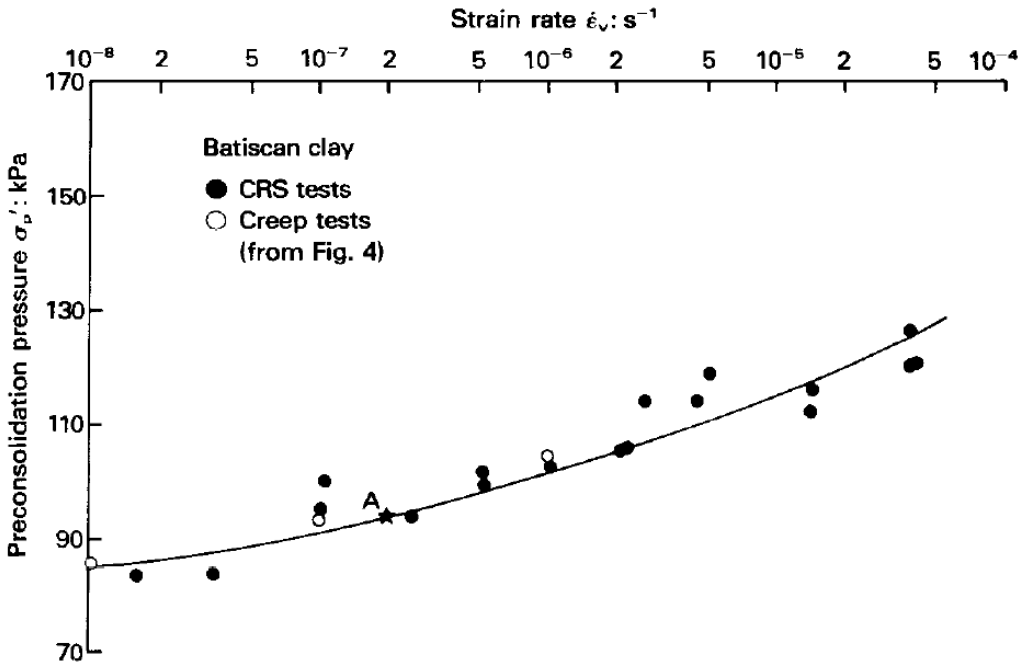

Figure 1.34 Preconsolidation pressure variation with strain rate (from Leroueil et al., 1985).

Based on the experimental results, the value of c_α/c_c represents the same behaviour of the variation in the preconsolidation pressure per logarithmic cycle of time or strain rate, i.e., $\alpha = c_\alpha/c_c$ (Leroueil et al., 1985) especially that the isotach approach considers $\Delta log\dot{\varepsilon} = \Delta logt$.

Table 1.9 Viscous characteristics of geotechnical materials (from Mesri et al. 1995).

Material	$C_{\alpha e}/C_c$ equal to $\alpha = \Delta \log \sigma_p'/\Delta \log \dot{\varepsilon}$	$\frac{\Delta\sigma'}{\sigma'}/\Delta \log \dot{\varepsilon}$ (%)
Granular soils including rockfill	0.02 ± 0.01	2.3 – 7.2
Shale and mudstone	0.03 ± 0.01	4.7 – 9.6
Inorganic clays and silts	0.04 ± 0.01	7.2 – 12.2
Organic clays and silts	0.05 ± 0.01	9.6 – 14.8
Peat and muskeg	0.06 ± 0.01	12.2 – 17.5

Note: $C_{\alpha e}=C_\alpha$ which is the creep index.

1.5.5 Conclusion

This section discussed the long term behaviour of clay soils. Two theories were proposed to describe the creep behaviour of clay soils named theory A (secondary consolidation starts after primary consolidation) and theory B (secondary consolidation starts during primary consolidation). Different mechanisms were suggested by researchers to interpret the creep deformation and the soil mineralogy has the main role in deformation. The main factors that

influence creep behaviour are fluid viscosity, effective stress, and temperature. The creep deformation can be determined as a function of the primary compression.

1.6 Modeling of thermo-hydro-mechanical behaviour of clay soil

1.6.1 Modeling of elasto-viscoplastic behaviour of clay

Taylor (1942)

The first theory where creep behaviour was at least partly involved was proposed by Taylor & Merchant (1940). Taylor (1942) developed the first model that describes the variation of void ratio with effective stress at different times as shown in Figure 1.35 (as cited in Olsson, 2010; Suhonen, 2010; Takeda et al. 2013). In fact, Taylor (1942) generated two different theories A and B for one dimensional consolidation behaviour (Suhonen, 2010). Theory A suggests that creep occurs only after the end of primary consolidation. Hypothesis B suggests that creep occurs at least partly during primary consolidation.

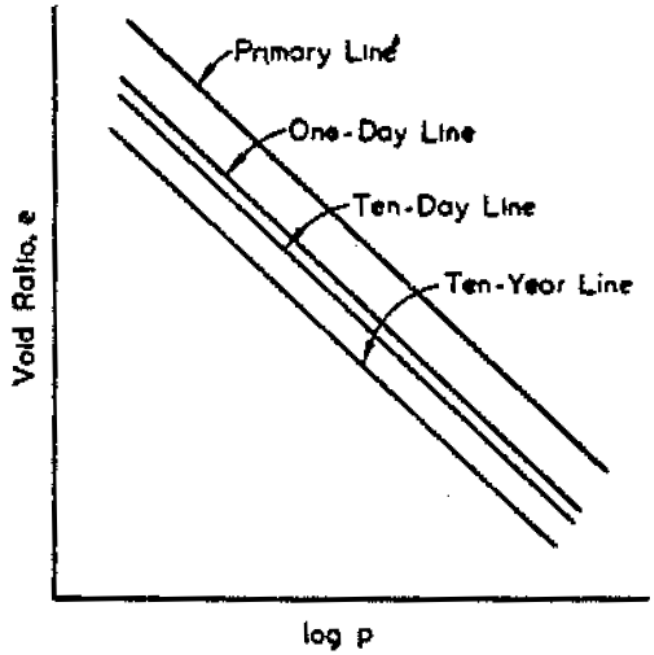

Figure 1.35 Void ratio-effective stress relationship at different times (from Taylor, 1942).

Suklje (1957)

Suklje (1957) was the first researcher who introduced a general theory called isotache model which considers that the behaviour of clay soils can be controlled by a unique relationship between effective stress, void ratio, and rate of void ratio (or strain rate). He proposed a set of isotaches that determine the effective stress-void ratio-void ratio rate relationship based on a series of incremental loading oedometer tests on lacustrine chalk samples (Figure 1.36). The effective stress void ratio relationship continuously changes with the rate of void ratio in

association with the viscosity. According to this model, the creep behaviour does not occur only after the dissipation of excess pore pressure but rather occurs during the entire consolidation process. Hence, there is no separation between primary consolidation and creep effects during consolidation. The model also suggested that the time-dependent strains are affected by the layer thickness of clay, the permeability, and the drainage conditions. Obviously, the isotache concept corresponds to hypothesis B of creep.

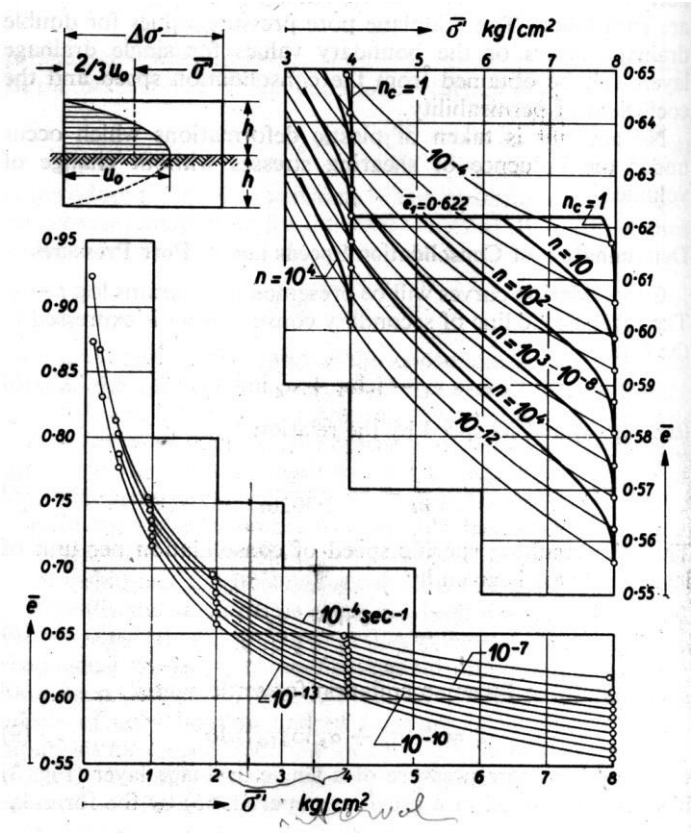

Figure 1.36 Isotache model by Suklje (1957).

Model of Perzyna (1963)

Perzyna (1963) proposed a general rate dependent constitutive model for the behaviour of clays. According to this model, the strain rate sensitivity of the material causes the difference between the static and dynamic behaviour of the material. This sensitive rate behaviour is called viscoplastic behaviour. Accordingly, the total strain rate is composed of elastic and viscoplastic strain rate and it is written as follows:

$$\dot{\varepsilon} = \dot{\varepsilon}^{e} + \dot{\varepsilon}^{vp} \tag{1.20}$$

where $\dot{\varepsilon}^{e}$ is the elastic strain rate, and $\dot{\varepsilon}^{vp}$ is the viscoplastic strain rate.

The plastic component only expresses the viscous behaviour of the material. The assumed function for the static yield stress is:

$$F(\sigma,\ \varepsilon^{vp}) = \frac{f(\sigma,\ \varepsilon^{vp})}{k_s} - 1 \tag{1.21}$$

where function $f(\sigma,\ \varepsilon^{vp})$ depends on the states of stress σ and plastic strain ε^{vp}. k_s is the work-hardening parameter. F=0 indicates the static domain function, and $F > 0$ indicates the dynamic domain function. Figure 1.37 shows the elastic and viscoplastic domains for isotropically consolidated clay materials. Based on the Drucker's formulation (pressure-dependent model), Perzyna suggested a flow rule for the viscoplastic deformations as follows:

$$\dot{\varepsilon}^{vp} = \gamma < \varphi(F) > \frac{\partial f}{\partial \sigma'} \tag{1.22}$$

The material function $\varphi(F)$ can be expressed as follows:

$$< \varphi(F) >= \begin{cases} 0, & F \le 0 \\ \varphi(F), & F > 0 \end{cases} \tag{1.23}$$

where γ is the viscoplastic parameter, f is the dynamic domain function, and φ is the material function due to strain rate effect.

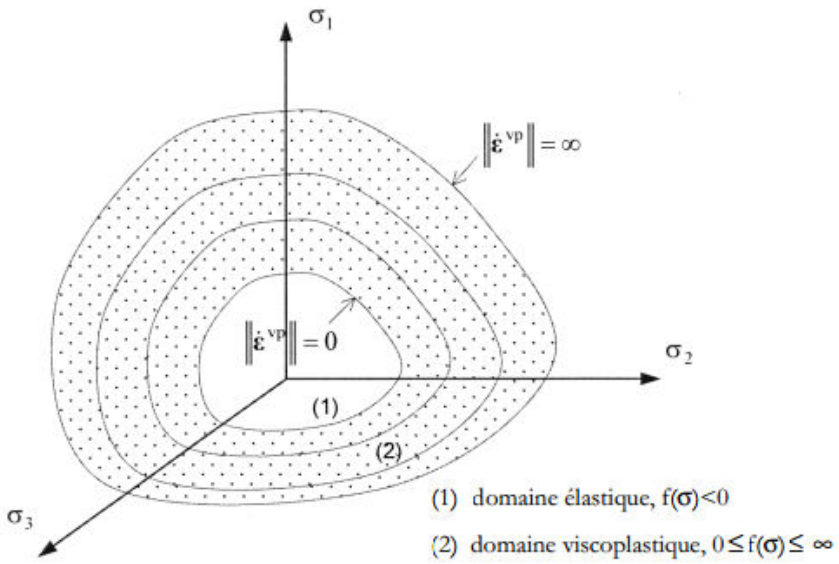

Figure 1.37 Elastic and viscoplastic domain for isotropically consolidated clay material (after Fabre, 2005).

Bjerrum (1967)

Bjerrum (1967) proposed a model that explains the apparent preconsolidation pressure and over-consolidation ratio, resulting from geological ageing, and also the determination of settlement and creep effects which occur over time. He defined a unique relationship between void ratio, effective stress, and time. This relationship is determined by parallel time lines (isochrones), and each line represents the void ratio corresponding to different values of effective stress at specific time of constant loading (Figure 1.38 (a)). The time durations

represented by these lines are related to the multi-stage loading tests, delayed compression at constant effective stress under engineering structures, and aging in natural deposits. Time step is 24 hrs, 3 years, 30, 300, 3000, etc. The model divided the reaction of the clay soil due to an increase in the effective stress into two components, instant and delayed compression. Instant compression occurs simultaneously with the effective stress increase and reduces the void ratio value until the structure effectively supports the overburden pressure. Delayed compression represents the volume reduction at constant effective stress. Figure 1.38 (b) shows the instant and delayed compression behaviour of clay soils with time under uniform loading. In the case of drained soil (dotted line), the load will be transferred simultaneously to the clay structure as effective stress. However, due to water viscosity, the effective stress will increase gradually when the pore pressure dissipates, and hence the compression occurs (the bold line). The dissipation of pore pressure depends on the soil permeability, drainage condition, and thickness of clay layer. According to this concept, the secondary consolidation cannot be separated from the primary consolidation as introduced by Gray (1936).

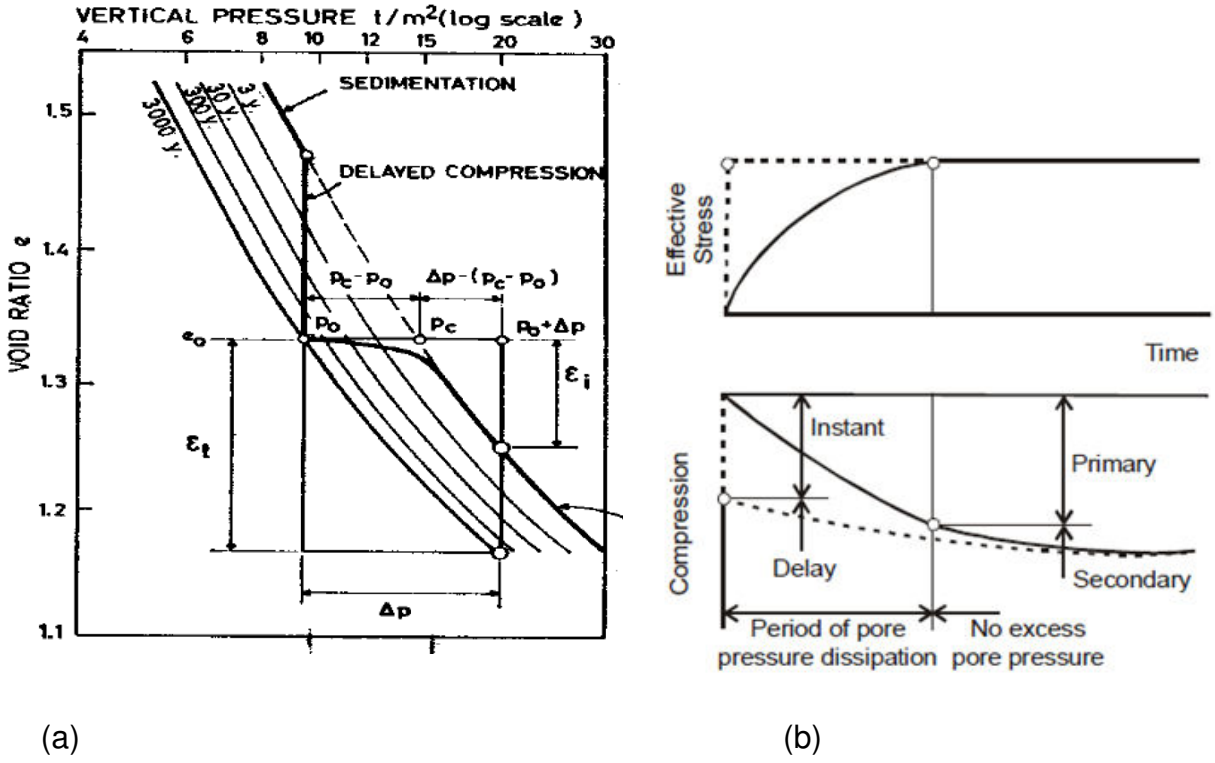

Figure 1.38 (a) clay compressibility (b) Instant and delayed compression concept (from Bjerrum, 1967).

1.6.2 Modeling of thermo-elasto-viscoplastic behaviour of clay

Thermally activated creep model of Kuhn & Mitchell (1993)

Kuhn & Mitchell (1993) proposed a new concept for creep deformation which is due to a sliding movement between the particles. The mechanism of this model describes soil creep generally under the effects of shear stress and temperature. The sliding movement is caused by the tangential component of the contact forces between soil particles, f_t, as a result of the nature of viscous friction. The relationship between the sliding velocity ($\dot{s}$), the sliding force and the friction ratio between the tangential force and the normal force (f_t/f_n) represents the deformation of the clay. The proposed equation model for sliding velocity between the clay particles ($\dot{s}$) can be given as follows,

$$\dot{s} = \lambda v' = \lambda \frac{2kT}{h} \exp\left(\frac{-\Delta F}{RT}\right) sinh\left(\frac{1}{2kT} \frac{\lambda}{n_1} \frac{f_t}{f_n}\right) \quad \textbf{(1.24)}$$

where λ is the distance between neighbouring equilibrium positions, suggested to have the order of 2.89×10^{-10}m (2.8 A°), T is the absolute temperature, k is Boltzmann's constant of 1.38 * 10^{-16}erg/K, h is Planck's constant of 6.626 * 10^{-27}erg/s, R is the universal gas constant (8.31 J/(mol K)), n_1 is the number of bonds per unit of normal contact force, and ΔF is free energy of activation in range of 84–190 kJ/ mol. ΔF represents the bonding strength, as ΔF is the total energy required to break down all the energy barriers to allow the displacement of the flow units to a new position without applied potentials.

An increase in temperature accelerates the sliding velocity between the particles and consequently, the creep rate increases. The temperature causes a decrease in strength and weakens the soil structure according to physical interpretation of this model.

Boudali et al. (1994) model

Boudali et al. (1994) performed constant rate of strain (CRS) oedometer tests at different strain rates and temperatures on a soft silty clay from Berthierville, Canada. They observed a linear preconsolidation pressure-strain rate relationship at a given temperature, and these lines are parallel at different temperatures. By considering the results of different oedometer tests performed by Kabbaj (1985) and Boudali et al. (1994), Figure 1.39 shows the preconsolidation pressure-strain rate relationship at different temperatures, and Figure 1.40 shows the normalized stress-strain behaviour at different strain rates and temperatures. It is observed form Figure 1.42 that all data come into a narrow range around a unique normalized effective stress-strain curve. Based on the experimental results, the viscous behaviour of clay soils can be extended to include temperature dependent behaviour. Boudali et al. (1994) extended the

viscous behaviour model of Leroueil et al. (1985) to include the temperature dependent behaviour as follows,

$$\sigma'_p = f(\dot{\varepsilon}, T) \quad \textbf{(1.25)}$$

$$\sigma' / \sigma'_p(\dot{\varepsilon}, T) = g(\varepsilon) \quad \textbf{(1.26)}$$

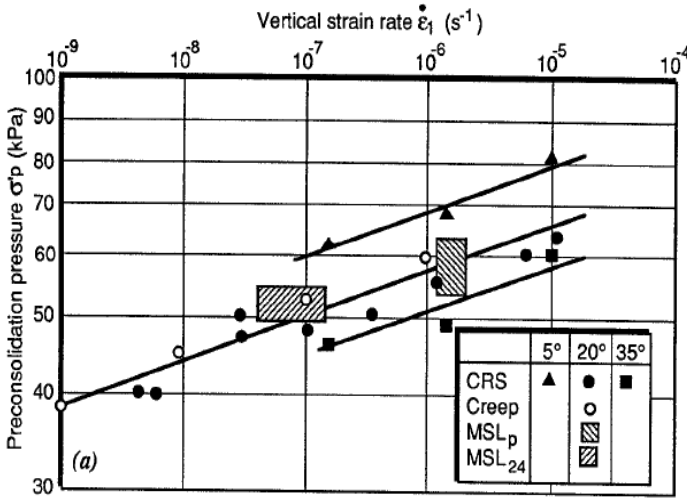

Figure 1.39 Preconsolidation pressure-strain rate relationship at different temperatures from oedometer tests(from Kabbaj 1985 and Boudali et al. 1994).

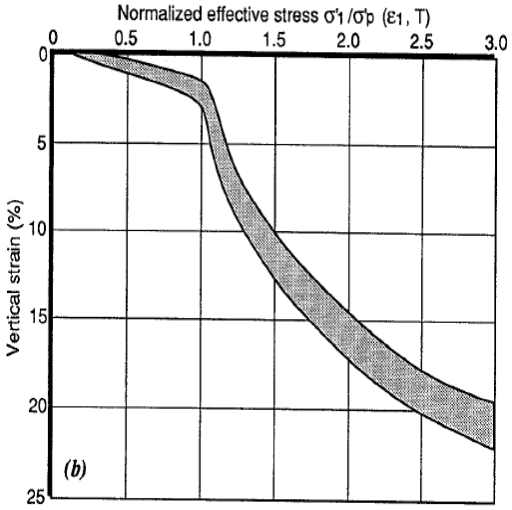

Figure 1.40 Normalized stress-strain behaviour at different temperatures from oedometer tests (from Kabbaj 1985 and Boudali et al. 1994).

Model of Yashima et al. (1998)

Yashima et al. (1998) developed an elasto-thermo-viscoplastic constitutive model to represent the clay behaviour at different strain rates and temperatures. Based on the experimental and models studies, the viscoplastic strain rate in the case of one dimensional consolidation process can be identified as follows:

$$\dot{\varepsilon}^{vp} = C(T).exp\left\{\alpha\left(ln\frac{\sigma'}{\sigma'_o} - \frac{1+e}{c_c - c_s}\varepsilon^{vp}\right)\right\} \quad \textbf{(1.27)}$$

$$C(T) = C_o exp\left\{\alpha\left(-ln\frac{\sigma'_p}{\sigma'_o}\right)\right\} \quad \textbf{(1.28)}$$

where α is the constant parameter in eq. 1.19, σ'_o is the initial effective stress, σ'_p is the preconsolidation pressure, c_c is the compression index, c_s is the swelling index, C is viscoplastic parameter. The viscoplastic parameter C (T) is only temperature dependent and can be written as follows:

$$C(T) = C(T_r)exp\left\{\alpha\left(-ln\left(\frac{T_r}{T}\right)^{\theta}\right)\right\} \quad \textbf{(1.29)}$$

with a temperature reference T_r , the viscoplastic parameter $C(T)$ can be expressed as follows:

$$\frac{C(T)}{C(T_r)} = \left(\frac{T}{T_r}\right)^{\alpha\theta} \quad \textbf{(1.30)}$$

where the viscoplastic parameter θ can be determined from the preconsolidation pressure-temperature relationship. In fact, this model can be considered approximately as a function of the unique effective stress-strain-strain rate temperature relationship. To validate the model results, it was compared with the experimental results of CRS tests on Berthierville clay at different strain rates and temperatures performed by Boudali et al. (1994). It well simulated the experimental work on Berthierville clay as shown in Figure 1.41.

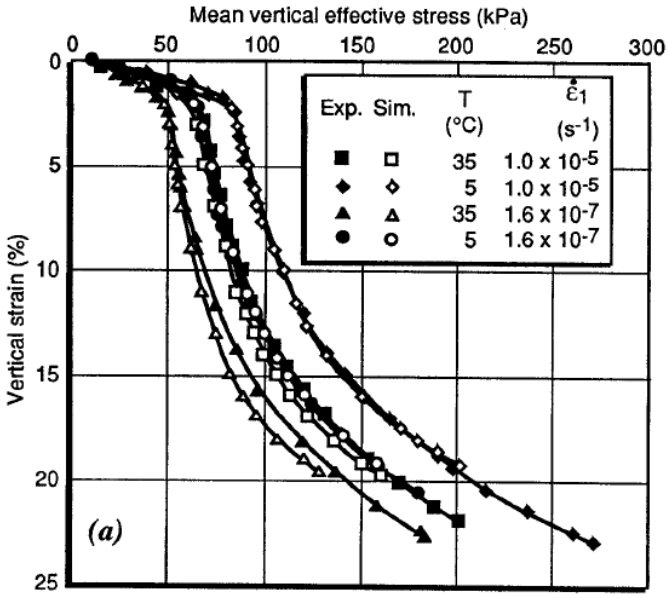

Figure 1.41 Simulated the experimental results on Berthierville clay at different strain rates and temperatures (Yashima et al., 1998).

Kim & Leroueil (2001) model

Kim and Leroueil (2001) developed a viscoplastic model for one dimensional consolidation in which a unique effective stress-viscous strain-viscous strain rate is used as a base to model the viscous behaviour of clay during consolidation. Indeed, this model is an extension to the viscous behaviour model of Leroueil et al. (1985) (section 1.5.1) to include the temperature effect. The viscoplastic strain is considered in the model instead of the total strain since the soil behaviour is appropriate when the vertical stress continuously increases as follows,

$$\sigma'_y = f(\dot{\varepsilon}_{vp}, T) \quad \textbf{(1.31)}$$

$$\sigma' / \sigma'_y (\dot{\varepsilon}_{vp}, T) = g (\varepsilon_{vp}) \quad \textbf{(1.32)}$$

where $\dot{\varepsilon}_{vp}$, and ε_{vp} are the viscoplastic strain rate and viscoplastic strain respectively. According to the obtained results from the experimental work on different clays, in particular those obtained on Berthierville clay presented in Figure 1.40, equation can be displayed by a linear function in $\log\sigma'_p$ -$\log\dot{\varepsilon}_{vp}$ diagram as follows:

$$\sigma'_y = A + \alpha \log\dot{\varepsilon}_{vp} \quad \textbf{(1.33)}$$

$$\sigma' / \sigma'_y (\dot{\varepsilon}_{vp}, T) = g (\varepsilon_{vp}) \quad \textbf{(1.34)}$$

where A is a temperature-dependent soil parameter. α is essentially constant, independent of temperature, represents the slope of the preconsolidation pressure-strain rate relationship (or equal c_α/c_c as discussed in section 1.5.4). Accordingly, equation 3 can be written as follows:

$$\sigma'_y = f_1(\dot{\varepsilon}_{vp}) f_2(T) \quad \textbf{(1.35)}$$

Similar to experimental evidence of Boudali et al. (1994), Marques et al. (2004) also found experimentally parallel lines of the preconsolidation pressure-strain rate relationship at different temperatures for St-Roch-de-l'Achigan clay from Canada using CRS tests (Figure 1.42).

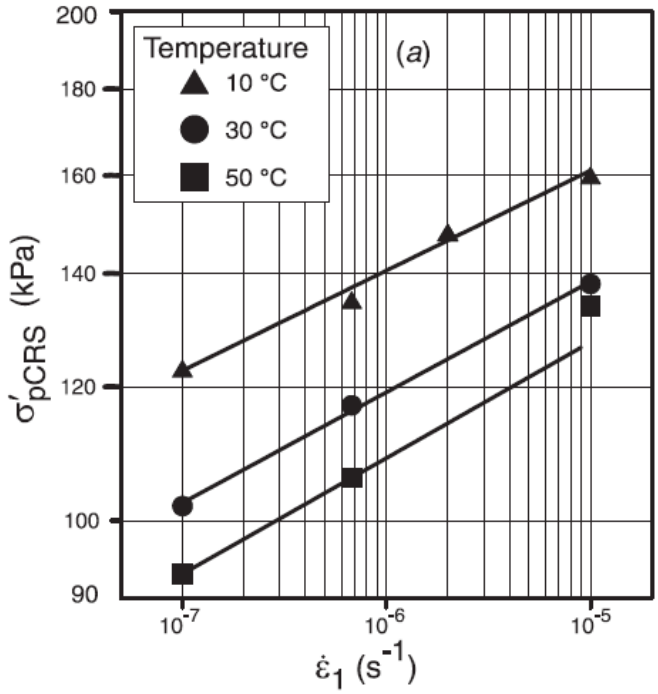

Figure 1.42 Preconsolidation pressure-strain rate relationship at different temperatures from oedometer tests (from Marques et al. 2004).

Laloui et al. (2008) model

Laloui et al. (2008) developed a thermo-visco-plastic model for soil that includes the effects of temperature and strain rate on the soil behaviour. The model is based on two concepts: the

unique effective stress-strain-strain rate concept and the evolution of the vertical yield stress with temperature. According to the model, the total volumetric strain increment can be divided into two components as follows:

$$d\varepsilon_v = d\varepsilon_v^e + d\varepsilon_v^{vp} \quad \textbf{(1.36)}$$

where $\mathbf{d\varepsilon_v^e}$ is the volumetric elastic strain increment, and $\mathbf{d\varepsilon_v^{vp}}$ is the volumetric viscoplastic strain increment.

The elastic strain increment can be related to the stress condition as follows,

$$d\varepsilon_v^e = \frac{1}{K} dp' \quad \textbf{(1.37)}$$

where p' is the mean effective stress, and K is the bulk modulus.

Along with Laloui and Cekerevak (2003) suggestion for temperature dependent yield stress (f_2 in eq. 1.35), the evolution of the vertical yield stress with temperature in eq. 1.35 can be expressed as follows:

$$\sigma'_{y,\dot{\varepsilon}_v^{vp},T} = \sigma'_{y,\dot{\varepsilon}_v^{vp},T_o} \left(\frac{\dot{\varepsilon}_v^{vp}}{\dot{\varepsilon}_{vo}^{vp}}\right)^{\alpha} \left(1 - \gamma \log \frac{T}{T_o}\right) \quad \textbf{(1.38)}$$

where $\sigma'_{y,\dot{\varepsilon}_v^{vp},T}$ is the vertical yield stress at strain rate $\dot{\varepsilon}_v^{vp}$ and temperature T, $\sigma'_{y,\dot{\varepsilon}_v^{vp},T_o}$ is the vertical yield stress at strain rate $\dot{\varepsilon}_v^{vp}$ and initial temperature T_o, $\dot{\varepsilon}_{vo}^{vp}$ is initial strain rate, γ is a soil parameter, and α is a constant parameter shown in eq. 1.33.

The isotropic yield limit can be represented as follows,

$$f = p' - \sigma'_y \quad \textbf{(1.39)}$$

where

- In the strain rate and temperature independent conditions:

$$\sigma'_y = \sigma'_{yo} \exp(\beta \varepsilon_v^{vp}) \quad \textbf{(1.40)}$$

- In the strain rate and temperature dependent conditions:

$$\sigma'_y = \sigma'_{yo} \exp\left(\beta \varepsilon_v^{vp}\right) \left(\frac{\dot{\varepsilon}_v^{vp}}{\dot{\varepsilon}_{vo}^{vp}}\right)^{\alpha} \left(1 - \gamma \log \frac{T}{T_o}\right) \quad \textbf{(1.41)}$$

with σ'_{yo} the initial vertical yield stress, and β the plastic compressibility.

For the purpose of validation, the constitutive model consolidation results are compared to the experimental results of consolidation tests at different strain rates and temperatures on Berthierville clay performed by Boudali et al. (1994). The predicted consolidation paths at different strain rates and temperatures using the proposed model show a good agreement with the experimental consolidation paths as show in Figure 1.43.

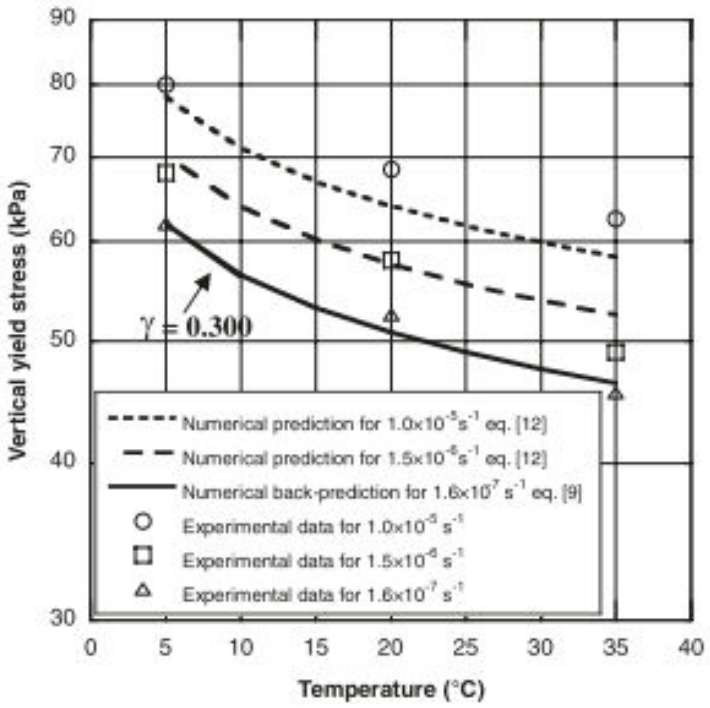

Figure 1.43 Prediction of the evolution of the vertical yield stress of Berthierville clay at different strain rates and temperatures (from Laloui, Leroueil et Chalindar, 2008).

1.6.3 Summary

The modeling of the elasto-viscoplastic (Taylor, 1942; Suklje, 1957; Perzyna, 1963; Bjerrum, 1967) and thermo-elasto-viscoplastic (Kuhn and Mitchell, 1993; Boudali et al., 1994; Yashima, 1998; Kim and Leroueil, 2001; Laloui et al., 2008) behaviour of clayey soils was discussed in this section. Most of the proposed models show a good agreement with the experimental work at different types of clays.

1.7 Conclusion

This chapter discussed the main characteristics of the thermo-hydro-mechanical behaviour of clay soils. It focused on the thermal properties of soil, variation of permeability with temperature using the direct method, temperature effect on the short and long term consolidation behaviour of clay soils beside the relevant experimental methods. In addition, it discussed the modeling of thermo-hydro-mechanical behaviour of clay.

As mentioned above, most of the experimental works performed by researchers have been focused on the natural clays. In this context, this research investigated the short- and long-term consolidation behaviour of two compacted clay soils. The impacts of clay nature, stress history and temperature variations on the thermo-hydro-mechanical behaviour of compacted clay soils were studied. In fact, the structure of compacted clay soils is different from the natural clays

and which may lead to different behaviour with the external factors. Constant rate of strain consolidation (CRS) tests with different strain rates and temperatures were performed on the compacted clays. In comparison with the incremental loading in classical oedometer tests, the constant rate of strain consolidation (CRS) tests are rapid and provide a large amount of data within a short time. These data are useful for the evaluation of the long-term hydro-mechanical and creep behaviours of clayey soils. A detailed description for constant rate of strain consolidation (CRS) test is presented in the Chapter 2 -Materials characteristics and experimental method.

Chapter 2 Materials characterization and experimental method

2.1 Introduction

The current chapter identifies the clayey soils, the apparatus used in this research, and the validation of the experimental protocols. To investigate the impact of clay nature on the hydro-mechanical behavior of clay with temperature variations, two different clays were used in this study. This chapter presents the basic characteristics of the studied clays. The relevant details of the experimental device and techniques are presented.

Constant rate of strain consolidation tests (CRS) were performed to investigate the temperature and strain rate impact on the hydro-mechanical behaviour of clay soils. The relevant theory of CRS test, the sample preparation method, the experimental procedures, are presented in this chapter. The detailed experimental program of this research is also presented.

2.2 Characteristics of soil materials

This section presents the main characteristics of the studied materials. It includes the mineralogical and chemical composition, particle size distribution and atterberg limits, Proctor curve of compaction for studied clays. Two different clays are presented in this study, clay A and clay B.

2.2.1 Mineralogical and chemical composition

Table 2.1 shows the mineralogical and chemical composition of the studied soils. Clay A used in this study is called Arginotech® (East of Germany). Clay A consists of 77% illite, 10% kaolinite, 12% calcite and traces of quartz and feldspar. Illite is a non-expanding, micaceous clay material which is common in many argillaceous sediments (Srodon et al., 1986; Lynch, 1997; Gaudette et al., 1964; Adamis et al., 2005). Alteration of silicates such as feldspar, muscovite or other clay minerals forms the illite. The chemical formula of illite is $(K,H_3O)(Al,Mg,Fe)_2(Si,Al)_4O_{10}[(OH)_2]$.

The second material has been sampled in the East of France. It is a natural clayey material composed of 43% kaolinite, 30% illite, 20% smectite, and 7% chlorite. It has been labelled

clay B in the remaining part of the manuscript. The mineralogical composition of these clays was determined using x-ray diffraction (XRD) technique.

Table 2.1 Mineralogical and chemical composition of the studied clays.

Mineral	**%**	**%**
	Clay A	**Clay B**
Illite	77.0	30
Calcite	12.0	-
Kaolinite	10.0	43
Smectite	-	20.0
Chlorite	-	7.0
Chemical composition		
- Clay A		
Oxides	%	
SiO_2	46.0	
Al_2O_3	20.0	
Fe_2O_3	7.0	
CaO	6.0	
K_2O	5.5	
MgO	3.0	
Na_2O	0.15	
TiO_2	0.80	
P_2O_5	0.30	
Organic material	11%	
- Clay B		
Minerals	%	
SiO_2	63	
Clay minerals	18.0	
Ca	15	
Feldspar	1.0	
Gypsum	1.0	
Plagioclase	1.0	
Pyrite	Traces	

Illite is one of the most common clay minerals with three-layer sheets (silica and gibbsite). Generally, the three layer sheet is a combination of an octahedral sheet in the middle with two silica sheets, one at the top and one at the bottom. The repetition of layers of these sheets forms the clay mineral. In detail, the basic structure of illite consists of gibbsite sheet with two silica sheets, one at the top and one at the bottom. The layers of illite are bonded together by relatively weak bonding due to non exchangeable potassium ions held between them. Illite particles have lateral dimensions of 1000–5000Å and thicknesses of 50–500Å. Figures 2.1 and 2.2 show the symbolic structure and structure sheets of illite.

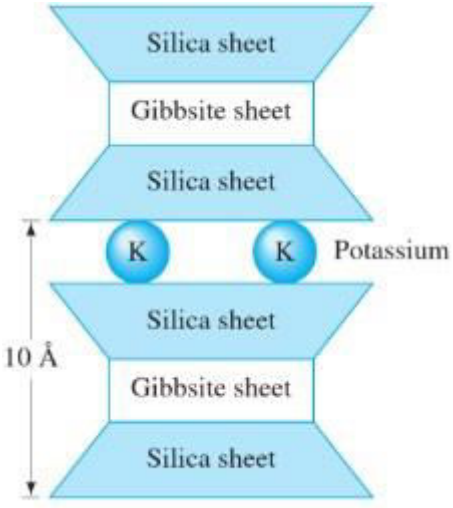

Figure 2.1 Simple structure of illite (from Craig, 2004).

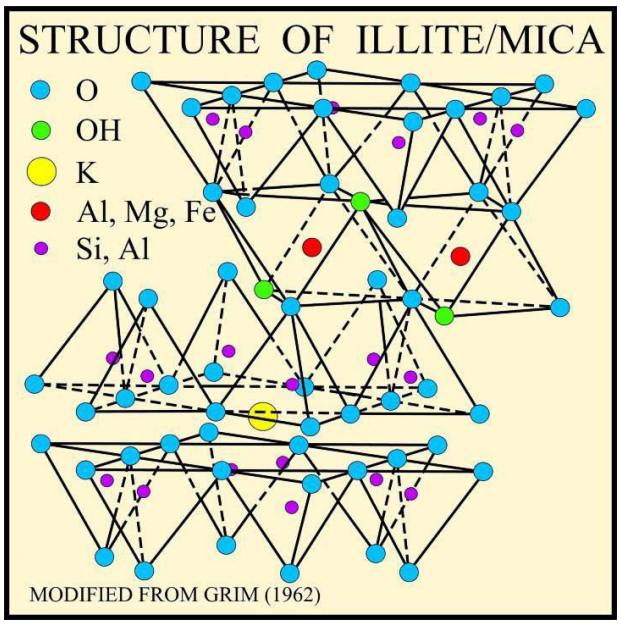

Figure 2.2 Structure sheets of illite (Poppe et al., 2001).

Kaolinite is one of the important clay minerals and it consists of repeating layers of a single sheet of silica combined with a single sheet of gibbsite. The combined silica-gibbsite sheets

are held together by hydrogen bonding. The thick of each layer is about 7.2 Å. Kaolinite appears as platelets with a lateral dimension of 1000 to 20000 Å and a thickness of 100 to 1000 Å. Figures 2.3 and 2.4 show the symbolic structure and structure sheets of Kaolinite.

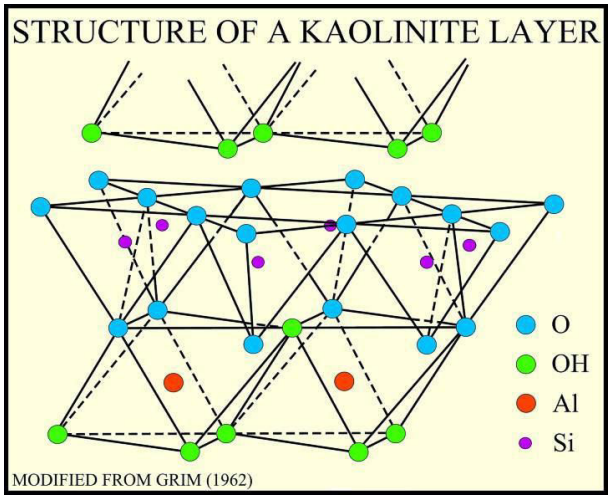

Figure 2.3 Structure sheets of kaolinite clay (Poppe et al., 2001).

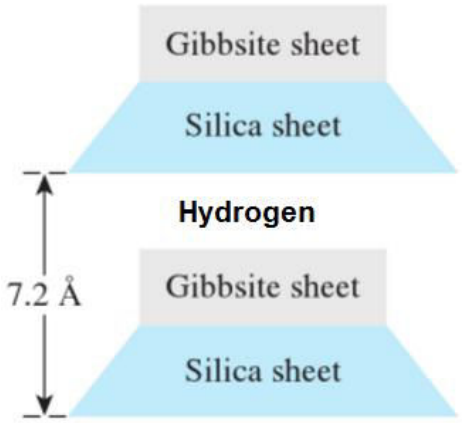

Figure 2.4 Simple structure of Kaolinite (from Craig, 2004).

2.2.2 Particle size distribution and Atterberg limits

Laser diffraction particle size analyser (Malvern Mastersizer 2000®) was used to determine the particle size distribution of the two soils. Figure 2.5 show particle size distribution for clay A and clay B. Clay A contains about 85% of clay particles (smaller than 0.002 mm) and 15% of silt particles (smaller than 0.02 mm). Clay B is composed of about 72% of silt particles (smaller than 0.02 mm) and the remaining particles (25.5%) are smaller than 0.08mm.

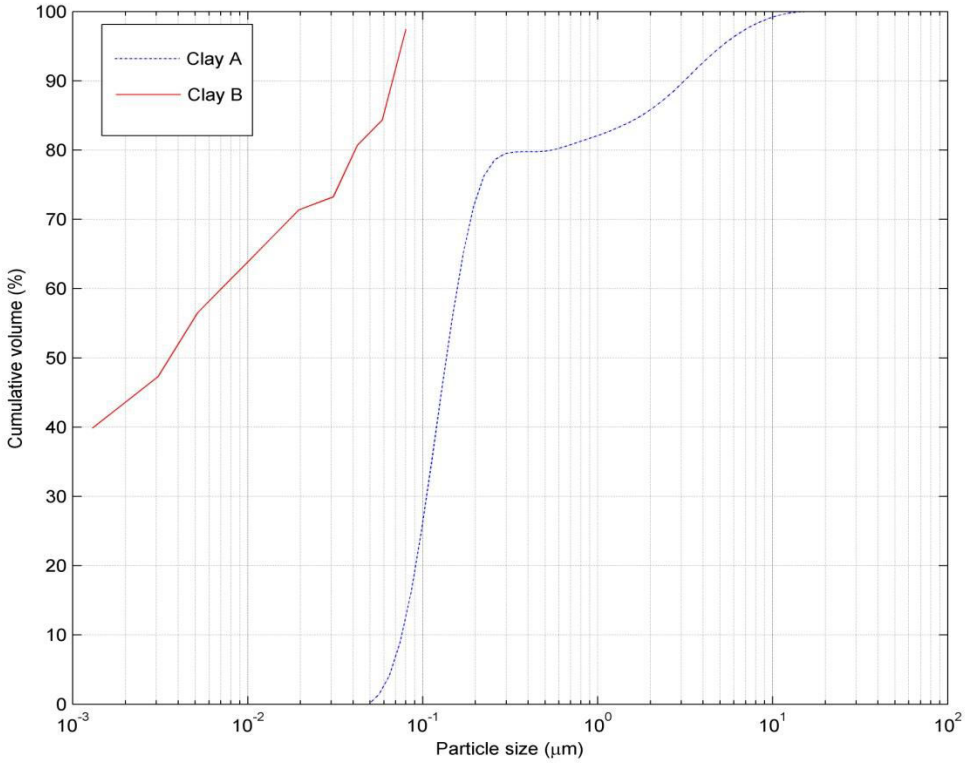

Figure 2.5 Particle size distribution of clay A and clay B.

Atterberg limits (AFNOR, 1993) for studied clays were determined (Table 2.2). According to the particle size distribution and Atterberg limit, the classification of clay A according to the French standard for soil classification (GTR, 2000) is A3. However, it is classified as fat clay, and CH in accordance with the Unified Soil Classification System (Standard ASTM, 2006). On the other hand, the classification of clay B according to the French standard for soil classification (GTR, 2000) is A2. However, it is classified as lean clay, and CL in accordance with the Unified Soil Classification System (Standard ASTM, 2006).

Table 2.2 Atterberg limits of studied clays.

	Clay A	**Clay B**
Liquid limit (w_L)	65.0%	43.5%
Plastic limit (w_p)	34.0%	19.7%
Plasticity index (I_p)	31.0%	23.8%
Specific gravity (G_s)	2.65	2.65

2.2.3 Compaction characteristics

To determine the maximum dry density at optimum water content for studied clays, Proctor compaction test (AFNOR, 1999) was performed. Different samples were prepared at different water contents using a mechanical mixer. The samples were stored for 24 hrs to achieve good

homogeneity. After that, the samples were compacted dynamically using a mechanical compactor at a given compactive effort. The compaction process was performed based on the recommendations of Proctor compaction test NF P94-093: AFNOR (1999). The samples were compacted in 3 layers with 56 blows per layer in a compaction mold with size of 15.2 cm diameter × 11.7 cm height. The data points obtained from the compaction of several samples at different water content forms the compaction curve are shown in Figure 2.9 and Figure 2.10 for clay A and clay B respectively.

The maximum dry density of clay A was 1.43 Mg/m^3 at the optimum water content of 31.3%. The compaction curve (Figure 2.6) shows that the dry density varies from 1.22 to 1.43 Mg/m^3. On the other hand, the maximum dry density of clay B was 1.74 Mg/m^3 at the optimum water content of 16.5%. The compaction curve (Figure 2.7) shows that the dry density varies from 1.63 to 1.74 Mg/m^3.

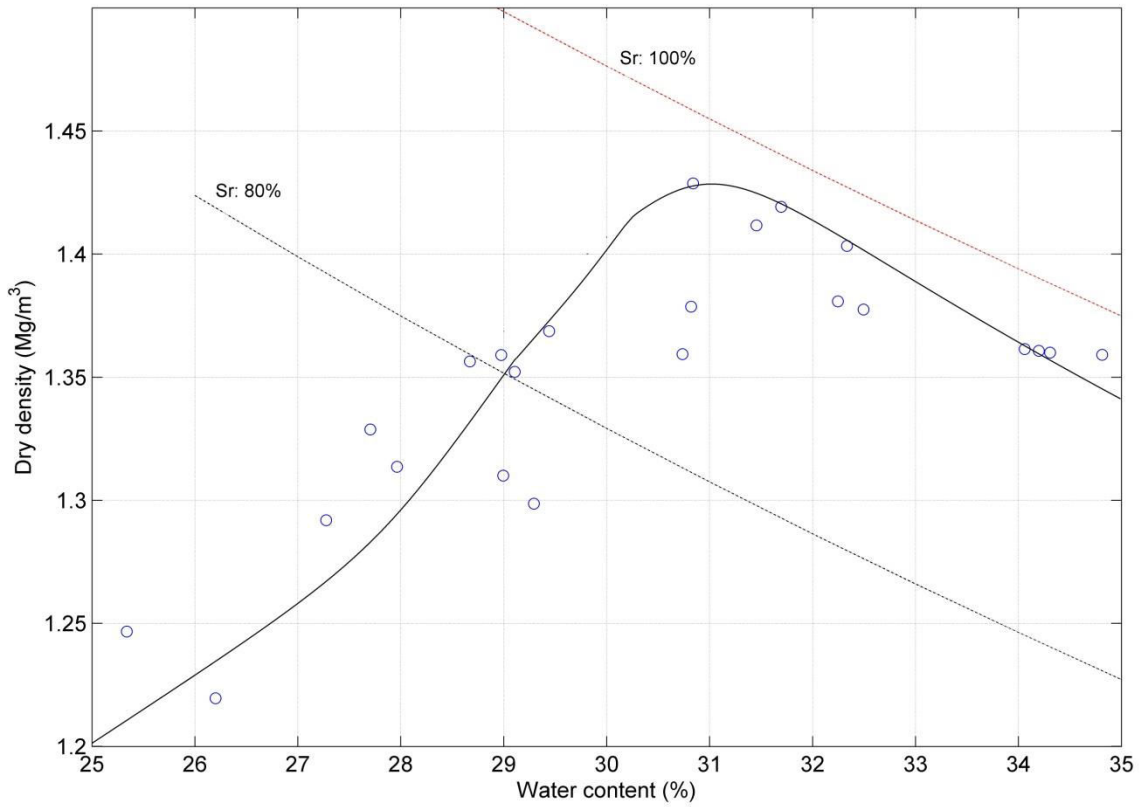

Figure 2.6 Compaction curve of clay A.

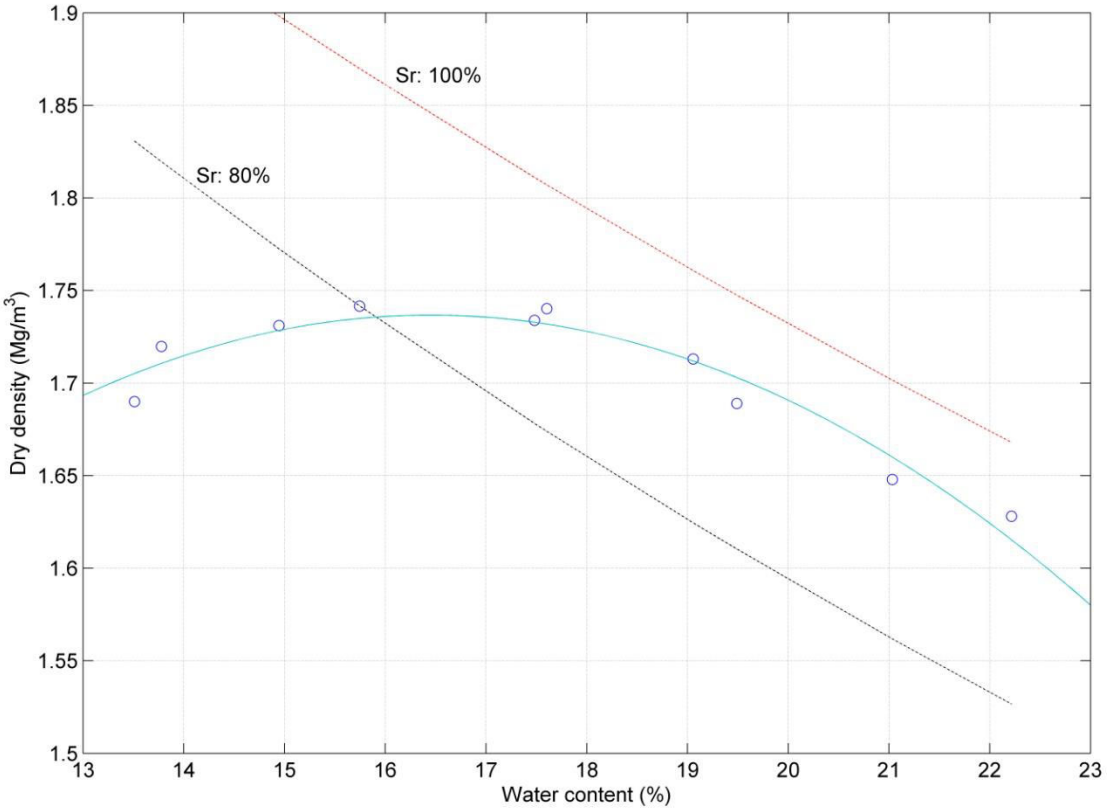

Figure 2.7 Compaction curve of clay B.

2.3 Temperature controlled oedometric cell

This section describes the experimental device used in this research. It presents an overview of the oedometric cell. The experimental device system including the mechanical, hydraulic and thermal systems are presented. In addition, the calibration of the oedometric device deformation due to temperature variations is presented.

2.3.1 Overview of the oedometric cell

The oedometric cell is designed to resist high temperatures up to 90° C, and to reach maximum axial stress up to around 5000 kPa. The main parts of the oedometric cell are cell base, sample room, pressure piece (piston), water room, water connections, hydraulic and thermal connections, and bracket and support of settlement sensor (see Figure 2.8).

One ceramic porous stone (pore size of 100 μm) locates at the base of the cell (underneath the sample), while the second porous stone is connected to the pressure piece (top of the sample). The o-ring was fitted in the groove around the ceramic filter plate in the cell base to prevent water seepage. The cell base contains two drainage lines, one of them extends to the center of the base (underneath the porous stone), and the other extends to the edge of porous stone (underneath).These lines are used for flushing air out, saturation, and pore pressure measuring.

The water room is separated from the sample room by the porous stone, and connects to the water connections at the top of the cell.

The sample room has a sample surface area of 40 cm^2 (sample diameter of 71.4 mm) with sample height of 20 or 40 mm. The maximum water pressure inside the cell does not exceed 15 MPa.

The oedometric cell is installed into the load frame after assembly. A shear-free connection between the cell and the test press was available. Connections between pressure generator, test cell and pressure monitor were set up.

The oedometric cell is used to perform compression tests, shrink swell tests and porosity tests on cohesive and non-cohesive soils in saturated or unsaturated cases (soil/water system or soil/water/air system). Accordingly, the tests which can be performed are incremental loading, continuous loading, constant rate of loading, constant gradient, constant pore pressure ratio, and constant rate of strain tests. The constant rate of strain and incremental loading tests on saturated cohesive soils were used in this study.

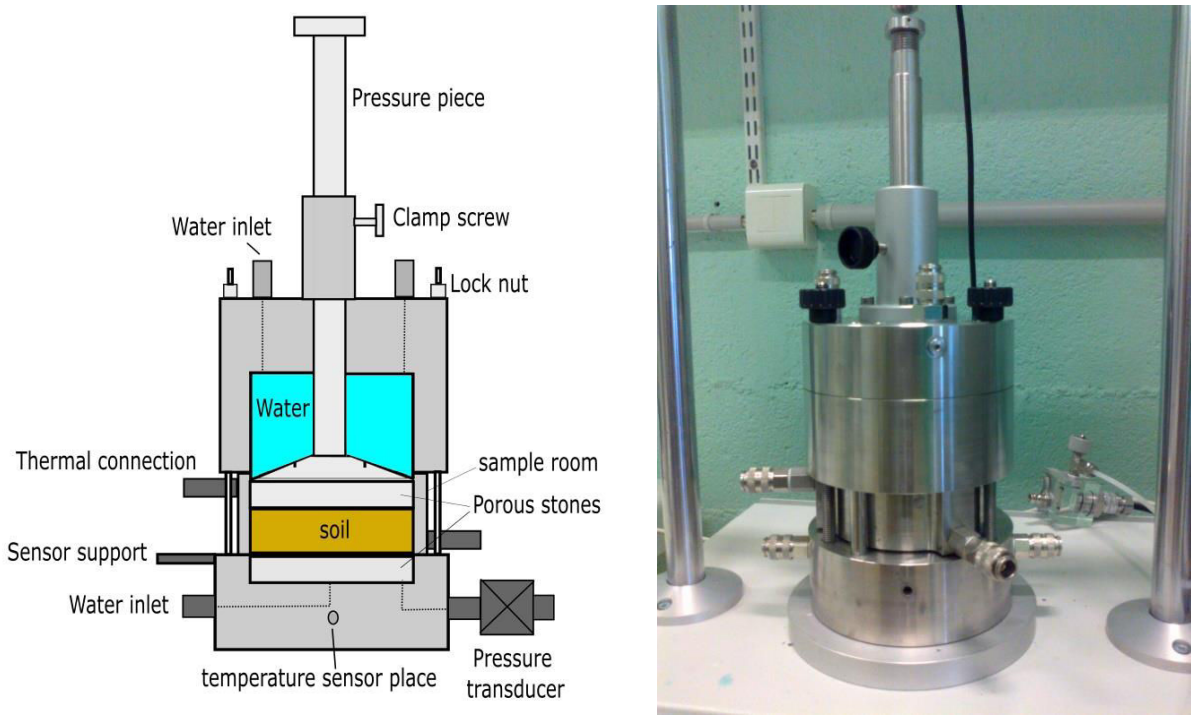

a) b)

Figure 2.8 (a) Schematic diagram of the oedometric cell (b) photograph of the oedometric cell.

2.3.2 Overview of the experimental device systems

A schematic diagram for the modified temperature controlled oedometric cells is shown in the Figure 2.9. The whole system includes the main following parts:

- load frame,
- oedometric cell,
- temperature device,
- and water injector (GDS).

The systems of the device include three coupled systems of working during testing, and all data of sensors are stored in the data logger, and then are displayed on the PC. These systems of working are,

- mechanical system,
- hydraulic system,
- thermal system.

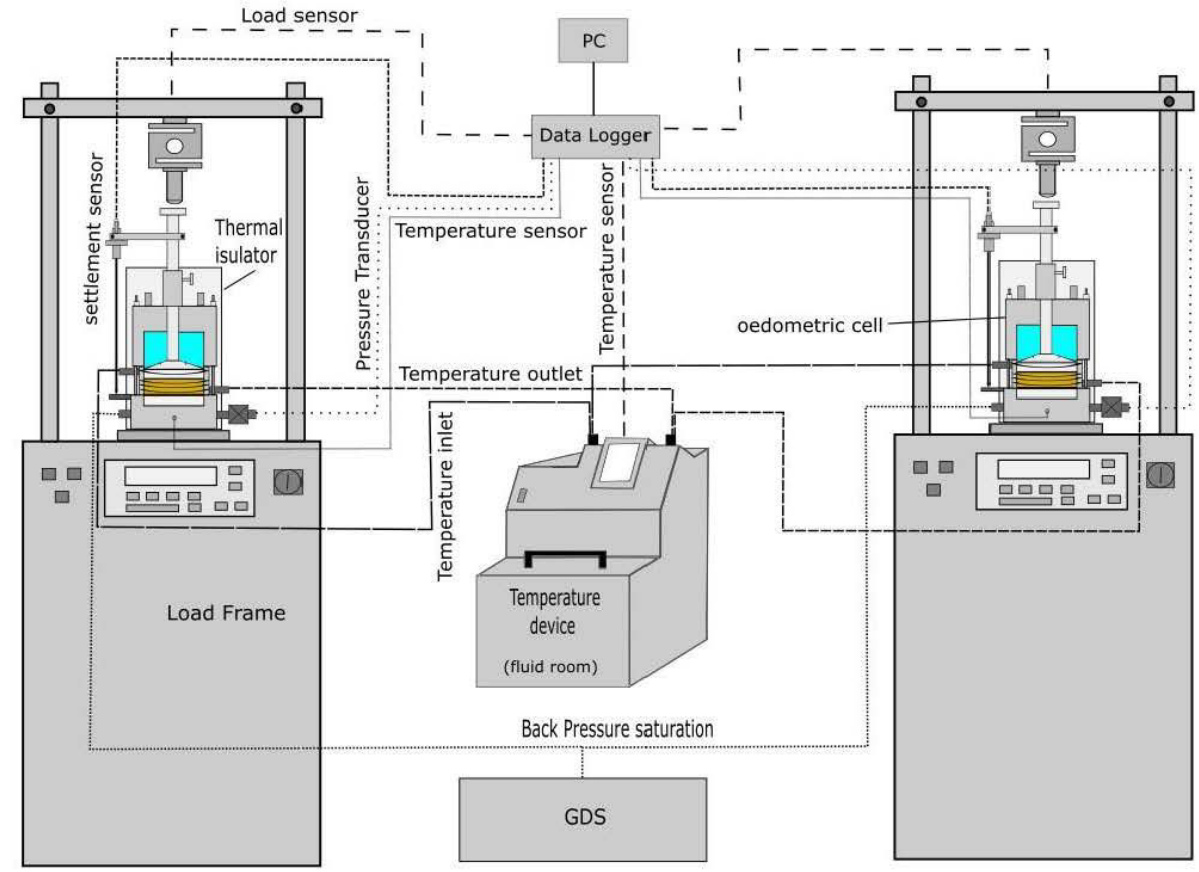

(a)

(b)

Figure 2.9 (a) Schematic diagram for the modified temperature controlled oedometric cell system (b) Photograph for the modified temperature controlled oedometric cell system.

A) Mechanical system

An external load is applied to the pressure piece of the oedometric cell using the load frame to generate a load on the specimen. The vertical deformation of the specimen can be measured by observing the movement of the settlement sensor stem which moves in parallel to the movement of pressure piece during loading.

Load frame

The basic apparatus of the load frame consists of a load frame to support loads up to 25 kN, electrical motor drive, electrical control system, and integrated electronic load regulator. In addition, an external path sensor is required for the operation of path regulation. The load frame can be operated (manually or using PC-remote control) in three cases:

- tests with constant velocity (up to 10mm/min),
- tests with load regulations (constant or linear increasing load),
- tests with path regulation (constant position).

In this study, the velocity controlled mode was utilized. In this mode, the drive receives a set speed which remains constant until cancelled. The sample yield path and load results represent the current conditions during testing and results in responses at the monitoring PC or through monitoring limiting values.

B) Hydraulic system

The main elements of the hydraulic system include the water injector, the pore pressure transducer, oedometric cell water room, and water connections (Figures 2.8 and 2.9). Water injector (GDS) is used as a water supply to saturate the sample by applying back pore water pressure, and it is fitted to the bottom water connector.

Pore pressure transducer

The pore water pressure which is generated by increasing the applied load or the back pressure can be measured through a cell pressure transducer which is connected to the pore water connector (underneath the sample). It measures the pore pressure at the base of the sample and the pore pressure ranges are from 0.1 to 2 MPa. A special de-airing unit is used for the avoidance of bubble inclusions, which would disturb a precised and correct pressure measurement. In addition, an incorporated built-in amplifier is used to remove any electrical influence on the measuring signals.

C) Thermal system

The thermal system is working independently from the mechanical and hydraulic systems in order to regulate and monitor the temperature of the testing specimen. The main elements of the thermal system include the temperature device, the thermal chamber of the sample, and the thermal isolator, in addition to the thermal sensor.

Temperature device

The temperature device has dimensions of 255 x 450 x 476 mm and weight of 35kg. It has a powerful pressure/suction pump with a controlled rotational speed that ensures optimal circulation. The pressure pumb max power is 27 l/min (0.7 bar) while the suction pump max power is 20 l/min (0.4 bar). The temperature device can be operated in the temperature range from -40° to 80° C within temperature stability of ±0,02 °C. It has a heating capacity of 2 kW and its cooling capacity varies with temperature value. The permissible ambient temperature for working is within the range between 5 and 40°C.

Thermal chamber of the sample

The thickness of the sample room contains a thermal spiral tube in which the thermofluid circulates around the sample to heat or cool the soil. The spiral tube is connected to the thermic inlets which are connected to the insulated thermal tubes of the temperature device (Figure 2.9). Figure 2.10 shows the description of the thermal chamber of the sample.

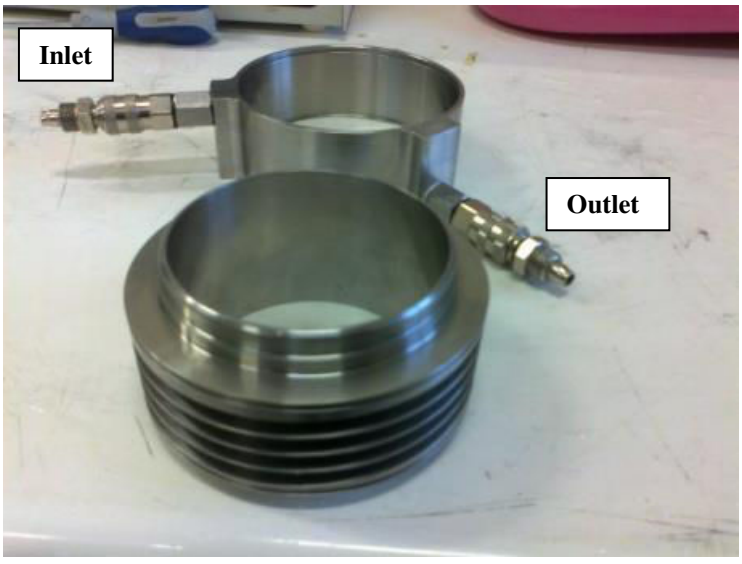

Figure 2.10 Thermal chamber of the sample.

Themal process

The temperature device supplies a thermal fluid to the sample of the oedometric cell through insulated tubes to control the sample temperature. The thermal fluid circulates through these tubes from the device to the cell and vice versa to keep a constant temperature. The temperature can be controlled through the control unit of the temperature device. A thermal isolator is used to cover the oedometric cell as shown in Figure 2.9 to minimize heat loss. The actual temperature of the sample is measured by a temperature sensor, and the way of measurement is described later (section 2.5.2).

2.3.3 Calibration of Oedometric device deformation due to temperature variations

The calibration required to correct measurement errors due to the temperature effects on the testing apparatus is one of the main problems encountered with thermo-mechanical experimental devices (Tang et al., 2007; François and Laloui, 2010). To determine the cell's deformability due to temperature variations, a cell deformation-temperature-relationship was determined. The thermal deformation of the oedometric cell was observed by measuring the vertical displacement of the piston during cycles of heating and cooling. The heating cycle was from 20°C to 75°C in steps of 10°C, and the cooling cycle was from 20°C to 0.1°C in three steps at 10.0°C, 5.0°C and 0.1°C. Figure 2.11 shows the relationship between the measured thermal vertical displacement of the oedometric cell and the applied temperature to the cell. A linear equation can be approximated to determine the thermal vertical displacement of the oedometric cell, $\Delta h_{T(cell)}$, at different temperatures as follows:

$$\Delta h_{T(cell)} = -0.0027 \Delta T \quad \textbf{(2.1)}$$

where $\Delta h_{T(cell)}$ in mm.

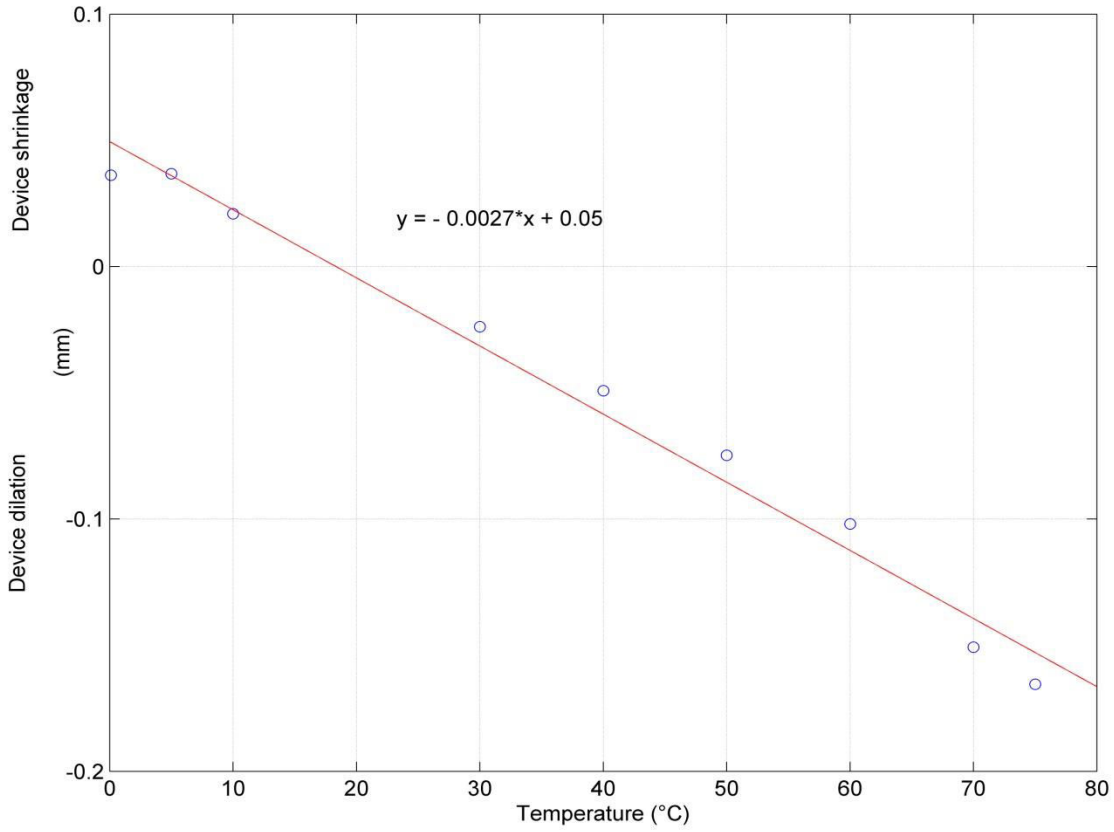

Figure 2.11 Oedometric cell vertical deformation due to temperature variations.

Generally, the heating cycle causes dilation in the oedometric cell, while the cooling causes a contraction in the cell. The abovementioned relationship was used to evaluate the effect of the thermal deformation of the oedometric cell on the measured vertical displacement of the sample. These evaluated thermal deformations of the cell would be useful to obtain the correct measurements of the sample deformation during temperature variations. Accordingly, the actual thermal deformation of the sample will be according to the following:

$$\Delta h_{T(sample)} = \Delta h_{T(measured)} - \Delta h_{T(cell)} \quad (2.2)$$

where $= \Delta h_{T(measured)}$ is the measured total displacement during heating or cooling phases.

2.4 CRS test

2.4.1 Introduction

The constant rate or strain consolidation test is considered as one of the fast consolidation tests for determining the consolidation characteristics of cohesive soils. It was first performed by Hamilton and Crawford (1959) and Crawford (1964) as a rapid method for measuring the preconsolidation pressure. The main advantage of this test over the classical incremental

oedometer test is that it is faster than the conventional oedometer test (Gorman, 1981; Gonzalez, 2000; Shimizu and Imamura, 2001). On the other hand, it is difficult to distinguish the secondary compression using this method. In addition, more attention for selection of suitable strain rate is required before starting the test to obtain meaningful data (Gorman, 1981; Gonzalez, 2000).

2.4.2 CRS test method

In this test, the sample is located between two porous stones. The drainage is prevented from one side (typically at the base) and the other side is free for drainage. The sample is saturated with a back pore pressure before starting the test. After full saturation, the sample is loaded axially at a constant rate of deformation. During deformation, the time, deformation, reaction load, and the generated excess pore pressure at the base are recorded. A standard test consists of loading phase, constant load phase (excess pore pressure return to zero), and unloading phase. The constant strain rate value is selected to generate pore pressure equal to 3% to 15% relative to total stress.

2.4.3 CRS test theories

A theoretical solution for the test was first developed by Smith & Wahls (1969). Afterwards, a complete theory for the test was developed by Wissa et al. (1971). Some researchers take into consideration the large strain effect (Umehara & Zen, 1980; Lee, 1981). Generally, CRS test theories can be divided into small strain theory and large strain theory.

A. Small strain theory

Smith and Wahls (1969)

A theoretical solution was proposed by Smith and Wahls (1969) to evaluate both magnitude and rate of consolidation. The mathematical modeling of this test is similar to the Terzaghi's one dimensional theory. The basic model depends on the following assumptions:

1. The soil is both homogeneous and saturated.
2. The water and solids are incompressible.
3. Darcy's law is applied for flow through the soil.
4. The drainage occurs only in the vertical direction.
5. The total and effective stresses are uniform along a horizontal plane.

The basic equation of consolidation based on the continuity of flow through a soil element is used:

$$\frac{d}{dz}\left(\frac{k}{\gamma_w}\frac{du}{dz}\right) = \frac{1}{1+e}\frac{de}{dt} \quad \textbf{(2.3)}$$

where k, u, $\boldsymbol{\gamma_w}$, e, z, t are the coefficient of permeability, the pore pressure, The unit weight of water, The void ratio, depth, and time respectively.

The coefficient of permeability is considered as a function of the average void ratio (ē) of the sample, k becomes only time dependent but independent of position. The void ratio varies linearly with depth. The assumption appears correct for the relatively thin samples that were used in consolidation tests with relatively slow rates of deformation. Eq. 2.3 becomes:

$$\frac{k}{\gamma_w}\frac{d^2u}{dz^2} = \frac{1}{1+e}\frac{de}{dt} \quad \textbf{(2.4)}$$

The rate of volume change and the rate of vertical strain in this test are constant and can be represented as:

$$\frac{dV}{dt} = -RA \quad \textbf{(2.5)}$$

where V, R, and A are volume of the sample, constant rate of deformation, and the sectional area of the specimen respectively.

The rate of change of average void ratio according to Eq. 2.5 is:

$$\frac{d\bar{e}}{dt} = \frac{1}{V_s}\frac{dV}{dt} = -\frac{RA}{V_S} = -r = constnt \quad \textbf{(2.6)}$$

where V_s is the volume of solids.

And ē can be expressed as

$$\bar{e} = \frac{1}{H}\int_0^H e\ dz \quad \textbf{(2.7)}$$

where H is the sample height.

According to Eq. 2.6 and 2.7, the void ratio as a function of time and depth can be written as a linear function of time as the following,

$$e(z,t) = g(z)t + e_o \quad \textbf{(2.8)}$$

where g (z) is a function of depth only and e_o is the initial void ratio.

A linear function is considered and Eq. 2.8 becomes,

$$e = e_o - rt\left[1 - \frac{b}{r}\left(\frac{z-0.5H}{H}\right)\right] \quad \textbf{(2.9)}$$

where b is a constant and it depends on the variation of void ratio with depth and time.

The ratio b/r refers to the variation of void ratio with depth. At the base of the sample, eq. 2.9 becomes,

$$e_B = e_o - rt\left[1 - \frac{1}{2}\left(\frac{b}{r}\right)\right] \quad \textbf{(2.10)}$$

In Eq. 2.10, if b/r equal 2, the void ratio at the base remains constant. If b/r equal 0, the void ratio becomes uniform with depth. The practical range of b/r is between 0 and 2.

Eq. 2.4 can be solved by integrating twice with respect to z and by using eq. 2.9 and using boundary conditions:

$$\text{u(0, t)} = 0 \;\&\; \frac{du}{dz}\,(H, t) = 0$$

If b/r = 0, the pore pressure is:

$$u = \frac{\gamma_w r}{k(1+\bar{e})}\left[Hz - \left(\frac{z^2}{2}\right)\right] \quad \textbf{(2.11)}$$

If b/r is not equal to 0, the pore pressure is:

$$u = \frac{\gamma_w r}{k}\left\{zH\left(\frac{1+e_o-bt}{rt(bt)}\right) + \frac{z^2}{2rt} - \left[\frac{H(1+e_o)}{rt(bt)}\right]\left[\frac{H(1+e)}{bt}\ln(1+e) - zln(1+e_B) - \frac{H(1+e_T)}{bt}\ln(1+e_T)\right]\right\} \quad \textbf{(2.12)}$$

where

$$e_T = e_o - rt\left[1 + \frac{1}{2}\frac{b}{r}\right] \quad \textbf{(2.13)}$$

To simplify Eq. 2.12, it is suggested to replace the term (1+e) in eq. 2.4 by (1+ $\bar{e}$) and $\bar{e}$ is not a function in z, pore pressure becomes:

$$u = \frac{\gamma_w r}{k(1+\bar{e})}\left[\left(Hz - \frac{z^2}{2}\right) - \frac{b}{r}\left(\frac{z^2}{4} - \frac{z^3}{6H}\right)\right] \quad \textbf{(2.14)}$$

At z=H, the pore pressure at the base is:

$$u_b = \frac{\gamma_w r H^2}{k(1+\bar{e})}\left[\frac{1}{2} - \frac{b}{r}\left(\frac{1}{12}\right)\right] \quad \textbf{(2.15)}$$

An expression for effective stress was suggested by Smith and Wahls (1969) which is in terms of total stress, and base pore pressure as the following,

$$\sigma' = \sigma - \alpha\, u_b \tag{2.16}$$

where σ is the total stress, and α is the ratio between the average pore (ū) pressure to the base pore pressure u_b and can be expressed from eq (2.14) and (2.15) as:

$$\alpha = \frac{\bar{u}}{u_b} = \frac{\frac{1}{H}\int_0^H u dz}{u_b} = \frac{\frac{1}{3} - \frac{b}{r}\left(\frac{1}{24}\right)}{\frac{1}{2} - \frac{b}{r}\left(\frac{1}{12}\right)} \tag{2.17}$$

Using the Terzaghi definition of the coefficient of consolidation (c_v) which is:

$$c_v = \frac{k(1+e)}{a_v \gamma_w} \tag{2.18}$$

where a_v is the coefficient of compressibility.

and the eq. (2.15) to find k, and replacing e by ē, and substitution to eq. (2.18), the coefficient of consolidation becomes:

$$c_v = \frac{rH^2}{a_v u_b}\left[\frac{1}{2} - \frac{b}{r}\left(\frac{1}{12}\right)\right] \tag{2.19}$$

Wissa et al. (1971)

Wissa et al. (1971) proposed a theoretical solution including both initial transient and steady state phases of the constant strain rate test. They used the basic equation of consolidation:

$$c_v \frac{d^2\varepsilon}{dz^2} = \frac{d\varepsilon}{dt} \tag{2.20}$$

where $\boldsymbol{c_v = k/\gamma_w m_v}$, $\boldsymbol{c_v}$,$\boldsymbol{\varepsilon}$,$\boldsymbol{z}$, t, $\boldsymbol{k}$, $\boldsymbol{\gamma_w}$, and $\boldsymbol{m_v}$ are coefficient of consolidation, vertical strain, the vertical coordinate of a point, time, permeability, unit weight of water, and coefficient of volume compressibility respectively.

They considered that the coefficient of consolidation is depth independent and the ratio k/m_v is also depth independent.

To solve eq. 2.20, they used the following parameters,

$$X = \frac{z}{H}; T_v = \frac{c_v t}{H^2} \tag{2.21}$$

where H is the sample height.

The solution of eq. 2.20 gives the strain as a function of depth and time,

$$\varepsilon (X,T_v) = rt[1+F(X, T_v)] \quad \textbf{(2.22)}$$

where r is the strain rate and,

$$F(X, T_v) = \frac{1}{6T_v}(2\text{-}6X+3X^2) - \frac{2}{\pi^2 T_v}\sum_{n=1}^{\infty}\frac{cosn\pi X}{n^2}\exp(-n^2\pi^2, T_v) \quad \textbf{(2.23)}$$

The first part of eq. 2.23 represents the average strain (the strains everywhere in the sample are the same). The second part consists of two parts as shown in eq. 2.23. The first part is the deviation from the average strain in the steady state condition and it is time independent (it exists to provide a necessary gradient for constant flow of pore fluid). The second part represents the transient condition of the solution at the beginning of the test.

Figure 2.12 shows the development of the strains at early times until it becomes steady by $T_v = 0.5$.

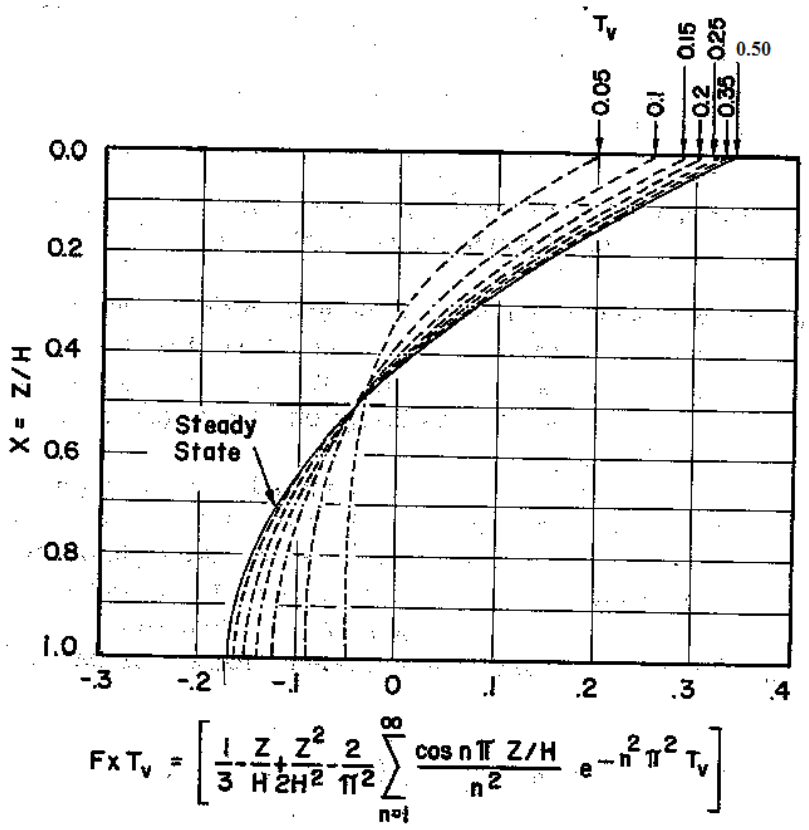

Figure 2.12 Deviation of strain from its average as a function of depth for different time factors (from Wissa et al., 1971).

Steady state conditions

After the dissipation of transients, Eq. 2.22 and 2.23 become:

$$\varepsilon\,(z,t) = rt + \frac{rH^2}{c_v}\left\{\frac{1}{6}\left[3\left(\frac{z^2}{H}\right) - 6\frac{z}{H} + 2\right]\right\} \quad \textbf{(2.24)}$$

By applying the boundary conditions, the strain difference between the top and the bottom of the sample at any time is $\frac{rH^2}{2c_v}$. At any position, the difference at any two times is r (t_2-t_1).

The difference between the vertical effective stress at the top and the bottom of the sample is,

$$\Delta\sigma' = u \quad \textbf{(2.25)}$$

where the effective stress at the top is σ and at the bottom is $\sigma - u$. If the soil is assumed linear, i.e., the relation between stress and strain is defined by a constant coefficient of volume compressibility,m_v:

$$\Delta\sigma' = \frac{\Delta\varepsilon}{m_v} \quad \textbf{(2.26)}$$

The permeability can be evaluated by using eq. 2.26 since the differences of stress and strain between the top and bottom are known:

$$k = \frac{rH^2\gamma_w}{2u} \quad \textbf{(2.27)}$$

At any point, the rate of change of effective stress and distribution of pore pressure are constant because the change of strain is constant. Then, Eq. 2.26 can be rearranged as a function of total stress change:

$$m_v = \frac{\Delta\varepsilon}{\Delta\sigma} = r\frac{\Delta t}{\Delta\sigma} \quad \textbf{(2.28)}$$

The coefficient of consolidation can be expressed as:

$$c_v = \frac{H^2}{2u}.\frac{\Delta\sigma}{\Delta t} \quad \textbf{(2.29)}$$

To investigate the validity of the linear assumption of stress strain relation, plot the values of total stress at the top and bottom against the related strains:

$$\varepsilon\,(0,t) = rt + \frac{rH^2}{3c_v} \text{ and } \varepsilon\,(H,t) = rt - \frac{rH^2}{6c_v} \quad \textbf{(2.30)}$$

If the soil is assumed nonlinear, i.e., the relation between stress and strain is non linear or non linear void ratio e then:

$$-\frac{de}{d(log\Delta\sigma')} = c_c \quad \textbf{(2.31)}$$

where c_c is the compression index. A new expression for small strains called strain index:

$$c_{\varepsilon} = \frac{-d\varepsilon}{d(log\Delta\sigma')} = \frac{c_c}{1+e} \quad \textbf{(2.32)}$$

Eq. 2.32 is valid for wider range of material properties than eq. 2.31. By using the boundary conditions, eq. 2.32 can be expressed as,

$$\frac{\varepsilon\,(0,t) - \varepsilon\,(\mathrm{H},t)}{\log(\sigma) - \log(\sigma - u)} = c_{\varepsilon} \quad \textbf{(2.33)}$$

$$\frac{rH^2}{2c_v \log\left(\frac{\sigma - \mathrm{u}}{\sigma}\right)} = c_{\varepsilon} \quad \textbf{(2.34)}$$

The difference at two times at the top surface gives:

$$\frac{r\Delta \mathrm{t}}{\log\left(\frac{\sigma_2}{\sigma_1}\right)} = c_{\varepsilon} \quad \textbf{(2.35)}$$

By comparing eq. 2.34 and eq. 2.35 leads to:

$$c_{\mathrm{v}} = -\frac{H^2 \log\left(\frac{\sigma_2}{\sigma_1}\right)}{2\Delta \mathrm{t} \log\left(1 - \frac{\mathrm{u}}{\sigma}\right)} \quad \textbf{(2.36)}$$

The coefficient of volume compressibility and permeability can be calculated as,

$$m_v = \frac{.434 c_{\varepsilon}}{\sigma'} \quad \textbf{(2.37)}$$

$$k = m_v c_{\mathrm{v}} \gamma_{\mathrm{w}} \quad \textbf{(2.38)}$$

Since the strain has parabolic distribution over the depth of the sample in any case, the average strain is:

$$\varepsilon_{\ avg} = \frac{1}{3}\ [2\ \varepsilon\ (\mathrm{H},t) + \varepsilon\ (0,t)] = \mathrm{rt} \quad \textbf{(2.39)}$$

The average effective stress for linear soil due to the average strain is:

$$\sigma'_{\ avg} = \frac{1}{3}\ [2\ \sigma'\ (\mathrm{H},t) + \sigma'\ (0,t)] = \sigma - \frac{2}{3}u \quad \textbf{(2.40)}$$

The average effective stress for nonlinear soil due to the average strain is:

$$\sigma'_{\ avg} = \frac{1}{3}\ (\sigma^3 - 2\sigma^2 u + \sigma u^2)^{1/3} \quad \textbf{(2.41)}$$

Transient conditions

By using eq. 2.23 to interpret the transient conditions for both stress strain relations at any time, it becomes:

$$\frac{\varepsilon\,(\mathrm{H},t)}{\varepsilon\,(0,t)}=\frac{1+\mathrm{F}\,(1,T_v)}{1+\mathrm{F}\,(0,T_v)}=\mathrm{F}_3(T_v) \tag{2.42}$$

Figure 2.13 shows how to find T_v then c_v with $\mathrm{F}_3(T_v)$.

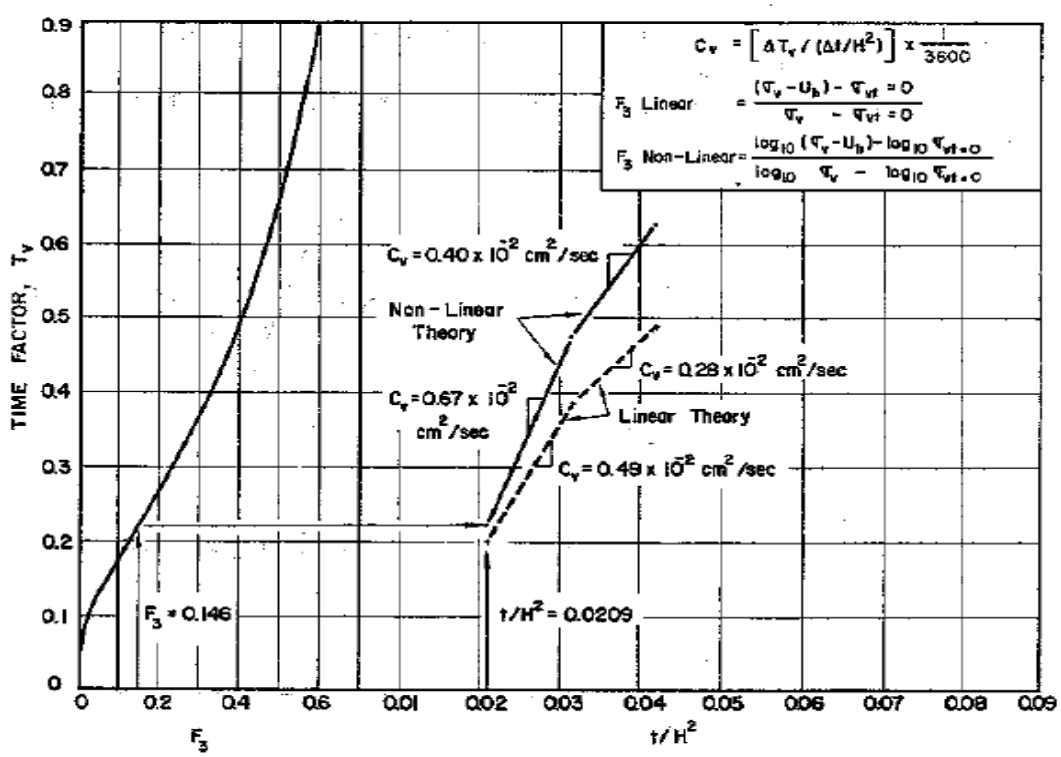

Figure 2.13 Values of c_v during transient condition (from Wissa et al., 1971).

F_3 can be calculated for the linear material as:

$$\mathrm{F}_3=\frac{(\sigma-\sigma_{t=0})-\mathrm{u}}{(\sigma-\sigma_{t=0})} \tag{2.43}$$

where the strain is proportional to the change of effective stress from the beginning of the test until time t. F_3 for nonlinear material is the same but with logarithm change as the following,

$$\mathrm{F}_3=\frac{\log(\sigma-\mathrm{u})-\log(\sigma_{t=0})}{log(\sigma)-log(\sigma_{t=0})} \tag{2.44}$$

By using eq. 2.28 and 2.29, the c_v for linear material is:

$$c_\mathrm{v}=\frac{rH^2}{2um_v} \tag{2.45}$$

And for nonlinear material by using eq. 2.36 and 2.37,

$$c_\mathrm{v}=-\frac{0.434\,rH^2}{2\sigma' m_v \log\left(1-\frac{u}{\sigma}\right)} \tag{2.46}$$

where $\sigma' = \sigma$ for small pore pressure.

So, the ratio between the c_v of linear and nonlinear is,

$$\frac{c_v\ linear}{c_v\ nonlinear} = \frac{\log\left(1-\frac{u}{\sigma}\right)}{0.434\frac{u}{\sigma}} \quad \textbf{(2.47)}$$

Figure 2.14 shows the difference between the linear and nonlinear C_v against the ratio of $\frac{u}{\sigma}$ for small values of $\frac{u}{\sigma}$ only.

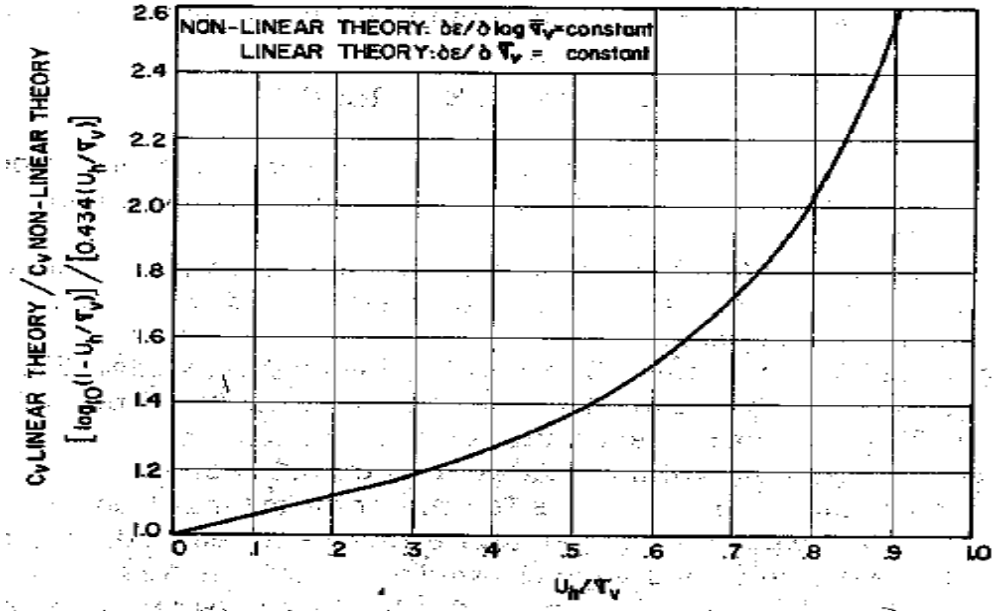

Figure 2.14 The difference between the linear and nonlinear of c_v (from Wissa et al., 1971).

B. Large strain theory

Umehara and Zen (1980)

The large strain consolidation theory developed by Mikasa (1963) was used as a basic for the Umehara and Zen (1980) method. The base equation is:

$$\frac{\partial \xi}{\partial t} = c_v \xi^2 \frac{\partial^2 \xi}{\partial z_0^2} \quad \textbf{(2.48)}$$

where $\xi = \frac{1+e_o}{1+e} = \frac{1}{1-\varepsilon}$, and it is called the consolidation ratio.

The boundary conditions were employed for different values of the parameter $\frac{c_v R}{H_o}$ to solve the equation numerically. Where R is the deformation rate and H_o is the initial thickness of the sample. A series of curves are constructed to determine the coefficient of consolidation and effective stress-void ratio relationship. The consolidation ratio, the strains, and the non-

dimensional parameter $\frac{c_v R}{H_o}$ are the elements of constructed curves. The ratio of the bottom strain to the top strain (used for curves) can be determined as following:

$$F = \frac{\log(\sigma - u) - \log(\sigma_o)}{\log(\sigma) - \log(\sigma_o)} \quad \textbf{(2.49)}$$

where σ_o is the initial effective stress. Figure 2.15 shows the strain distribution inside the sample.

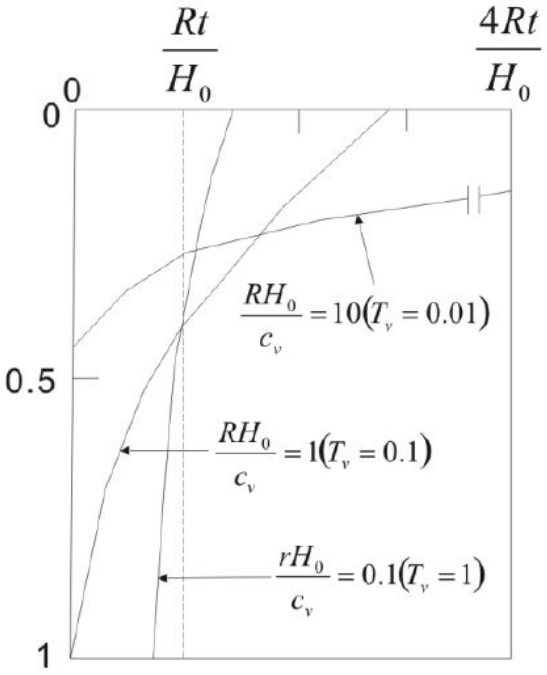

Figure 2.15 Distribution of the strain in the sample (after Umehara and Zen, 1980).

Lee (1981)

Lee (1981) proposed a method depending on the porosity n, and the base equation for his solution as the following,

$$\frac{\partial n}{\partial t} = \frac{\partial}{\partial z}\left(\frac{\partial n}{\partial z}\right) \quad \textbf{(2.50)}$$

where z is the coordinate system, and it is a function of time.

By assuming constant coefficient of consolidation throughout the test, the equation was solved numerically using suitable boundary conditions. Several values of dimensionless parameter $\beta = \frac{rH_o^2}{c_v}$ which represents the normalized strain rate were used in the solution to determine the coefficient of consolidation, and then the effective stress-void ratio relationship. The solution includes transient and steady state conditions. The transient state is treated after Wissa et al.

(1977) analysis. A parabolic distribution of strain within the sample is assumed for steady state conditions, and therefore the coefficient of consolidation can be determined as following:

$$C_V = \frac{H^2}{2u} \cdot \frac{\Delta\sigma}{\Delta t} \quad \textbf{(2.51)}$$

The strain can be determined depending on the obtained coefficient of consolidation value. Figure 2.16 shows the strain distribution inside the sample.

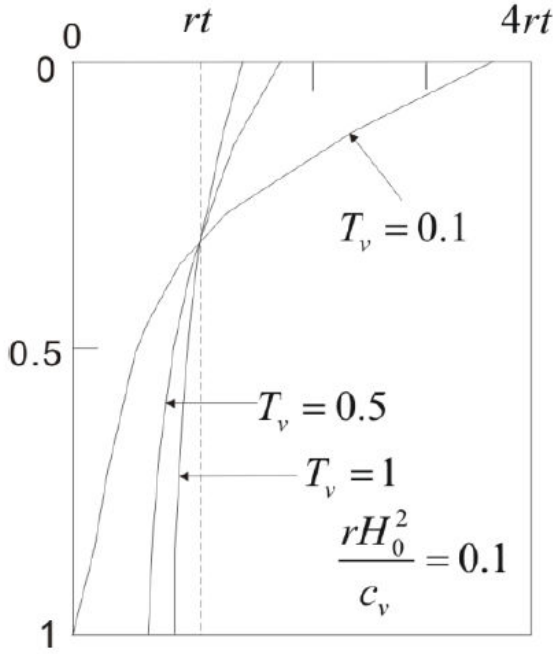

Figure 2.16 Distribution of the strain in the sample (after Lee, 1981).

2.4.4 Strain rate selection

The main question of CRS test is how to select appropriate strain rate for the test materials. Generally, the strain rate selection depends on the liquid limit, pore pressure relative to total stress, permeability, and coefficient of consolidation of the material. If the strain rate is too low, the generated excess pore pressure will be very low so, the results cannot be interpreted by this method. In addition, too high strain rate will cause high hydraulic gradients that do not reflect the field conditions. For Wissa et al. (1971), a value of u/σ lower than or equal to 0.05 seems reasonable for strain rate based on their observations at specific material. ASTM (2008) recommended selecting strain rate in which the ratio of pore pressure relative to total stress within a range between 3% and 15% for different materials.

2.4.5 Conclusion

This section presents the existing theories of CRS test and the interpretation methods of the results. Each theory has specific assumptions based on the strain distribution within the sample

that makes the interpretation method of results different from other theories. CRS test theories can be classified to small strain theory and large strain theory depending on the deformation through time interval. Small strain theory is in the ASTM (2008). Large strain theory deals with the large strain conditions, and this occurs in the very soft clayey soils.

2.5 Experimental procedures

This section shows the experimental procedures followed in this research. It presents the sample preparation method, the actual temperature measurements of the sample and the test phases. The test phases include the saturation phase, the heating phase, and the loading phase.

2.5.1 Sample preparation

The powders of both clayey soils were mixed with distilled water at room temperature to adjust the water content corresponding to the value of the optimum water content (at maximum dry density). The prepared soils were then kept in closed bags for 24 hrs at least to obtain the moisture homogeneity. Samples from the stored slurries were statically compacted into a rigid mold in one layer to form specimens with 71.4 mm diameter and 20 mm height.

The weights of the compacted specimens are representative of the maximum dry density at optimum water content. The average compaction stresses for materials A and B are 467 kPa, and 926 kPa, respectively. At this condition, the initial void ratios of the compacted samples are 0.85 for clay A, and 0.53 for clay B which is denser. The compacted sample was then transferred after releasing the load directly from the compaction mold, which was greased to minimize the side friction, to the oedometric cell.

2.5.2 Temperature measurements of the sample

Due to heat loss in the temperature system because of different external environment, a soil temperature- device temperature -relationship was determined. A saturated compacted sample with dimensions of 71.4 mm diameter, and 20 mm height was used for measurements. The upper part of the sample was protected using an insulator to minimize heat loss beside the thermal insulator of the oedometric cell. To measure the temperature of the sample, the temperature sensor of the device was inserted at the middle of the sample (at depth of 10 mm). The relationship between the device temperature and the sample temperature was determined by running different temperatures. Figure 2.17 explains the procedures of measuring the actual temperature of the soil sample.

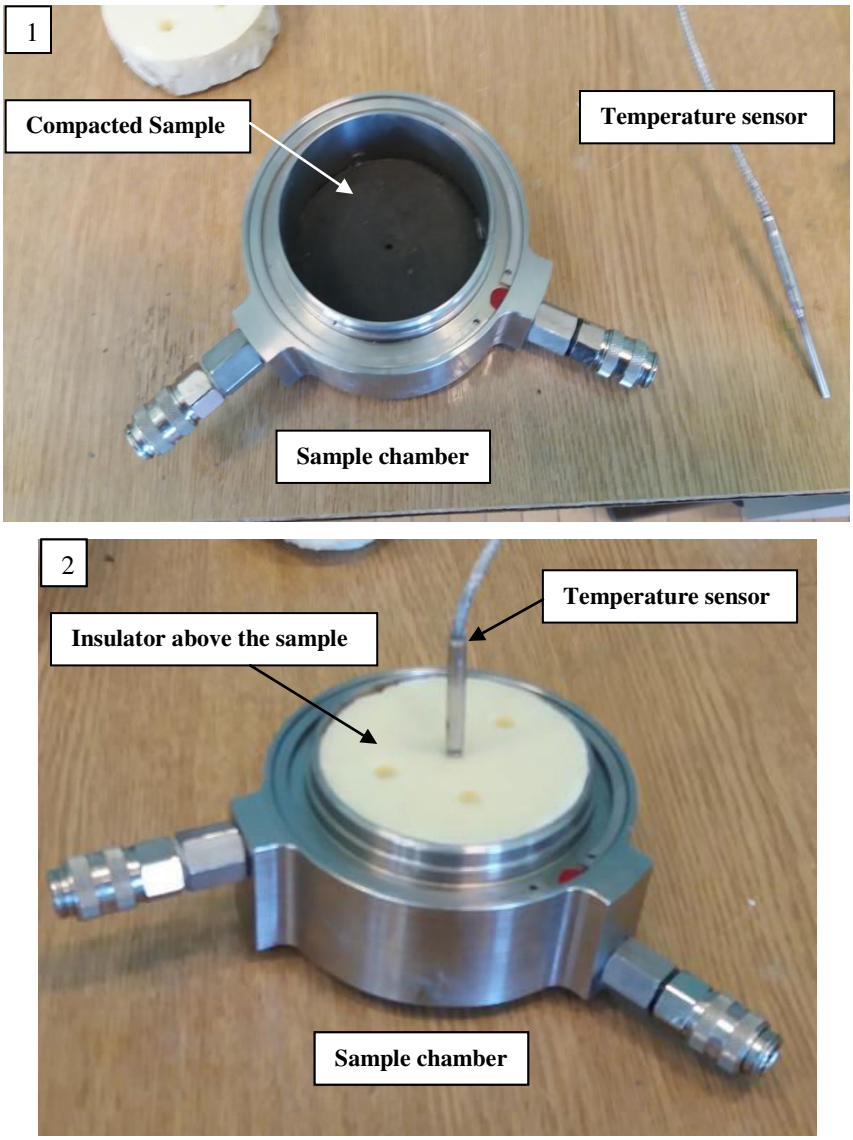

Figure 2.17 (1) Compacted sample inserted in the room. (2) Sample with temperature sensor and the thermal insulator for heating and cooling cycles after installation and saturation.

Figure 2.18 shows the curve that represents the determined relationship. A linear equation for the soil temperature- device temperature -relationship was estimated as follows:

$$\Delta T_{sample} = 0.856 \Delta T_{device} \quad (2.52)$$

According to that relationship, the selected target temperature in the sample can be used for setting the temperature of the device. In addition, all the tests were performed with temperature insulator to minimize heat losses.

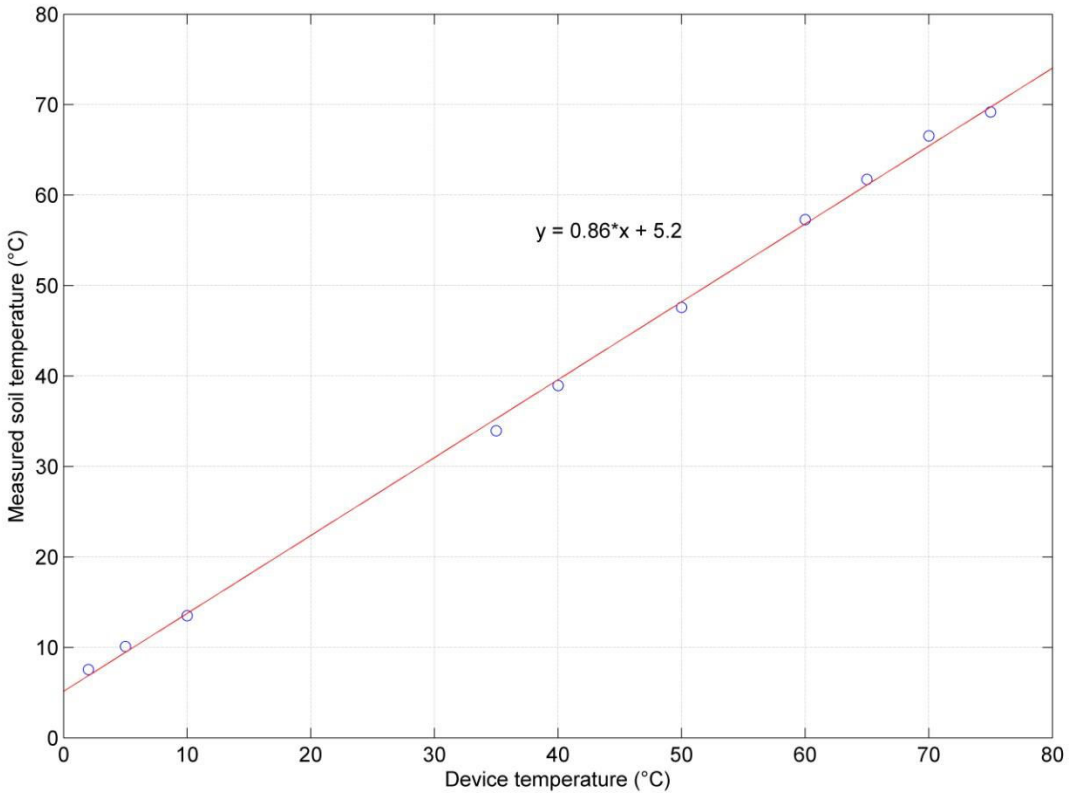

Figure 2.18 Relationship between the temperature of the sample at the middle and the temperature of the device.

2.5.3 Test phases

The main experimental procedures consist of three or four phases which are (i) saturation phase, (ii) over-consolidation phase (for heavily over-consolidated clay), (iii) thermal phase, and finally, (iv) the constant rate of strain consolidation phase.

Saturation phase

Before starting the saturation phase, the sample was loaded vertically under constant vertical stress of 10 kPa. Both porous stones at the bottom and top were saturated, and the air was flushed out from the base and top of the cell. One of the base drainages was closed off for pore water pressure reading, while the top drainage was permitted. A back pore water pressure of 10 kPa was applied through the porous element of the base to saturate the sample. In addition, the water room of the oedometric cell was filled.

The saturation level was checked firstly by measuring the injected water volume as a linear function of time as indicated by Figure 2.19 and Figure 2.20 for clay A and clay B respectively and secondly by measuring the water content of the sample at the end of the phase. The direct measurement of permeability at room temperature (20°C) during saturation for clay A was 1.16×10^{-10} m/s, while it was 5.93×10^{-10} m/s for clay B. The permeability value is consistent with the one obtained with flexible wall permeameters.

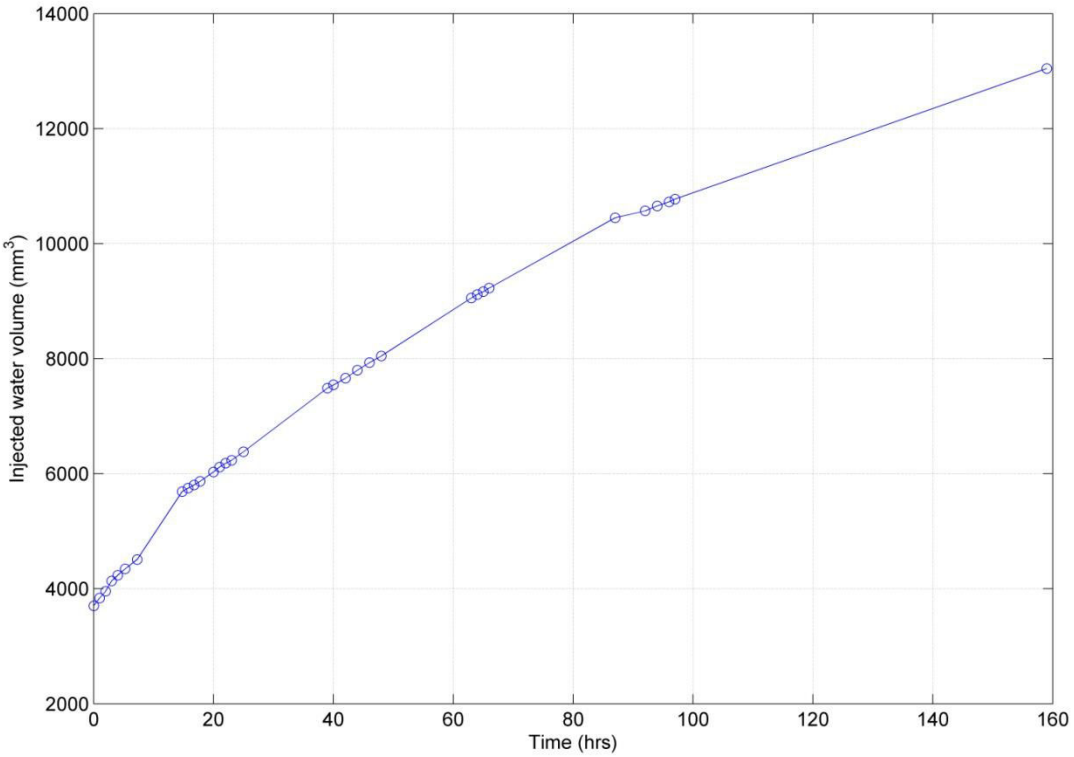

Figure 2.19 Injected water volume-time relationship for clay A.

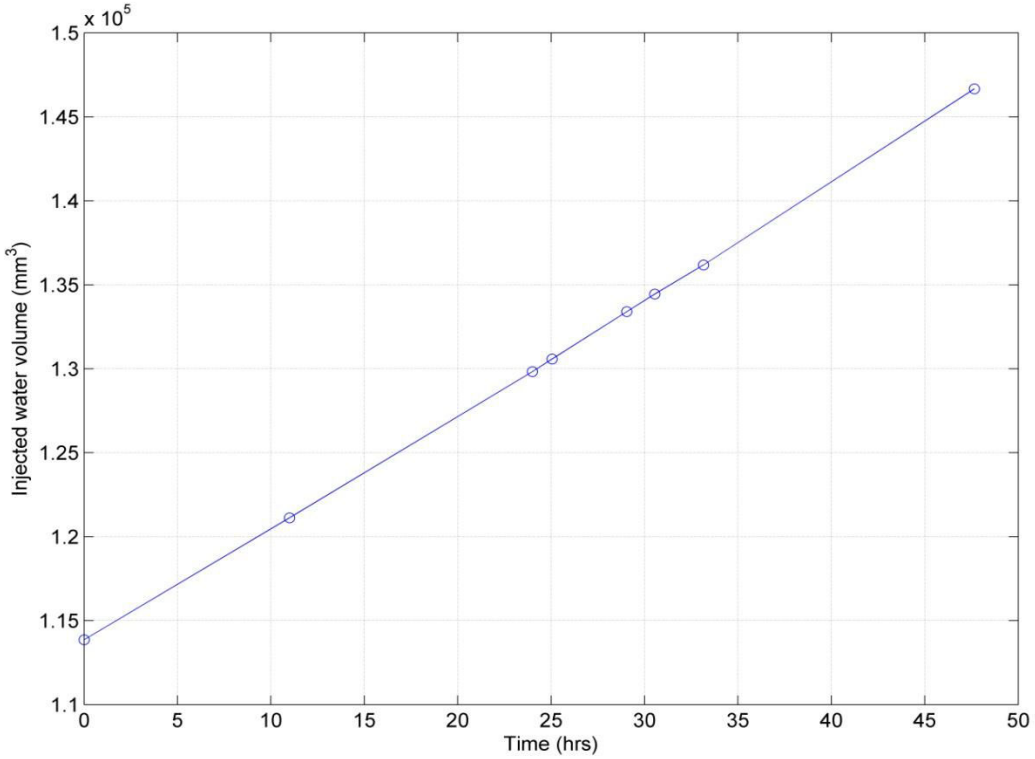

Figure 2.20 Injected water volume-time relationship for clay B after 5 days.

Heating phase

After full saturation (Figure 2.19 and 2.20) with deaired water, and loading-unloading phase for heavily overcosolidated clay, the sample temperature was changed to the desired temperature. The temperature reference is 20° C, and the sample temperature was changed up or down this value in order to observe the temperature effect. The thermal phase was achieved when the deformation variation of the sample was less than ±0.001% after temperature change.

Constant rate of strain (CRS) consolidation test

The constant rate of strain (CRS) consolidation test which is explained in section 2.4 was carried out on the sample according to ASTM (2008) recommendations. In CRS test, the sample is loaded at a constant rate of vertical deformation. Drainage is possible only at the top surface of the specimen. During testing, the excess pore water pressure is generated through the sample with the variation from the maximum at the base until zero at the top surface. The reaction force, axial deformation, and pore water pressure at the base have been measured during the testing at certain time interval. The sample was loaded from 10 kPa until reaching, the maximum fixed value of stress, 5120 kPa.

- Strain rate selection

The strain rate was selected according to the ASTM (2008) recommendations that take into consideration the soil classification. Accordingly, the starting value of strain rate for clay A is 0.002%/min. To observe the strain rate effect on the soil behavior, strain rate values of 5 times and ten times larger than the selected starting value were selected.

Similar procedures followed for clay B, a good starting value of strain rate is 0.02%/min. For the purpose of comparison with clay A and to observe the strain rate effect, strain rate values of 5 times and 10 times lower than the selected starting value were selected. Then, the selected strain rate values for consolidation tests at different temperatures for both materials are 0.002%/min, 0.01%/min, and 0.02%/min.

Summary of test phases

Figure 2.21 shows the schematic diagram for the experimental path of lightly over-consolidated clay for both materials in general.

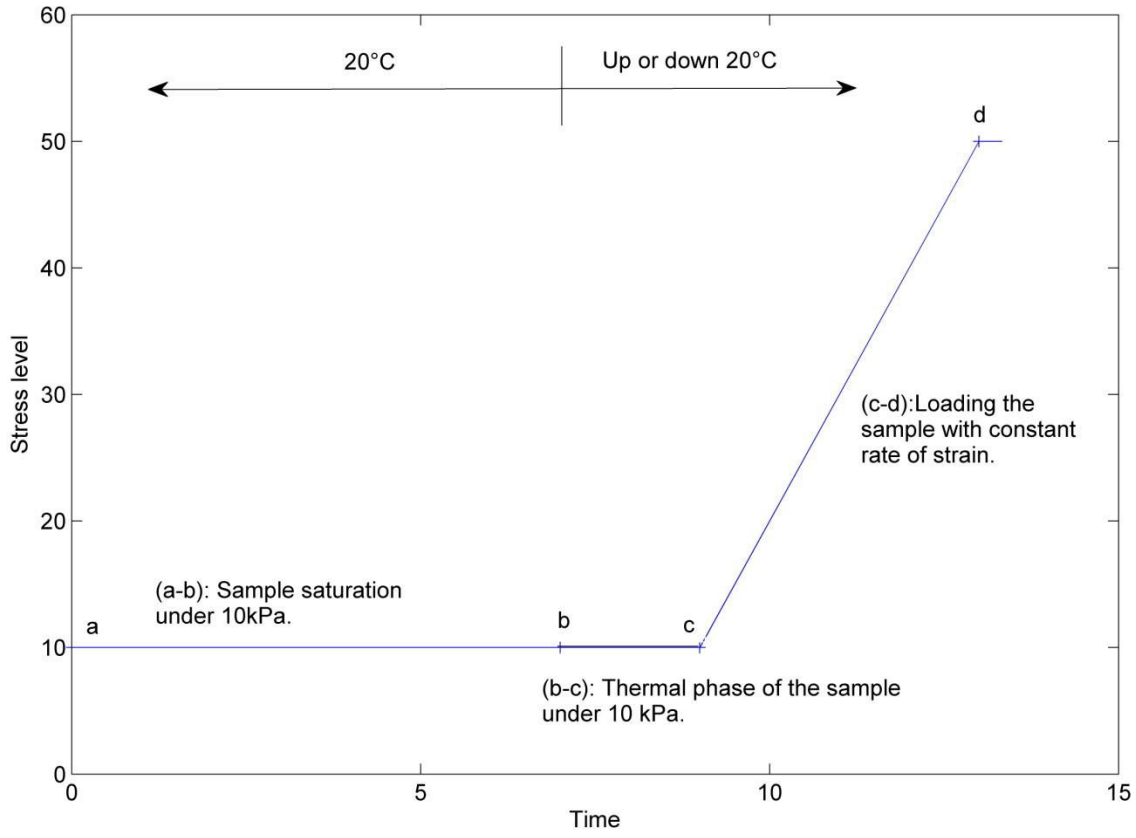

Figure 2.21 Schematic diagram for the experimental path of lightly over-consolidated clay.

2.6 Validation of the results

The following sections show the method used to investigate the validity of the experimental results for both materials, clay A and clay B.

2.6.1 Validation of the results of clay A

The validity of CRS tests results carried out on the illitic clay (clay A) was determined using three factors which are the repeatability of the tests, the comparison with the classical oedometric test, and fulfillment of the criteria recommended by ASTM (2008) based on the relationship between total stress and excess pore water pressure.

A) Repeatability of the tests

Most of the CRS tests performed on illitic clay in this research were repeated under the same conditions. The repeatability of tests can measure the accuracy and validity of tests and its results.

Figure 2.22 and 2.23 show repeated CRS tests for strain rate of 0.02%/min at 70°C and 0.002%/min at 50°C as examples. It is clear from the figures that the repeated tests at given strain rate and temperature have approximately the same consolidation curves, while the

generated excess pore pressure during these tests slightly changed. The difference between two repeated test results is small and this reflects the validity of the results of performed CRS tests.

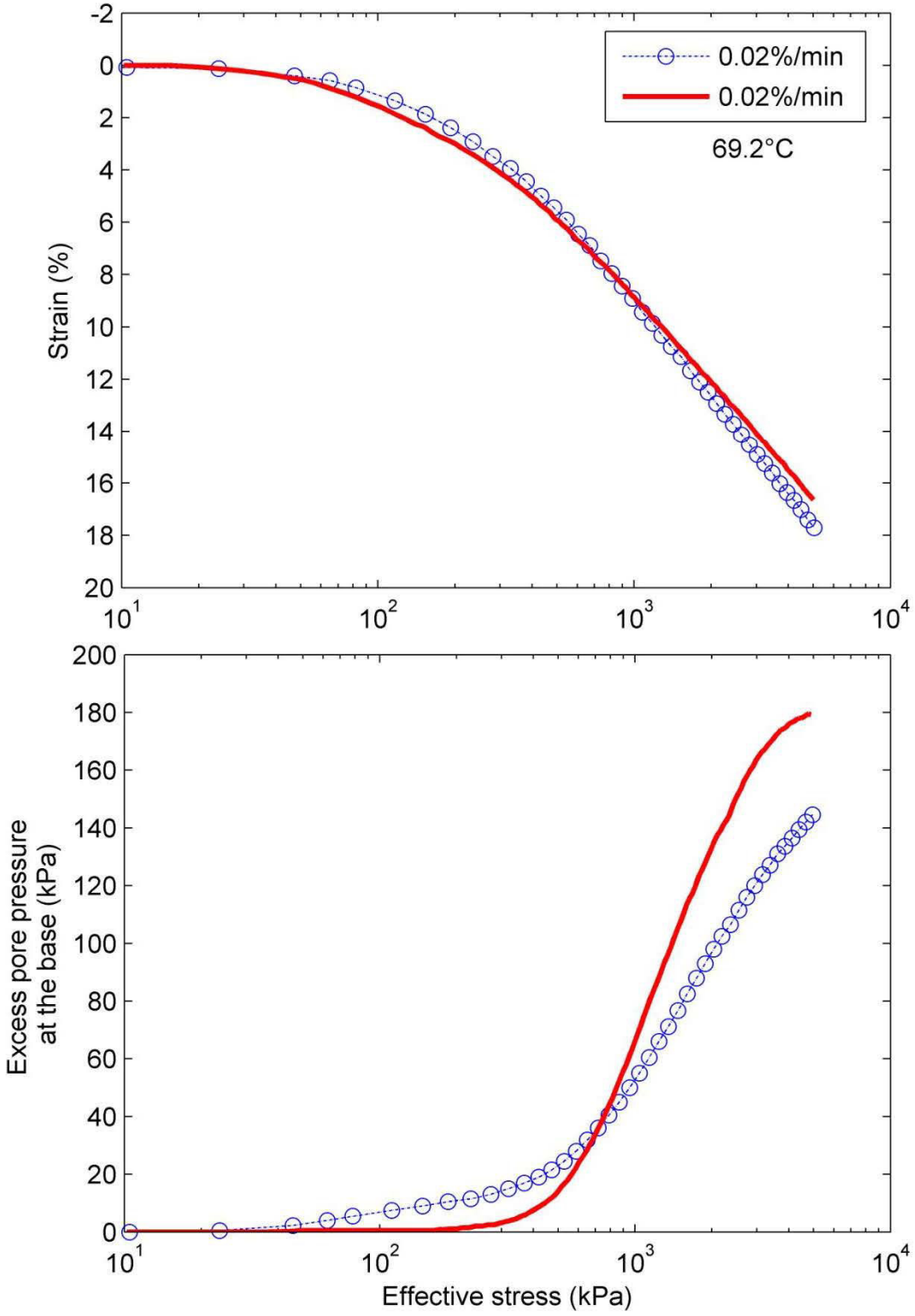

Figure 2.22 Repeated CRS tests at strain rate of 0. 02%/min at 70°C for lightly over-consolidated clay A.

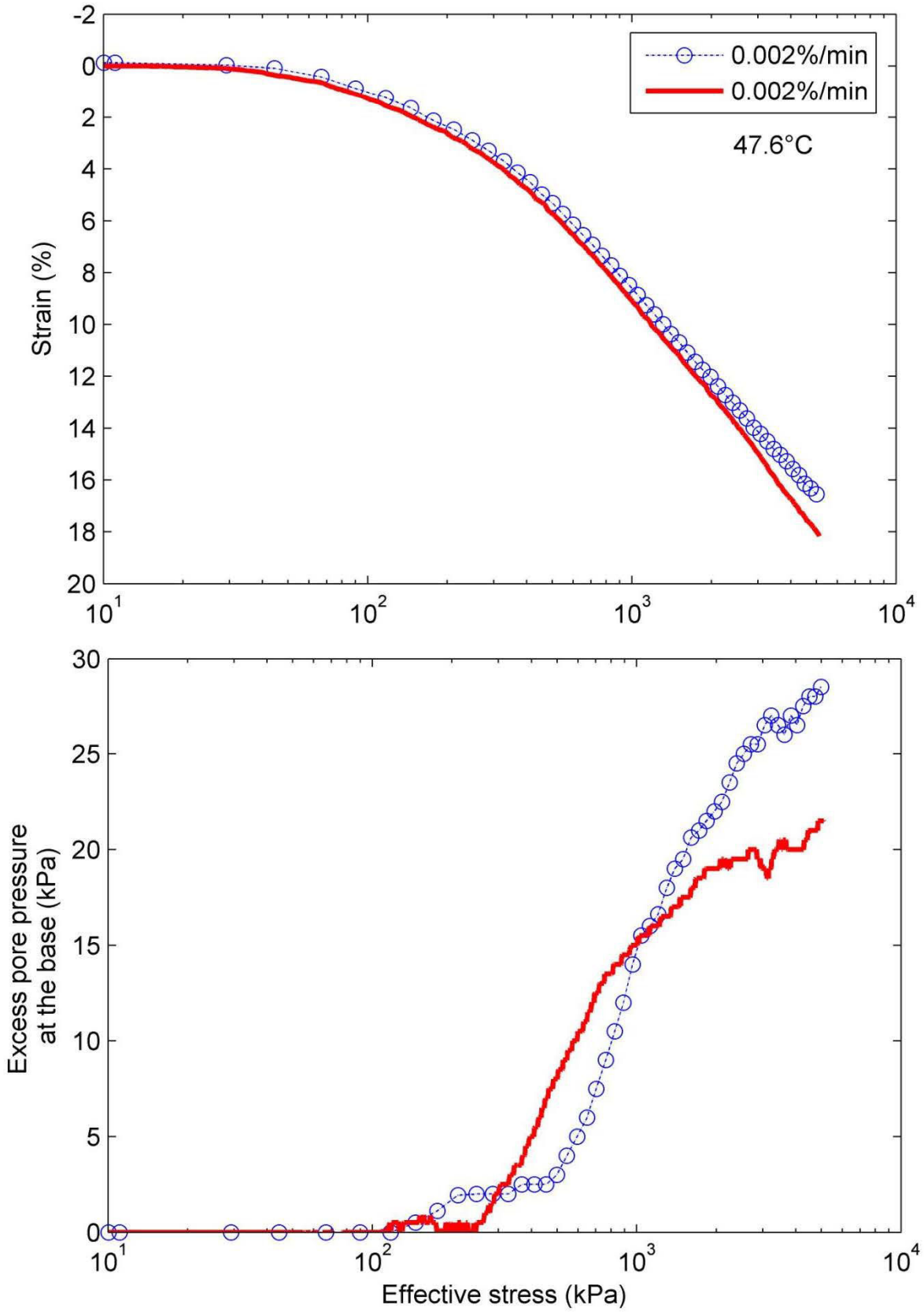

Figure 2.23 Repeated CRS tests at strain rate of 0.002%/min at 50°C for lightly over-consolidated clay A.

B) Incremental loading (IL) test Vs. CRS test

To analyze the validity of CRS test results using small strain rate, the CRS test results at strain rate of 0.002%/min was compared with the results of IL oedometer test. The selected small strain rate was chosen according to the ASTM (2008) recommendations for strain rate selection. The IL oedometer test results were considered as a reference in comparison with CRS tests.

Figure 2.24 shows a comparison between stress-strain curves obtained from CRS test and IL oedometer test performed on clay A. It can be seen that the stress-strain curves are similar at the over-consolidated part of the consolidation curve, while in the normal consolidation part of the curve, the IL curve shows slightly stiffer response than the CRS test consolidation curve. In the conventional oedometric tests, the effective stress is considered equal to the total stress, while in the CRS tests, the effective stress was determined as a function of total stress and excess pore pressure at the base as mentioned previously ($\sigma'=\sigma-2/3*u$).

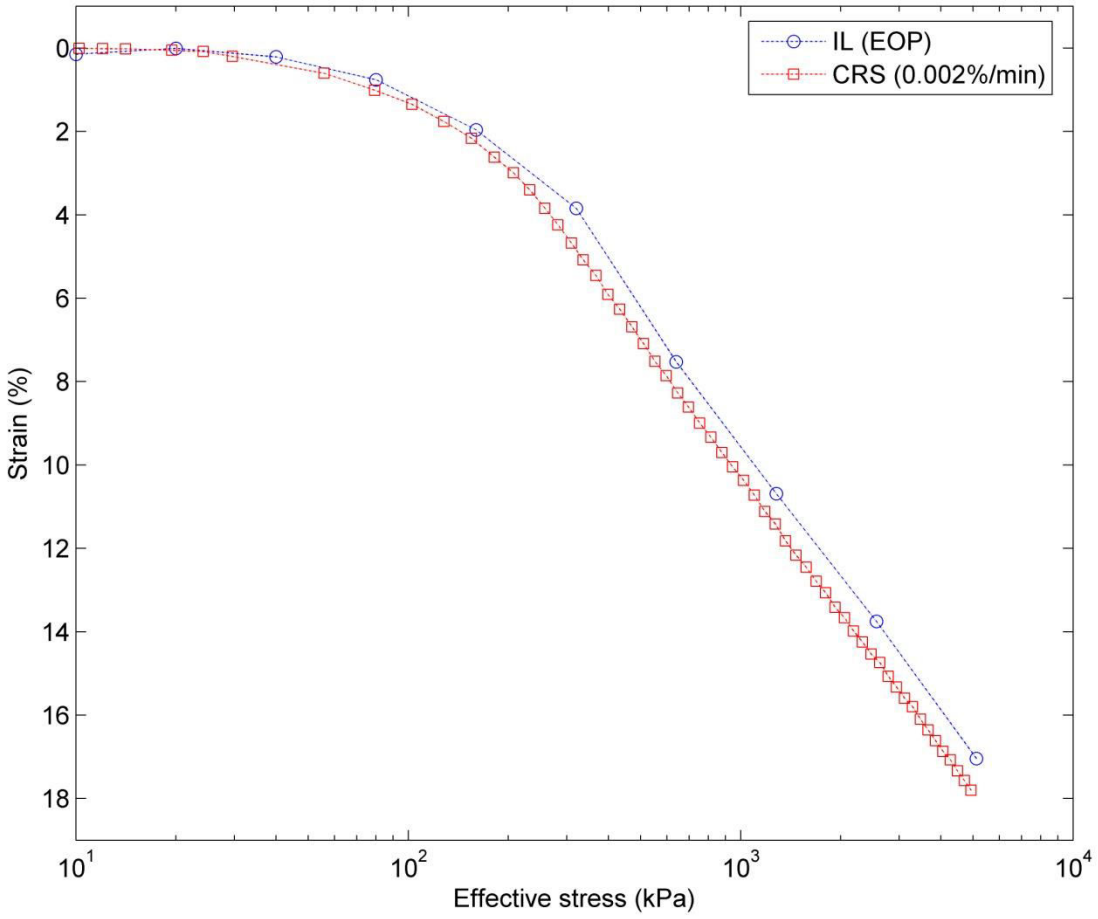

Figure 2.24 Comparing CRS test at strain rate of 0.002%/min with IL test at the EOP consolidation for lightly over-consolidated clay A.

C) Relationship between total stress and excess pore water pressure

The pore pressure relative to the total stress (pore pressure ratio) variation with vertical effective stress at different temperatures for different strain rates for clay A tests has been depicted in Figure 2.25. Generally, at the beginning of the test, the pore pressure ratio is very small since the generated pore pressure at the base of the sample is very small. After a period of time, the value of pore pressure ratio increased gradually until reaching a peak value then it decreased gradually to the end of the test. This increasing and decreasing behavior is due to relatively high pore water pressure relative to the total stress before the peak value then the total stress became high relative to the pore pressure after the peak value.

The tests performed at strain rates of 0.02 and 0.01%/min at 5.5° C showed that the excess pore pressure relative to the total stress is more than 15% (Figure 2.25). Hence, the method of interpretation for these tests is probably doubtful according to the ASTM (2008) method, as mentioned in CRS test theory regarding the acceptance limit for the excess pore pressure/total stress ratio. However, the tests performed at different temperatures at low strain rate of 0.002%/min produced very small pore pressure ratio since the generated excess pore pressure at the base of the sample is very small.

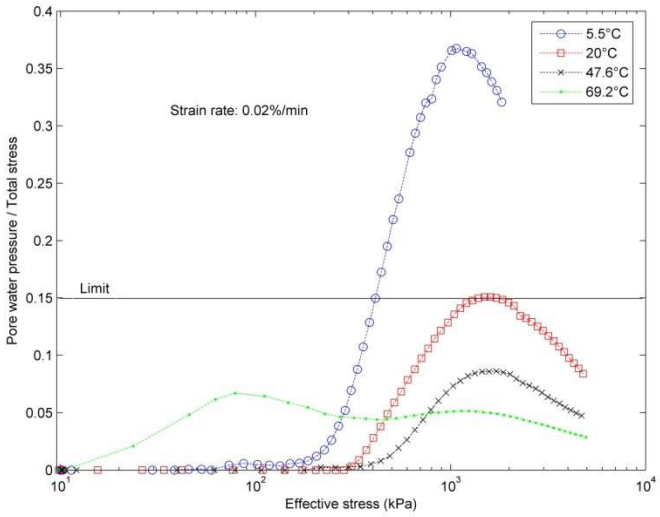

(a)

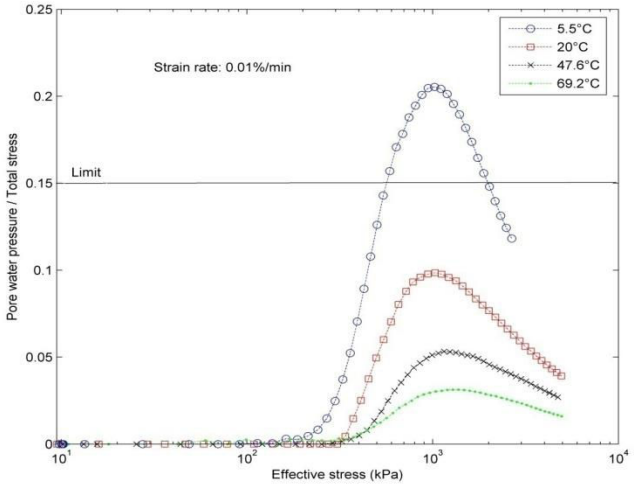

(b)

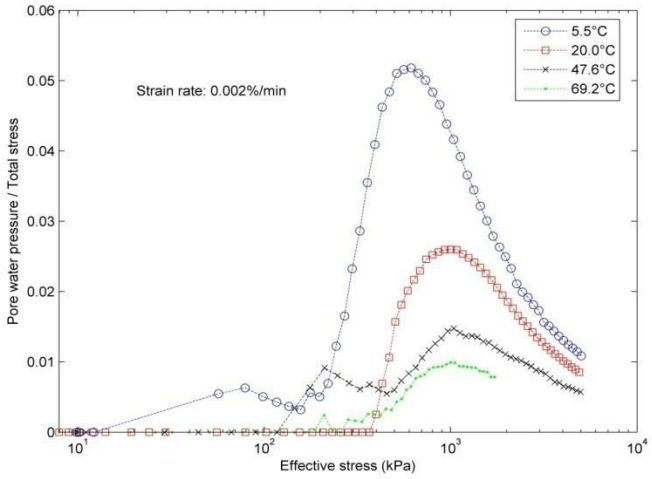

(c)

Figure 2.25 Variation of pore pressure ratio (pore pressure/total stress) with vertical effective stress at different temperatures at strain rates of (a) 0.02%/min. (b) 0.01%/min. (c) 0.002%/min. for lightly over-consolidated clay A.

2.6.2 Validation of the results of clay B

The validity of experimental results of clay B was checked before presenting and comparing. The repeatability of some tests was performed. In addition, the following section shows the relationship between total stress and excess pore water pressure to investigate the agreement of results with criteria of ASTM (2008).

Relationship between total stress and pore water pressure

To study the trend and pattern of variation of pore water pressure in clay B, the ratio of developed excess pore water pressure at the base of the sample to the total stress against vertical effective stress has been described in Figure 2.29. The Figure shows rise and fall in the curve of the pore pressure ratio, and this is related to the variation of pore pressure and total stress during CRS tests. The relatively fast development of pore water pressure against relatively slow development of total stress caused the rise in the curve while the high total stress at the last duration of the test caused the drop in the curve.

The pore pressure ratio for the strain rate of 0.02%/min at 5.5° C passed the limit recommended by ASTM (2008) to compute the representative mean effective stress (Figure 2.26a). However, at strain rate of 0.01%/min at 5.5°C, the pore pressure ratio passed the limit but with small percentage (Figure 2.26b). At strain rate of 0.002%/min, the pore pressure ratio still far lower from the recommended limit at all tested temperatures (Figure 2.26c).

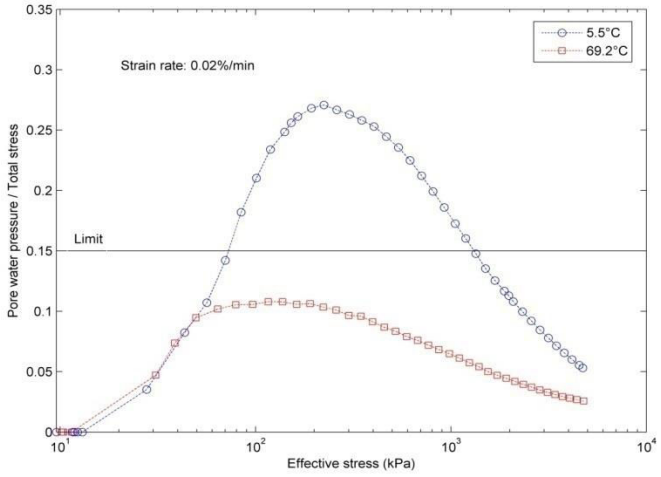

a)

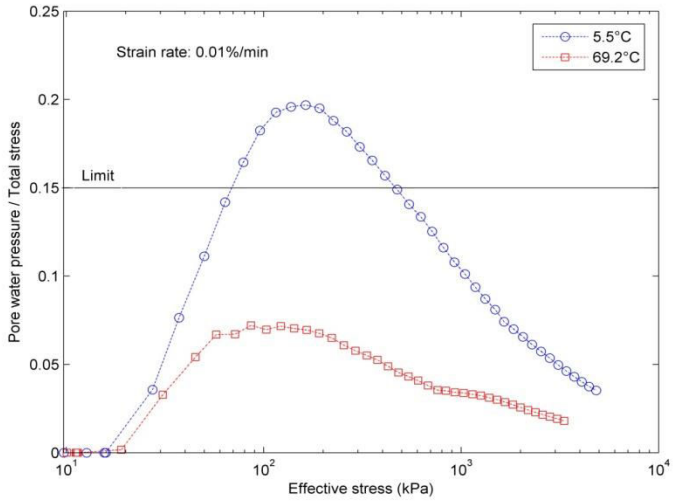

b)

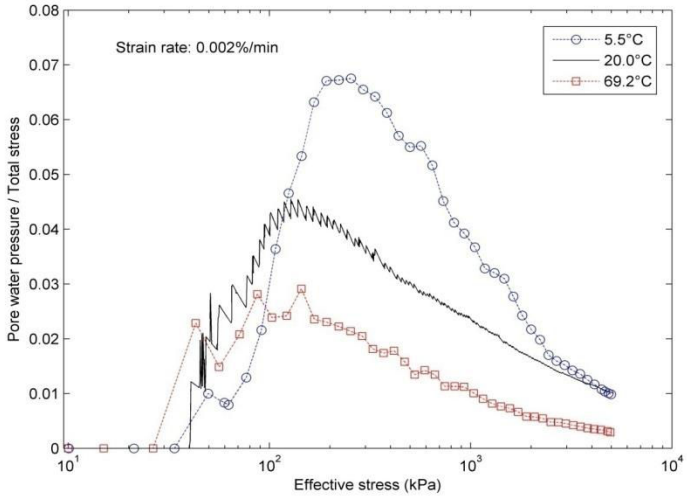

c)

Figure 2.26 Variations of pore pressure ratio (pore pressure/total stress) with vertical effective stress at different temperatures for strain rates of (a) 0.02%/min (b) 0.01%/min (c) 0.002%/min.for lightly over-consolidated clay B.

2.7 Experimental program

A total of thirty constant rate of strain (CRS) consolidation tests at different temperatures were performed on the selected clays. Nineteen of these tests were presented in the study. To observe the strain rate effects, three vertical strain rates were used in these tests includes 0.002%/min (the lowest rate), 0.01%/min (equal 5 times the lowest rate), and 0.02%/min (equal 10 times the lowest rate). The temperatures used for all tests to observe the temperature influence are 5.53, 20, 47.6, and 69.2° C. In detail, lightly over-consolidated samples of clay A were tested under all used temperatures (four different temperatures) at each strain rate, while clay B (also lightly over-consolidated) was tested under the lowest and highest temperatures (5.53 and 69° C) at each strain rate and at ambient temperature (20°C) at lowest strain rate (0.002%/min). Table 2.3 shows the detailed experimental program for both materials.

Table 2.3 Experimental program for clay A and clay B.

Clay type	Temperature (C°)	Strain rate (%/min)		
Lightly over-consolidated clay (LOC)				
		0.002	0.01	0.02
Clay A	5.53	✓	✓	✓
	20.0	✓	✓	✓
	47.6	✓	✓	✓
	69.2	✓	✓	✓
Clay B	5.53	✓	✓	✓
	20	✓		
	69.2	✓	✓	✓

2.8 Chapter Summary

In this chapter, the main characteristics of the studied materials are described as well as the experimental device set-up and testing procedures used. The main characteristics such as the mineralogical and chemical composition, particle size distribution and Atterberg limits, and Proctor curve of compaction for studied clays, clay A and clay B, are presented. The question of the results validity was also answered in this chapter.

The overview of the modified temperature controlled oedometric cell and the mechanical, hydraulic, and thermal systems of the experimental device are presented. The chapter also shows the oedometric cell deformation due to temperature variations. The interpretation of the experimental test used in this study (CRS test) is discussed in details. Sample preparation and actual temperature measurements of the sample are also presented. Test phases which include saturation phase, thermal phase, and loading phase are presented. Finally, a detailed experimental program which was used in this research is presented.

Chapter 3 Thermo-hydro-mechanical behaviour of illitic clay

3.1 Introduction

A series of CRS tests was performed at different strain rates and temperatures on illitic clay (clay A) to answer one of the questions raised in this research through the literature review. The issue is about investigation of the short- and long-term consolidation behaviour of clay soils with temperature and strain rate. This chapter discusses the results of these performed tests on the illitic clay soil.

The impact of the temperature (T) and the strain rate ($\dot{\varepsilon}$) on the consolidation characteristics including the stress-strain behaviour (ε-log σ'), compression index (c_c), swelling index (c_s), excess pore water pressure (u), hydraulic conductivity (k), coefficient of consolidation (c_v), coefficient of volume compressibility (m_v), preconsolidation pressure (p_c), and creep on statically compacted saturated illitic clay are successively introduced in this chapter. The influence of temperature on the p_c-$\dot{\varepsilon}$ relationship is also presented. Results and their validity which are presented in this chapter are for lightly over-consolidated illitic clay behaviour.

3.2 Excess pore water pressure variation with total stress at different temperatures

Figure 3.1 presents the variation of generated excess pore pressure at the base during loading with the total stress at different strain rates (0.02%/min, 0.01%/min, and 0.002%/min) and temperatures (5.5°C, 20°C, 47.6°C, 69.2°C). As shown in these figures, the magnitude of the generated pore water pressure at the base of the sample decreased when temperature increased from 5.5°C to 69.2°C at a given strain rate. For example, at strain rate of 0.02%/min at a given total stress of 1600 kPa, the generated pore water pressure at 5.5°C was 7 times larger than the generated pore pressure at 69.2°C. In addition, these figures show that the pore water pressure developed at strain rate of 0.02%/min (highest strain rate) was the highest in comparison with lower strain rates at a given temperature. For example, at 5.5°C at a given total stress of 1600 kPa, the generated excess pore water pressure at strain rate of 0.02%/min was 12 times larger than the generated pore pressure at strain rate of 0.002%/min.

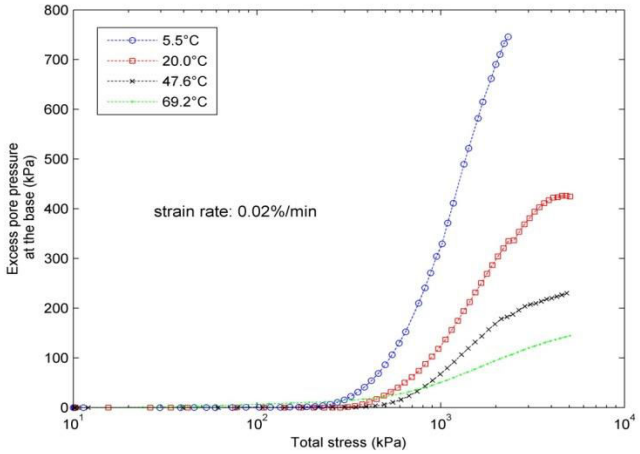

(a)

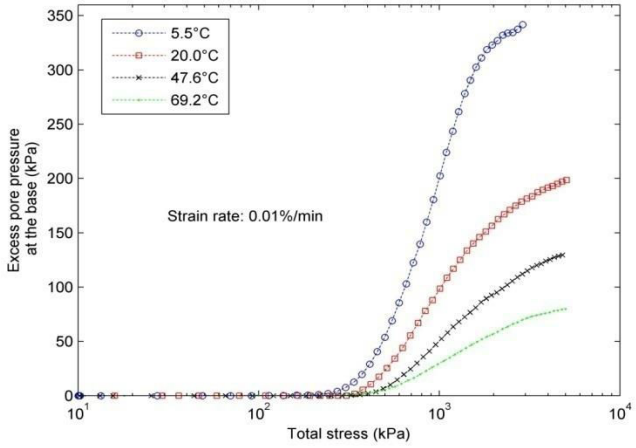

(b)

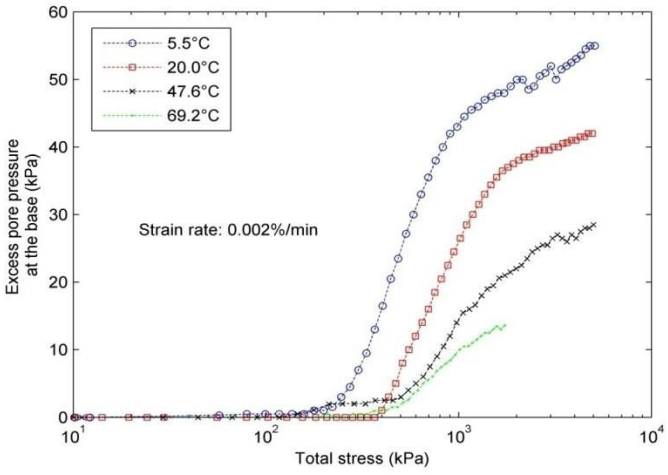

(c)

Figure 3.1 Excess pore water pressure variation with total stress at different temperatures for strain rates (a) 0.02%/min (b) 0.01%/min (c) 0.002%/min.

It is clear from the results that the generated excess pore pressure at the base of the sample increased with total stress increase but with different values at different strain rates and temperatures. The increase of temperature and the decrease of strain rate make the generated excess pore pressure at the base of the sample to be lower relative to the total stress and this behaviour leads to accepted results to a certain extent according to ASTM (2008) standard. However, both temperature and strain rate have strong effect on the pore water pressure.

3.3 Stress-strain behaviour with temperature

The influence of temperature on the compressibility under constant strain rates are evaluated by comparing the ε-log σ' curves at different temperatures of 5.5°C, 20°C, 47.6°C, and 69.2°C for lightly over-consolidated illitic clay. Figures 3.2 to 3.4 show the variation of the strain and excess pore pressure at the base with a vertical effective stress for different temperatures for the CRS tests with strain rates of 0.02%/min, 0.01%/min and 0.002%/min for lightly over-consolidated illitic clay. The tests were performed at 5.5°C for strain rates of 0.02%/min and 0.01%/min were presented within the ASTM limit for pore pressure relative to total stress as shown in the figures.

Under the larger strain rate of 0.02%/min, the strain values obtained at different temperatures for a given effective stress are close to each other, especially before reaching the preconsolidation pressure value approximately. However, for strain rate of 0.01%/min, a higher strain was found at a given effective stress at high temperature of 69.2° C in comparison with other temperatures. At 50°C for strain rate of 0.01%/min, ε-log σ' curve moved to the right with small percent in comparison with other temperatures.

Under the low strain rate of 0.002%/min, it was observed, approximately, the same value of strain at different temperatures for a given effective stress, especially before reaching the preconsolidation pressure value with a small shift to the right for ε-log σ' curve at temperature of 50°C.

Generally, for all CRS tests at different temperatures and strain rates, the ε-log σ' curves changed slightly as the temperature increased.

Excess pore water pressure variation with temperature

The generated excess pore pressure during strain loading was examined at four different temperatures (5.5°C, 20°C, 47.6°C, 69.2°C) at a given strain rate for lightly over-consolidated illitic clay to observe the temperature effect. Figures 3.2 to 3.4 show the variation of excess pore pressure with effective stress at different temperatures for a given strain rate.

Figure 3.2 for example shows the variation of excess pore pressure at the base of the specimen with effective stress at different temperatures for a given strain rate of 0.02%/min. The Figure shows that the generated excess pore pressure at 69.2°C was the lowest comparing with other temperatures. On the other hand, the generated excess pore pressure was the highest at lowest temperature (5.5°C).

It is clearly observed also at other given strain rates (0.01%/min, and 0.002%/min) that the excess pore pressure decreased with temperature increase at a given effective stress. For example at 0.01%/min strain rate, the maximum excess pore pressure generated at 47.6°C is 1.53 times smaller than at room temperature (20°C), while the pore pressure generated at 69.2° C is 2.5 times smaller than at room temperature.

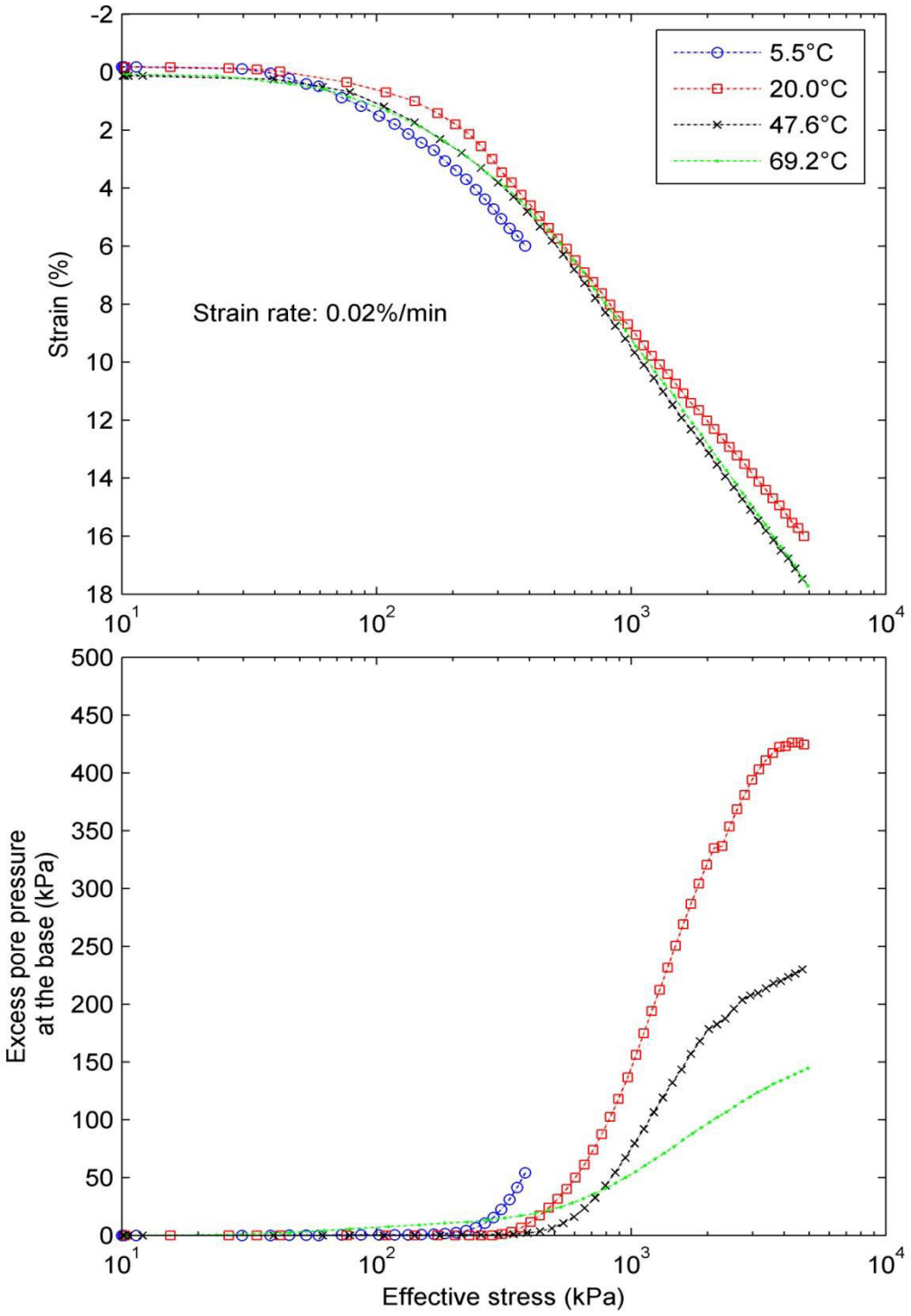

Figure 3.2 Effect of temperature on the effective stress-strain curve and excess pore water pressure for lightly over-consolidated illitic clay at strain rate of 0.02%/min (Strain=$\Delta h/h_0$).

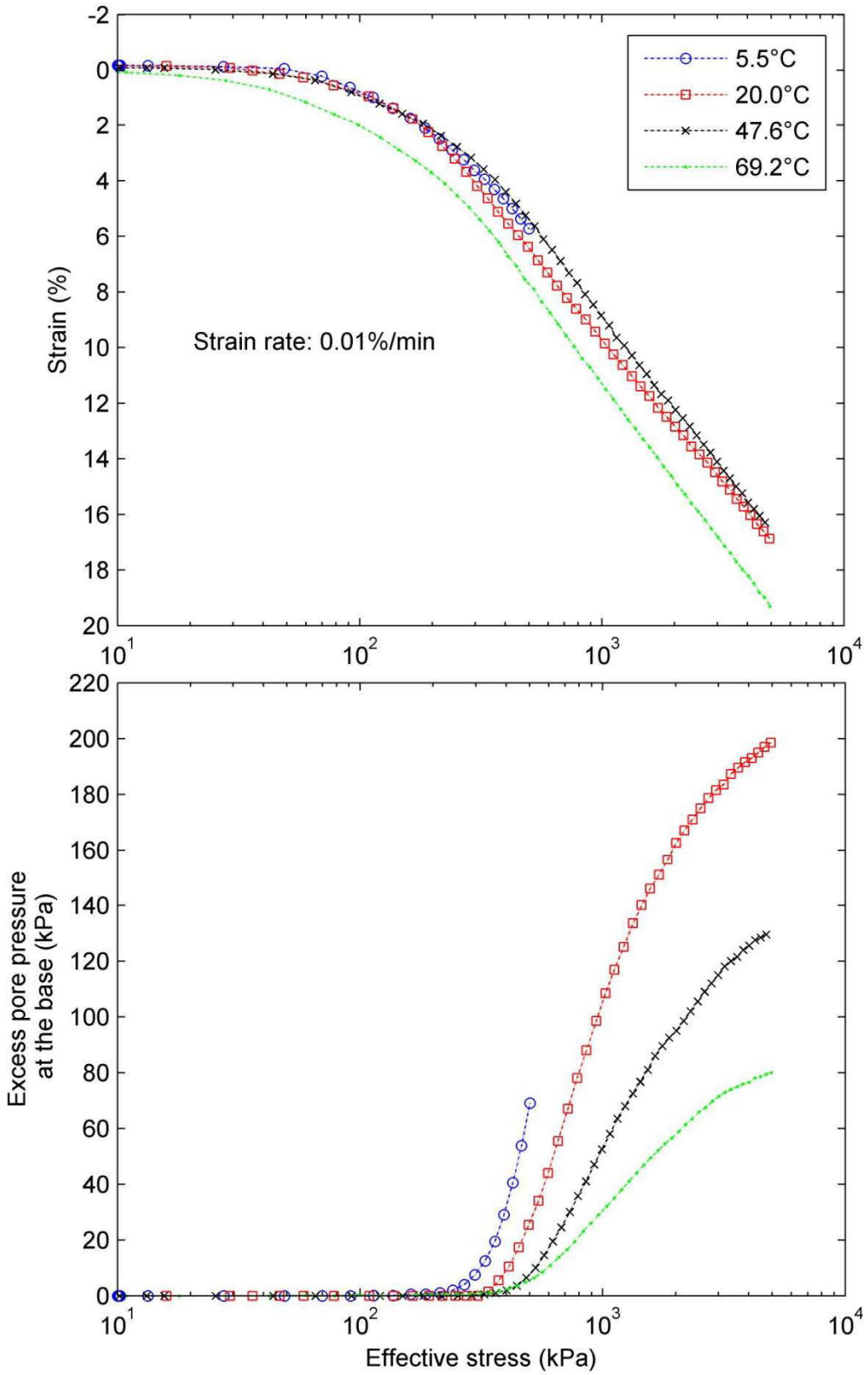

Figure 3.3 Effect of temperature on the effective stress-strain curve and excess pore water pressure for lightly over-consolidated illitic clay at strain rate of 0.01%/min (Strain=$\Delta h/h_0$).

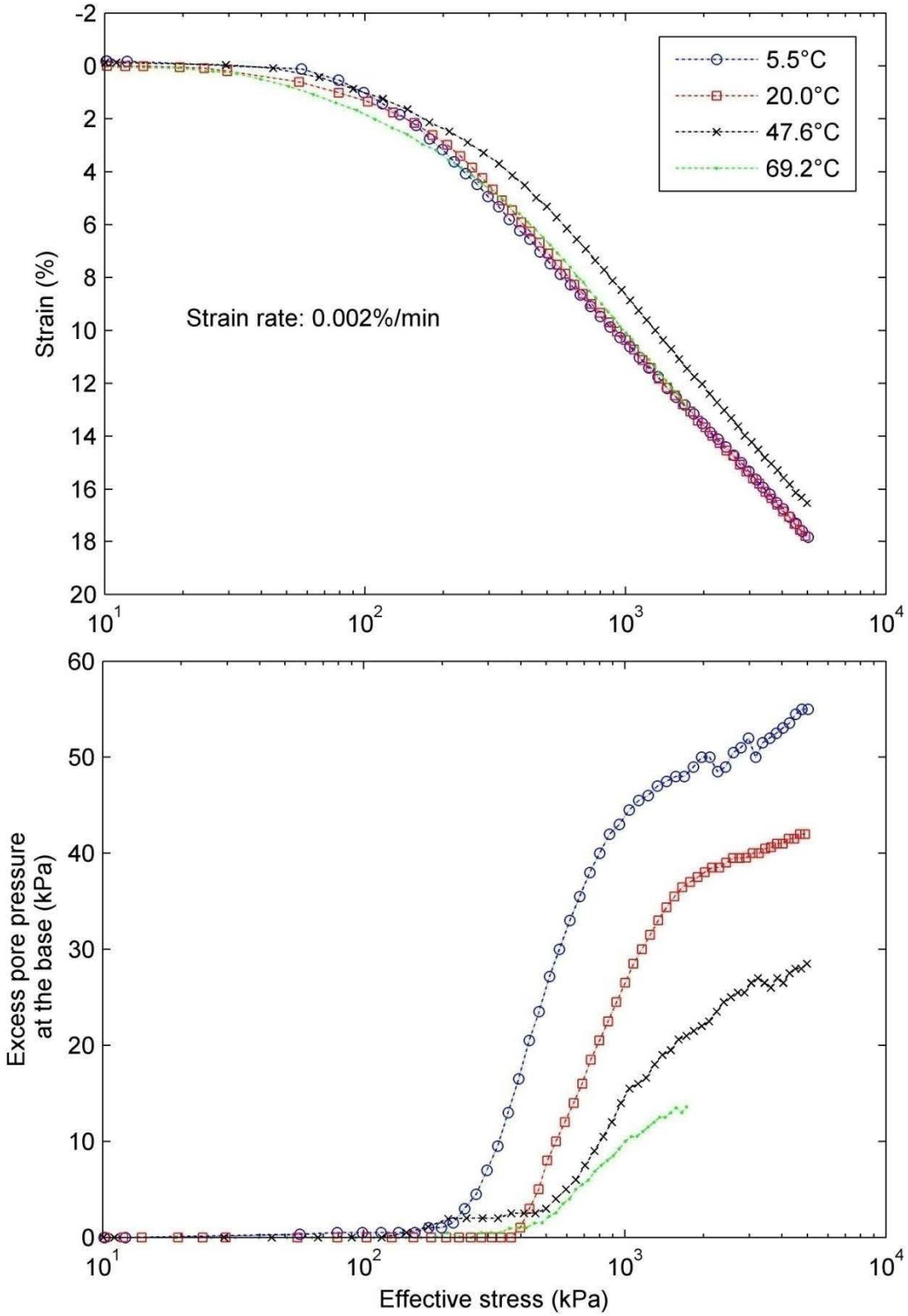

Figure 3.4 Effect of temperature on the effective stress-strain curve and excess pore water pressure for lightly over-consolidated illitic clay at strain rate of 0.002%/min (Strain=$\Delta h/h_0$).

The variation of the excess pore pressure at the base of the specimen is strongly dependent on the temperature as observed in the results. Generally, a higher temperature results in a smaller excess pore pressure at the base of the specimen at given strain rate. This behavior could be directly related to the decrease in the water viscosity as the temperature increases, which facilitates expulsion or dissipation of the water.

3.4 Stress strain behaviour with strain rate

Regardless of the temperature effect, the impact of strain rate on the compressibility under constant temperature is evaluated by comparing the ε-log σ' curves at different strain rates of 0.02%/min, 0.01%/min, and 0.002%/min for lightly over-consolidated illitic clay. Figures 3.5 to 3.8 show the variation of strain and excess pore water pressure with vertical effective stress for illitic clay for different strain rates at different given temperatures of 5.5° C, 20.0° C, 47.6° C, and 69.2° C, respectively.

At the room temperature for example, Figure 3.6 highlights the stress-strain behaviour at different strain rates. The figure shows that at a given effective stress, the value of strain was the largest at strain rate of 0.002%/min, while the value was the lowest at strain rate of 0.02%/min. A similar behaviour was observed approximately for CRS tests at temperature of 5.5°C, 47.6°C, and 69.2°C.

Generally, the value of strain increased when the strain rate decreased for a constant level of effective stress.

Excess pore pressure variation with strain rate

The generated excess pore pressure during constant strain loading was examined at three different strain rates (0.02%/min, 0.01%/min, and 0.002%/min) at a given temperature for illitic clay to observe the strain rate effect. Figures 3.5 to 3.8 show the variation of the excess pore pressure with the vertical effective stress at different strain rates for a given temperature.

Figure 3.6 for example shows the variation of generated excess pore pressure at the base with vertical effective stress for different strain rates at the room temperature (20°C). The figure shows that the generated excess pore pressure at a strain rate of 0.02%/min was the largest compared to the other strain rates. A similar behaviour was observed for CRS tests at temperatures of 5.5°C, 47.6°C, and 69.2°C.

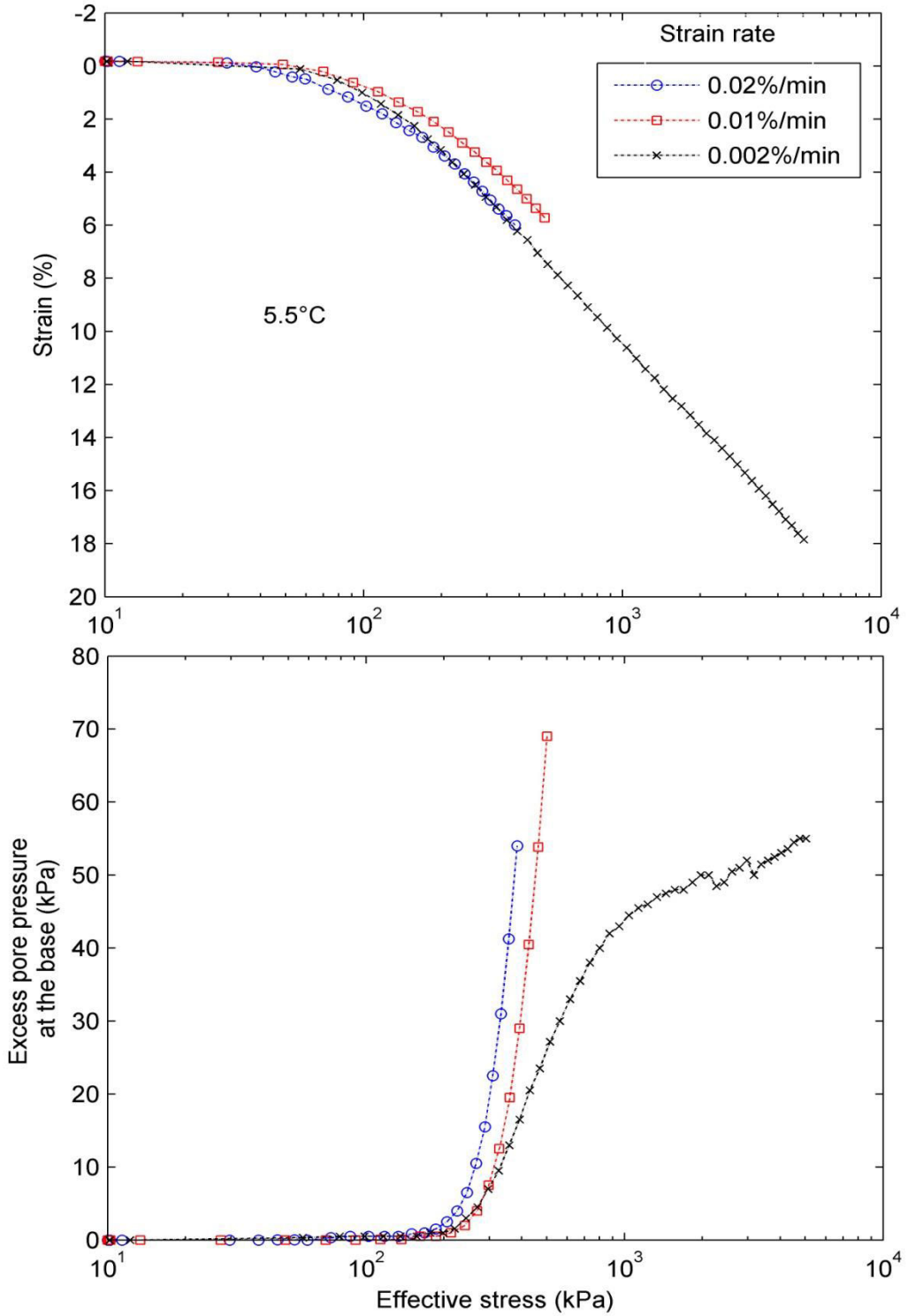

Figure 3.5 Effect of the strain rate on the effective stress-strain curve and excess pore water pressure at 5.5° C for lightly over-consolidated illitic clay (Strain=$\Delta h/h_0$).

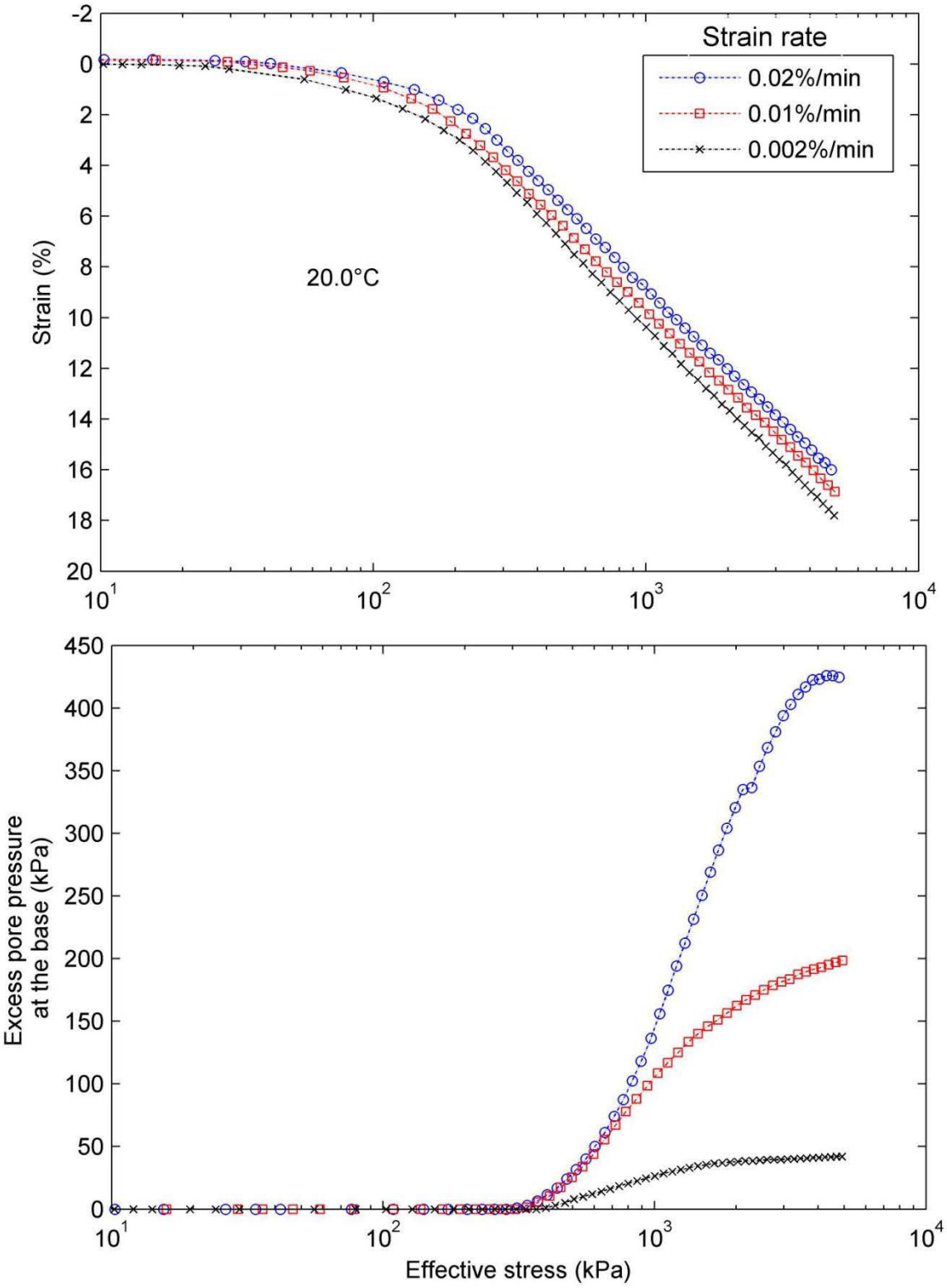

Figure 3.6 Effect of the strain rate on the effective stress-strain curve and excess pore water pressure at 20.0° C for lightly over-consolidated illitic clay (Strain=$\Delta h/h_0$).

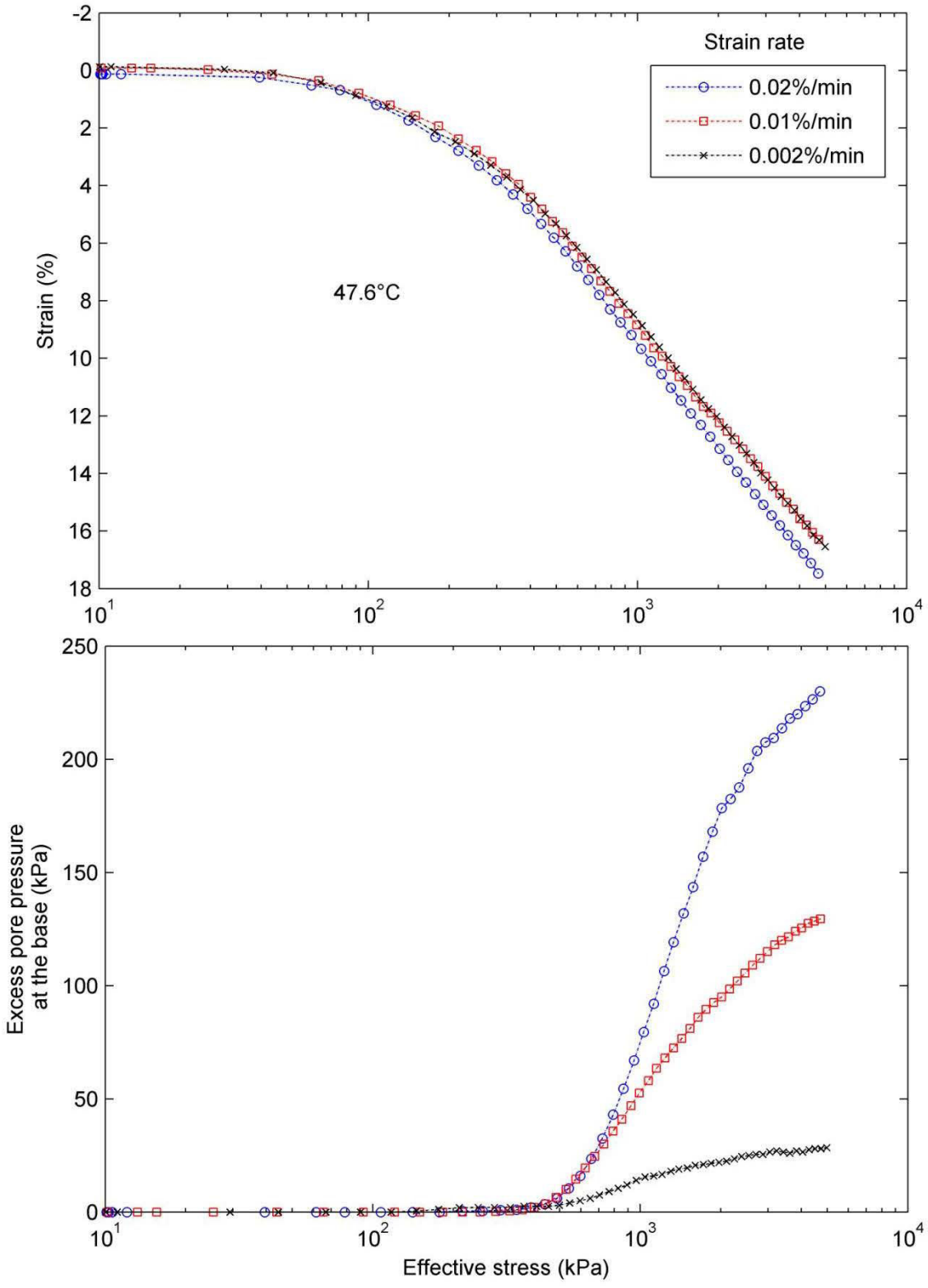

Figure 3.7 Effect of the strain rate on the effective stress-strain curve and excess pore water pressure at 47.6° C for lightly over-consolidated illitic clay (Strain=$\Delta h/h_0$).

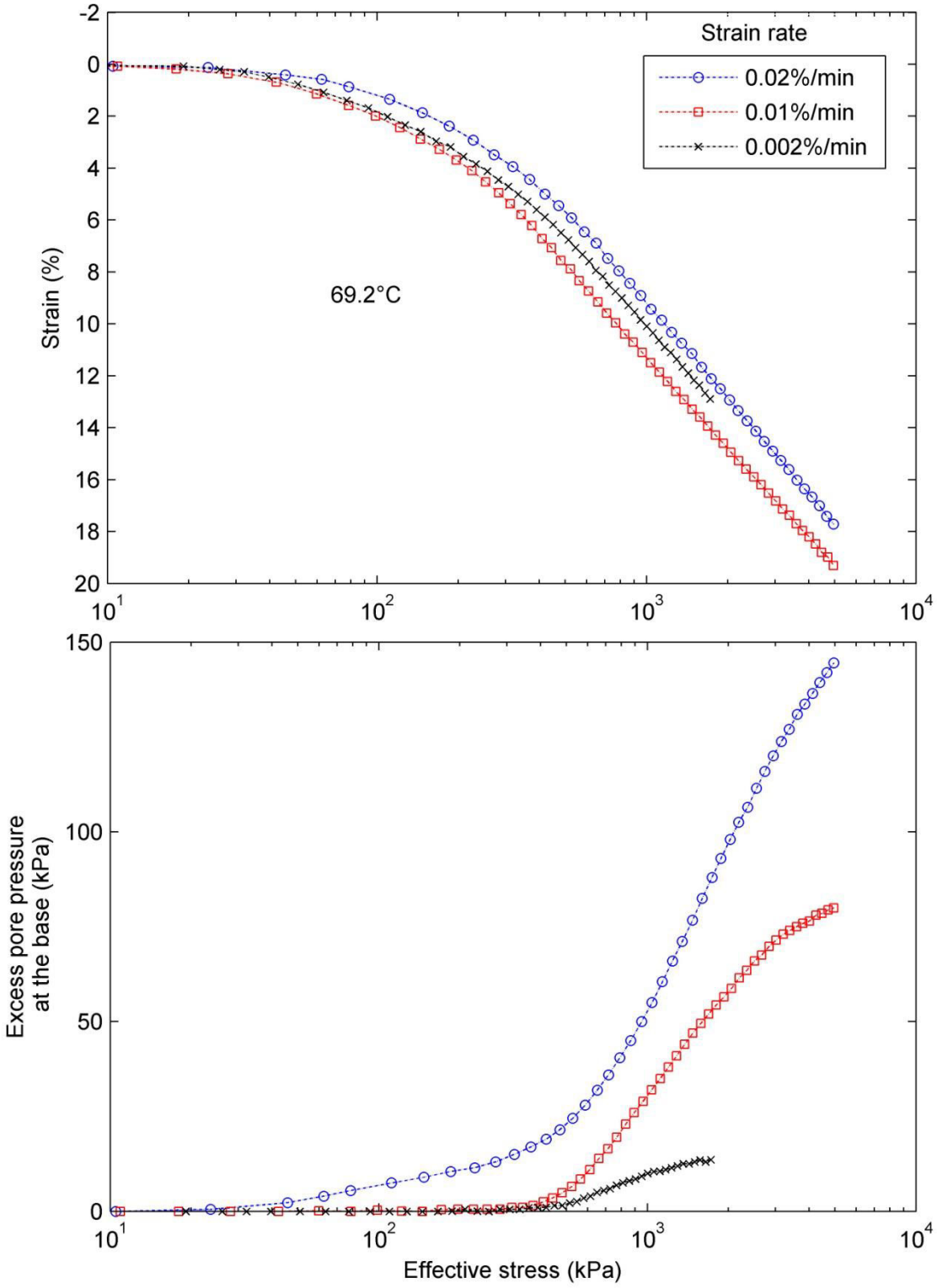

Figure 3.8 Effect of the strain rate on the effective stress-strain curve and excess pore water pressure at 69.2° C for lightly over-consolidated illitic clay (Strain=$\Delta h/h_0$).

Based on the obtained results at a given temperature, the generated excess pore water pressure at the base of specimen increases with strain rate increase. The non dissipated water will not be drained immediately during large strain rate and it will show more resistance.

3.5 Temperature and strain rate effect on the coefficient of volume compressibility

The coefficient of volume compressibility was determined using the method mentioned in CRS test theory. Figure 3.9 shows the variation of the coefficient of volume compressibility (m_v) with vertical effective stress at different temperatures for strain rate of 0.002%/min. As shown in the figure, the differences between the values of m_v for the lowest and highest temperatures during loading are very small. This behaviour has also been observed for other strain rates.

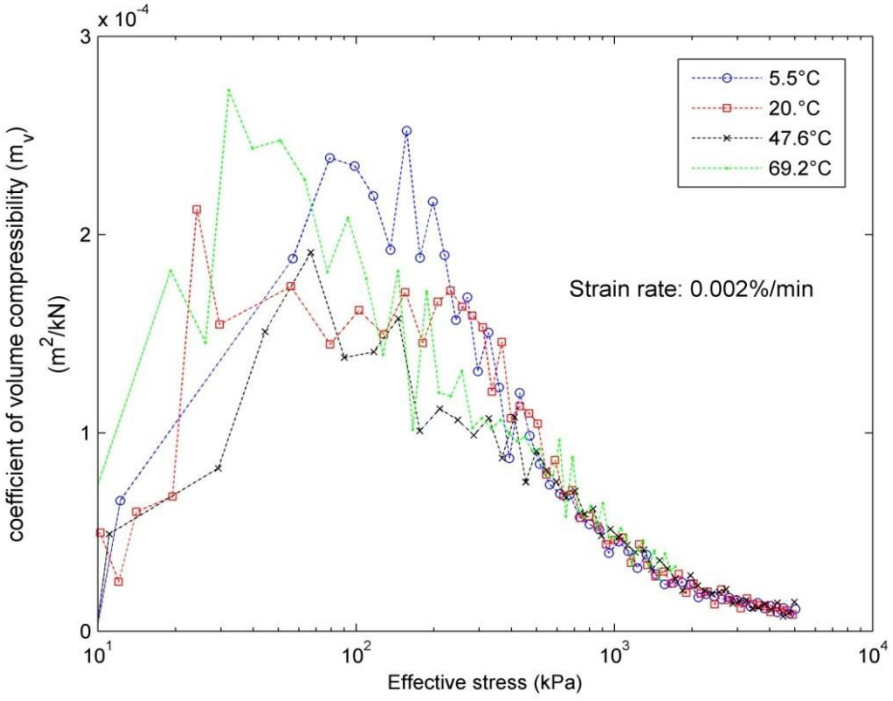

Figure 3.9 Effect of temperature on the coefficient of volume compressibility for lightly over-consolidated illitic clay at strain rate of 0.002%/min.

In fact, for the illitic clay, the coefficient of volume compressibility at a given strain rate changed slightly with temperature and it is not easy to note clearly the temperature impact. On the other hand, the variation of the coefficient of volume compressibility with strain rate is not significant. At a given temperature, the coefficient of volume compressibility have approximately the same value at different strain rates.

3.6 Compression and swelling indices variation with temperature and strain rate

Figure 3.10 shows the variation of the compression and swelling indices with temperature and strain rate for 10 tests on lightly over-consolidated illitic clay. The values of compression index (c_c) for all tests ranged between 0.191 and 0.217 at 5.5°C, 20.0°C, 47.6°C, and 69.2°C. Also, the compression indices at different strain rates of 0.002, 0.01, and 0.02%/min for a given temperature changed slightly. The values of the swelling index, which was obtained from the slopes of the elastic part of the compression curves at different temperatures, vary between 0.0035 and 0.016 for the illitic clay.

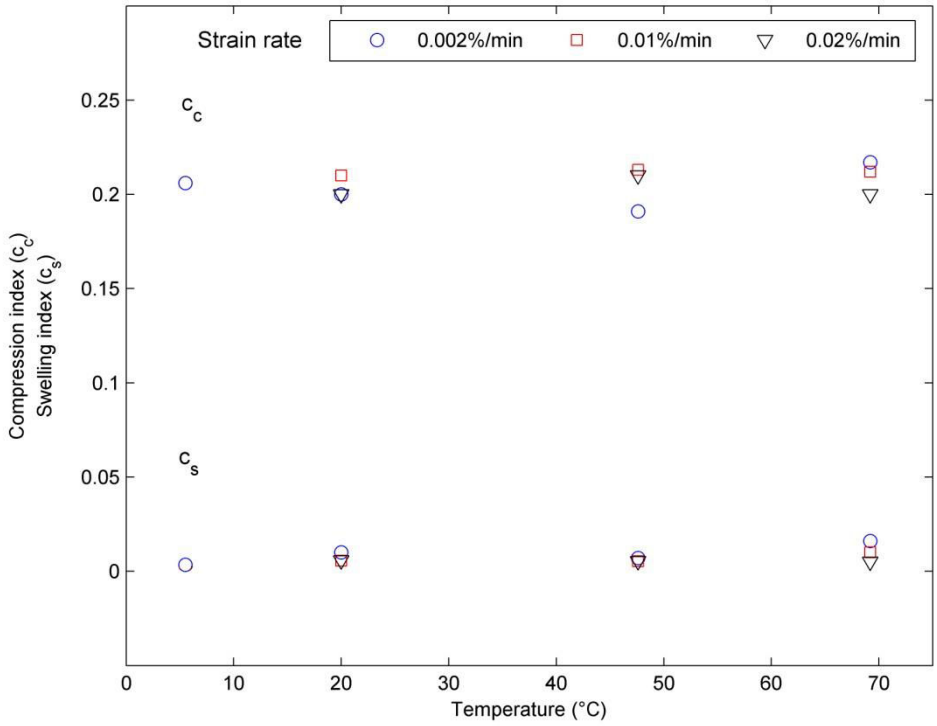

Figure 3.10 Effect of temperature and strain rate on the compression and swelling indices of lightly over-consolidated illitic clay.

Accordingly, the compression index increased slightly as the temperature increased while it could be considered strain rate independent. The extent of change in the values for all tests on the same clay indicates that the swelling index is not strongly dependent on temperature and strain rate.

3.7 Temperature and strain rate effect on the preconsolidation pressure

The preconsolidation pressure can be defined as the pseudo-elastic limit which separates elastic from the elasto-plastic behaviour in oedometric conditions. Figure 3.11 presents the variation range of the preconsolidation pressure with temperature, which was determined from

10 CRS tests on lightly over-consolidated illitic clay at different strain rates. Since there is no a clearly defined pressure separating the elastic part from plastic part on the compression curve, a variation range of the preconsolidation pressure was estimated using Burmister (1951) method. The preconsolidation pressure at 69.2°C was smaller than the preconsolidation pressures at lower temperatures.

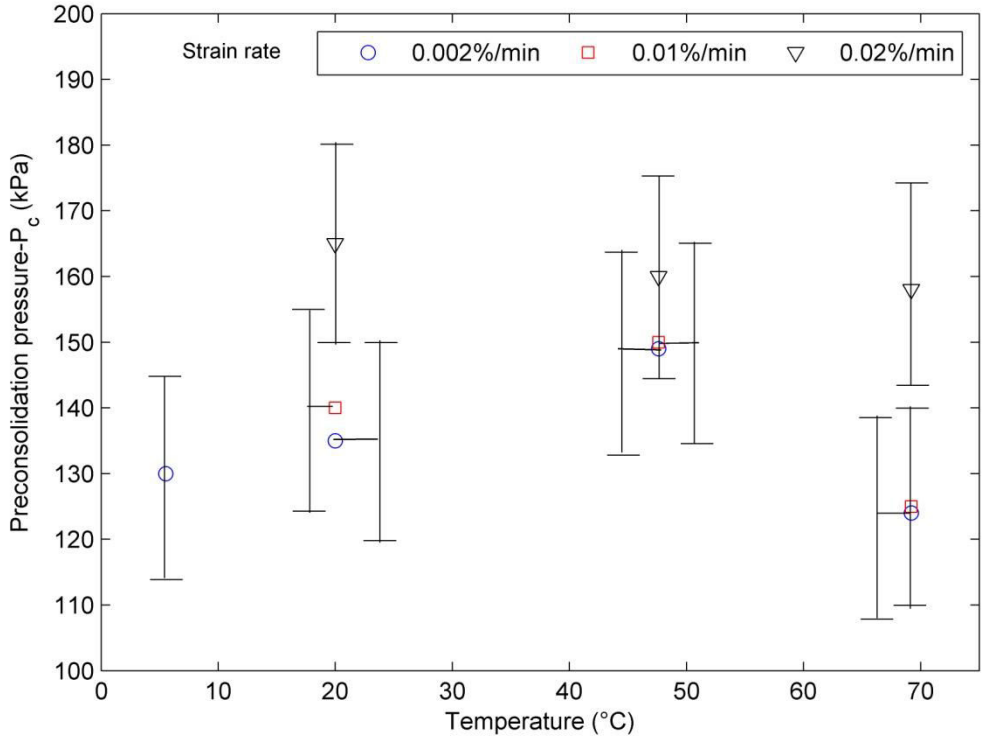

Figure 3.11 Effect of temperature and strain rate on the preconsolidation pressure of lightly over-consolidated illitic clay.

The determined preconsolidation pressure for lightly over-consolidated illitic clay for all tests at different temperatures (5.5°C, 20.0° C, 47.6° C, and 69.2° C) shows that preconsolidation pressure slightly decreased as the temperature increased. On the other hand, the preconsolidation pressure was affected by the strain rate change as presented on the same figure. The higher the strain rate, the higher the preconsolidation pressure at any given temperature.

3.8 Temperature and strain rate effect on the permeability

The permeability was determined using the method mentioned in CRS test theory (indirect method). To illustrate the influence of temperature on the hydraulic behaviour, a given void ratio was selected for lightly over-consolidated illitic material in the normally consolidated zone. Figure 3.12 shows the variation of hydraulic conductivity with temperature and strain rate for a void ratio of 0.65 for lightly over-consolidated illitic clay. As shown in the figure, at

a given strain rate, the hydraulic conductivity increased as the temperature increased from 5.5°C to 69.2°C. Meanwhile, the intrinsic permeability was not affected by temperature at a given strain rate (Table 3.1). In other words, the hydraulic conductivity increases as strain rate increases.

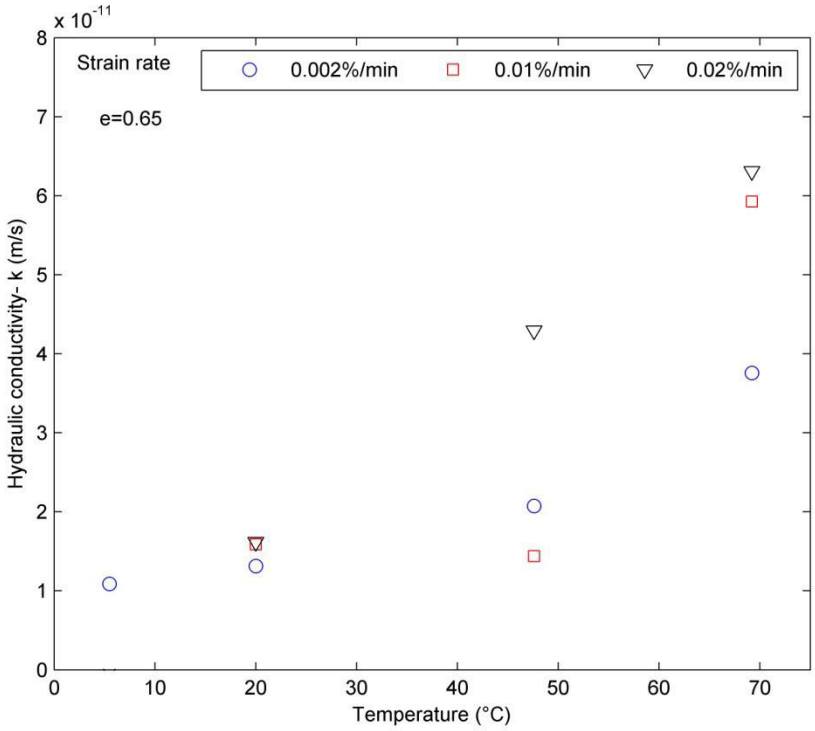

Figure 3.12 Effect of temperature and strain rate on the permeability (k) for lightly over-consolidated illitic clay.

Table 3.1 Intrinsic permeability variation with temperature and strain rate for lightly over-consolidated illitic clay at e=0.65.

Temperature (°C)	Strain rate (%/min)	K (m^2)
20	0.02	1.64E-19
20	0.01	1.61E-19
20	0.002	1.33E-19
47.6	0.02	2.62E-19
47.6	0.01	8.79E-20
47.6	0.002	1.27E-19
69.2	0.02	2.75E-19
69.2	0.01	2.58E-19
69.2	0.002	1.64E-19

According to the results obtained for the studied material, the hydraulic conductivity is strongly dependent on temperature, while the variation of the intrinsic permeability with temperature is negligible. Actually, the permeability depends on the viscosity and the porosity, while the intrinsic permeability depends on the porosity.

3.9 Temperature and strain rate effect on the coefficient of consolidation

To present the influence of temperature on the coefficient of consolidation, Figure 3.13 shows the results in terms of constant void ratio of 0.65 for lightly over-consolidated illitic clay. To illustrate the behaviour, here the strain rate of 0.01%/min is discussed. Results are similar for other strain rate values. At the highest temperature of 69.2° C, the value of C_v is 2.7 times higher than the value of C_v at room temperature, 20.0° C.

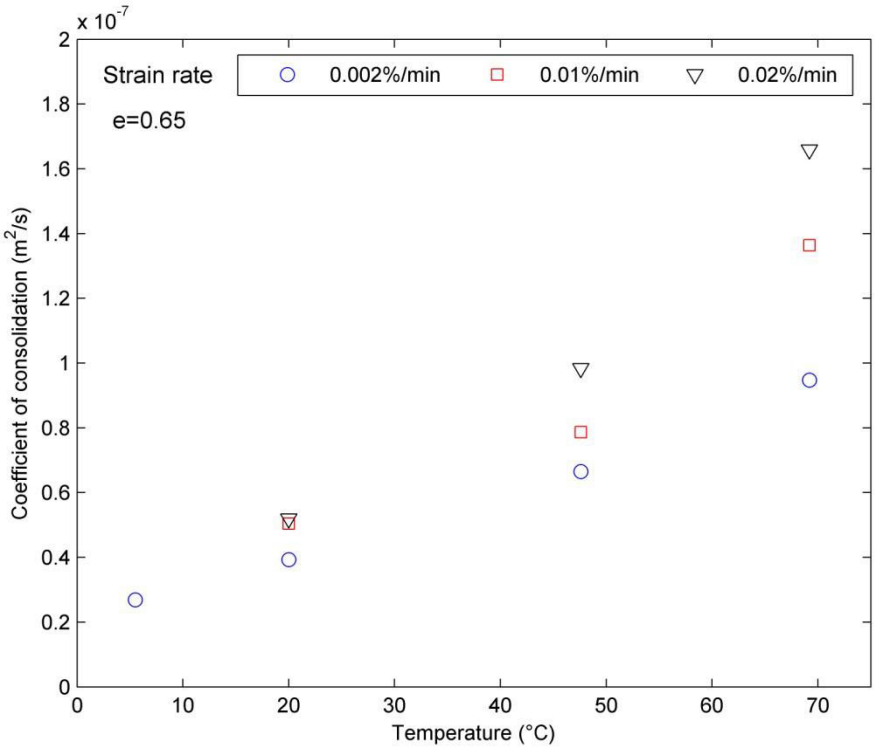

Figure 3.13 Effect of temperature and strain rate on the coefficient of consolidation for lightly over-consolidated illitic clay.

Based on those results, for a given strain rate, the value of coefficient of consolidation increases for high temperatures. The increased permeability at high temperatures makes the rate of consolidation greater than at low temperatures.

3.10 Temperature effect on the long-term consolidation

Mesri and Godlewski (1977) developed a method for determining the creep index (c_α) as a function of the compression index, c_c. This method is based on the result that the magnitude and behaviour of the secondary compression index, c_α, with time is directly related to the magnitude and behaviour of the compression index, c_c, with the consolidation stress (See section 1.5.4). The relationship between the creep index and compression index is linear with a constant slope of c_α/c_c. This method was used in this study to determine the creep index value, c_α.

At a given temperature, the value of c_α/c_c together with the compression index, c_c, were used to determine the value of the creep index. The value of c_α/c_c is equal to the slope of the preconsolidation pressure–strain rate logarithmic curve (log $\dot{\varepsilon}$ - log p_c) as mentioned in section 1.5.5:

$$\alpha = c_\alpha/c_c = \Delta log\dot{\varepsilon}/\Delta log P_c$$

$$c_\alpha = \alpha\, c_c$$

3.10.1 Variation of preconsolidation pressure–strain rate relationship with temperature

Figure 3.14 shows the variation range of the preconsolidation pressure with strain rate for different temperatures for illitic clay. The figure shows that the estimated values of $\Delta log\dot{\varepsilon}/\Delta log P_c$ (=c_α/c_c) varied with temperature.

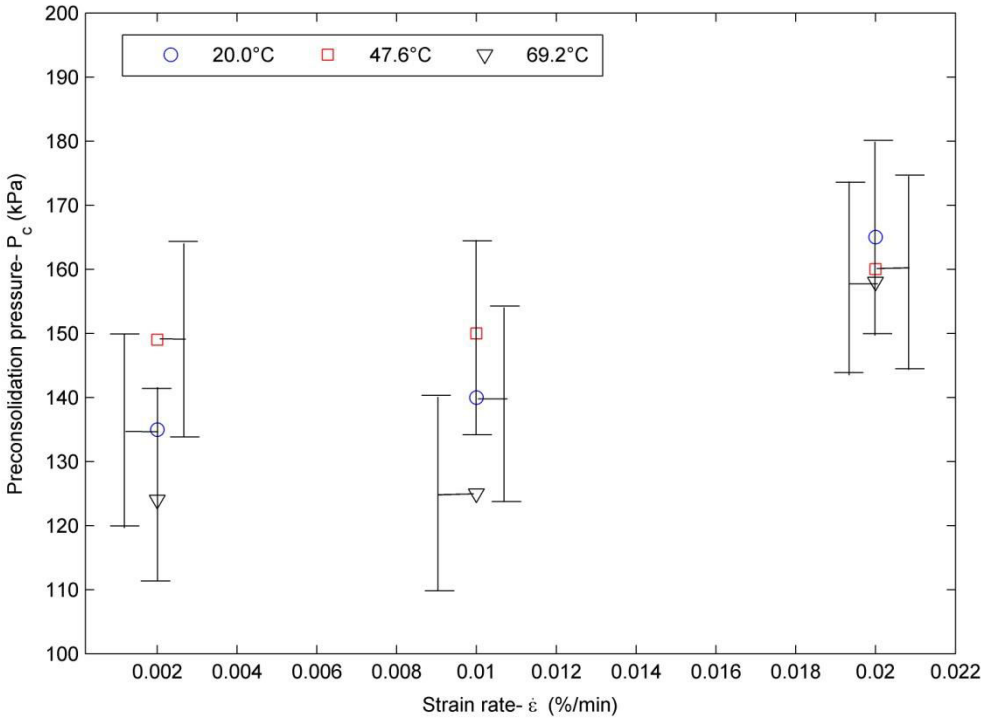

Figure 3.14 Variation of preconsolidation pressure with strain rate at different temperatures for illitic clay.

These estimated values were 0.081, 0.056, and 0.106 at 20.0° C, 47.6° C, and 69.2° C, respectively. The estimated values of c_α/c_c varied with temperature alteration between 0.039 and 0.125.

3.10.2 Effect of temperature on the creep index (c_α)

According to the values of c_α/c_c and c_c, Figure 3.15 shows the variation range of the creep index with temperature for illitic material. The estimated values of the creep index were 0.0165, 0.012, and 0.0223 corresponding to temperatures of 20.0° C, 47.6° C, and 69.2° C,

respectively. Compression index, c_c, was obtained from the slope of the void ratio versus logarithm of the effective stress curve (e-logσ') at the end of primary consolidation (EOP) for a given temperature, as mentioned before in section 3.5. The figure shows that creep index at 69.2°C was the largest in comparison with other temperatures.

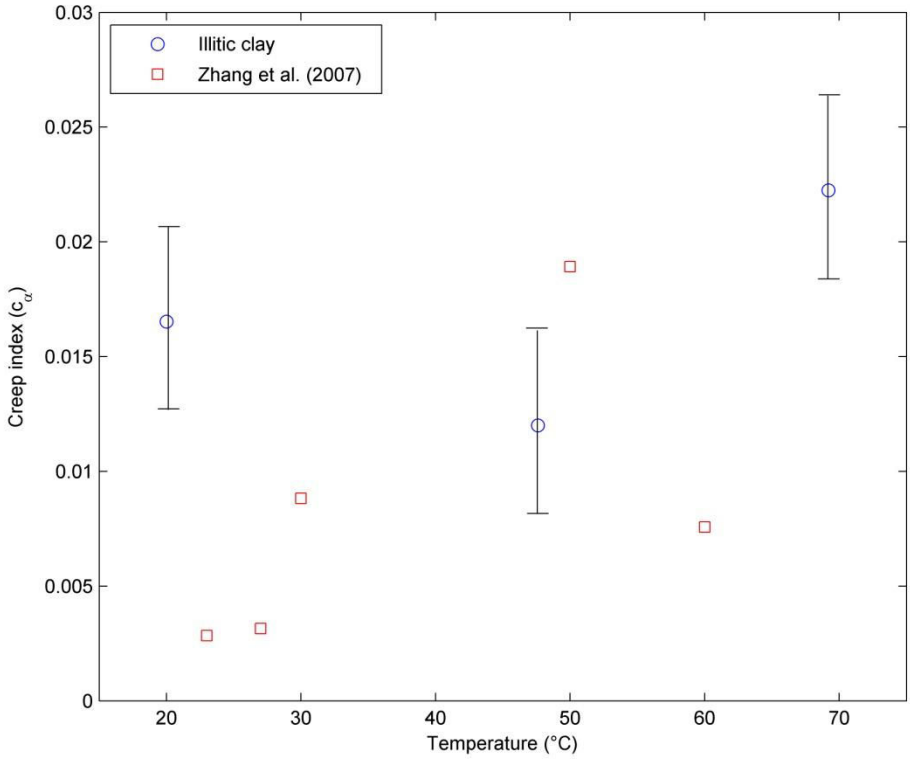

Figure 3.15 Influence of temperature on the creep index of illitic clay.

Based on the obtained results, the creep index, c_α, of illitic clay increases as the temperature increase. This finding depends on the variation of preconsolidation pressure with strain rate as a function of temperature.

3.11 Results discussion

The obtained results for the illitic clays are discussed in this section. As can be seen in the results, there is a slight temperature effect on the compression curves of lightly over-consolidated illitic clay at the highest strain rate of 0.02%/min. On the other hand, the highest strain was found at a given effective stress at the highest studied temperature of 69.2° C for a strain rate of 0.01%/min. The lower effective stress at higher temperatures could be interpreted as a decrease in preconsolidation pressure (Moritz, 1995). Akagi (1995) indicated that the compression curves of remolded clay (PI=62.7%) which were obtained from CRS tests at strain rate of 0.02%/min had almost the same behaviour at 50°C and 80°C.

A small shift to the right for ε-log σ' curve at temperature of 50°C was observed in this study in comparison with other temperatures for performed tests at strain rate of 0.002%/min. A similar behaviour was observed by Tsutsumi and Tanaka (2012) for low strain rates at high temperatures but for reconstituted clays. Tsutsumi and Tanaka (2012) indicated that the curve shift to the right at high temperatures for low strain rates may be related to the creation of some types of structure during loading in the CRS test, and its creation is accelerated by heating. The closer rearrangement of clay particles due to reduced thickness of adsorbed water layer on the surface of clay particles during heating creates a new structure with higher stiffness against loading, and the new structure formation is accelerated by heating.

It is observed for all CRS tests that the excess pore pressure at the base of the sample decreases with temperature increase. These results are consistent with Tsutsumi and Tanaka (2012) who observed that the generated excess pore pressure at 10°C was larger than the generated one at 50°C during CRS tests on different reconstituted clays at different strain rates. The reduction of the viscosity with temperature increase was the main reason for this behaviour (Tsutsumi & Tanaka, 2012). On the other hand, the increased permeability with temperature accelerates the pore water dissipation.
To focus on strain rate effect, results showed a higher strain at lower strain rate for a given effective stress. Leroueil et al. (1985) found a similar behaviour when they performed CRS tests on soft natural clay at different strain rates. They proposed a unique stress-strain-strain rate relationship for different clays.

On the other hand, a higher value of excess pore pressure was observed at higher strain rate. The increase of pore pressure with strain rate increase is because of lesser time available for the dissipation of developed pore pressure in comparison with lower strain rates (Ahmadi et al., 2014).

Results show different effects of temperature on the consolidation parameters of the illitic clay. The coefficient of volume compressibility (m_v) slightly changed with temperature alteration. Akagi et al. (1995) found small differences in volume change of clay with effective stress increase at different temperatures which indicated that the coefficient of volume compressibility changed slightly with temperature. Consistency with this study, results can be seen in section 1.4.4.

The compression index (c_c) increased slightly as the temperature increased while the swelling index (c_s) was not dependent on temperature. Campanella and Mitchell (1968) indicated that

the variation of compression and swelling indices with temperature change were insignificant for illitic clay which is consistent with this study results.

Results indicated that the preconsolidation pressure decreased as the temperature increased. At higher temperatures, the elastic domain is reduced (softening) due to the reduction in the viscosity. The reduced viscosity at high temperature increases the contacts between the clay minerals; i.e., mineral-to-mineral contacts, which causes plastic deformation (Shariatmadari & Saeidijam, 2012). Accordingly, the preconsolidation pressure decreases with temperature increase as has been referred in section 1.4.3 in details.

The hydraulic conductivity increased as the temperature increased while the intrinsic permeability variation with temperature is insignificant. The viscosity reduction that occurs as the temperature increases causes a higher hydraulic conductivity. Similar findings were recorded by other researchers but for different clays with different preparation; e.g., Towhata et al. (1993) and Abuel-Naga et al. (2005) using the same method (indirect method) (section 1.4.5).

A higher coefficient of consolidation was observed at higher temperature. An increase in the coefficient of consolidation with temperature increase is because of increased permeability at higher temperatures (Delage et al., 2000). Agreement with this study results was mentioned in section 1.4.4.

Mesri and Godlewski (1977) method (see section 1.5.4) was used in this study to observe the long term behaviour of illitic clay with temperature. According to the obtained results, the slope of the preconsolidation pressure-strain rate relationship ($=c_\alpha/c_c$) varied with temperature variation. Marques et al. (2004) obtained approximately parallel slopes of log $\dot{\varepsilon}$ - log p_c at different temperatures from CRS tests which were performed on natural clay.

Based on the obtained results of c_c and c_α/c_c at different temperatures, the estimated values of creep index (c_α) increased with temperature increase. This result showed the temperature impact on the long term behaviour of illitic clay. In comparison with this study results, Zhang et al. (2007) observed the same tendency of creep index of Callovo-Oxfordian clay (γ=2.25 Mg/m^3) with temperature (Figure 3.15) after creep tests. They suggested that the long term behaviour with temperature could be related to the weakness of particles bonds or shear resistance between particles at high temperatures, and hence, the creep increases. The reduction in the apparent viscosity of the contacts between the particles at higher temperatures may be the reason that the creep increased as the temperature increased (Gupta, 2013).

3.12 Conclusion

This chapter discussed the main features of the thermo-hydro-mechanical behaviour of lightly over-consolidated illitic clay. The validity of CRS test results for this clay was checked using three factors which are the repeatability of tests, comparison with IL (Incremental loading) oedometer test, and fulfillment of the ASTM (2008) criteria. The CRS tests performed at strain rates of 0.02%/min and 0.01%/min at 5°C cannot be interpreted according to the CRS reduction method since it does not fit the criteria. Figure 3.2 shows the consolidation parameters variation with temperature and strain rate for lightly over-consolidated illitic clay.

The results in this chapter show the impact of temperature and strain rate on the short term consolidation characteristics of lightly over-consolidatedd illitic clay. The stress-strain behaviour slightly changed with temperature alteration. The excess pore water pressure at the base was strongly affected by temperature alteration. At a given strain rate, as temperature increases, the excess pore pressure at the base of the specimen decreases. On the other hand, the stress-strain behaviour and excess pore pressure at the base were affected by strain rate at a given temperature. At a given temperature, the strain value increases at constant effective stress with strain rate decrease, while the excess pore pressure at the base decreases. The change of compression and swelling indices with temperature and strain rate fluctuations could be considered negligible. The results showed that the preconsolidation pressure decreased with temperature increase. In addition, the hydraulic conductivity was temperature dependent, while the intrinsic permeability variation with temperature was negligible. The coefficient of volume compressibility was slightly affected by temperature and strain rate, while the coefficient of consolidation increased with temperature and strain rate increase.

Table 3.2 consolidation parameters variation with temperature and strain rate for lightly over-consolidated illitic clay (e=0.65).

Temperature (°C)	**5.5**		**20.0**		**47.6**		**69.2**	
Strain rate (%/min)	**C_c**	**C_s**	**C_c**	**C_s**	**C_c**	**C_s**	**C_c**	**C_s**
0.02	-	-	0.20	0.0057	0.21	0.0053	0.20	0.0051
0.01	-	-	0.21	0.0056	0.213	0.0053	0.212	0.01
0.002	0.206	0.0035	0.20	0.01	0.191	0.007	0.217	0.016
Strain rate (%/min)	**Pc (kPa)**							
0.02	-		165		160		158	
0.01	-		140		150		125	
0.002	130		135		149		124	
Strain rate (%/min)	**$m_v \times 10^{-5}$ (m^2/kN)**							
0.02	-		3.341		3.155		4.056	

0.01	-		3.148		1.849		4.444	
0.002	2.867		3.115		4.417		3.888	
Strain rate (%/min)	**k $\times10^{-11}$ (m/s)**	**K $\times10^{-19}$ (m^2)**	**k $\times10^{-11}$ (m/s)**	**K $\times10^{-19}$ (m^2)**	**k $\times10^{-11}$ (m/s)**	**K $\times10^{-19}$ (m^2)**	**k $\times10^{-11}$ (m/s)**	**K $\times10^{-19}$ (m^2)**
0.02	-	-	1.616	1.64	4.291	2.62	6.307	2.75
0.01	-	-	1.588	1.61	1.438	0.879	5.927	2.58
0.002	1.086	1.74	1.313	1.33	2.074	1.27	3.759	1.64
Strain rate (%/min)	**$c_v \times10^{-8}$ (m^2/s)**							
0.02	-		5.187		9.835		16.59	
0.01	-		5.045		7.868		13.64	
0.002	2.692		3.93		6.654		9.479	
-	**c_α**							
-	**-**		0.0165		0.012		0.022	

The results also showed that the long term behaviour of lightly over-consolidated illitic clay was affected by temperature. The value of creep index was slightly increased with temperature increase. The long term index (c_α) change with temperature was estimated according to the variation of preconsolidation pressure-strain rate link with temperature. This index varies with temperature.

Chapter 4 Impact of clay nature on the thermo-hydro-mechanical behaviour

4.1 Introduction

The impact of clay nature on the thermo-mechanical behavior was assessed in this study. A set of experiments was conducted on a second material (which has less percentage of fines), it mainly consists of kaolinite and interstratified illite/smectite.

A series of CRS tests was performed at different strain rates and temperatures on clay B to compare it with clay A. The validation of clay B results is presented. The short and long term consolidation behaviour of studied materials with temperature and strain rate was compared and discussed in this chapter to investigate the impact of clay nature. The effect of clay content (percentage of fines) and soil plasticity index was also discussed.

4.2 Temperature effect on the stress-strain behaviour

Figures 4.1 to 4.3 show the impact of temperature on the stress-strain behavior of lightly over-consolidated clays A and B at different strain rates. The stress-strain behavior of lightly over-consolidated clay B was investigated at two temperatures of 5.5°C and 69.2°C at given strain rates of 0.02%/min, 0.01%/min, and 0.002%/min. In comparison with clay A, the results indicated that the stress-strain behaviour of clay B was less affected by temperature, at least between 5.5°C and 69.2°C. At a given effective stress, the change in strain due to temperature effect for clay A is larger than in clay B. For clay B, at a given strain rate of 0.02%/min, the variation of the strain with the vertical effective stress converged at temperatures of 5.5° C and 69.2° C. A similar behavior was observed for strain rates of 0.01%/min and 0.002%/min.

In general, the experimental results at different temperatures in any case of strain rate indicated that the stress-strain behaviour of lightly over-consolidated clay B is not significantly temperature dependent and it is less affected by temperature than clay A .

Excess pore pressure variation with temperature

Figures 4.1 to 4.3 show the variation of pore pressure with vertical effective stress for different strain rates at different temperatures for studied materials. For example for clay B at strain rate

of 0.01%/min, the maximum excess pore pressure generated at 5.5° C is 2.7 times larger than the excess pore pressure generated at 69.2° C.

It is found that the pore water pressure generated in clay A samples are more affected by temperature than clay B. At a strain rate of 0.01%/min for example, for a temperature change from 5.5°C to 69.2°C, the pore water pressure generated in clay A samples showed a larger decrease than the decrease in clay B by a factor of 1.77.

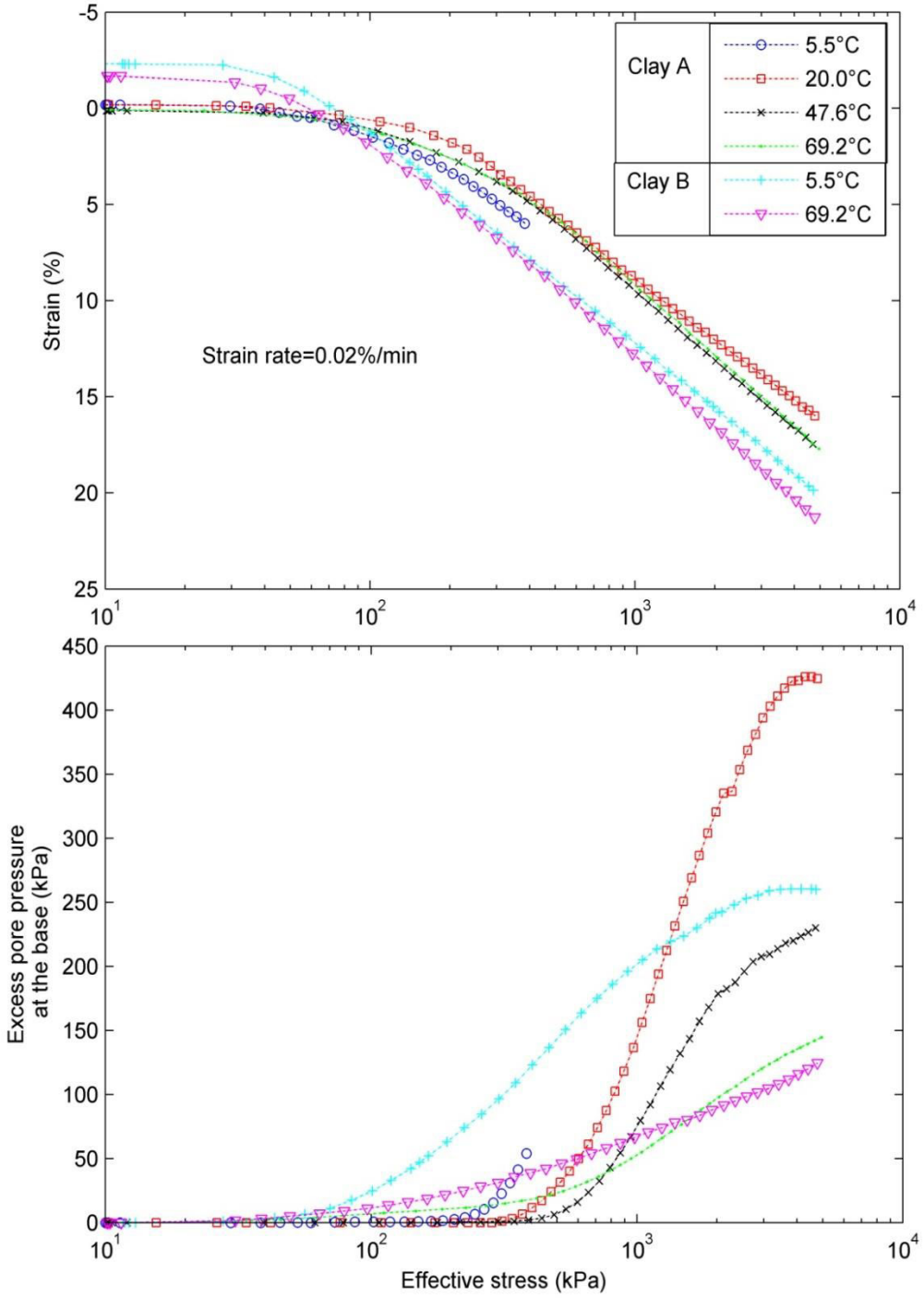

Figure 4.1 Effect of temperature on the effective stress-strain curve and excess pore water pressure at strain rate of 0.02%/min for studied lightly over-consolidated clays (Strain=$\Delta h/h_0$).

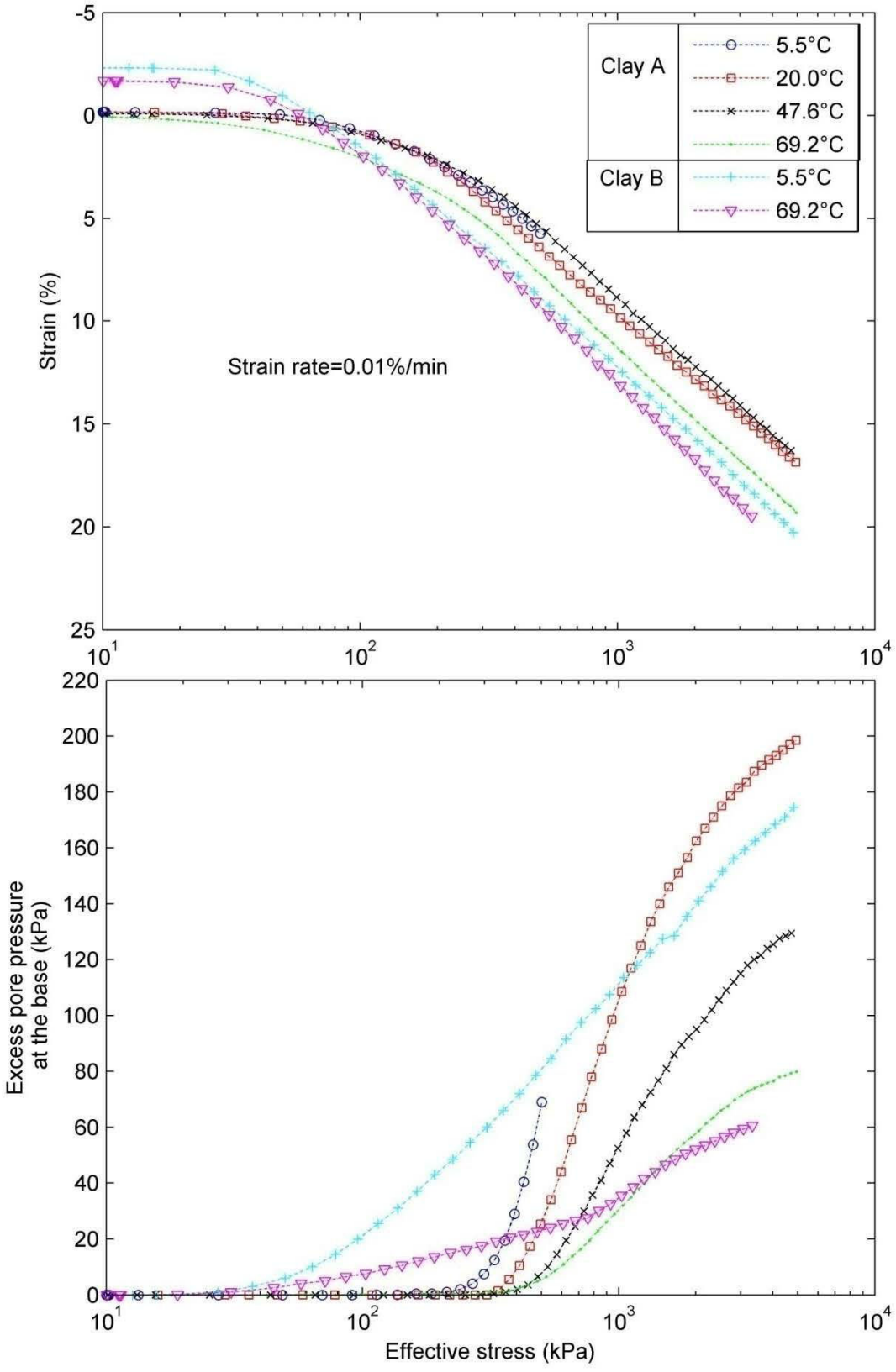

Figure 4.2 Effect of temperature on the effective stress-strain curve and excess pore water pressure for studied lightly over-consolidated materials at strain rate of 0.01%/min (Strain=$\Delta h/h_0$).

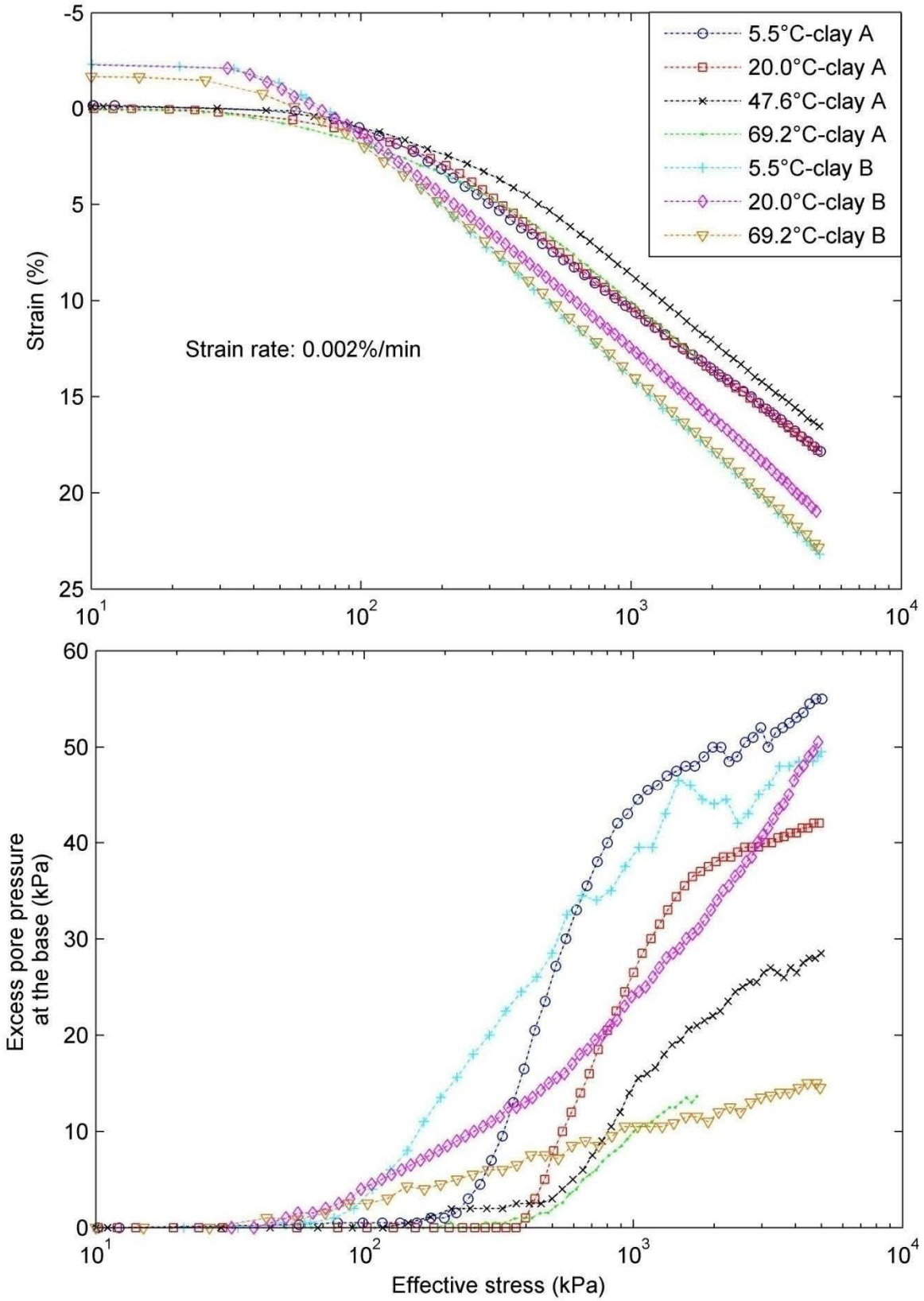

Figure 4.3 Effect of temperature on the effective stress-strain curve and excess pore water pressure at strain rate of 0.002%/min for studied lightly over-consolidated clays (Strain=$\Delta h/h_0$).

Depending on the obtained experimental results, the pore pressure variation due to temperature variations is significant. For any strain rate status, at a given vertical effective stress, the higher the temperature, the lower the generated excess pore pressure at the base of the clay sample for both materials.

4.3 Strain rate effect on the stress strain behaviour

Figures 4.4 and 4.5 show the variation of strain with vertical effective stress for clay A and clay B for different strain rates at temperatures of 5.5°C and 69.2°C. For clay B for example, the results in Figure 4.5 show that the strain increased at the strain rate of 0.002%/min for a given vertical effective stress at temperature 69.2°C. However, at temperature of 5.5°C for the same clay, a small difference in strain values was observed for the strain rates of 0.02 and 0.01%/min at a given effective stress.

Generally, for both materials, at a given temperature, results showed that the strains at the highest strain rate are lower than other strain rates at given effective stress because the pore pressure increased as the strain rate increased.

Furthermore, it is noted that for the combination of high temperature and low strain rate, the generated excess pore pressure is smaller (for example, at the 0.002%/min strain rate at 69.2° C). The generated excess pore pressure that was measured at the base of the specimen showed a strong dependency on the temperature and strain rate for both clays.

Excess pore water pressure variation with strain rate

Regardless of whether the temperature is high or low, a remarkable variation of excess pore pressure with vertical effective stress at different strain rates was recorded as shown in Figures 4.4 and 4.5 for both materials. At any temperature, the generated excess pore pressure for the strain rate of 0.002%/min was the smallest, while it was the largest for the strain rate of 0.02%/min. At temperature of 5.5°C for clay B for example, the maximum generated excess pore pressure at strain rate of 0.02%/min was 5.2 times larger than the maximum generated excess pore pressure at strain rate of 0.002%/min. It is clear that the excess pore pressure of clay A is more affected by temperature than clay B.

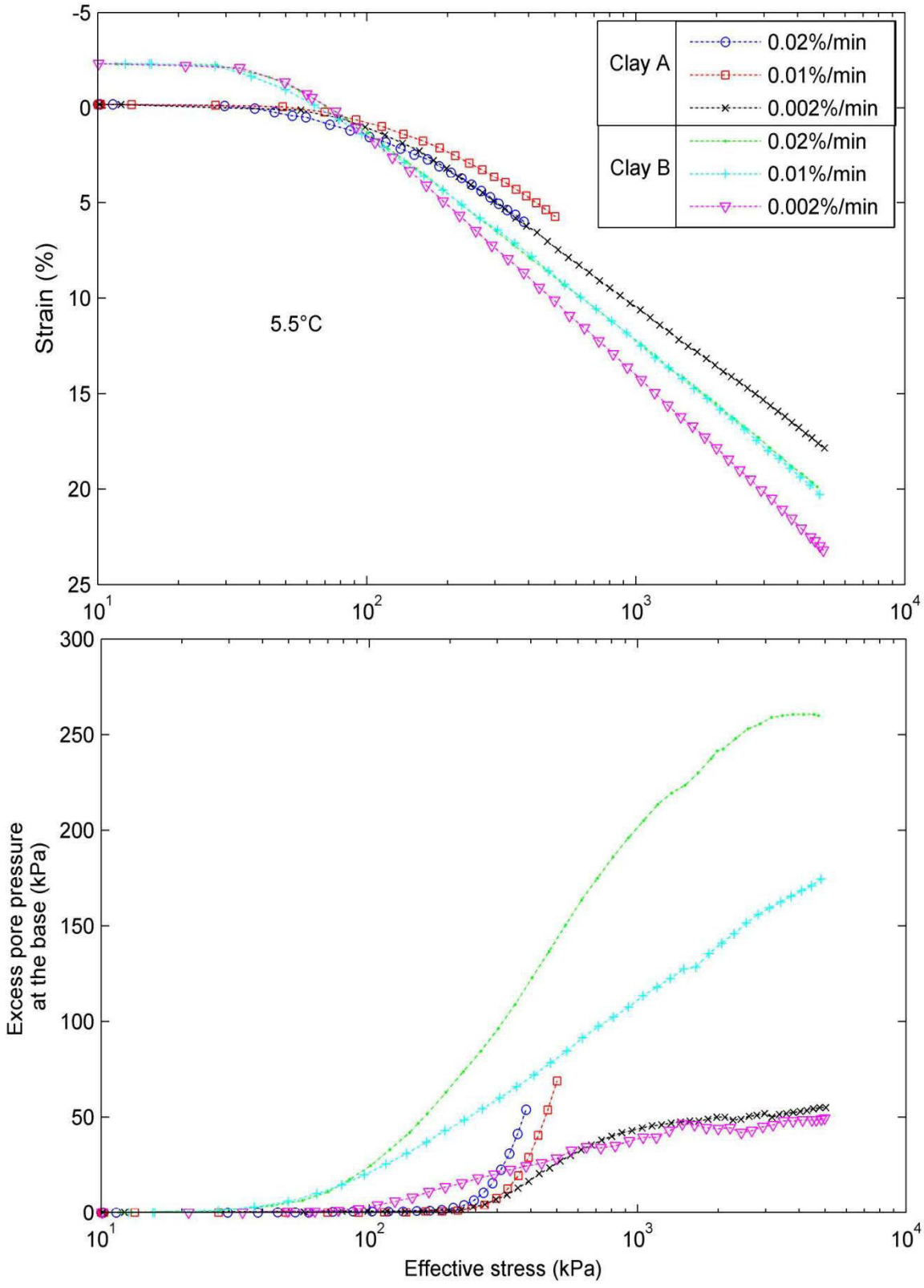

Figure 4.4 Effect of strain rate on the effective stress-strain curve and excess pore water pressure at 5.5°C for studied lightly over-consolidated clays(Strain=$\Delta h/h_0$).

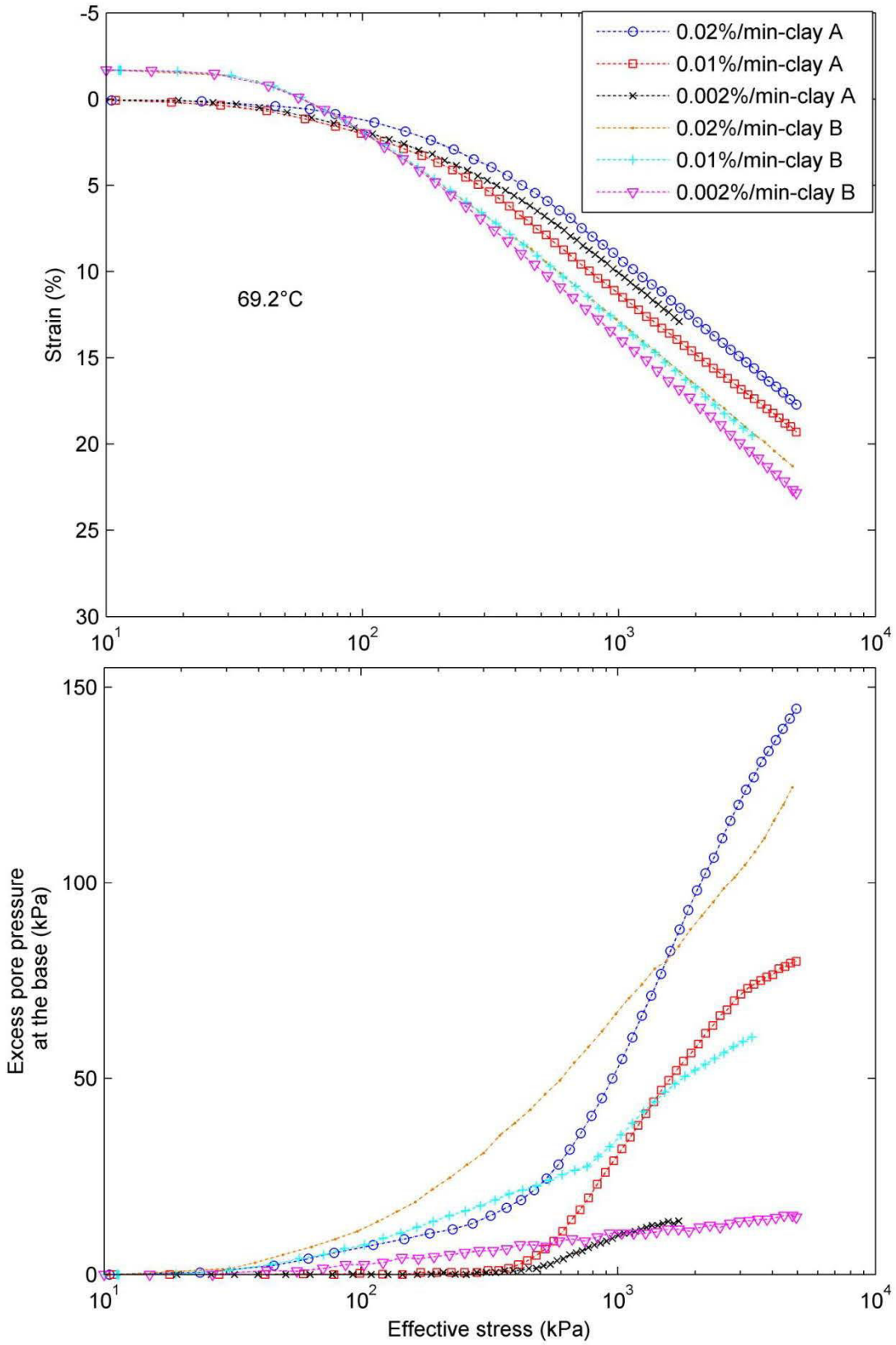

Figure 4.5 Effect of strain rate on the effective stress-strain curve and excess pore water pressure at 69.2°C for studied lightly over-consolidated clays(Strain=$\Delta h/h_0$).

Generally, for both materials, results showed that the excess pore pressure decreased as the strain rate decreased, and the smallest value was obtained at the lowest strain rate of 0.002%/min. Therefore, at very low strain rates, the generated excess pore water pressure was negligible.

4.4 Compression and swelling indices variation with temperature and strain rate

Figure 4.6 shows the variation of the compression and swelling indices with temperature and strain rate for 10 tests on lightly over-consolidated clay A and 7 tests on lightly over-consolidated clay B. For clay B for example, the obtained values of compression index at different temperatures (5.5°C, 20.0°C, 69.2°C) and strain rates (0.02%/min, 0.01%/min, 0.002%/min) extended from 0.182 to 0.205, while the obtained values of swelling index was between 0.009 to 0.019.

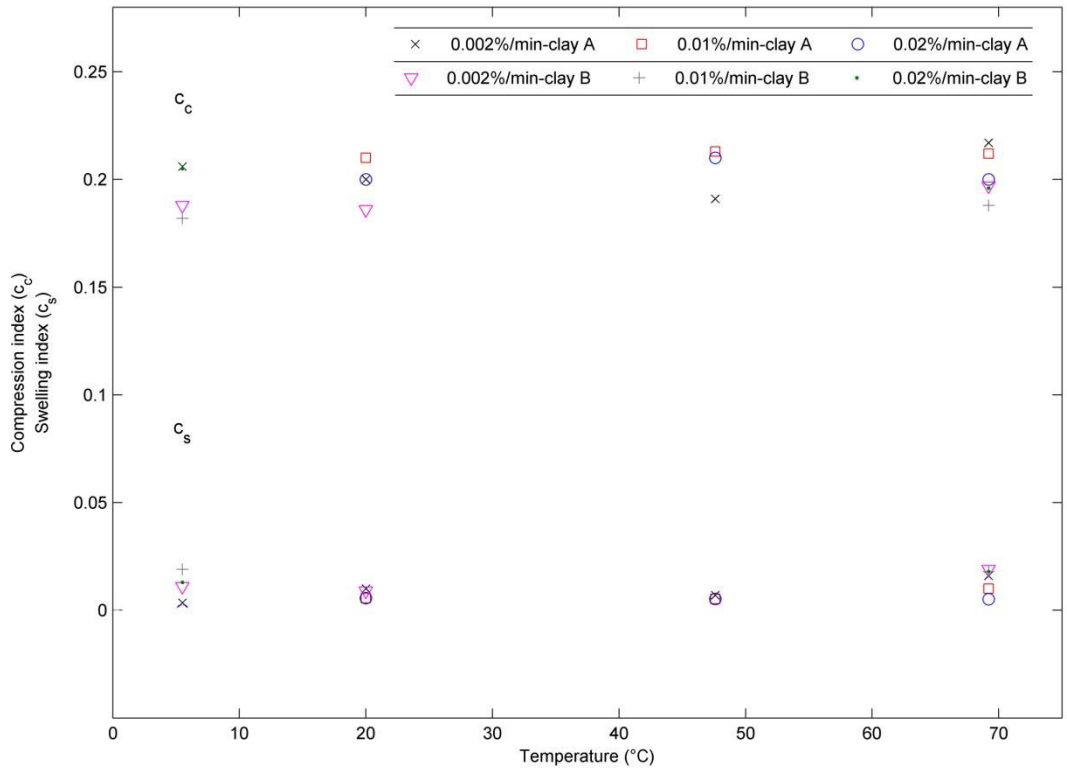

Figure 4.6 Effect of temperature and strain rate on the compression and swelling indices of studied lightly over-consolidated clays.

According to the obtained results, the compression index (c_c) slightly changed with temperature for clay A while its variation is negligeable for clay B. The swelling index (c_s) variation with temperature seems to be essentially independent of temperature for both clays. On the other hand, the compression (c_c) and swelling indexes (c_s) also remain unaffected by strain rate change for both materials.

4.5 Temperature and strain rate effect on the preconsolidation pressure

Temperature and strain rate effect on the evolution of the preconsolidation pressure for studied lightly over-consolidated clays had been investigated experimentally. Figure 4.7 displays the variation range of preconsolidation pressure with temperature and strain rate for 10 tests on lightly over-consolidated clay A and 7 tests on lightly over-consolidated clay B. For clay B, the evaluated preconsolidation pressures at 69.2° C decreased slightly compared to 5.5° C but less than clay A. The experimental results demonstrated also the strain rate effect on the preconsolidation pressure. At a given temperature, the preconsolidation pressure at strain rate of 0.02%/min was the largest comparing to other strain rates for both materials.

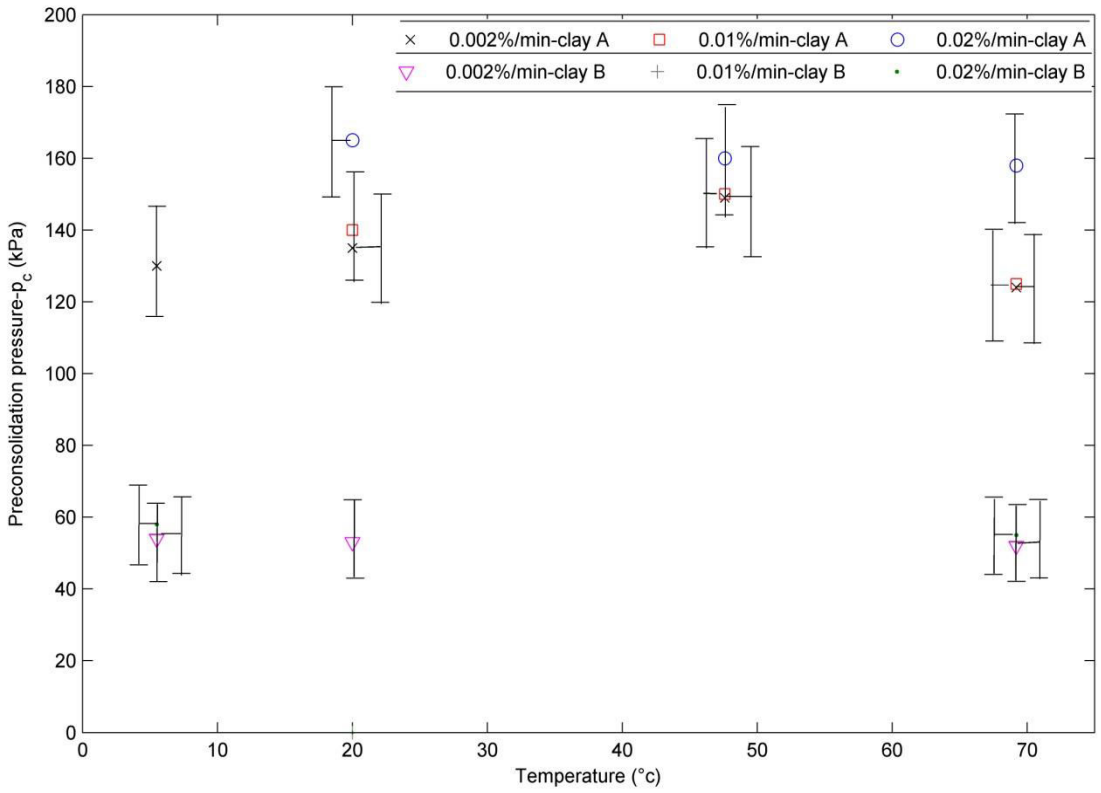

Figure 4.7 Effect of temperature and strain rate on the preconsolidation pressure of studied lightly over-consolidated clays.

It appears from the curves that the preconsolidation pressure of clay A was more affected by temperature than clay B, i.e., the elastic domain of clay A was more affected by temperature. The preconsolidation pressure increased with strain rate increase for both clays.

4.6 Temperature and strain rate effect on the coefficient of volume compressibility

To highlight the influence of temperature and strain rate on the coefficient of volume compressibility (m_v) for studied lightly over-consolidated clays, a strain rate of 0.002%/min

was chosen as an example for clay A and clay B. Figure 4.8 presents the values of coefficient of volume compressibility with vertical effective stress at different temperatures at the selected strain rate. At the selected strain rate, the value of coefficient of volume compressibility at 5.5°C is not far from its counterpart at 20.0 °C and 69.2°C. From another perspective, at a given temperature, values of coefficient of volume compressibility at strain rates of 0.02%/min, 0.01%/min, and 0.002%/min superimpose approximately at the same value.

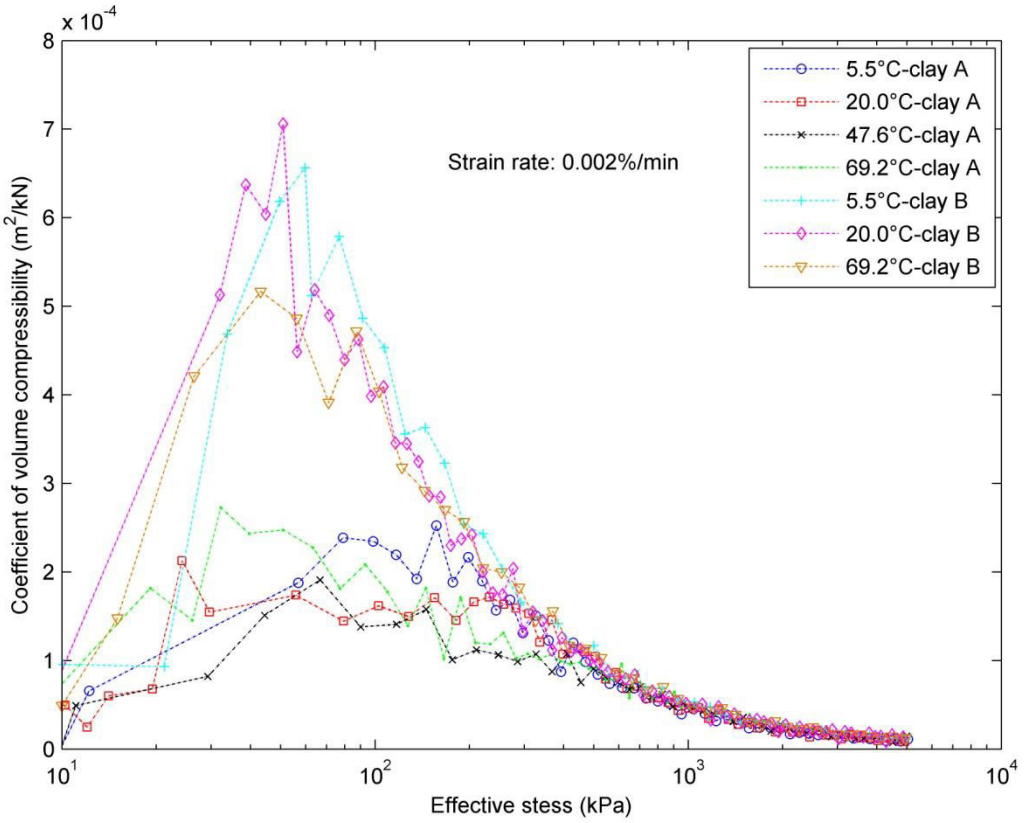

Figure 4.8 Effect of temperature on the coefficient of volume compressibility for studied lightly over-consolidated clays at strain rate of 0.002%/min.

It seems that the coefficient of volume compressibility (m_v) is not significantly affected by temperature and strain rate for both materials according to the obtained results.

4.7 Temperature and strain rate effect on the permeability

To evaluate the temperature and strain rate effect on the permeability of studied lightly over-consolidated clays, two void ratios, 0.40 and 0.65, were selected for clay B and A respectively. Using the indirect method of CRS test theory to determine permeability, Figure 4.9 presents the impact of temperature and strain rate on the permeability at the selected void ratios. For clay B for example, at a strain rate of 0.01%/min, the hydraulic conductivity at 69.2°C increased by approximately three times the hydraulic conductivity at 5.5°C. A positive

relationship was also observed for clay A. The difference in the intrinsic permeability at different temperatures was small for both materials (Table 4.1). On the other hand, for temperature of 5.5°C, the hydraulic conductivity at strain rate of 0.002%/min was the lowest in comparison with other strain rates for both materials.

Table 4.1 Intrinsic permeability variation with temperature and strain rate for lightly over-consolidated clay A at e=0.65 and clay B at e=0.40.

Temperature (°C)	Strain rate (%/min)	K (m^2) Clay A	K (m^2) Clay B
5.5	0.02	-	6.80E-19
5.5	0.01	-	5.38E-19
5.5	0.002	1.22E-19	3.23E-19
69.2	0.02	2.75E-19	4.98E-19
69.2	0.01	2.58E-19	5.61E-19
69.2	0.002	1.64E-19	3.00E-19

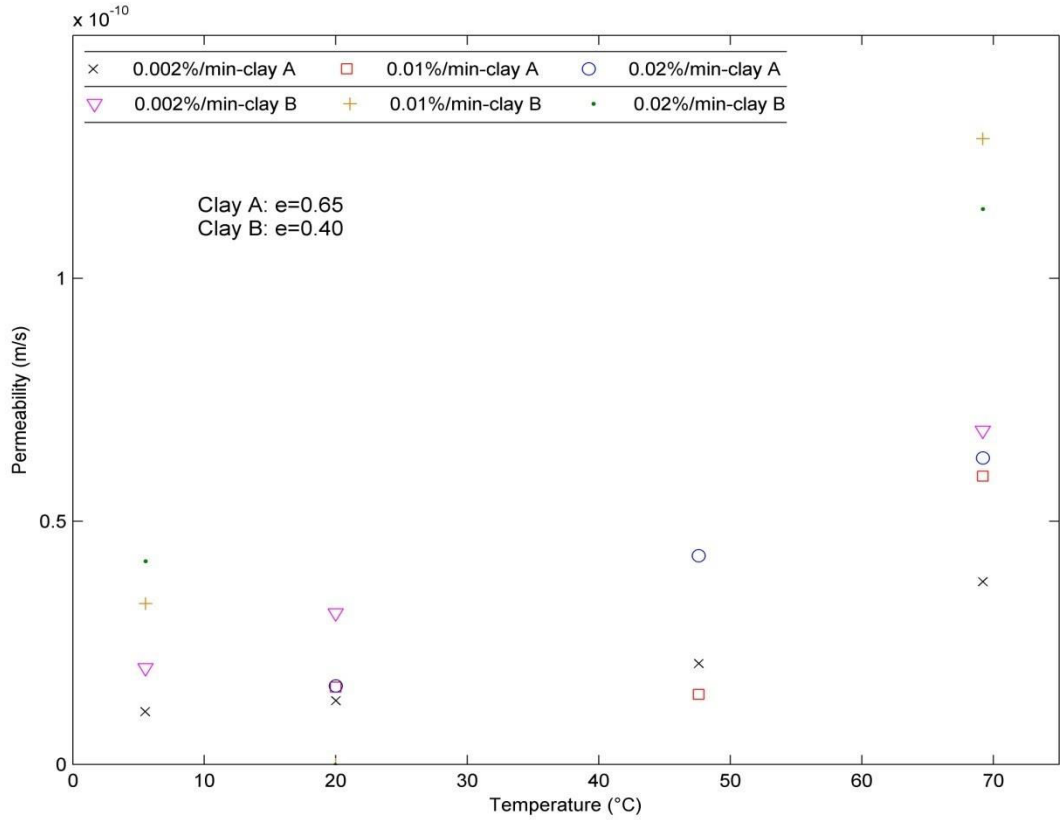

Figure 4.9 Effect of temperature and strain rate on the permeability (k) for lightly over-consolidated studied clays.

The results indicated on the one hand that the water involved in transfer at different temperatures is free water and on the other hand that there is apparently no changes in the status of the porosity with respect to different temperatures.

4.8 Temperature and strain rate effect on the coefficient of consolidation

At selected constant void ratio of 0.65 for clay A and 0.40 for clay B, observation of results presented in Figure 4.10 indicated that the relationship between coefficient of consolidation (C_v) and temperature is important. For clay B for example, at strain rate of 0.01%/min, the value of C_v at 69.2° C is three times larger than the value of C_v at 5.5° C. C_v was increased with temperature for clay A. To investigate strain rate effect, it was observed at different temperatures that the lower the strain rate, the lower the coefficient of consolidation for both materials (Figure 4.10).

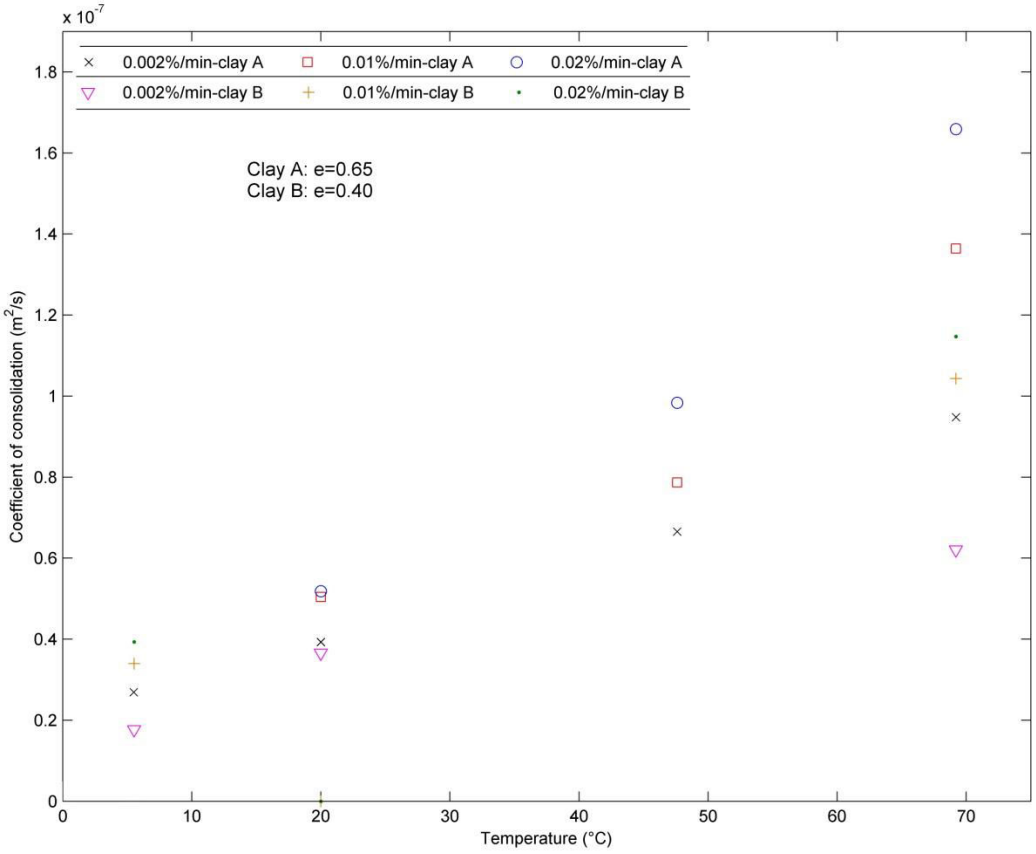

Figure 4.10 Effect of temperature and strain rate on the coefficient of consolidation (c_v) for studied clays.

It appears reasonable from obtained data that the coefficient of consolidation which is a function of permeability is temperature dependent for both materials. Moreover, it was affected positively by strain rate.

4.9 Temperature effect on the long-term consolidation

The long term behaviour of studied clays was evaluated at different temperatures using the method of Mesri and Godlewski (1977) which is mentioned in Chapter 3. The following sections present the variation of preconsolidation pressure-strain rate relationship with temperature and the creep index (c_α) variation with temperature for both clays.

4.9.1 Variation of preconsolidation pressure–strain rate relationship with temperature

Figure 4.11 presents the variation range of the preconsolidation pressure with strain rate for different temperatures for both materials. The estimated values of c_α/c_c were relatively close to each other at two different temperatures for clay B. These estimated values were 0.032 and 0.033 at 5.5° C and 69.2° C, respectively. Generally, the estimated values of c_α/c_c varied between 0.013 and 0.051 for the different temperatures. The estimated values of c_α/c_c varied with temperature alteration between 0.039 and 0.125 for clay A as mentioned previously.

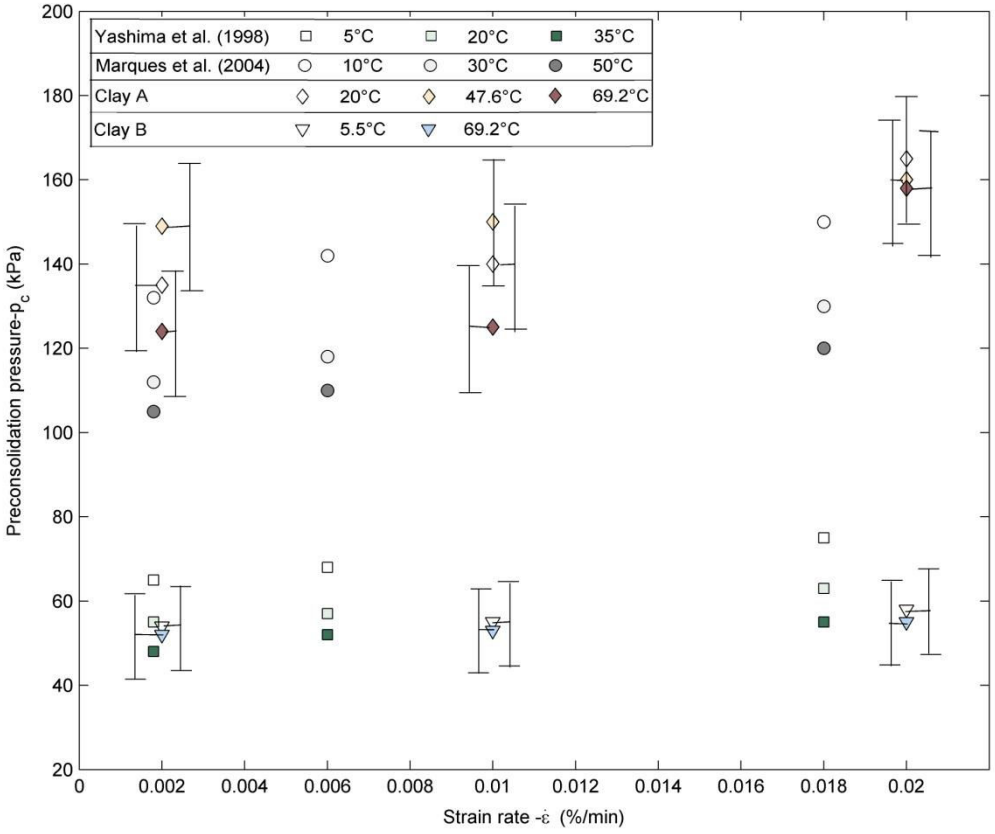

Figure 4.11 Variation of preconsolidation pressure with strain rate at different temperatures for studied clays and different researchers.

Based on the obtained results in this study, the estimated values of c_α/c_c varied with temperature for both compacted materials.

4.9.2 Effect of temperature on the creep index (c_α)

Figure 4.12 shows the variation range of the creep index with temperature for studied materials. c_α was obtained according to the estimated values of c_α/c_c and c_c, where c_c is the slope of compression curve at the end of primary consolidation (EOP). Results indicated that the creep index of clay B increased slightly as temperature increased, but less significantly

than clay A. At temperatures of 5.5 and 69.2° C, the corresponding estimated c_α were 0.0061 and 0.0064, respectively.

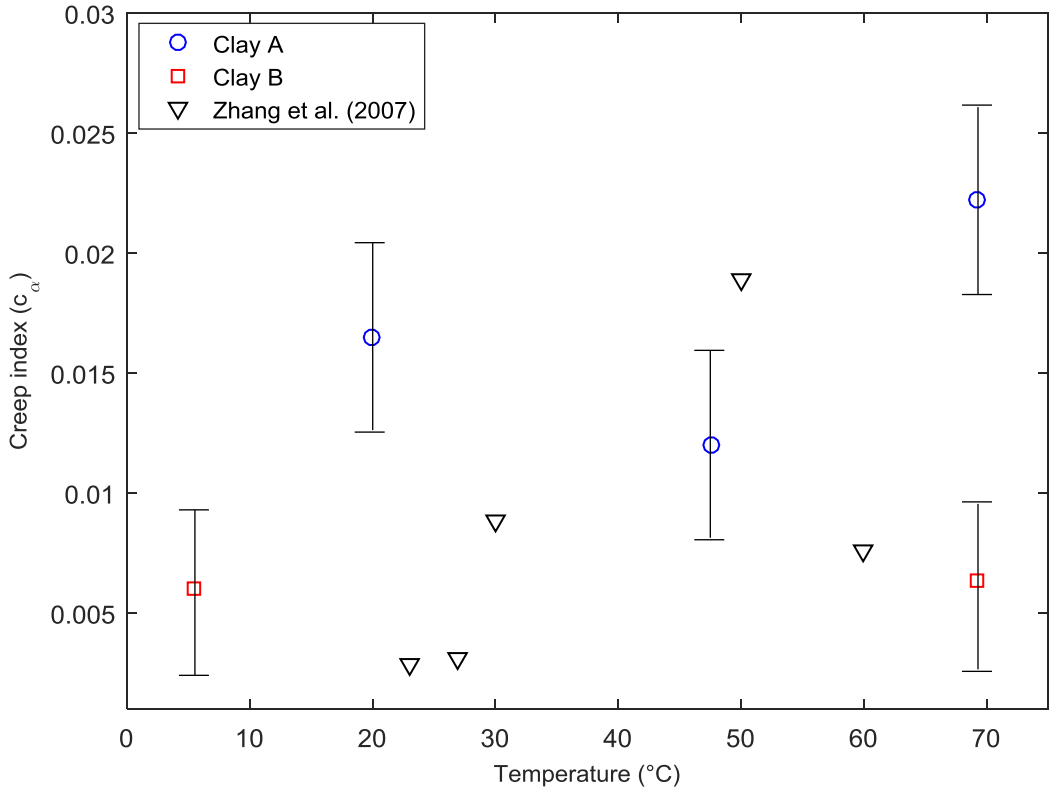

Figure 4.12 Influence of temperature on the creep index (c_α) of studied clays.

The results indicated that the creep behaviour of clay A was more affected by temperature than clay B.

4.10 Soil plasticity index effect

An attempt was made to correlate the soil plasticity index effect on the thermally induced volumetric strain for the studied materials. Figure 4.13 shows the impact of soil plasticity index on the thermally induced volumetric strain for different clays. When the temperature increased within the range from 5.5°C to 69.2°C, the thermally induced volumetric strain for clay with larger plasticity index was larger than other clays.

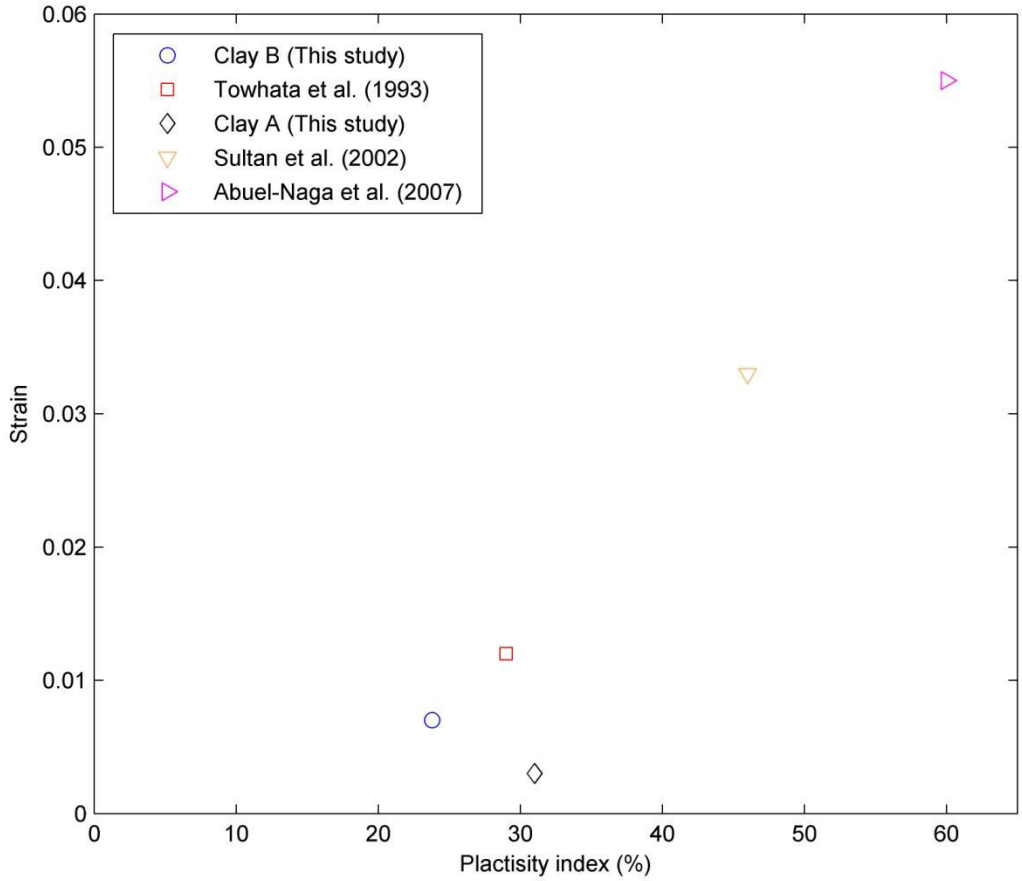

Figure 4.13 Effect of soil plasticity index on the thermally induced volumetric strain for different clay soils (ΔT=63 to 70) (Strain=$\Delta h/h_0$).

In general, it is observed in this study that the thermally induced volumetric strain was influenced by the soil plasticity index for lightly over-consolidated samples.

4.11 Clay content effect

A study on the relationship between the clay content and the thermally induced volumetric strain under constant total stress has been performed. Figure 4.14 shows the thermally induced volumetric strain variations with clay content under 1500 kPa for 0.01%/min CRS tests on the studied materials. It has been found for lightly over-consolidated samples that during temperature change ΔT = 63°C, the thermally induced volumetric strain of clay with 85% clay content (clay A) was more than the thermally induced volumetric strain of clay with 45% clay content (Clay B).

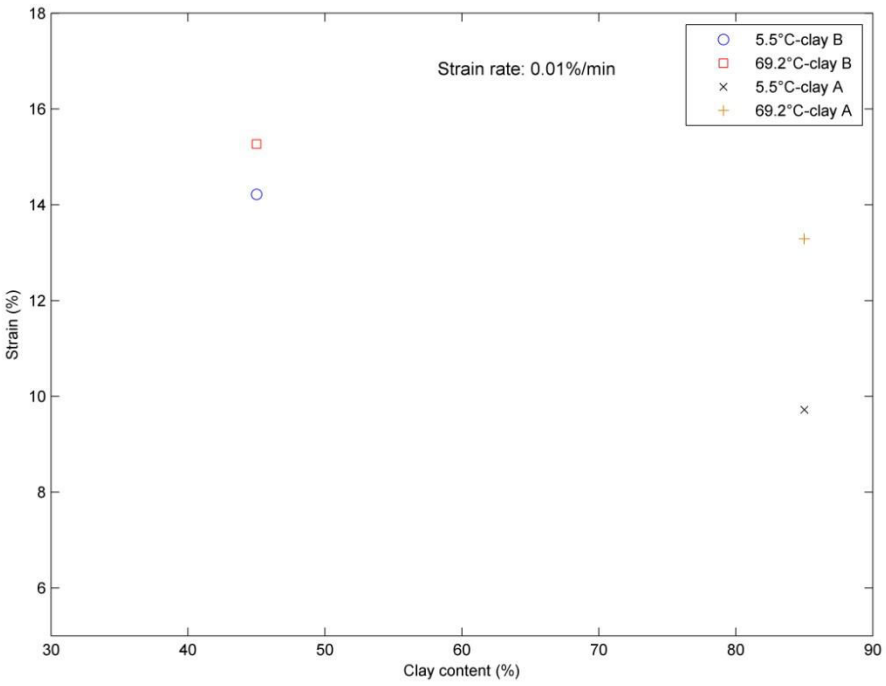

Figure 4.14 Effect of clay content on the thermally induced volumetric strain under constant total stress of 1500 kPa for lightly over-consolidated clays (LOC) (Strain=$\Delta h/h_0$).

Based on the obtained results, it can be concluded that there is a correlation between clay content and temperature effect on the soil behaviour. The percentage of clay could control the thermo-mechanical behaviour of fine graded soils.

4.12 Results discussion

The results indicated that the compression curve (ε-σ') of clay B was less affected by temperature than clay A after CRS tests with temperature range between 5.5°C and 69.2°C. In fact, clay B is denser than clay A. A similar behavior for dense granitic soil was reported by Kholghifard et al. (2014). They mentioned that for dense samples, the soil response is controlled by the compression caused by the applied load. However, Boudali et al. (1994) and Marques et al. (2004) observed that the strain increased with temperature increase at a given effective stress through CRS tests on natural clays and this is related to the viscous behaviour of clay with temperature. Their results of the stress-strain response to temperature were more affected compared with the current study results which focused on compacted clays. The main reason for the difference in the stress-strain behaviour with temperature between studied clays could be related to the difference in the characteristics and mineralogy of these clays (section 2.2).

The results showed different effects of temperature on the consolidation characteristics of studied clays. The compression index of clay A slightly changed with temperature but clay B

compression index was less affected. A similar behaviour to clay A, Tanaka et al. (1997) observed non parallel normally consolidated lines at different temperatures (28, 65, 100 °C) for reconstituted illitic clay. In agreement with this study, François et al. (2007) using sandy silt soil and Tang et al. (2008a) using bentonite indicated that the effect of temperature on the compressibility indices is not significant.

In comparison with clay B, the preconsolidation pressure of clay A was more affected by temperature. In fact, clay A is more plastic than clay B. The change in the preconsolidation pressure due to temperature change was larger for soils with higher clay content (Tidfors & sallfors, 1989). This is consistent with these study results. A reduction in the preconsolidation pressure was monitored by Moritz (1995) for natural clay, Sultan et al. (2002) for Boom clay, and Tang et al. (2007) for bentonite at high temperatures as observed also in this study. The viscosity reduction at high temperature softens the soil and reduces the elastic domain of the clay and hence the preconsolidation pressure decreases.

In addition, results show that the excess pore pressure at the base decreased with temperature increase but it is less affected in the case of clay B. Lower pore pressure value at higher temperature during CRS tests on soft natural clays was observed by Marques et al. (2004) and Tsutsumi and Tanaka (2012).Their findings are in agreement with the current study results. In fact, the occurrence of high permeability at high temperatures (Towhata et al., 1993; Villar & Lloret, 2010) beside the drainage from one side limits the buildup of pore pressure in the specimen. In other words, the high strain rates caused lower strain of the sample, and this resulted in the generation of higher excess pore water pressure. Leroueil et al. (1985), Marques et al. (2004), and Jia et al. (2010) observations on natural clays are consistent with this study results. In fact, the results indicated that the clay nature has small effect on its behaviour with different strain rates.

As it can be seen from the results, lower strain rate generates lower pore water pressure at the base of the sample for both materials. At low strain rate, there is enough time for excess pore pressure to dissipate, and so, lower value of pore water pressure was observed. In fact, it is noted from the results that the clay nature has not an important effect on the pore pressure variation with strain rate. The study observations are in agreement with Leroueil et al. (1985), and Ahmadi et al. (2014) findings on natural clays.

The testing of hydraulic conductivity (indirect method) at different temperatures for both materials showed that it increases with temperature increase. Referring to section 1.4.5, a similar behaviour to this study was observed by Towhata et al (1993) using bentonite and

kaolin clays and Abuel-Naga et al. (2005) using soft Bangkok clay (PI=60%). They used the indirect method to measure the permeability at different temperature after performing isothermal consolidation tests at different temperatures. The direct measurements of permeability (See section 1.3) showed also that it increases with temperature increase (Cho et al., 2000; Villar & Lloret, 2004). Delage et al. (2000) noted that the effect of temperature (20-100°C) on the soil porosity is not significant. The increased permeability with temperature increase is because of decreased viscosity with temperature increase (Towhata et al., 1993). The investigated values of coefficient of consolidation at different temperatures for clay A and clay B show that the coefficient of consolidation was larger at higher temperatures. Using isothermal oedometer tests at different temperatures, Abuel-Naga et al. (2005) observed that the coefficient of consolidation at 20°C is lower than at 90°C. This point is consistent with this study. The decrease of viscosity of pore water with temperature increase makes the consolidation amount greater at high temperatures (Akagi et al., 1995).

Referring to section 1.5.4, the method of Mesri and Godlewski (1977) was used to evaluate the long term behaviour of studied clays ($\alpha=c_\alpha/c_c=\Delta\log P_c/\Delta\log \dot{\varepsilon}$). According to the obtained results, the estimated values of $\Delta\log P_c/\Delta\log \dot{\varepsilon}$ changed with temperature alteration for both materials. In comparison with this study, Boudali et al. (1994) carried out different constant rate of strain (CRS) consolidation tests at different temperatures to investigate the viscous behavior of natural clay (PI=40%). They found that the strain rate-preconsolidation pressure relationship is independent of temperature. A similar behavior of natural clay (PI=41-46%) was also observed by Marques et al. (2004). Boudali et al. (1994) and Marques et al. (2004) found approximately parallel slopes of strain rate-preconsolidation pressure relationship at different temperatures (Figure 4.11). These studies were however focused on the natural and structured clays only, while this study focused on the compacted clays. The differences in the results may relate to the differences in the clay nature and mineralogy.

Based on the estimated values of (c_α/c_c) and c_c at different temperatures, results indicated that the creep index of both materials increased slightly with temperature increase, but the creep index of clay B was less affected by temperature than clay A. In line with this study, Towhata et al. (1993) found that the amount of secondary deformation at high temperatures is more than the case under room temperature. The high temperatures may cause the starting of creep earlier (Moritz et al., 1995). This difference in findings could be related to the differences in mineralogy and nature.

It is observed from our results that the plasticity index has an effect on the thermally induced volumetric strain (Figure 4.13). By comparing with different clays, thermally induced

volumetric strain increases with PI increase. Abuel-Naga et al. (2005) compared also the thermally induced volumetric strain with plasticity index of different types of normally consolidated clays that were subjected to temperature change, $\Delta T \approx 65$ to 70 °C, and they found a linear trend between the thermally induced volume change and plasticity index (PI). The temperature effect on the physico-chemical interactions between the clay particles (See section 1.4.1) contributes to the thermally induced volumetric strain (Laloui and Cekerevac, 2003). According to Abuel-Naga et al. (2005) results, the PI (plasticity index) gives a qualitative indication to the physico-chemical interactions between the clay particles.

It is also found that the percentage of fines could control the thermo-mechanical behaviour (Figure 4.14). According to the obtained results, the higher the percentage of fines in clay, the higher the thermally volumetric strain under constant effective stress. The physico-chemical interactions between the clay particles at different temperatures (See section 1.4.1) which depend on the clay lattice constitution, the chemical nature of the interstitial fluid, and interlayer distance affect the thermally induced volumetric strain (Laloui and Cekerevac, 2003). Accordingly, the clay content could contribute to the thermally induced volumetric strain.

4.13 Conclusion

This chapter discussed the impact of clay nature on the thermo-hydro-mechanical behaviour based on a comparison between two different clays. The studied materials were an illitic clay (clay A) and a clay which was composed mainly of kaolinite, illite, and smectite (clay B). Table 4.2 shows the consolidation parameters variation with temperature and strain rate for lightly over-consolidated clay A and clay B.

The differences in temperature impact on the short- and long- term behaviour for clay A and clay B were presented in this chapter. Based on the results, the stress-strain behaviour of clay A was more affected by temperature than clay B because of different nature and mineralogy beside different dry densities. The results indicated that the long term behaviour of clay A was more affected by temperature than clay B. The preconsolidation pressure-strain rate relationship varied with temperature alteration for both materials. According to that relationship, the value of creep index of clay A was slightly increased with temperature increase, while it was less affected by temperature for clay B. It was also observed that the thermally induced volumetric strain was influenced by the soil plasticity index and clay content.

Table 4.2 Consolidation parameters variation with temperature and strain rate for lightly over-consolidated clay A (e=0.65) and clay B (e=0.40).

Temperature (°C)	5.5		20.0		47.6		69.2	
Clay A								
Strain rate (%/min)	C_c	C_s	C_c	C_s	C_c	C_s	C_c	C_s
0.02	-	-	0.20	0.0057	0.21	0.0053	0.20	0.0051
0.01	-	-	0.21	0.0056	0.213	0.0053	0.212	0.01
0.002	0.206	0.0035	0.20	0.01	0.191	0.007	0.217	0.016
Strain rate (%/min)	Pc (kPa)							
0.02	-		165		160		158	
0.01	-		140		150		125	
0.002	130		135		149		124	
Strain rate (%/min)	$m_v \times 10^{-5}$ (m^2/kN)							
0.02	-		3.341		3.155		4.056	
0.01	-		3.148		1.849		4.444	
0.002	2.867		3.115		4.417		3.888	
Strain rate (%/min)	k $\times 10^{-11}$ (m/s)	K $\times 10^{-19}$ (m^2)	k $\times 10^{-11}$ (m/s)	K $\times 10^{-19}$ (m^2)	k $\times 10^{-11}$ (m/s)	K $\times 10^{-19}$ (m^2)	k $\times 10^{-11}$ (m/s)	K $\times 10^{-19}$ (m^2)
0.02	-	-	1.616	1.64	4.291	2.62	6.307	2.75
0.01	-	-	1.588	1.61	1.438	0.879	5.927	2.58
0.002	1.086	1.74	1.313	1.33	2.074	1.27	3.759	1.64
Strain rate (%/min)	$c_v \times 10^{-8}$ (m^2/s)							
0.02	-		5.187		9.835		16.59	
0.01	-		5.045		7.868		13.64	
0.002	2.692		3.93		6.654		9.479	
-	c_α							
-	-		0.0165		0.012		0.022	
Clay B								
Strain rate (%/min)	C_c	C_s	C_c	C_s	C_c	C_s	C_c	C_s
0.02	0.205	0.013	-	-	-	-	0.196	0.018
0.01	0.182	0.019	-	-	-	-	0.188	0.018
0.002	0.188	0.011	0.186	0.009	-	-	0.197	0.019
Strain rate (%/min)	Pc (kPa)							
0.02	58		-		-		55	
0.01	55		-		-		53	
0.002	54		53		-		52	
Strain rate (%/min)	$m_v \times 10^{-4}$ (m^2/kN)							
0.02	1.121		-		-		1.132	
0.01	1.212		-		-		1.262	
0.002	1.063		9.92		-		1.019	
Strain rate (%/min)	k $\times 10^{-11}$ (m/s)	K $\times 10^{-19}$ (m^2)	k $\times 10^{-11}$ (m/s)	K $\times 10^{-19}$ (m^2)	k $\times 10^{-11}$ (m/s)	K $\times 10^{-19}$ (m^2)	k $\times 10^{-11}$ (m/s)	K $\times 10^{-19}$ (m^2)
0.02	4.180	6.80	-	-	-	-	11.42	4.98

0.01	3.309	5.38	-	-	-	-	12.87	5.61
0.002	1.983	3.23	3.111	4.971	-	-	6.871	3.0
Strain rate (%/min)	**$c_v \times 10^{-8}$ (m^2/s)**							
0.02	3.933		-		-		11.47	
0.01	3.40		-		-		10.43	
0.002	1.77		3.655		-		6.207	
-	**c_α**							
-	0.0061		-		-		0.0064	

Clay B was denser than clay A, and clay A was more plastic than clay B. In addition, both clays were different in the mineralogy. Based on the observed behaviour of studied materials with temperature, the clay nature could be considered as an important factor controlling the thermo-hydro-mechanical behaviour of lightly over-consolidated samples.

Chapter 5 Impact of the over-consolidation ratio (OCR) on the thermo-hydro-mechanical behaviour of clayey soils

5.1 Introduction

The impact of stress history (OCR) on the thermo-hydro-mechanical behaviour of saturated compacted clayey soils is discussed in this chapter. In order to do that, CRS tests were performed at different temperatures on two different materials which were loaded at different stress histories. These two different materials were illitic clay (clay A) and clay composed of kaolinite, and illite/smectite (clay B). The over-consolidated sample preparation for studied materials is presented in this chapter.

The impact of OCR on the consolidation characteristics variation with temperature for studied materials are presented and discussed in this chapter. The results of lightly and heavily over-consolidated clayey soils are compared and presented.

5.2 Over-consolidation method

Figure 5.1 shows the total experimental path for the heavily over-consolidated samples. To obtain heavily over-consolidated clay samples for both materials, the sample was firstly loaded from 10 kPa to 1000 kPa at a constant rate of stress in drained conditions (one side drainage) after saturation phase (path a-b). The constant rate of stress was equivalent to strain rate of 0.01%/min. This rate of stress was determined from a constant rate of strain consolidation test at a strain rate of 0.01%/min for each type of soil. For clay A, the sample was loaded by a stress rate of 0.823 kPa/min (=0.01%/min strain rate), while it was loaded by a stress rate of 0.618 kPa/min (=0.01%/min strain rate) for clay B. The sample was then kept under the constant vertical stress of 1000 kPa until the pore pressure dissipation without reaching the secondary consolidation phase. The sample was then unloaded to 10 kPa at a constant rate of stress equal to twice the loading rate (1.646 kPa/min for clay A, and 1.236 kPa/min for clay B) (path c-d). The unloaded sample was considered stabilized when the deformation variation of the sample was less than 0.001% per minute. The unloaded sample was then heated to a given temperature T (path d-e). After stabilization of thermal deformation of the sample (0.001%/min), CRS tests with strain rate of 0.01%/min were performed (path e-f). Table 5.1

shows the experimental program for the studied heavily over-consolidated clays. Figures 5.2 and 5.3 show the experimental path for heavily over-consolidated clays at strain rate of 0.01%/min at different temperatures.

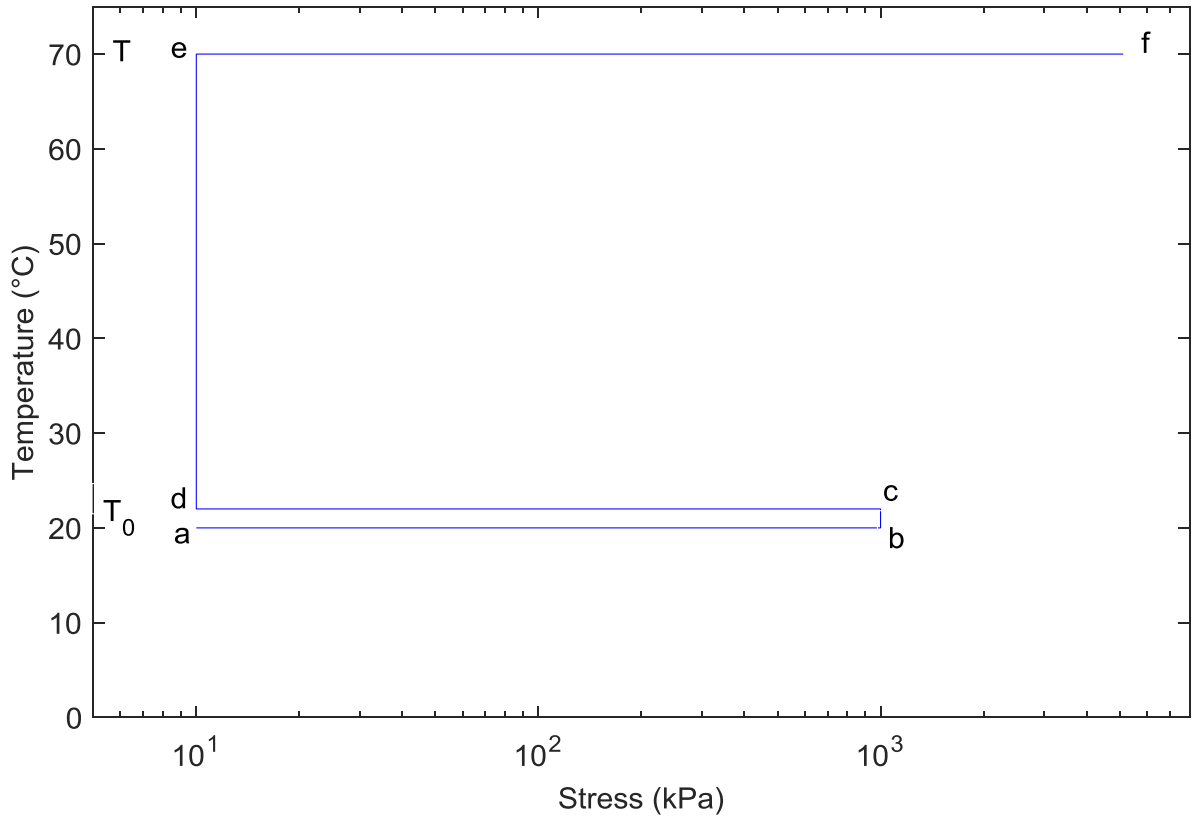

Figure 5.1 Applied mechanical and thermal paths for heavily over-consolidated clay (T0=20°C and T = 5.5 and 69.2°C).

Table 5.1 Experimental program for studied heavily over-consolidated clays.

Temperature (°C)	Strain rate (%/min)	Clay type	
		Clay A (OCR=67.5)	Clay B (OCR=26)
5.53	0.01	✓	✓
69.2	0.01	✓	✓

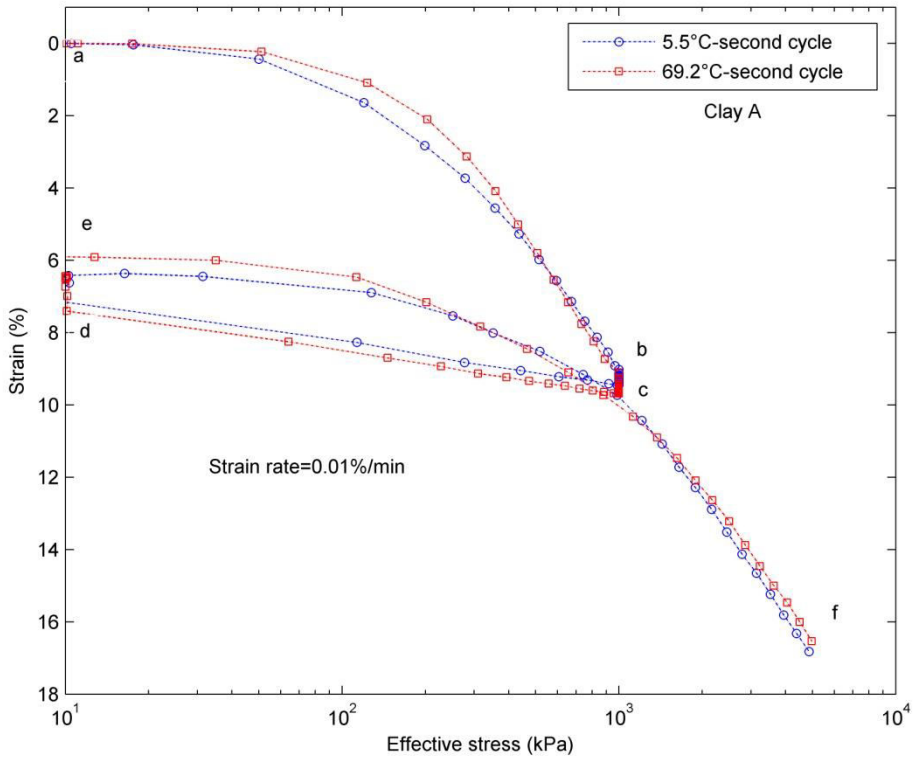

Figure 5.2 Experimental path for the effective stress-strain curve of heavily over-consolidated clay A at strain rate of 0.01%/min (Strain=$\Delta h/h_0$).

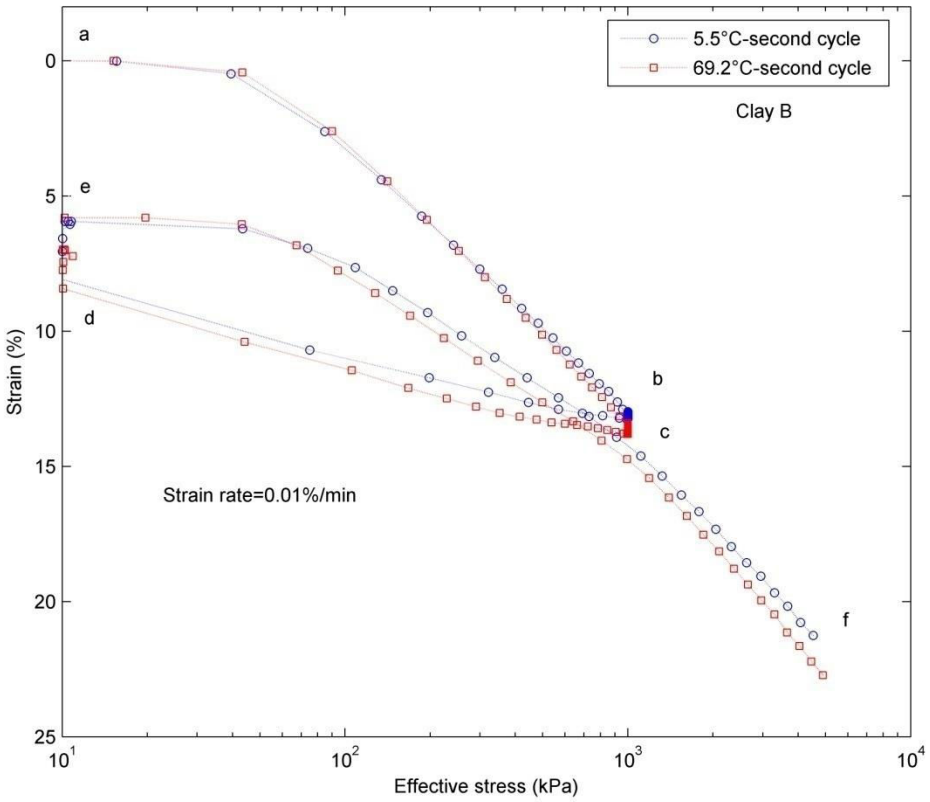

Figure 5.3 Experimental path for the effective stress-strain curve of heavily over-consolidated clay B at strain rate of 0.01%/min (Strain=$\Delta h/h_0$).

The path a-b-c-d-e-f in Figure 5.2 and 5.3 represents loading until 10^3 kPa, constant loading at 10^3 kPa, unloading until 10 kPa, constant loading at 10 kPa and process of heating, and constant rate of strain loading respectively.

5.3 Relationship between total stress and pore water pressure

Figure 5.4 shows the variation of pore water pressure relative to total stress against the vertical effective stress at different temperatures for heavily over-consolidated samples of clay A. The maximum ratio of pore water pressure relative to the total stress at 5.5°C during loading was 3.4%, while it was 3.6% at 69.2°C. These findings are within the limit recommended by ASTM (2008) method to interpret the results according to the theory of CRS test.

Generally, the maximum produced pore pressure ratio during the loading phase in the CRS tests at all testing temperatures is very low compared to the normally consolidated samples for heavily over-consolidated samples of clay A.

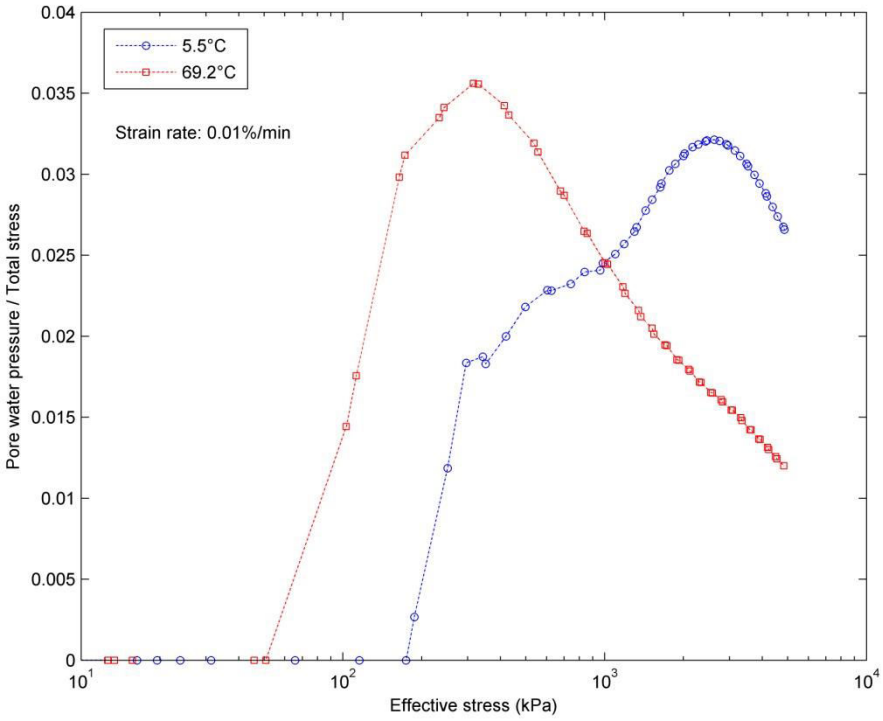

Figure 5.4 Variation of pore pressure ratio (pore pressure/total stress) with vertical effective stress at different temperatures at strain rates of 0.01%/min for heavily over-consolidated clay A.

On the other hand, the variations of pore water pressure relative to total stress against the vertical effective stress at different temperatures for heavily over-consolidated samples of clay B are shown in Figure 5.5. The maximum produced pore water pressure ratio during CRS test at 69.2°C was 0.12 which is larger than the maximum produced pore water pressure ratio at

5.5°C (0.105). The obtained pore pressure ratios from CRS tests at different temperatures for 0.01%/min strain rate are consistent with the limit recommended by ASTM (2008) for results interpretation.

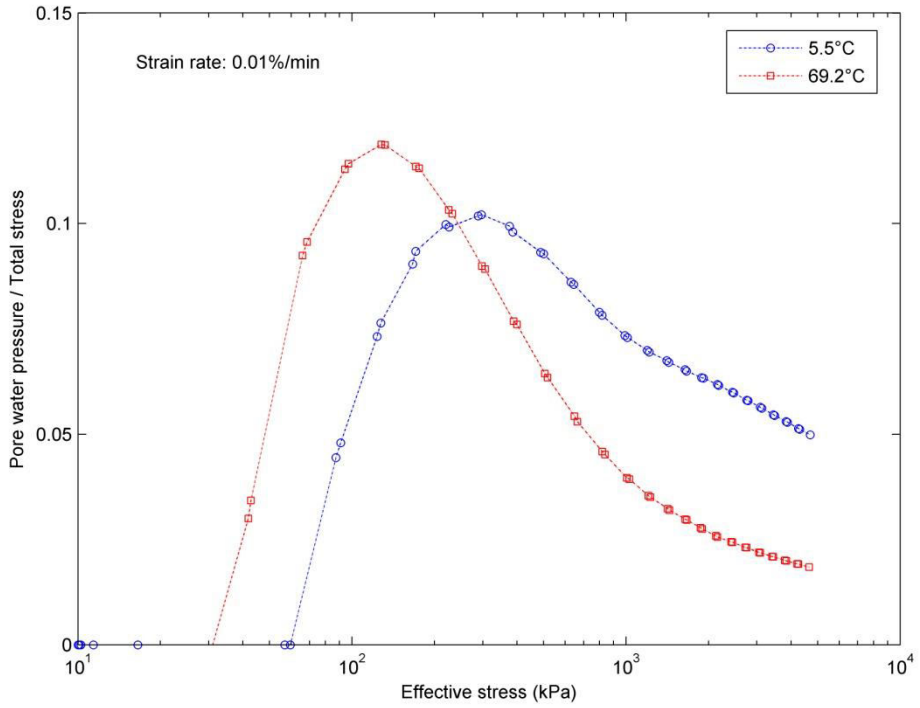

Figure 5.5 Variation of pore pressure ratio (pore pressure/total stress) with vertical effective stress at different temperatures for strain rate of 0.01%/min for heavily over-consolidated clay B.

Generally, the laboratory results show that the produced pore water pressure ratios at different temperatures for heavily over-consolidated samples of clay B are low.

5.4 Stress strain behaviour with temperature

In order to express the mechanical behaviour of heavily over-consolidated samples of clay A with temperature, the stress-strain behaviour has been determined at two different temperatures of 5.5°C and 69.2°C using tests at strain rate of 0.01%/min. Experimental results for these tests are shown in comparison with the lightly over-consolidated samples in Figure 5.6. The compression curve at 5.5°C converged to the compression curve at 69.2°C with a small difference in the elastic part of the curve.

It is obvious from the results that the compression curves of heavily over-consolidated samples are not strongly affected by temperature variations especially the plastic part of the curve. However, the compression curves of lightly over-consolidated samples were more affected by temperature.

Considering the effect of temperature on the hydraulic behaviour of over-consolidated samples, Figure 5.6 presents the results of pore water pressure variation with vertical effective stress at different temperatures. For heavily over-consolidated samples, in the drained tests at strain rate of 0.01%/min, the increased water viscosity at 5.5°C caused the excess pore water pressure at the base of the sample is larger than the generated excess pore water pressure at temperature of 69.2°C by a factor of 2.25.

Based on the results, it appears that temperature is an important factor that affects the excess pore water pressure of lightly and heavily over-consolidated samples under drained conditions.

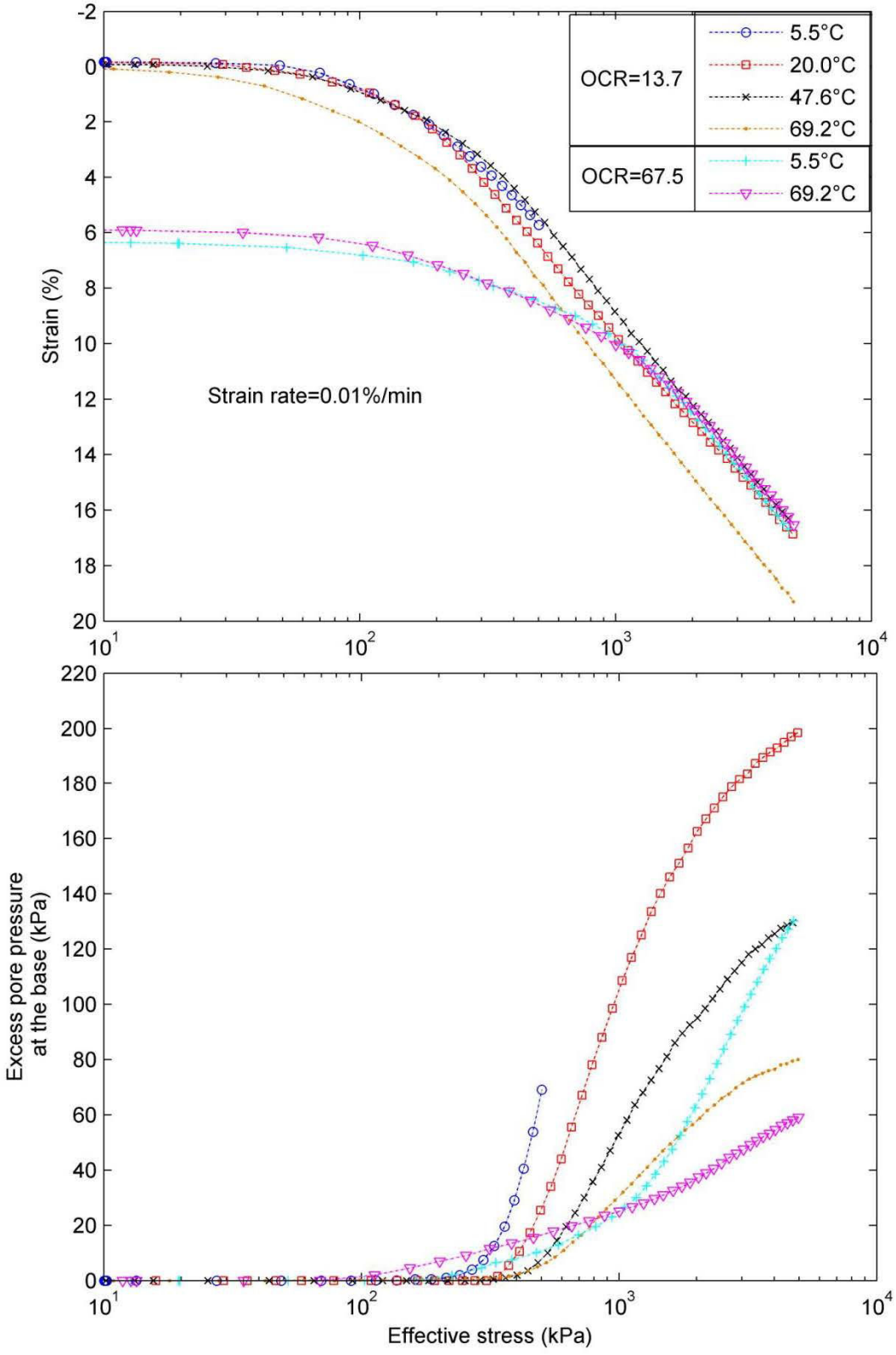

Figure 5.6 Effect of temperature on the effective stress-strain curve and excess pore water pressure for lightly and heavily over-consolidated clay A at strain rate of 0.01%/min (Strain=$\Delta h/h_0$).

An experimental comparison between the stress-strain behaviour of heavily over-consolidated samples of clay B at different temperatures has been made. The samples were tested at 5.5°C and 69.2°C using CRS tests with strain rate of 0.01%/min. As seen on Figure 5.6, the deformation at 69.2°C increased slightly in comparison with observed deformation at 5.5°C for heavily over-consolidated samples. The compression curves of heavily over-consolidated samples show small differences in deformation due to temperature effect. It is relatively more affected by temperature than the lightly over-consolidated samples (Figure 5.7).

Based on the obtained results, the stress-strain behaviour of heavily over-consolidated samples could be considered slightly temperature dependent. In another words, the temperature as an external factor has not strong effect on the mechanical behaviour of heavily over-consolidated samples.

Figure 5.7 compares the pore pressure variation with vertical effective stress curves obtained from CRS tests at different temperatures for over-consolidated samples of clay B. As seen in the figure, at the end of the test at the same vertical effective stress, the value of maximum excess pore water pressure corresponding to temperature 5.5°C exceeds the maximum excess pore water pressure value corresponding to temperature 69.2°C by a factor of 2.8 for heavily over-consolidated samples.

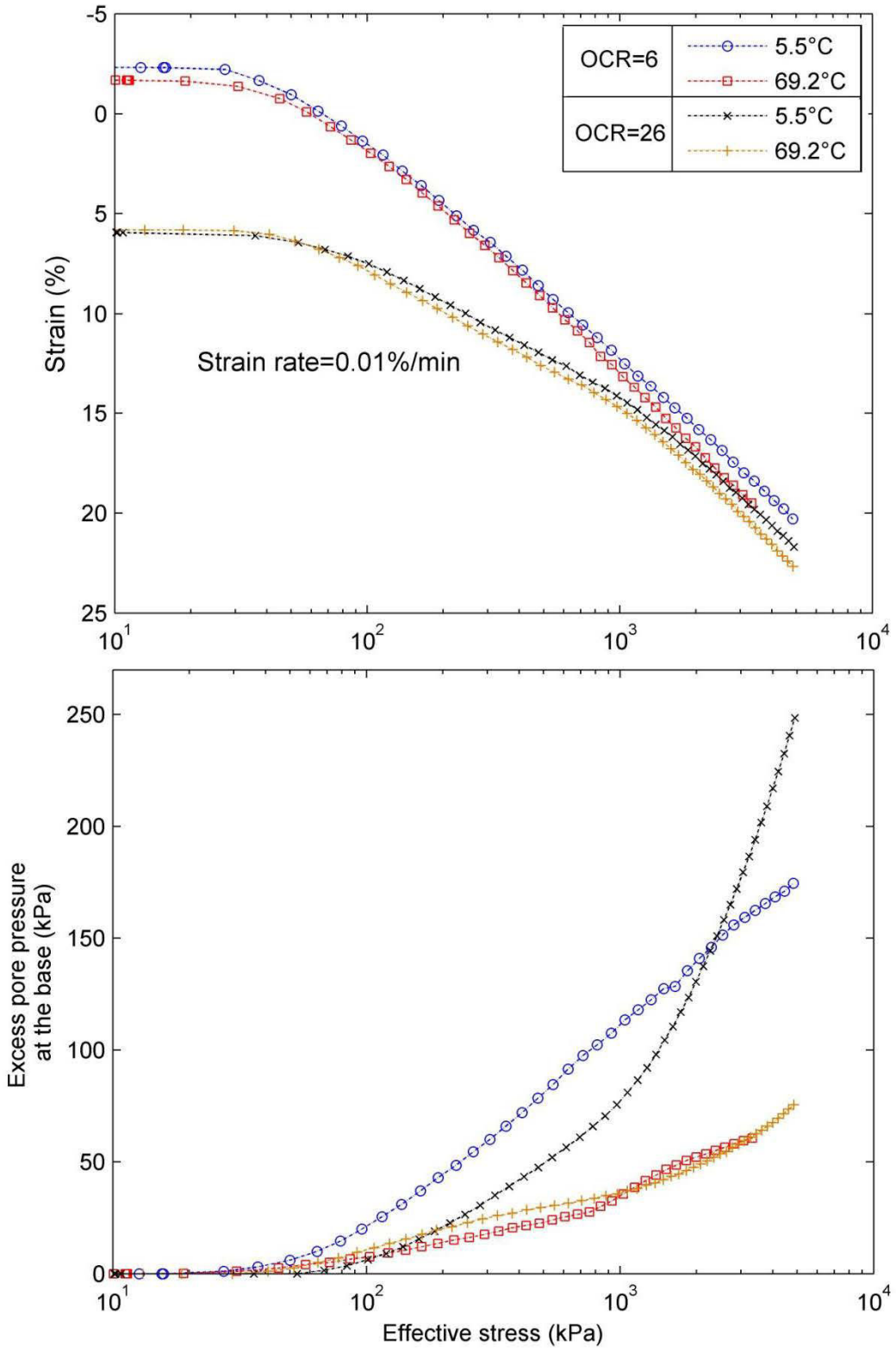

Figure 5.7 Effect of temperature on the effective stress-strain curve and excess pore water pressure at strain rate of 0.01%/min for lightly and heavily over-consolidated clay B (Strain=$\Delta h/h_0$).

It becomes quite clear that when temperature changed, the pore water pressure significantly changed for lightly and heavily over-consolidated samples. The developed pore water pressure through CRS tests are affected by temperature increase at a given effective stress.

5.5 Compression and swelling indices variation with temperature

Table 5.2 shows the variation of compression and swelling indices at different temperatures obtained from CRS tests at 0.01%/min strain rate for lightly and heavily over-consolidated samples of clay A. It appears from the values that with the temperature change, the compression index (c_c) changed very slightly. The same result was observed for swelling index (c_s). For heavily over-consolidated samples, the compression indexes values lie between 0.191 and 0.195, while the swelling indexes lie between 0.0038 and 0.0055 (Table 5.2).

It could be considered that the variation of compression index of heavily over-consolidated samples of clay A with temperature is not important as seen in the presented results. Likewise, the swelling index variation with temperature is not important. On the other hand, compression and swelling indices of lightly over-consolidated samples are not strongly temperature dependent.

Table 5.2 Compression (c_c) and swelling (c_s) indices variation with temperature for lightly and heavily over-consolidated clay A.

Symbol		OCR=13.7		OCR=67.5	
Temperature (°C)	Strain rate (%/min)	c_c	c_s	c_c	c_s
5.5	0.01	-	-	0.191	0.0055
20	0.01	0.210	0.0056	-	-
47.6	0.01	0.213	0.0053	-	-
69.2	0.01	0.212	0.01	0.195	0.0038

For heavily over-consolidated samples of clay B, the compression index value obtained from CRS test under 0.01%/min strain rate at high temperature condition (c_c=0.193 at 69.2°C) was relatively larger than the value obtained at low temperature condition (c_c=0.187 at 5.5°C). A similar behaviour was obtained for swelling index at different temperatures (c_s=0.006 at 5.5°C, c_s=0.009 at 69.2°C). These variations are presented Table 5.3.

Table 5.3 Compression (c_c) and swelling (c_s) indices variation with temperature for lightly and heavily over-consolidated clay B.

Symbol		OCR=6.0		OCR=26	
Temperature (°C)	Strain rate (%/min)	c_c	c_s	c_c	c_s
5.5	0.01	0.182	0. 019	0.187	0.006
69.2	0.01	0.188	0.018	0.193	0.009

The observed differences at a wide range of temperature are very small and according to that, the compression and swelling indices could be considered independent of temperature for heavily over-consolidated samples of clay B. On the other hand, the compression and swelling indices of lightly over-consolidated samples slightly varied with temperature (Table 5.3).

5.6 Preconsolidation pressure variation with temperature

The evaluated preconsolidation pressure from the laboratory CRS tests decreased by about 7.14% when conducted at temperature of 69.2°C compared to temperature of 5.5°C for heavily over-consolidated samples of clay A (Figure 5.8). The samples were examined at 0.01%/min strain rate. Figure 5.8 shows the observed influence of temperature on the preconsolidation pressure for lightly and heavily over-consolidated samples of clay A with a variation range at different temperatures.

In general, the preconsolidation pressure of lightly and heavily over-consolidated samples of clay A decreased under elevated temperatures according to the experimental works. However, the variation of the preconsolidation pressure for these over-consolidated samples either lightly or heavily is not large under high temperatures.

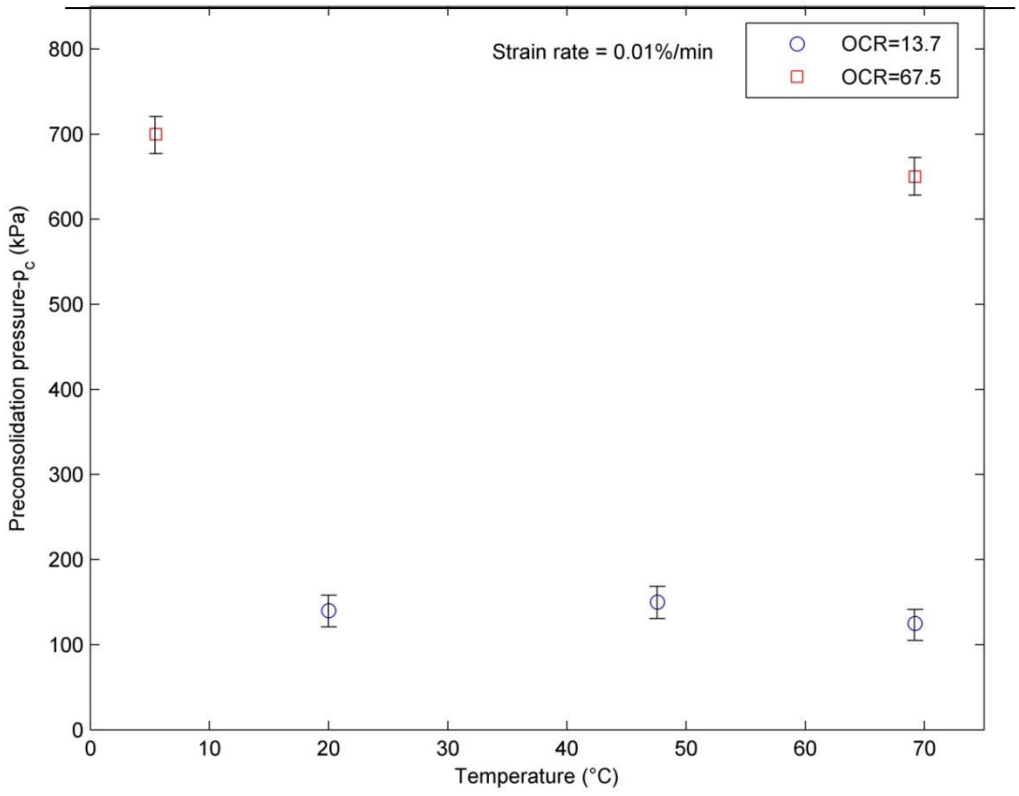

Figure 5.8 Effect of temperature on the preconsolidation pressure of lightly (OCR=13.7) and heavily over-consolidated (OCR=67.5) clay A.

The obtained preconsolidation pressure for heavily over-consolidated samples of clay B at 69.2°C was slightly less than those obtained at 5.5°C. The monitored difference due to temperature effect was less than 7.5% (Figure 5.9). Figure 5.9 shows the variation range of preconsolidation pressure with temperature for lightly and heavily over-consolidated samples of clay B which obtained from CRS tests at strain rate of 0.01%/min.

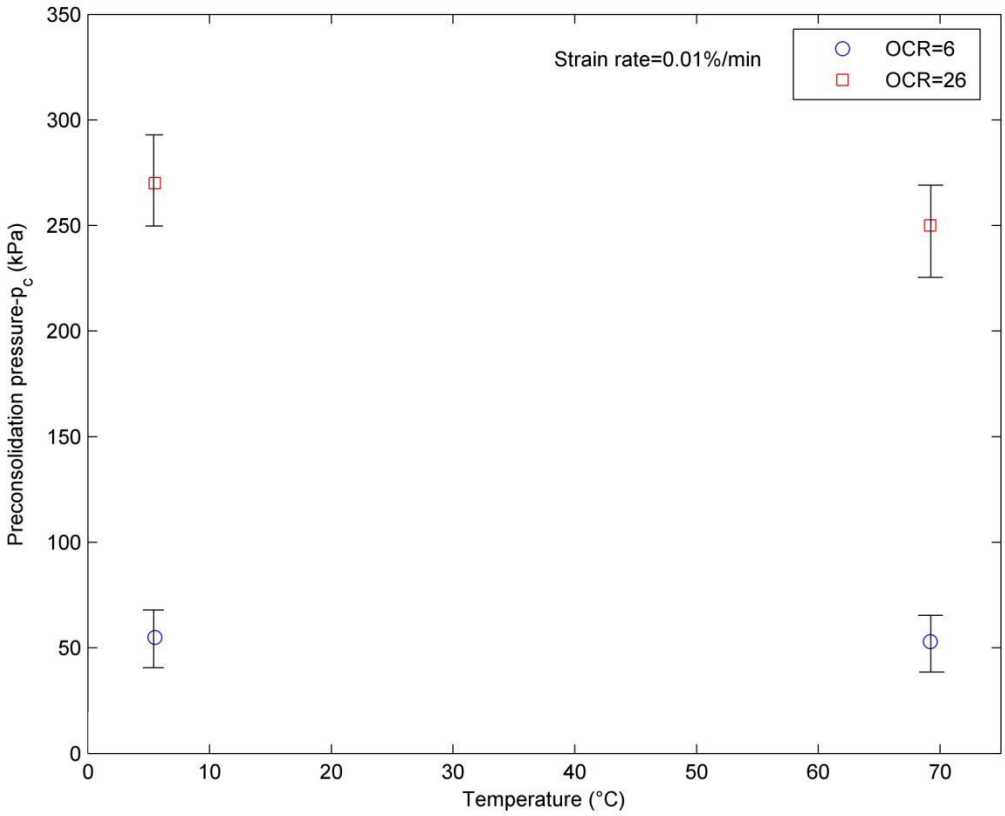

Figure 5.9 Effect of temperature on the preconsolidation pressure of lightly (OCR=6) and heavily over-consolidated (OCR=26) clay B.

The observed behaviour for lightly and heavily over-consolidated samples of clay B at wide range of temperature implies a slight decrease in the preconsolidation pressure with increased temperature. It is indicated to limited temperature dependency.

5.7 Coefficient of volume compressibility variation with temperature

Figure 5.10 compares the values of coefficient of volume compressibility against effective stress with the change of temperature condition under 0.01%/min CRS loading for lightly and heavily over-consolidated samples of clay A. The comparison has been done for values variation with effective stress. It is clearly observed from the figure that the difference

between the values of coefficient of volume compressibility at 5.5°C and 69.2°C is very small for heavily over-consolidated samples (Figure 5.10).

The variation of coefficient of volume compressibility with temperature is considered to be small for lightly and heavily over-consolidated samples of clay A even using a wide range of temperatures to observe the influence.

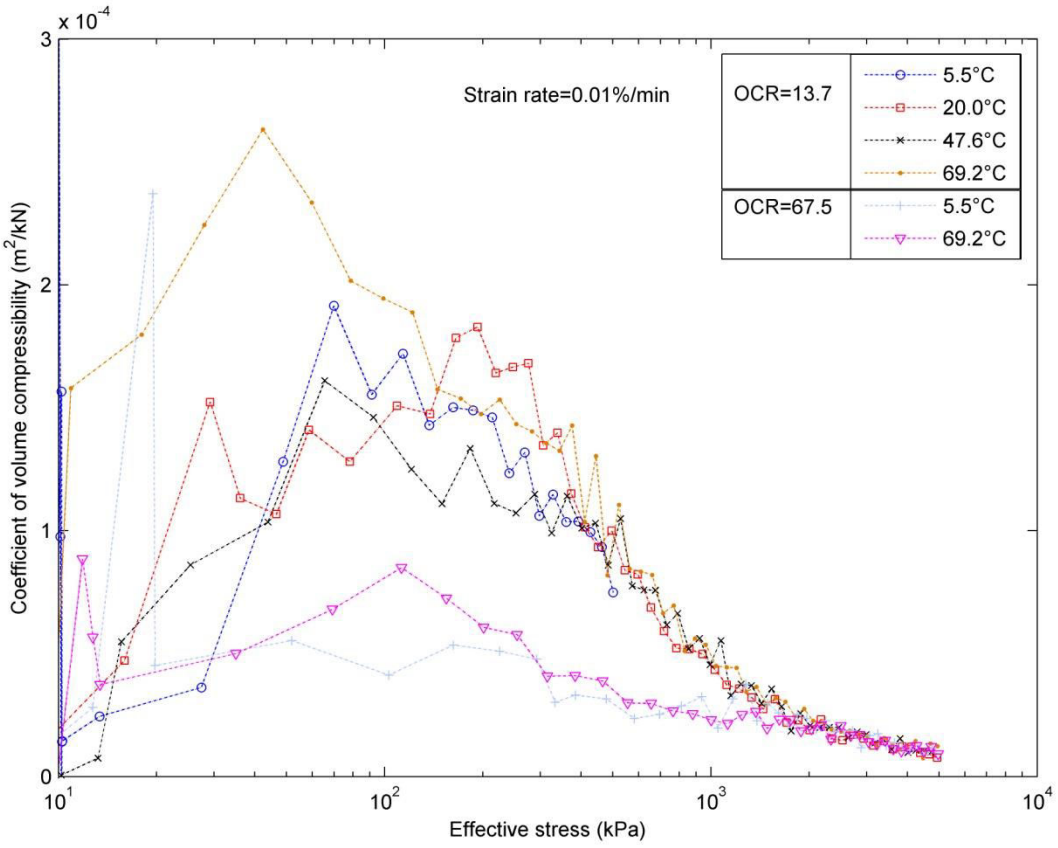

Figure 5.10 Coefficient of volume compressibility (m_v) variation with temperature for lightly (OCR=13.7) and heavily over-consolidated (OCR=67.5) clay A.

Figure 5.11 presents the values of coefficient of volume compressibility variation with vertical effective stress obtained from 0.01%/min strain rate CRS tests carried out at 5.5°C and 69.2°C for lightly and heavily over-consolidated samples of clay B. As shown in the figure for heavily over-consolidated soil, the coefficient of volume compressibility at 69.2°C is close to the value at 5.5°C.

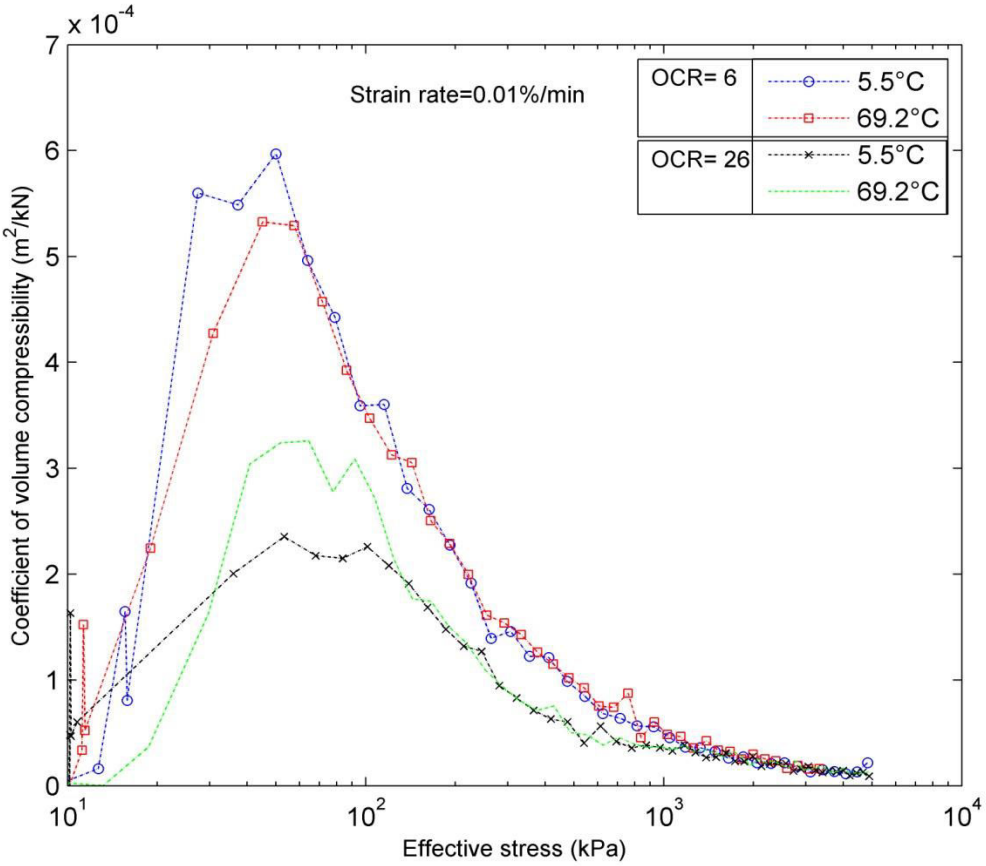

Figure 5.11 Coefficient of volume compressibility (m_v) variation with temperature for lightly (OCR=6) and heavily over-consolidated (OCR=26) clay B.

For lightly and heavily over-consolidated samples of clay B, results showed that the coefficient of volume compressibility changed very slightly with temperature increase. Therefore, the effect of temperature could be considered negligible.

5.8 Permeability variation with temperature

To evaluate the influence of temperature on the permeability and intrinsic permeability of over-consolidated samples of clay A, a constant void ratio of 0.65 was selected for CRS tests under 0.01%/min strain rate. Table 5.4 shows the variation of permeability and intrinsic permeability at different temperatures at the selected void ratio. The permeability increased slightly with temperature increase, while the intrinsic permeability is almost the same (Table 5.4).

The permeability of heavily over-consolidated samples of clay A which was calculated in terms of the measured pore water pressure and deformation rate could be considered temperature dependent, while the intrinsic permeability could be considered independent of temperature. A similar behaviour was observed for lightly over-consolidated samples.

Table 5.4 Permeability (k) and intrinsic permeability (K) variation with temperature for lightly and heavily over-consolidated clay A at e=0.65.

Symbol		OCR=13.7		OCR=67.5	
Temperature (°C)	Strain rate (%/min)	k (m/s)	K (m^2)	k (m/s)	K (m^2)
5.5	0.01	-	-	2,9007E-11	4.7260E-19
20	0.01	1.5882E-11	1.61E-19	-	-
47.6	0.01	1.4378E-11	8.79E-20	-	-
69.2	0.01	5.9274E-11	2.58E-19	4,6715E-11	2.0364E-19

The hydraulic conductivity and intrinsic permeability variations with temperature change are presented in Table 5.5 for lightly and heavily over-consolidated samples of clay B at constant void ratio of 0.40. Results showed that the hydraulic conductivity of heavily over-consolidated samples increased by a factor of 1.23 when temperature increased from 5.5°C to 69.2°C. On the other hand, there is no significant difference in the intrinsic permeability evaluated when temperature changed (Table 5.5).

Table 5.5 Permeability (k) and intrinsic permeability (K) variation with temperature for lightly and heavily over-consolidated clay B at e=0.40.

Symbol		OCR=6.0		OCR=26	
Temperature (°C)	Strain rate (%/min)	k (m/s)	K (m^2)	k (m/s)	K (m^2)
5.5	0.01	3.3091E-11	5.38E-19	3.6252E-09	5.91E-17
69.2	0.01	1.2871E-10	5.61E-19	4.441E-09	1.94E-17

The results indicated that the temperature influenced the characteristics of pore fluid of both lightly and heavily over-consolidated samples of clay B. The temperature effect on the intrinsic permeability could be ignored.

5.9 Coefficient of consolidation variation with temperature

Figure 5.12 presents the values of coefficient of consolidation (c_v) at different temperatures as a function of constant void ratio (e=0.65) for 0.01%/min CRS tests on consolidated samples of clay A at different values of OCR. The values of coefficient of consolidation obtained from high temperature CRS test (69.2°C) was greater than those of low temperature test (5.5°C) for all tested over-consolidated samples. As can be seen from the figure, the values of coefficient of consolidation at 69.2°C are larger than those at 5.5°C by a factor of 1.81 for heavily over-consolidated samples.

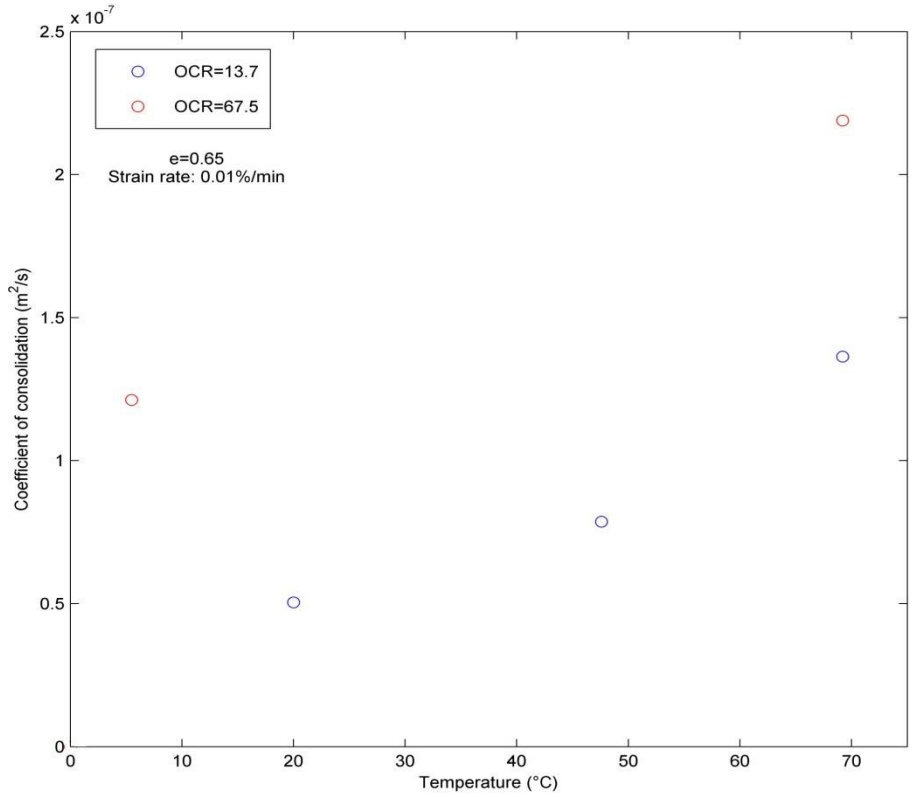

Figure 5.12 Effect of temperature on the coefficient of consolidation for lightly (OCR=13.7) and heavily over-consolidated (OCR=67.5) clay A.

At a constant void ratio of 0.40, Table 5.6 presents the coefficient of consolidation values at different temperatures for lightly and heavily over-consolidated samples of clay B which are obtained from CRS tests at 0.01%/min strain rate. The study showed that the temperature rise from 5.5°C to 69.2°C results in an increase in the coefficient of consolidation by a factor of 1.6 for heavily over-consolidated samples. On the other hand, the coefficient of consolidation of lightly over-consolidated samples was more affected by temperature as shown in Table 5.6. The change in hydraulic conductivity with temperature as shown previously could, in particular, explain why the coefficient of consolidation increased with temperature increase.

Table 5.6 Coefficient of consolidation (c_v) variation with temperature for lightly and heavily over-consolidated clay B at e=0.40.

Symbol		OCR=6	OCR=26
Temperature (°C)	Strain rate (%/min)	c_v	c_v
5.5	0.01	3.40E-08	4.77E-06
69.2	0.01	1.0433E-07	7.64E-06

The results of CRS tests performed on clay B at a particular strain rate and different temperatures with different OCR confirmed that the coefficient of consolidation is temperature dependent and it changed with temperature increase.

5.10 Comparison of stress strain behaviour at different temperatures for the studied clays

The impact of clay nature beside OCR on the thermo-hydro-mechanical behaviour of heavily over-consolidated samples was examined. Figure 5.13 presents a comparison between the stress-strain behaviour of heavily over-consolidated clay A and clay B. It is clear from the figure that the change in strain due to temperature effect is difficult to observe for both clays.

Small differences between the thermo-mechanical behaviour of clay A and clay B were observed. In this case, the effect of clay nature beside OCR on the mechanical behaviour of heavily over-consolidated samples can be considered negligeable.

Regarding the clay nature beside OCR impact on the hydraulic behaviour of heavily over-consolidated samples, Figure 5.13 compares the pore water pressure variation with vertical effective stress at different temperatures for clay A and clay B.

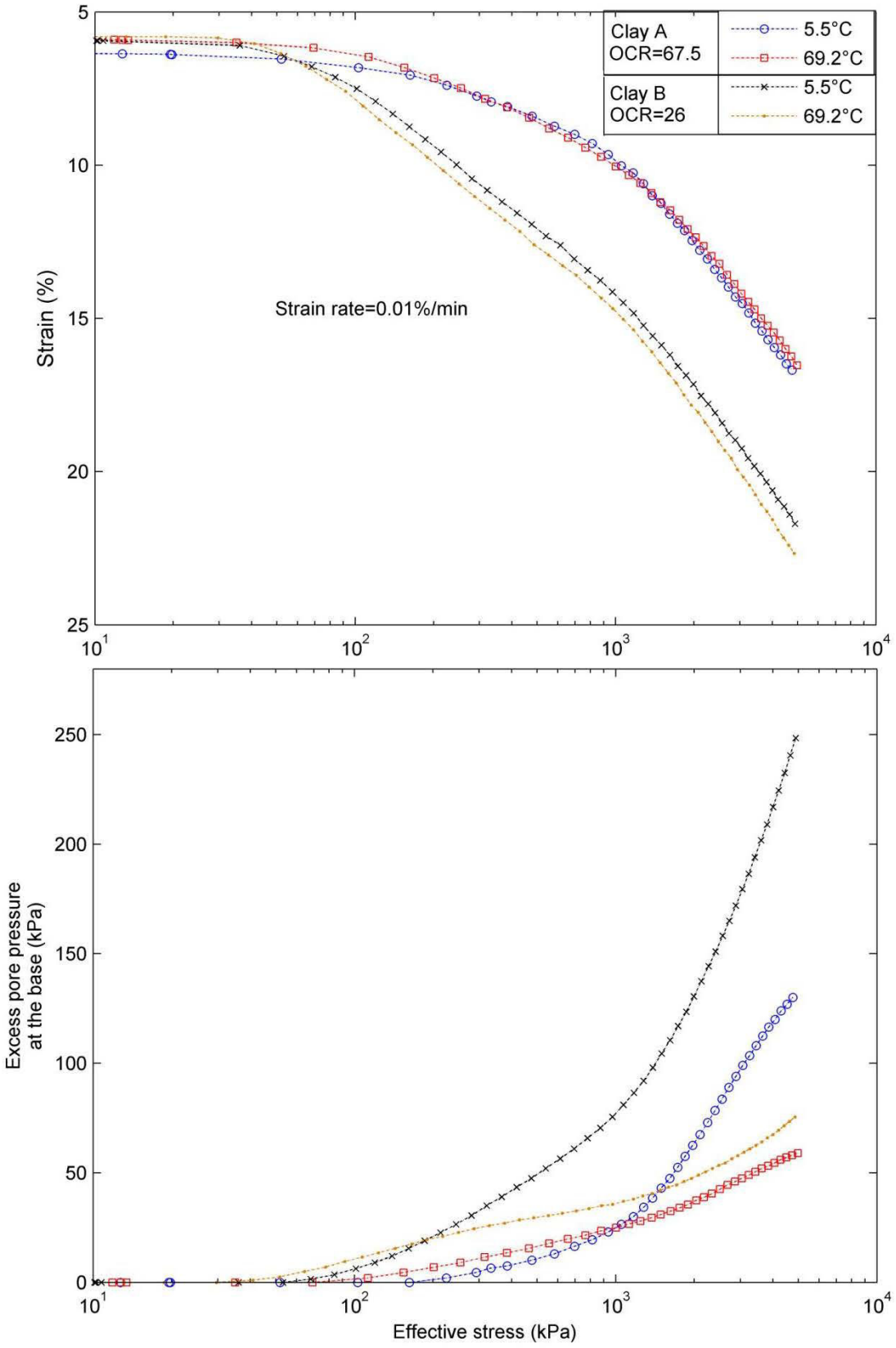

Figure 5.13 Effect of temperature on the effective stress-strain curve and excess pore water pressure at strain rate of 0.01%/min for heavily over-consolidated clays (Strain=$\Delta h/h_0$).

The temperature increase from 5.5°C to 69.2°C showed that the pore pressure variation in clay B was 1.26 times larger than the variation in clay A. The thermo-hydraulic behaviour of heavily over-consolidated samples could be considered clay nature and OCR dependent.

5.11 Soil plasticity index effect

An attempt was made to correlate the soil plasticity index effect on the thermally induced volumetric strain under constant total stress for the studied materials. Figure 5.14 exhibits the impact of soil plasticity index on the thermally induced volumetric strain under constant total stress of 1000 kPa for 0.01%/min CRS tests. In the case of heavily over-consolidated samples, when the temperature altered from 5.5°C to 69.2°C, the thermally induced volumetric strain for clay A was lower than clay B (has lower plasticity index than clay A).

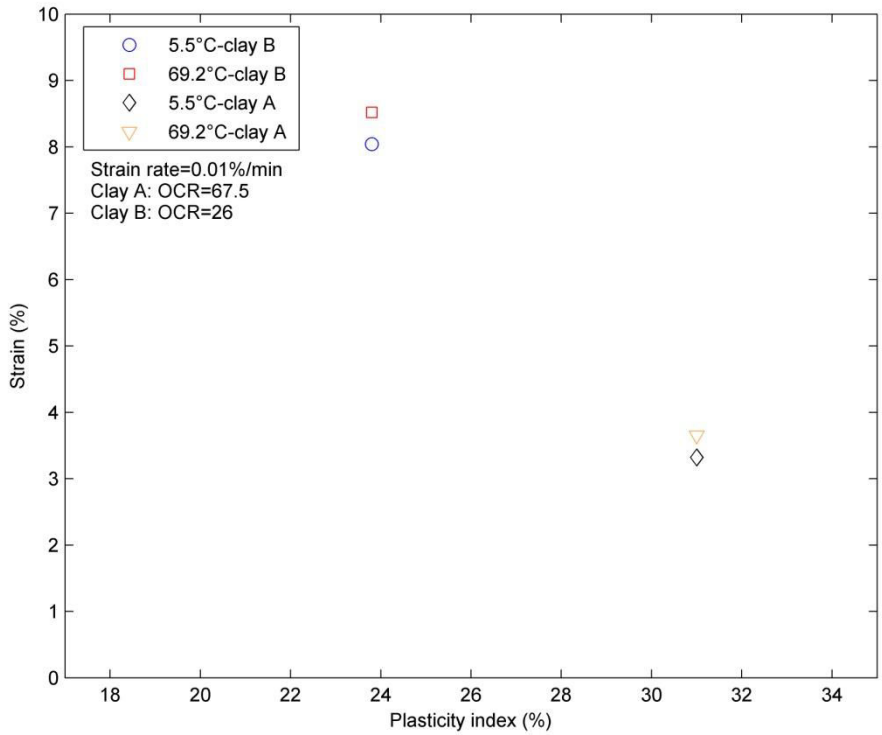

Figure 5.14 Effect of soil plasticity index on the thermally induced volumetric strain under constant total stress of 1000 kPa for heavily over consolidated clay (HOC) (Strain=$\Delta h/h_0$).

In general, it is observed that the thermally induced volumetric strain was slightly influenced by the soil plasticity index for heavily over-consolidated samples (See section 1.4.1).

5.12 Clay content effect

A study on the relationship between the clay content and the thermally induced volumetric strain under constant total stress has been performed. Figure 5.15 shows the thermally induced volumetric strain variations with clay content under 1500 kPa for 0.01%/min CRS tests on the studied materials. It has been found for heavily over-consolidated samples that during

temperature change ΔT = 63°C, the thermally induced volumetric strain of clay with 85% clay content (clay A) was lower than the thermally induced volumetric strain of clay with 45% clay content (clay B).

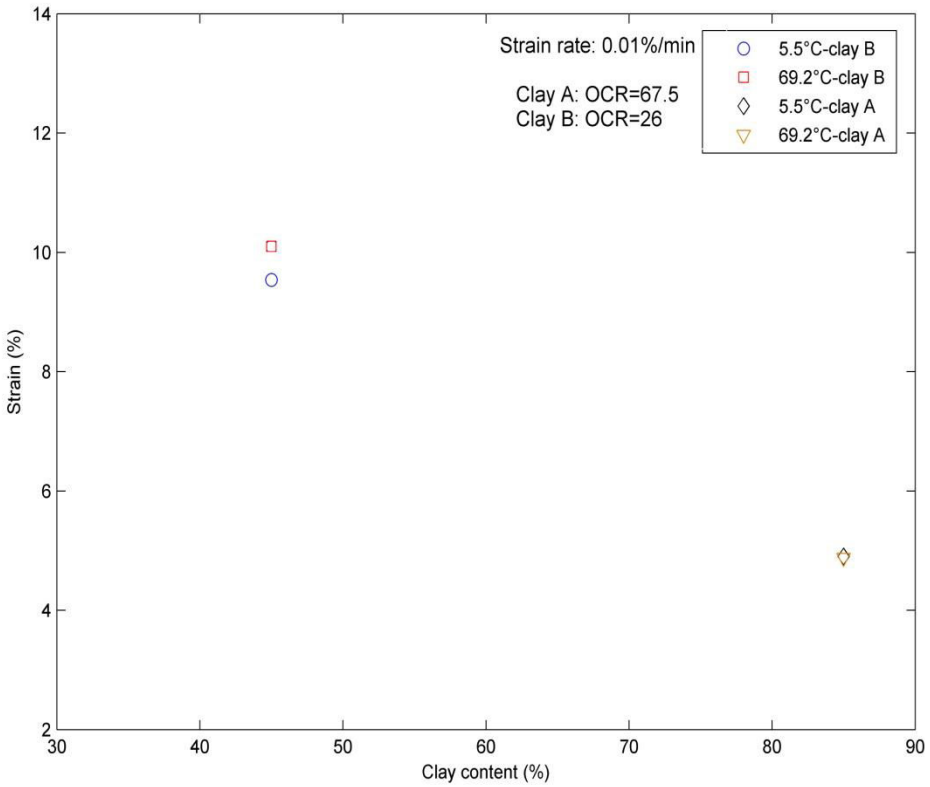

Figure 5.15 Effect of clay content on the thermally induced volumetric strain under constant total stress of 1500 kPa for heavily over-consolidated clays (HOC) (Strain=$\Delta h/h_0$).

According to the obtained results, it can be considered that in general for over-consolidated soils, the clay content has a negligible effect on the thermo-mechanical behaviour.

5.13 Thermally induced volumetric strain

The observed thermally induced volumetric strain of clay A is shown if Figure 5.16. The samples were tested under different stress histories which can be divided into lightly over-consolidated (LOC) samples (OCR=13.7) and heavily over-consolidated (HOC) samples (OCR=67.5). It can be seen that if temperature increased from 20°C to 69.2°C, lightly over-consolidated samples show contraction behaviour. However, the decrease in temperature to 5.5°C reflects expansion behaviour for the lightly over-consolidated samples. On the other hand, heavily over-consolidated samples exhibited expansion when the temperature increased from 5.5°C to 69.2°C.

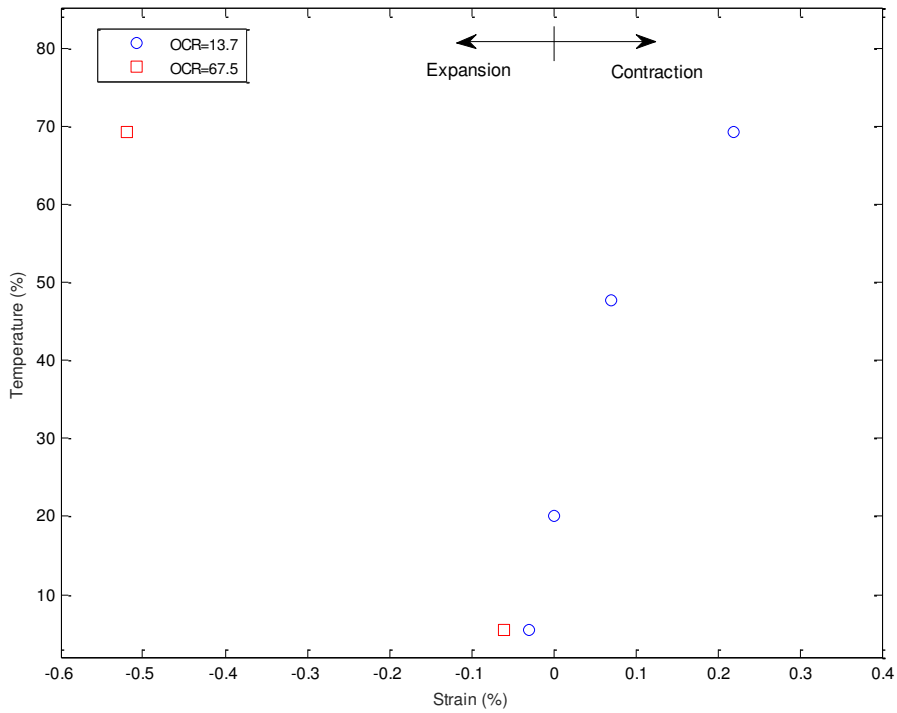

Figure 5.16 Thermally induced volumetric strain of clay A (Strain=Δh/h$_0$).

Figure 5.17 presents the thermally induced volumetric strain of clay B. Lightly over-consolidated (LOC) samples (OCR=6) and heavily over-consolidated (HOC) samples (OCR=26) were tested at 5.5°C and 69.2°C. It was clearly found a contraction behaviour with temperature increase for lightly over-consolidated samples, while the heavily over-consolidated samples showed expansion increase with temperature increase.

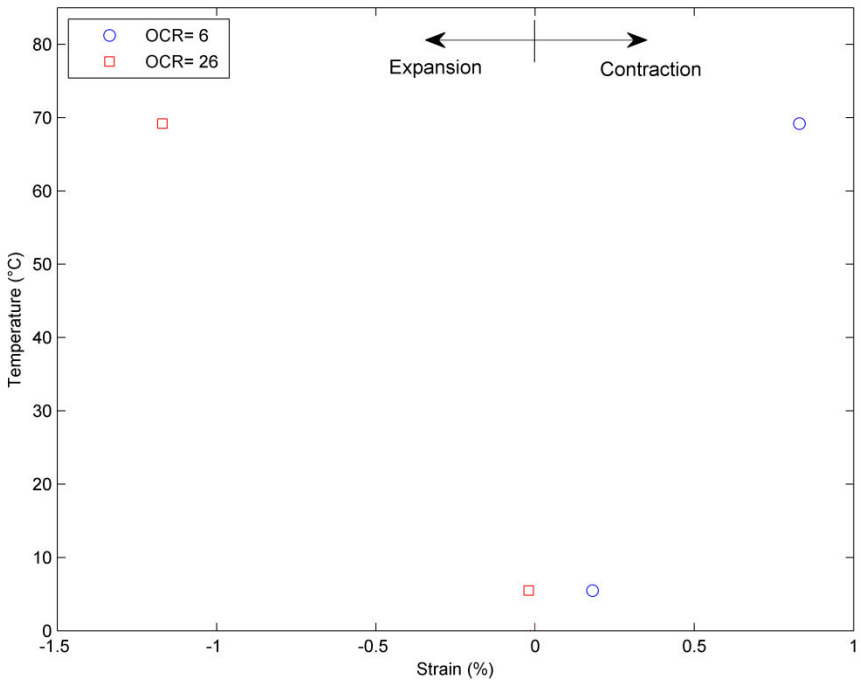

Figure 5.17 Thermally induced volumetric strain of clay B (Strain=Δh/h$_0$).

It is clear that the temperature change affects the thermally induced volumetric strain for both lightly and heavily over-consolidated soils.

5.14 Results discussion

Based on the obtained results, the stress-strain behaviour of heavily over-consolidated samples was relatively less affected by temperature than lightly over-consolidated samples for clay A. The excess pore pressure generated in heavily over-consolidated samples was less than the case of lightly over-consolidated samples for clay A. On the other hand; the stress-strain behaviour of heavily over-consolidated samples was relatively more affected by temperature than lightly over-consolidated samples for clay B. The excess pore pressure generated in heavily over-consolidated samples was more than the case of lightly over-consolidated samples for clay B. Observed stress-strain behaviour with temperature referred to the effect of viscous property of clay (Tsutsumi and Tanaka, 2012).

The value of preconsolidation pressure reduced due to the thermal expansion of the clay volume (thermal softening) at high temperatures. Phase (d-e) in Figure 5.1 and 5.2 shows the coupled result of mechanical and thermal deformation of the sample. The preconsolidation pressure of heavily over-consolidated clays was more affected by temperature than lightly over-consolidated samples for both materials. In general, the preconsolidation pressure at any case of stress history decreased with temperature increase which is consistent with researcher findings on different clays as mentioned in section 1.4.3.

Similar to the behaviour of lightly over-consolidated clay, results indicated that the hydraulic conductivity of heavily over-consolidated samples increased with temperature rise. One of the reasons is the reduction in water viscosity with heating that causes an increase in the hydraulic conductivity as pointed out in section 1.3.2. A number of researchers obtained the same results of temperature dependency for different materials (- section 1.3 and 1.4.5).

Results indicated that the compression index and swelling index of heavily over-consolidated samples are not strongly affected by temperature as well as the lightly over-consolidated samples for both materials. Independency of temperature for compression index of over-consolidated soft Bangkok clay (PI=60%) was found by Abuel-Naga et al. (2007a), but the swelling index increased slightly at higher temperature. The coefficient of volume compressibility (m_v) of over-consolidated clays under different stress histories varied slightly with temperature for studied materials. A similar behaviour for the coefficient of volume compressibility of lightly over-consolidated Boom clay (PI=50%) was reported by Delage (2000). On the other hand, results showed that the coefficient of consolidation (c_v) for samples

with higher OCR was higher at a given high temperature. The slight increased value of coefficient of consolidation (c_v) with temperature for lightly and heavily over-consolidated samples during consolidation tests with constant strain rate is likely to be related to the decreased viscosity of pore water at elevated temperatures; i.e., hydraulic conductivity increase. Similar results were obtained by Delage (2000) for over-consolidated Boom clay (PI=50%).

A contraction behaviour for lightly over-consolidated samples (OCR=13.7 & 6 for clay A and clay B respectively) was observed upon heating, while the heavily over-consolidated samples (OCR=67.5 & 26 for clay A and clay B respectively) showed a dilation behaviour. Similar results were obtained by Baldi et al. (1988) using natural and reconstituted clays, Cekerevac and Laloui (2004) on Kaolin clay, and Cui et al. (2000) on Boom clay. Expansion of soil constituents (soil and water), and mechanical weakening of the contacts between soil aggregates are two phenomena produced during heating. The expansion of soil constituents clarifies the phenomenon of macroscopic thermal dilation under high OCR, while the mechanical weakening of the contacts between soil aggregates could explain the phenomenon of thermal contraction under low OCR (Tang et al, 2008(a)). Towhata et al. (1993) suggested that the thermal contraction is caused by the thermal deterioration of clay skeleton. The physico-chemical clay-water interactions, based on the double layer thickness (Eqn. 1.9) variation with increased temperature may induce the thermal contraction, while the thermal expantion of soil minerals causes the thermal expansion of clay (Delage et al., 2000). Baldi et al. (1988) indicated that the over-consolidated clays have thermoelastic behaviour. As described in section 1.4.1, the changes in clay volume due to temperature variation reasonably depend on the stress history of the soil.

5.15 Conclusion

This chapter discussed the impact of stress history (OCR) on the thermo-hydro-mechanical behaviour of two different clays. Illitic clay (clay A) was tested under different stress histories including OCR = 13.7 and OCR=67.5, and kaolinite clay (clay B) was tested under stress histories of OCR=6 and OCR=26. CRS tests at strain rate of 0.01%/min at different temperatures were performed on these clays. Table 5.7 shows the consolidation parameters variation with temperature and strain rate for lightly and heavily over-consolidated clay A and clay B.

The consolidation characteristics of lightly and heavily over-consolidated samples of studied clays were presented in this chapter. The stress-strain behaviour of heavily over-consolidated

samples does not show a strong dependency on temperature for both materials. For clay B, the compression curve of heavily over-consolidated samples was more affected by temperature than lightly over-consolidated samples, while it was approximately the same for clay A. The excess pore water pressure was increased with temperature derease for lightly and heavily over-consolidated samples for both materials. The compression (c_c) and swelling (c_s) indices were slightly affected by temperature for lightly and heavily over-consolidated samples of both materials. The preconsolidation pressure was slightly decreased with temperature increase for both materials at different OCR values. In addition, the hydraulic conductivity was strongly dependent on temperature, while the intrinsic permeability variation with temperature was negligible for both heavily and lightly over-consolidated samples. The coefficient of volume compressibility was independent of temperature at any value of OCR for both clays. On the other hand, the coefficient of consolidation increased with temperature increase.

Clay A	**Temperature (°C)**															
	5.5				**20.0**				**47.6**				**69.2**			
OCR	**13.7**		**67.5**		**13.7**		**67.5**		**13.7**		**67.5**		**13.7**		**67.5**	
Strain rate (%/min)	**C_c**	**C_s**	**C_c**	**C_s**	**C_c**	**C_s**	**C_c**	**C_s**	**C_c**	**C_s**	**C_c**	**C_s**	**C_c**	**C_s**	**C_c**	**C_s**
0.02	-	-	-	-	0.20	0.0057			0.21	0.0053	-	-	0.20	0.0051	-	-
0.01	-	-	0.191	0.0055	0.21	0.0056	-	-	0.213	0.0053	-	-	0.212	0.01	0.195	0.0038
0.002	0.206	0.0035	-	-	0.20	0.01	-	-	0.191	0.007	-	-	0.217	0.016	-	-
Strain rate (%/min)	**Pc (kPa)**															
0.02	-		-		165		-		160		-		158		-	
0.01	-		700		140		-		150		-		125		650	
0.002	130		-		135		-		149		-		124		-	
Strain rate (%/min)	**$m_v \times 10^{-5}$ (m^2/kN)**															
0.02	-		-		3.341		-		3.155		-		4.056		-	
0.01	-		2.447		3.148		-		1.849		-		4.444		2.182	
0.002	2.867		-		3.115		-		4.417		-		3.888		-	
Strain rate (%/min)	**k $\times 10^{-11}$ (m/s)**	**K $\times 10^{-19}$ (m^2)**	**k**	**K**	**k**	**K**	**k**	**K**	**k**	**K**	**k**	**K**	**k**	**K**	**k**	**K**
0.02	-	-	-	-	1.616	1.64	-	-	4.291	2.62	-	-	6.307	2.75	-	-
0.01	-	-	2,901	4.726	1.588	1.61	-	-	1.438	0.879	-	-	5.927	2.58	4,672	2.037
0.002	1.086	1.74	-	-	1.313	1.33	-	-	2.074	1.27	-	-	3.759	1.64	-	-
Strain rate (%/min)	**$c_v \times 10^{-8}$ (m^2/s)**															
0.02	-		-		5.187		-		9.835		-		16.59		-	
0.01	-		12.12		5.045		-		7.868		-		13.64		21.89	
0.002	2.692		-		3.93		-		6.654		-		9.479		-	
-	**c_α**															
-	**-**				0.0165				0.012				0.022			
Clay B																

OCR	6		26		6		26		6		26		6		26	
Strain rate (%/min)	C_c	C_s	C_c	C_s	C_c	C_s	C_c	C_s	C_c	C_s	C_c	C_s	C_c	C_s	C_c	C_s
0.02	0.205	0.013	-	-	-	-	-	-	-	-	-	-	0.196	0.018	-	-
0.01	0.182	0.019	0,187	0,006	-	-	-	-	-	-	-	-	0.188	0.018	0,193	0,009
0.002	0.188	0.011	-	-	0.186	0.009	-	-	-	-	-	-	0.197	0.019	-	-
Strain rate (%/min)	Pc (kPa)															
0.02	58		-		-		-		-		-		55		-	
0.01	55		270		-		-		-		-		53		250	
0.002	54		-		53		-		-		-		52		-	
Strain rate (%/min)	$m_v \times 10^{-4}$ (m^2/kN)															
0.02	1.121		-		-		-		-		-		1.132		-	
0.01	1.212		0.76		-		-		-		-		1.262		0.588	
0.002	1.063		-		9.92		-		-		-		1.019		-	
Strain rate (%/min)	k $\times 10^{-11}$ (m/s)	K $\times 10^{-19}$ (m^2)	k	K	k	K	k	K	k	K	k	K	k	K	k	K
0.02	4.180	6.80	-	-	-	-	-	-	-	-	-	-	11.42	4.98	-	-
0.01	3.309	5.38	36.25	591	-	-	-	-	-	-	-	-	12.87	5.61	44.41	194
0.002	1.983	3.23	-	-	3.111	4.971	-	-	-	-	-	-	6.871	3.0	-	-
Strain rate (%/min)	$c_v \times 10^{-8}$ (m^2/s)															
0.02	3.933		-		-		-		-		-		11.47		-	
0.01	3.40		477		-		-		-		-		10.43		764	
0.002	1.77		-		3.655		-		-		-		6.207		-	
-	c_α															
-	0.0061				-				-				0.0064			

Based on the obtained results, the thermo-hydro-mechanical behaviour could be considered OCR and clay nature dependent.

General conclusion and perspective

The understanding and the consideration of the thermo-mechanical behavior of clay soils is of primary importance in some engineering applications such as geothermal piles, nuclear waste storages, heat storage in embankments, etc.

The main objective of this study was to investigate the temperature impact on the consolidation and creep behaviour of compacted clayey soils. The impact of clay nature on the thermo-hydro-mechanical behaviour was also investigated. In addition, the impact of stress history on the thermo-hydro-mechanical behaviour of clay was investigated.

Indeed, the literature review showed that most of researchers investigated the thermo-hydro-mechanical behaviour of the natural clays. Temperature effects on the consolidation parameters and creep behaviour of clay soils were presented in this chapter. In addition, the literature review showed the studies on the modeling of elasto-viscoplastic and thermo-elasto-viscoplastic behaviour of clay. This chapter presented the scientific background which is necessary to the remaining parts of the study.

Accordingly, the main strategy of this research was to build up an experimental program as a tool to reach the study objectives. To achieve the research goals, a constant rate of strain consolidation tests (CRS) were performed on the selected compacted clays within a temperature range between 5°C and 70°C and strain rates between 0.002%/min and 0.02%/min using temperature controlled oedometric cells. The oedometric cells, the experimental procedures, and the theory of constant rate of strain test were introduced in chapter 2. The experimental protocol validity was checked through three factors which include the tests repeatability, comparing with the classical oedometric test. Two soils were employed in this study; their main characteristics were also exposed in this chapter 2.

To investigate the temperature impact on the consolidation and creep behaviour of compacted clayey soils which is one of the study objectives, Chapter 3 presents the results of the impact of temperature on the consolidation and creep behaviour of compacted illitic clay. Results show that the excess pore pressure increased with temperature decrease. The hydraulic conductivity (k) and coefficient of consolidation (c_v) increased with temperature increase. The stress-strain behaviour was slightly affected by temperature variations. The compression (c_c) and swelling (c_s) indexes could be considered slightly temperature dependent. The preconsolidation pressure (p_c) decreased with temperature increase, while the creep index (c_α) slightly increased with temperature increase.

Chapter 4 presents the impact of clay nature on the thermo-hydro-mechanical behaviour by comparing the consolidation tests results of clay A and clay B. Results show that the stress-strain behaviour of clay A was not strongly dependent on temperature, while it was less affected by temperature for clay B. The compression (c_c) and swelling (c_s) indexes was slightly affected by temperature for both materials. The preconsolidation pressure (p_c) of clay A decreased when temperature increased, while it decreased for clay B but lower than clay A. The creep index of clay A slightly increased with temperature increase, while creep index of clay B increased but lower than the case of clay A. The hydraulic conductivity (k) and the coefficient of consolidation (c_v) was higher at higher temperature, while the pore pressure was lower at higher temperature. The soil plasticity index and clay content could control the thermo-hydro-mechanical behaviour.

In chapter 5, a comparison between the tests results of lightly and heavily over-consolidated clays at different temperatures and strain rates was conducted to investigate the impact of over-consolidation ratio (OCR) on the thermo-hydro-mechanical behaviour. Results show that the compression curves of heavily over-consolidated samples for both clays were not strongly temperature dependent. The compression curves of clay B for heavily over-consolidated samples were more affected by temperature than lightly over-consolidated samples, while it was approximately the same behaviour for clay A. The compression (c_c) and swelling (c_s) indexes of lightly and heavily over-consolidated clays were slightly affected by temperature. Lower preconsolidation pressure (p_c) was obtained at higher temperature for both lightly and heavily over-consolidated clays. The hydraulic conductivity (k) and the coefficient of consolidation (c_v) values were higher at higher temperature, while the excess pore pressure values were lower at higher temperatures for both lightly and heavily overconsolidated clays. The soil plasticity index and clay content did not show strong effect on the thermo-hydro-mechanical behaviour. The lightly over-consolidated clays showed contraction behaviour upon

heating, while the heavily over consolidated samples showed expansion behaviour upon heating.

The investigated impact of the main study factors which includes the temperature, clay nature, and stress history on the behaviour of compacted clayey soils indicated that these factors could control the thermo-hydro-mechanical behaviour of the compacted clays.

Recommendations for future work

The impact of temperature on the long-term behaviour of heavily over-consolidated compacted clays needs to be investigated. The impact of heating/cooling cycles on the consolidation and creep behaviour of compacted clays needs also to be investigated. Conventional oedometric consolidation and creep tests needs to be performed to further investigate the temperature impact on the consolidation and creep behaviour of compacted clays.

References

Abuel-Naga, H. M., Bergado, D. T., Soralump, S., Rujivipat, P., 2005. Thermal consolidation of soft Bangkok clay. Lowland Technology International 7, 13-21.

Abuel-Naga, H. M., Bergado, D. T., Bouazza, A., Ramana, G. V., 2007a. Volume change behavior of saturated clays under drained heating conditions: experiamental results and constitutive modeling. Canadian Geotechnical Journal 44, 942-956.

Abuel-Naga, H. M., Bergado, D. T., Bouazza, A., 2007b. Thermally induced volume change and excess pore water pressure of soft Bangkok Clay. Engineering Geology 89, 144-154.

Abuel-Naga, H. M., Lorenzo, G. A., Bergado, D. T., 2013. Current state of knowledge on thermal consolidation using prefabricated vertical drains. Geotechnical Engineering Journal of the SEAGS & AGSSEA 44, 132-141.

Abu-Hamdeh, N., 2003. Thermal properties of soils as affected by density and water content. Biosystems Engineering 86, 97-102.

Aboshi, H., 1973. An experimental investigation on similitude in the consolidation of a soft clay, including the secondary creep settlement. Pro. 8th Int. Conf. on SMFE, Specialty Session 2, 4(3), 88.

Adachi, T., Oka, F., Tange, Y., 1982. Finite element analysis of two dimensional consolidation using an elasto-viscoplastic constitutive equation. International Journal for Numerical and Analytical Methods in Geomechanics 1, 287–296.

Adamis, Z., Richard, W., 2005. Bentonite, kaolin, and selected clay minerals. Geneva: International programme on chemical safety.

AFNOR., 1993. NF P94-051 Sols: reconnaissance et essais;Détermination des limites d'Atterberg – Limite de liquidité à la coupelle- Limite de plasticité au rouleau [Soil:Inverstigation and testing. Determination of Atterberg's li its. Liquid limit test using cassagrande apparatus. Plastic limit test on rolled thread] (p. 15). Paris: Association Française de Normalisation.

AFNOR., 1999. NF P 94-093 Sols: Reconnaissance et essais Détermination des références de compactage d 'un matériau. Essai Proctor Normal-Essai Proctor Modifié [Soils: Investigation

and testing. Determination of the compaction characteristics of a soil. Standard Proctor test. Modified Proctor test] (p. 18). Paris: Association Française de Normalisation.

Ahmadi, H., Rahimi, H., Soroush, A., Alén, C., 2014. Experimental research on variation of pore water pressure in constant rate of strain test. Acta Geotechnica Slovenica 11, 46-57.

Aiban, S. A., 1998. The effect of temperature on the engineering properties of oil-contaminated sands, Environment international 24, 153-161.

Alnefaie, Kh. A., Abu-Hamdeh, N. H., 2013. Specific heat and volumetric heat capacity of some saudian soils as affected by moisture and density. International Conference on Mechanics, Fluids, Heat, Elasticity and Electromagnetic Fields, 139-142.

Akagi, H., Komiya, K., 1995. Constant rate of strain consolidation properties of clayey soil at high temperature. In: Proceedings of the International Symposium on Compression and Consolidation of Clayey Soils (IS-Hiroshima's 95) 1, 3–8. Hiroshima.

Barden, L., 1969. Time dependent deformation of normally consolidated clays and peats. Journal of the SoilMechanics and FoundationsDivision, ASCE 95, 1–32.

Baldi, G., Hueckel, T., Pellegrini, R., 1988. Thermal Volume Changes of the Mineral Water System in Low-Porosity Clay Soils. Canadian Geotechnical Journal 25, 807-825.

Becker, B. R., Misra, A., Fricke, A. F., 1992. Development of correlations for soil thermal conductivity, Int. Comm. Heat Mass Transfer 19, 59-68.

Bjerrum, L., 1967. Engineering geology of Norwegian normally-consolidated marine clays as related to settlements of buildings. Goetechnique 17, 83-118.

Brinch Hansen, J., 1969. A mathematical model for creep phenomena in clay. In 7th International Conference on Soil Mechanics and Foundation Engineering 12, 12–18, Mexico City, Mexico.

Bouazza, A., Abuel-Naga, H. M., Gates, W. P., Laloui, L., 2008. Temperature effects on volume change and hydraulic properties of geosynthetic clay liners. The First Pan American Geosynthetics Conference & Exhibition, Cancun, Mexico.

Boudali, M., Leroueil, S., Srinivasa Murthy, B. R., 1994. Viscous behaviour of natural clays. In: Proceedings of the 13th International Conference on Soil Mechanics and Foundation Engineering 1, 411–416, New Delhi, India.

Burghignoli, A., Desideri, A., Miliziano, S., 1992. Deformability of clays under non isothermal conditions. Rivista italiana di Geotecnica 92, 227-236.

Burghignoli, A., Desideri, A., Milizia no, S., 2000. A laboratory study on the thermomechanical behaviour of clayey soils. Can. Geotech. J. 37, 764-780.

Campanella, R. G., Mitchell, J. K., 1968. Influence of temperature variations on soil behavior. ASCE 94, 709-734.

Campbell, G., Norman. J., 1998. An introduction to environmental biophysics, 2nd Edition. Library of Congress Cataloging-in-Publication Data, Springer-Verlag New York, Inc.

Cekerevac, C., Laloui, L., 2004. Experimental study of thermal effects on the mechanical behaviour of a clay. International Journal for Numerical and Analytical Methods in Geomechanics 28, 209-228.

Cho, W. J., Lee, J. O., Chun, K. S., 1999. The temperature effects on hydraulic conductivity of compacted bentonite. Applied Clay Science 14, 47–58.

Cho, W. J., Lee, J. O., Kang, C. H., 2000. Infuence of temperature elevation on the sealing performance of a potential buffer material for a high-level radioactive waste repository, Annals of Nuclear Energy 27, 1271–1284.

Cho, W. J., Lee, J. O., Kwon, S., 2011. An analysis of the factors affecting the hydraulic conductivity and swelling pressure of KYUNGJU ca-bentonite for use as a clay-based sealing material for a high-level waste repository. Annals of Nuclear Energy 27, 1271–1284.

Cui, Y., Le, T. T., Tang, A. M., Delage, P., Li, X. L. 2009. Investigating the time dependent behaviour of Boom clay under thermo mechanical loading, Géotechnique 59, 319-329.

Das, B. M., 2008. Advanced Soil Mechanics. Washington, New York, London.

Degago, S. A., 2011. On creep during primary consolidation of clays. Ph.D. thesis. Norwegian University of Science and Technology (NTNU), Trondheim, Norway.

Delage, P., Sultan, N., Cui, Y. J., 2000. On the thermal consolidation of boom clay. Canadian Geotechnical Journal 37, 343–354.

Delage, P., Cui, Y. J., and Sultan, N., 2004. On the thermal behavior of Boom clay. Proceeding Eurosafe 2004 Conference. Berlin, Germany.

Delage, P., Sultan, N., Cui, Y. J., Li, X. L., 2009. Permeability changes in Boom clay with temperature. International Conference and Workshop "Impact of Thermo Hydro-Mechanical-Chemical (THMC) processes on the safety of underground radioactive waste repositories". European Union, Luxembourg, September.

Derjaguin, B. V., Karasev, V. V., Khromova, E. N., 1986. Thermal expansion of water in fine pores. J. Coll. Interface Sci 106, 586–587.

Edil, T. B., Fox, P. J., Lan, L. T., 1994. An assessment of one-dimensional peat compression. In Proceedings of the 8th International Conference on Soil Mechanics and Foundation Engineering 1, 229–232. New Delhi. A.A. Balkema, Rotterdam, the Netherlands.

Eriksson, L. G., 1992. Compression properties of sulphide soils – Influence from time and temperature, a laboratory study. Licentiate thesis, Luleå University of Technology, Luleå [In Swedish].

Farouki, O., 1981. Thermal properties of soils. United States Army Corps of Engineers, Cold Regions Research and Engineering Laboratory, Hanover, New hampshire, U.S.A.

François, B., Salager, S., El Youssoufi, M., Ubals Picanyol, D., Laloui, L., Saix, C., 2007. Compression tests on a sandy silt at different suction and temperature levels. Computer Applications in Geotechnical Engineering, 1-10.

Finn, F. N., 1951. The Effect of Temperature on the Consolidation Characteristics of Remolded Clay. American Society for Testing and Materials, Special Technical Publication 126, 65-71, as reported by Schmidt, N.O. (1965).

Fricke, B. A., Misra, A., Beeker, B. R., Stewart, W. E., 1997. Soil thermal conductivity: effects of saturation and dry density. Department of Mechanical and Aerospace Engineering, University of Missouri Kansas City, Kansas City.

Gaudette, H. E., Eades, J. L., Grim, R. E., 1966. The nature of illite. Clays and Clay Minerals 13, 33-48.

Green, W. J., 1969. The influence of several factors on the rate of secondary compression of soil. Master thesis, The Missouri University of Science and Technology, Rolla, Missouri, USA.

Gupta, B., 1964. Creep of saturated soil at different temperatures. Master Thesis, The University of British Columbia, Canada.

Gupta, V. K., 2013. An Experimental Study on Secondary Consolidation of Organic Clay. Master Thesis, Jadavpur University, Kolkata, India.

GTR. 2000. Réalisation des remblais et des couches de forme (p. 102). Paris: Laboratoire Central des Ponts et Chaussées. (In French).

Haehnlein, S., Bayer, P., Blump, P., 2010. International legal status of the use of shallow geothermal energy. Renew. Sustain. Energy Rev 14, 2611-2625.

Hanson, J. L., Edi, T. B., Yesiller, N., 2000. Thermal properties of high water content materials. Geotechnics of High Water Content Materials, 137-151.

Hong, P. Y., Pereira, J. M., Tang, A. M., Cui, Y. J., 2013. On some advanced thermo-mechanical models for saturated clays. International Journal for Numerical and Analytical Methods in Geomechanics 37, 2952-2971.

Imai, G., Tang, Y., 1992. A constitutive equation of one-dimensional consolidation derived from inter-connected tests. Soils and Foundation 32, 83–96.

Jain, S. K., Nanda, A., 2010. On the nature of secondary compression in soils. Proc. Indian Geotechnical Conference (IGC-2010) 2, 1121-1124, IIT Bombay, , MACMILLAN Publishers India Ltd.

Kholghifard, M., Ahmad, K., Ali, N., Kassim, A., Kalatehiari, R., Babakanpour, F., 2014. Temperature effect on compression and collapsibility of residual granitic soil. GRAĐEVINAR 66, 1-10.

Krzeminska, D. M., Steele-Dunne, S. C., Bogaard, T. M., Rutten, M. M., Sailhac, P., Geraud, Y., 2012. High-resolution temperature observations to monitor soil thermal properties as a proxy for soil moisture condition in clay-shale landslide. Hydrol. Process 26, 2143-2156.

Kuhn, M. R., Mitchell, J. K., 1993. New perspectives on soil creep. Journal of Geotechnical Engineering, 119, 507–524, doi: 10.1061/(ASCE)0733-9410 (1993)119:3(507).

Kim, Y. T., Leroueil, S., 2001. Modelling the viscoplastic behaviour of clays during consolidation: application to Berthierville clay in both laboratory and field conditions. Can. Geotech. J. 38, 484–497.

Lynch, F. L., 1997. Frio shale mineralogy and the stoichiometry of the smectite-to-illite reaction: the most important reaction in clastic sedimentary diagenesis. Clays and Clay Minerals 45, 618-631.

Ladd, C. C., Foott, R., Ishihara, K., Schlosser, F., Poulos, H. G., 1977. Stress-deformation and strength characteristics. state-of-the-art report. In 9th International Conference on SoilMechanics and Foundation Engineering 2, 421–494, Tokyo.

Laloui, L., Cekerevac, C., 2003. Thermo-plasticity of clays: An isotropic yield mechanism. Computers and Geotechnics 30, 649-660.

Laloui, L., Leroueil, S., Chalindar, S., 2008. Modelling the combined effect of strain rate and temperature on one-dimensional compression of soils. Canadian Geotechnical Journal 45, 1765-1777.

Le, T. M., Fatahi, B., Khabbaz, H., 2012. Viscous behaviour of soft clay and inducing factors. Geotechnical and Geological Engineering 30, 1069-1083.

Leroueil, S., Kabbaj, M., Tavenas, F., Bouchard, R., 1985. Stress–strain-strain rate relation for the compressibility of sensitive natural clays. Geotechnique 35, 159–180.

Leroueil, Serge & Marques, M. E. S., 1996. Importance of strain rate and temperature effects in geotechnical engineering. Geotechnical Special Publication, ASCE 61(Session on Measuring and Modeling Time Dependent Soil Behavior),1–60.

Leroueil, S., 2006. The isotache approach. Where are we 50 years after its development by Professor Šuklje? (2006 Prof. Šuklje's Memorial Lecture). In: Proceedings of the 13th Danube-European Conference on Geotechnical Engineering, 55-88, Ljubljana 2006.

Lingnau, B. E., Graham, J., Yarechewski, D., Tanaka, N., and Gray, M. N., 1996. Effects of Temperature on Strength and Compressibility of Sand-Bentonite Buffer. Engineering Geology 41, 103-115.

Lipiec, J., Usowicz, B., Ferrero, A., 2007. Impact of soil compaction and wetness on thermal properties of sloping vineyard soil. International Journal of Heat and Mass Transfer 50, 3837-3847.

MacFarlane, J. W., 1959. Effect of Structure on Secondary Compression of Kaolinite. An M.S. Thesis Presented to the Graduate Council of The University of Florida.

Madsen, F. T., 1998. Clay mineralogical investigations related to nuclear waste disposal. Clay Minerals 33, 109-129.

Marshall, P. W., 1960. Permeability Studies on Selected Saturated Clays. A High Honors Project under a Fellowship from the National Science Foundation, University of Florida.

Marques, M. E., Leroueil, S., Almeida, M. S., 2004. Viscous behaviour of St Roch-de-l'Achigan clay, Can. Geotech. J. 41, 25-38, Quebec.

Masin, D., Khalili, N., 2011. A thermo-mechanical model for variably saturated soils based on hypoplasticity. International Journal for Numerical and Analytical Methods in Geomechanics 36, 1461-1485.

Mesri, G., 1973. Coefficient of secondary compression. J Soil Mech Found Div, ASCE 99, 123–137.

Mesri, G., Castro, A., 1987. C_α/C_c concept and K_0 during secondary compression. Journal of Geotechnical Engineering 113, 230-247.

Mesri, G., Godlewski, P. M., 1977. Time and Stress Compressibility Inter relationship. Journal of the Geotechnical Engineering Division, ASCE 103, 417-430.

Mesri, G. , Shahien, M. , Feng, T. W., 1995. Compressibility parameters during primary consolidation. Proc. Int. Symp. on Compression and Consolidation of Clayey Soils 2 , 1021–1037, Balkema, Rotterdam, Netherlands.

Midttomme, K., Roaldset , E., Aagaard, P., 1998. Thermal conductivity claystones and mudstones. Clay Minerals 33, 131-145.

Misra, A., Becker, B. R., Fricke, B. A., 1995. A Theoretical model of the thermal conductivity of idealized soil 1, 81-96, HVAC&R Research.

Morin, R., Silva, A. J., 1984. The effects of high pressure and high temperature on some physical properties of ocean sediments. Journal of Geophysical research 89, 511-526.

Moritz, L., 1995. Geotechnical properties of clay at elevated temperatures. Swedish Geotechnical Institute (SGI), Linköping, Sweden.

Mon, E. E., Hamamoto, K., Kawamoto, S., Komatsu, T., Møldrup, P., 2013. Temperature effects on geotechnical properties of kaolin clay: simultaneous measurements of consolidation characteristics, shear stiffness, and permeability using a modified oedometer. GSTF International Journal of Geological Sciences (JGS) 1.

Nayak, N. V., Christensen, R. W., 1971. Swelling characteristics of compacted, expansive soils, Clays and Clay Minerals 19, 251-261.

Ochiai, F. M., Yasufuku, M. N., Kobayashi, M. T., Delage, P., Li, X. L., 2005. Thermally Induced Consolidation of Soft Bangkok Clay, Civil Society Western Branch of Presentation 59, 319-329.

Oladunjoye, M. A., Sanuade, O. A., 2012. Thermal diffusivity, thermal effusivity and specific heat of soils in olorunsogo powerplant. IJRRAS 13, 502-521, southestern Nigeria.

Peters-Lidard, C. D., Blackburn, E., Liang, X., Wood, E. F., 1998. The effect of soil thermal conductivity parameterization on surface energy fluxes and temperatures. Journal of the Atmos Pheric Sciences 55, 1209-1224.

Perzyna, P., 1963. The Constitutive Equations for Rate Sensitive Plastic Materials. Quarterly of Applied Mathematics 20, 321-332.

Pramanik, P., Aggarwal, P., 2013. Comparison of thermal properties of three texturally different soils under two compaction levels. African Journal of Agricultural Research 8, 3679-3687.

Putkonen, J., 1998. Soil thermal properties and heat transfer processes near Ny-Alesund. Polar Re.setrrrh 17, 165-179, northwestern Spitsbergen, Svalbard.

Raude, S., Laigle, F., Giot, R., Fernandes, R., 2015. A unified thermoplastic/viscoplastic constitutive model for geomaterials. Acta Geotechnica, 10.1007/s11440-015-0396-6.

Reeves, G. M., Sims, I., Cripps, J. C., 2006. Clay Materials Used in Construction. Geological Society, London.

Romero, E., Gens, A., Lloret, A., 2001. Temperature effects on the hydraulic behaviour of an unsaturated clay. Geotechnical and Geological Engineering 19, 311-332.

Romero, E., Villar, M. V., Lloret, A., 2005. Thermo-hydro mechanical behaviour of two heavily overconsolidated clays. Engineering Geology 81, 255-268.

Saleh, Q. A., 2012. Study of factors affecting the thermal conductivity of Iraq bentonite. J. Baghdad for Sci. 9, 548-553.

Sällfors, G., 1975. Preconsolidation pressure of soft high plastic clays. PhD thesis, Chalmers University of Technology, Gothenburg, Sweden.

Schmertmann, J. H., 1976. Secondary consolidation and secondary shear, University of florida, Gainesville.

Schmertmann, J. H., 2012. New Concepts for the Mobilization of the Components of Shear Resistance in Clay. Publication 208, Norwegian Geotechnical Institute, Oslo.

Shariatmadari, N., Saeidijam, S., 2011. The effect of elevated temperature on compressibility and swelling of bentonite sand mixtures. Bund. A 16, 137-146.

Shariatmadari, N., Saeidijam, S., 2012. The effect of thermal history on thermo mechanical behavior of bentonite-sand mixture. International Journal of Civil Engineering 10, 162-167.

Smits, K. M., Sakaki, T., Limsuwat, A., Illangasekare, T. H., 2009. Determination of the thermal conductivity of sands under varying moisture, drainage/wetting, and porosity conditions applications in near-surface soil moisture distribution analysis. Proceedings of the 29th Annual American Geophysical Union Hydrology Days, 58-66, Colorado State University, Fort Collins.

Subba, K., Wadhawan, S. K., 1953. The effect of heating the soil on permeability under prolonged submergence of soil in water. Proc. 3rd Int. Conf. Soil Mechanics and Foundation Engineering 1, 178-179, Zurich, Switzerland.

Suhonen, K., 2010. Creep of soft Clay. Thesis submitted for Master in Civil and Environmental Engineering, Aalto University.

Šuklje, L., 1957. The analysis of the consolidation process by the isotache method. Proc. 4th Int. Conf. on Soil Mechanics and Foundation Engineering 1 , 200–206, Butterworths, London.

Sultan, N., Delage, P., Cui, Y. J., 2002. Temperature effects on the volume change behaviour of Boom clay. Engineering Geology 64, 135 145.

Srodon, J., Morgan, D. J., Eslinger, E. V., Eberl, D. D., Karlinger, M. A., 1986. Chemistry of illite/smectite and end-member illite. Clays and Clay Minerals 34, 368-378.

Standard ASTM., 2006. D2487 Standard practice for classification of soils for engineering purposes (Unified Soil Classification System) (p. 12). West Conshohocken. PA: ASTM International.

Standard ASTM., 2008. D4186-06 Standard test method for one-dimensional consolidation properties of soils using controlled-strain loading (American Society of Testing Materials). West Conshohocken. PA: ASTM International.

Tang, A. M., Cui, Y. J., Barnel, N., 2007. A new isotropic cell for studying the thermo-mechanical behavior of unsaturated expansive clays. Geotechnical Testing Journal 30, 341-348.

Tang, A. M., Cui, Y. J., Barnel, N., 2008a. Thermo-mechanical behaviour of a compacted swelling clay. Géotechnique 58, 45-54.

Tang, A. M., Cui, Y. J., Le, T. T., 2008b. A study on the thermal conductivity of compacted bentonites. Applied Clay Science 41, 181-189.

Tang, A. M., Cui. Y., 2009. Modelling the thermo-mechanical volume change behaviour of compacted expansive clays. Science China Technological Sciences 54, 190-202.

Tang, A. M., Cui, Y. J., 2010. Effects of mineralogy on thermo-hydro-mechanical parameters of MX80 bentonite, Journal of Rock Mechanics and Geotechnical Engineering 2, 91-96.

Tang, A. M., Cui, Y. J., 2011. Preliminary laboratory thermo-hydro-mechanical characterization of Opalinus clay. Proceedings of the 12th International Congress on Rock Mechanics, Chine.

Tanaka, N., Graham, G., Crilly, T., 1997. Stress-strain behaviour of reconstituted illitic clay at different temperatures. Engineering Geology 47, 339-350.

Taylor, D. W., 1942. Research on Consolidation of Clays. Department of Civil and Sanitary Engineering, Massachusetts Institute of Technology, Cambridge, Massachusetts

Towhata, I., Kuntiwattanakul, P., Seko, I., 1993. Volume change of clays induced by heating as observed in consolidation tests. Soils and Foundations 33, 170-183.

Tsutsumi, A., Tanaka, H., 2012. Combined effects of strain rate and temperature on consolidation behavior of clayey soils. Soils and Foundations 52, 207-215.

Villar, M. V., Gómez-Espina, R., Lloret, A. 2010. Experimental investigation into temperature effect on hydro-mechanical behaviours of bentonite. Journal of Rock Mechanics and Geotechnical Engineering 2, 171–78.

Villar, M. V., Lloret, A., 2004. Influence of temperature on the hydro-mechanical behaviour of a compacted bentonite, Applied Clay Science 26, 337–350.

Verruijt, A., 2012. Soil Mechanics. Delft University of Technology, Netherlands.

Watabe, Y., Udaka, K., Nakatani, Y., Leroueil, S., 2012. Long term consolidation behavior interpreted with isotache concept for worldwide clays. Soils and Foundations 52, 449-464.

YangPing, Y., YiFan, Y., Lei, N., 2011. UH model considering temperature effects. Science China Technological Sciences 54, 190-202.

Ye, W. M., Wan, M., Chen, B., Chen, Y. G., Cui, Y. J., Wang, J., 2013. Temperature effects on the swelling pressure and saturated hydraulic conductivity of the compacted GMZ01 bentonite, Environ Earth Sci 68, 281-288.

Yong, R., Taylor, L. O., Warkentin, B. P., 1963. Swelling pressures of sodium montmorillonite at depressed temperatures. Eleventh National Conference on Clays and Clay Minerals 11, 268-281.

Yu-Jun, C., Wei-min, Y., 2005. On modeling of thermo mechanical volume change behavior of saturated clays. Chinese Journal of Rock Mechanics and Engineering 24, 3903-3910.

Yashima, A., Leroueil, S., Oka, F., Guntoro, I., 1998. Modelling temperature and strain rate dependent behavior of clays: one dimensional consolidation. Soils and Foundations 38, 63–73.

Zhang, F., Zhang, Z. Z., Low, P. F., Roth, C. B., 1993. The effect of temperature on the swelling of montmorillonite. Clay Minerals 28, 25–31.

Temperature impact on the consolidation and creep behaviour of compacted clayey soils

Abstract

Consolidation of clay soils is one of the main challenges in engineering design and construction. Clayey soils could be exposed to thermal cycles in some engineering applications such as geothermal piles, nuclear waste storages, heat storage in embankments, etc. These temperature changes could affect the primary consolidation as well as the creep behaviour of the soils.

In this context, this study investigated the impact of temperature on consolidation behaviour and creep behaviour of saturated compacted clays. In addition, the impact of stress history and clay nature on the temperature dependent mechanical and hydraulic behaviours was also considered. Temperature controlled oedometric cells were employed to perform constant rate of strain (CRS) consolidation tests for different strain rates (0.002%/min to 0.02%/min) within a temperature range of 5° C to 70^{o} C. Two different compacted saturated clays with different stress histories were used in these CRS tests (clay A: PI=31%, clay B: PI=23.8%).

The results showed that the compression and swelling indices for both materials changed slightly with temperature and strain rate alteration. The preconsolidation pressure of both clays decreased as the temperature increased, but less in the case of clay B, while it decreased as the strain rate decreased for both materials. The hydraulic conductivity increased with temperature while the intrinsic permeability remained unchanged in the investigated range of temperature. The creep index increased as the temperature increased for both clays. In addition, the stress history has an impact on the temperature dependent mechanical and hydraulic behaviour of clay soils. Results showed a thermal dilation for highly overconsolidated soils and a thermal contraction for low and normally consolidated samples. The relative impact of several parameters on the modification of the behaviour of compacted clays with temperature was also assessed.

Keywords: Temperature, compacted clays, vertical consolidation, creep, Vertical oedometric test, behaviour.

Impact de la température sur le comportement de consolidation et de fluage des sols argileux compacts

Résumé

La consolidation des sols argileux est un enjeu majeur dans le domaine de la géotechnique pour la conception des ouvrages. Ceci est notamment le cas lorsque les sols argileux peuvent être exposés à des cycles thermiques, comme dans le cas des géostructures géothermiques, dépôts de stockage des déchets nucléaires, stockage de chaleur dans les remblais, etc. Ces changements de température pourraient avoir une incidence sur le comportement de consolidation des sols, tant du point de vue de la consolidation primaire que du fluage.

Dans ce contexte, cette étude a examiné l'impact de la température sur le comportement de consolidation et du fluage d'argiles compactées saturées. L'impact de la nature du sol et de son histoire mécanique a été considéré. Une cellule œdométrique à température contrôlée a été utilisée pour effectuer des essais à vitesse de déformation constante (CRS) pour différentes vitesses de déformation (0,002% / min à 0,02% / min) dans une gamme de température comprise entre 5 ° C et 70 ° C. Deux argiles compactées, avec différentes histoires de chargement mécanique, ont été utilisés.

Les résultats indiquent que les indices de compression et de gonflement pour les deux matériaux ne sont que légèrement modifiés par une augmentation de la température allant de 5 à 70°C. En revanche, la pression de préconsolidation des deux argiles diminue à mesure que la température augmente, cet effet étant cependant fonction de la nature du sol considéré. Le coefficient de consolidation augmente lorsque la température augmente pour les deux matériaux, ainsi que la conductivité hydraulique. La perméabilité intrinsèque reste stable en fonction de la température. L'indice de fluage augmente lorsque la température augmente pour les deux argiles. En outre, l'histoire des chargementsmodifie l'impact de la température sur le comportement mécanique. Ainsi, les résultats montrent une dilatation thermique pour les sols fortement surconsolidées et une contraction thermique des échantillons faibles et normalement consolidés.

Cette étude a ainsi permis de mettre en évidence l'impact relatif d'un certain nombre de paramètres sur l'évolution du comportement des argiles compactées avec la température.

Mots clés: Température, argiles compactées, consolidation verticale, fluage, test oedométrique vertical, comportement.